REPUBLIQUE DU CAMEROUN
Paix – Travail – Patrie
****
UNIVERSITE DE YAOUNDE I
FACULTE DES SCIENCES
DEPARTEMENT DE MATHÉMATIQUES
****
CENTRE DE RECHERCHE ET DE FORMATION DOCTORALE EN SCIENCES, TECHNOLOGIE ET GEOSCIENCES
Laboratoire de Mathématiques et Applications

REPUBLIC OF CAMEROUN
Peace – Work – Fatherland
****
UNIVERSITY OF YAOUNDE I
FACULTY OF SCIENCE
DEPARTMENT OF MATHEMATICS
****
POSTGRADUATE SCHOOL OF SCIENCE, TECHNOLOGY AND GEOSCIENCES
Laboratory of Mathematics and Applications

Contribution to the mathematical modelling and analysis of spatial distribution of the anopheles mosquito

THESIS
Submitted to the graduate school in partial fulfilment of the requirements for the degree of Doctor of Philosophy / PhD in Mathematics

Par : **MANN MANYOMBE Martin Luther**
Master degree

Sous la direction de
MBANG Joseph
Senior Lecturer
University of Yaoundé I
BOWONG Samuel
Professor
University of Douala

Année Académique : 2020

RÉPUBLIQUE DU CAMEROUN
PAIX-TRAVAIL-PATRIE
****
MINISTÈRE DE L'ENSEIGNEMENT SUPÉRIEUR
****
UNIVERSITÉ DE YAOUNDÉ I
****
CENTRE DE RECHERCHE ET DE FORMATION DOCTORALE EN SCIENCES, TE*CHNOLOGIES* ET *GEOSCIENCES*
****

REPUBLIC OF CAMEROON
PEACE-WORK-FATHERLAND
****
MINISTRY OF HIGHER EDUCATION
****
THE UNIVERSITY OF YAOUNDE I
****
POSTGRADUATE SCHOOL OF SCIENCE, TECHNOLOGY AND GEOSCIENCES
****

DÉPARTEMENT DE MATHÉMATIQUES
DEPARTMENT OF MATHEMATICS

ATTESTATION DE CORRECTION DE LA THESE DE DOCTORAT / Ph.D

Nous soussignés, **BEKOLLE David, Pr., UYI, Président du jury ; BOWONG Samuel, Pr., UD, MBANG Joseph, CC, UYI, Rapporteurs ; NOUNDJEU Pierre, MC, UYI, KAMGANG Jean Claude, MC, UN, Examinateurs,** membres du jury de la thèse de Doctorat / Ph.D présenté par **M. MANN MANYOMBE Martin Luther, Matricule 13Q2057,** intitulé: **«CONTRIBUTION TO THE MATHEMATICAL MODELLING AND ANALYSIS OF SPATIAL DISTRIBUTION OF THE ANOPHELES MOSQUITO »** et soutenue en vue de l'obtention du diplôme de Doctorat / Ph.D **en mathématiques**, Spécialité **: Mathématiques et Applications Fondamentales,** Option **: Modélisation mathématique et Systèmes dynamiques,** attestons que toutes les corrections demandées par le jury de soutenance en vue de l'amélioration de ce travail, ont été effectuées.

En foi de quoi la présente attestation lui est délivrée pour servir et valoir ce que de droit.

Président	Rapporteurs	Examinateurs
BEKOLLE David, Pr., UYI	**BOWONG Samuel, Pr., UD**	**NOUNDJEU Pierre, MC, UYI**
	MBANG Joseph, CC, UYI	**KAMGANG Jean Claude, MC, UN**

♣ Declaration ♣

I hereby declare that this submission is my own work and to the best of knowledge, it contains no materials previously published or written by another person. No material has been accepted for the award of any other degree or diploma at the University of Yaounde I or any other educational institution except where due acknowledgement is made in this thesis. Any contribution made to the research by others, with whom I have worked at the University of Yaounde I or elsewhere, is explicitly cited in the thesis. I also declare that the intellectual content of this thesis is the product of my own work, except to the extent that assistance from others in style, presentation and linguistic expression is acknowledge.

Martin Luther MANN MANYOMBE

♣ Dedication ♣

In memory of my parents ***Mr and Mrs MANN***

♣ Remerciements ♣

Tout seul on ne peut rien bâtir. Qu'il me soit permis d'adresser mes sincères remerciements et d'exprimer ma gratitude au Seigneur Dieu et à tous ceux qui de près ou de loin ont contribué à la réalisation de ce travail.

Tout d'abord, j'exprime ma profonde gratitude à mes encadreurs le Docteur Joseph MBANG, le Professeur Samuel BOWONG et le Professeur Berge TSANOU qui ont patiemment suivi mes recherches avec diligence, passion et créativité. Ils m'ont transmis bien au-delà des connaissances scientifiques de valeurs morales qui resteront à jamais gravées dans mon coeur. Malgré vos emplois du temps chargés vous avez toujours trouvé du temps à m'accorder. C'est par votre accompagnement que j'ai pu apprendre et que je continue d'apprendre tant de choses à vos côtés.

Je ne remercierai jamais assez le Docteur Joseph MBANG qui a co-dirigé cette thèse et qui m'a introduit dans le monde de la recherche. Vous n'avez pas cessé d'éclairer et d'inspirer mon esprit de jeune chercheur dans les différentes façons d'aborder les questions scientifiques depuis mes études de Master. Les discussions toujours éclairées avec vous et vos multiples remarques m'ont permis d'améliorer la qualité de ce travail. Vous n'avez jamais hésité à me soutenir socialement afin de faciliter mon insertion et me permettre de travailler dans la sérénité. Je souhaite humblement que la qualité de ce travail soit à la mesure des sacrifices que vous avez consentis durant ces années de recherche.

Toute ma reconnaissance au Professeur Samuel BOWONG qui a spontanément accepté de co-diriger cette thèse. Malgré vos multiples occupations, vous avez toujours consacré votre précieux temps à ma modeste personne pour me prodiguer des conseils et apporter des remarques qui m'ont permis d'améliorer la qualité de ce travail.

Je tiens à exprimer ma profonde gratitude au Professeur Berge TSANOU pour le suivi de mes recherches avec rigueur, passion et créativité. Vous avez spontanément accepté de m'accompagner dans mes recherches et m'avez inculquer la vision de la science et la rigueur scientifique. Vos multiples remarques m'ont permis de renforcer mon sens de la critique et d'améliorer la qualité de ce travail. Vous avez toujours réagi à mes mails et appels même à des heures tardives de la nuit pour me permettre d'avancer dans mes travaux. C'est par ce dévouement au travail et votre accompagnement que j'ai pu réaliser cette thèse. J'espère que grâce à ces quelques lignes j'aurai pu dire l'essentiel de la reconnaissance et tout le respect que je vous dois.

Je remercie le Professeur Jean LUBUMA pour avoir consacré très souvent de son précieux temps pour apporter des remarques qui m'ont permis d'améliorer la qualité de ce

travail.

Je remercie également tous les enseignants de mathématiques de l'Université de Yaoundé I pour la qualité de la formation qu'ils ont su transmettre aux étudiants. Je remercie particulièrement les Professeurs David BEKOLLE, Yves EMVUDU, Raoult AYISSI, Jean-Jules TEWA, NOUDJEU, MBEHOU Mohamed et les Docteurs Maurice KIANPI, Edgar TCHOUNDJA, MENGUE MENGUE, Patrice TAKAM, Antoine BOGSO, MBELE BEDIMA, Gilbert CHENDJOU, Romain NIMPA, DJIADEU, Hilaire MBIAKOP. Je n'oublie pas de remercier les responsables du Laboratoire de mathématiques et applications (LABOMAP) : les professeurs Nicolas ANDJIGA, Bertrand TCHANTCHO, Yves EMVUDU, Jean-jules TEWA, Moyouwou ISSOFA, Mohamed MBEHOU et les Docteurs Joseph MBANG, Hugues TCHANTCHO, Patrice TAKAM pour les nombreux séminaires qu'ils ont organisés pour permettre aux étudiants de s'exprimer et d'être orientés.

La préparation d'une thèse nécessite qu'on fasse régner autour de soi une ambiance conviviale, amicale et chaleureuse. Je remercie tous mes amis du département de mathématiques ainsi que tous mes camarades du laboratoire de mathématique et applications en particulier Valaire Yatat, Alexis Tamen, Israel Tankam, Abdoulaye Mendy, Plaire Tchinda, Surdive Atemewoue, Yannick Tenkeu pour les échanges fraternels que j'ai eu avec vous pendant toutes ces années d'études. J'ai également une pensée pour tous les doctorants en mathématiques : Bertrand Kouenkam, Hugues Deffo, Adriel Keumo, Simon Tega II, Leroy Siaka et plein d'autres avec qui j'ai toujours eu un grand plaisir à discuter de la passion des mathématiques qui nous habite tous.

J'adresse ma sympathie à tous mes amis et collègues, en particulier Serge Ndanou, Fabrice Tchoua, Romeo Feudjio, Jean-Claude Mbarga, Romaric Tchapnga, Yannick Messi, Telor Kamgang, Merlin Youdom, Rodrigue Tadjoukong, Arthur Ayissi, Auberlin Konlack pour leurs soutiens et leurs encouragements sans failles.

Que faire sans la famille ? C'est grâce à vos encouragements réguliers que j'ai trouvé la motivation nécessaire pour réaliser ce travail. Une pensée profonde va à l'endroit de tous mes parents en particulier monsieur et madame Belengue, monsieur Alain Roland Ndoumbe qui m'ont toujours encouragés et souhaités voir aboutir cette thèse. J'espère profondement que l'aboutissement de ce travail vous honore. Je remercie énormement tous mes frères et soeurs, particulièrement Stéphanie, Bérénice, Nathalie Denise, Thierry, Nanou, Adrienne, Frida, Pascaline, Gladice, Eric Dunand pour votre soutien et toute l'affection que vous m'avez toujours accordé. Enfin toute mon affection va à ma beauté Imelda Lucresse pour son soutien et son amour qui m'ont apporté réconfort dans les moments difficiles et les aléas de la thèse.

♣ Abstract ♣

Mosquitoes represent a major threat to public health. Constants efforts are being made to develop or improve control strategies in the framework of control vectors. Control vectors aims to maintain mosquitoes at a low levels that do not represent risk for health. Planning of efficient control strategies requires in-depth knowledge of the mosquito's biology and ecology, as well as good understanding of the processes governing the dynamics of the population in time and space. In malaria endemic regions, dispersal of mosquitoes from one location to another for survival and reproduction is a fundamental biological process that operates at multiple temporal and spatial scales. This dispersal behaviour is an important factor that causes uneven distribution of malaria vectors causing heterogeneous transmission. In published literature, most models that addressed mosquito dynamics rely on temporal modelling in which spatial dynamics and movements of mosquito are not taken into account. My investigations in this thesis deals with spatial distribution of anopheles mosquito. I develop spatio-temporal models that consider mosquito dispersal, spatial dynamics, environmental heterogeneity and age structure of the mosquitoes, which are needed for designing, planning, and management of the control strategies. In the first, I develop a spatio-temporal model of mosquito dynamics using discrete patches as a representation of space. I analyze and simulate the spreading of mosquitoes on a complex metapopulation, that is, network of population connected by migratory flows. The theoretical study of this model is done using the theory of monotone dynamical systems. This study allow to identify threshold values that ensure an effective control of mosquitoes. Secondly, using an alternative approach to discrete-space model developed previously, I develop an advection-reaction-diffusion model in order to take into account the mosquito dispersal and spatial heterogeneity of their resources. The model incorporates female mosquitoes of oviposition's cycle, which provides a framework to study the life style of the adult mosquito. I carry out a qualitative analysis that highlights some biological thresholds that summarize the dynamics of the systems. In addition, for these models, meaningful numerical schemes are developed through nonstandard finite difference methods. The aim is to illustrate the theoretical part and investigate the effect of heterogeneous distribution of resources used by mosquitoes. Results reveal that due to dispersal, the distribution of mosquitoes highly depends on the distribution of hosts and breeding sites.

Keywords : Anopheles mosquito ; Dispersal ; Metapopulation ; Advection-Reaction-Diffusion Equation ; Spatial heterogeneity ; Dynamical Systems ; Threshold analysis.

♣ Résumé ♣

Les moustiques représentent une menace majeure pour la santé publique. Des efforts constants sont faits pour développer ou améliorer les stratégies de contrôle des moustiques. Le contrôle des moustiques vise à maintenir la densité des moustiques à des niveaux bas ne représentant aucun danger pour la santé. La planification des stratégies de contrôle efficaces exigent une bonne connaissance de la biologie du moustique et une bonne compréhension du processus gouvernant la dynamique de la population dans le temps et l'espace. Dans les régions où la malaria est endémique, la dispersion des moustiques d'un endroit à l'autre, à la recherche de ressources pour leur survie et leur reproduction, est un processus biologique fondamental fonctionnant à l'échelle temporelle et spatiale. Ce comportement de dispersion est un important facteur qui cause une distribution inégale des moustiques et une transmission hétérogène du paludisme. Dans cette thèse j'étudie la distribution spatiale des moustiques en développant des modèles mathématiques qui prennent en compte la dispersion, la dynamique spatiale, l'hétérogénéité environnementale et la structure d'âge des moustiques, lesquels sont nécessaires pour la conception, la planification et la gestion des stratégies de contrôle. Premièrement, je développe un modèle spatio-temporel de la dynamique des moustiques en utilisant des patches discrets comme représentation de l'espace. J'analyse et simule la propagation des moustiques sur un réseau de noeuds de population relié par des flux migratoires. L'étude théorique de ce modèle est faite à l'aide de la théorie des systèmes dynamiques monotones. Cette étude permet d'identifier des valeurs seuils qui assurent un contrôle efficace des moustiques. Ensuite, je développe un modèle de réaction-advection-diffusion afin de prendre en compte la dispersion des moustiques et l'hétérogénéité spatiale de leurs ressources. Le modèle incorpore les moustiques femelles du cycle de reproduction. J'effectue une analyse qualitative qui met en évidence des seuils écologiques résumant la dynamique des systèmes. De plus, pour ces modèles, des méthodes numériques appropriées ont été construites dans le but d'illustrer les parties théoriques et d'explorer les effets de la distribution hétérogène des ressources utilisées par les moustiques. Les résultats révèlent qu'à cause de la dispersion, la répartition des moustiques dépend fortement de la répartition des hôtes et des sites de reproduction.

Mots Clés : Moustique Anopheles ; Dispersion ; Métapopulation ; Equation d'Advection-Reaction-Diffusion ; Hétérogénéité Spatiale ; Systèmes Dynamiques.

Summary

List of Figures

List of Tables

♣ General introduction ♣

General overview

Malaria is a vector-borne disease transmitted by anopheles mosquitoes. The disease is transmitted between humans through bites of infectious mosquitoes. It is estimated that more than 3 billion people live in malarious areas and most of them live in sub-Saharan Africa [151]. Most individuals in this region are infected by Plasmodium Falciparum parasite which is the most prevalent and prominent malaria parasite in sub-Sahara Africa [51]. This parasite is not only associated with severe malaria but is also life threatening, causing high morbidity and mortality rates in the region. The World Health Organization [151] estimates that in 2010, more than 200 million malaria cases occurred worldwide [151]. Of the 660.000 malaria deaths that occurred in 2010 around the world, 91% were in Africa and 86% were children under the age of five years [151]. Despite the growing international pressure and efforts to provide treatment, to develop vaccines, and implement vector control, malaria continues to remain a major problem worldwide. Due to this trend, it is unlikely that the set goals for reducing the global burden of malaria will be achieved. Therefore, countries where malaria is prevalent need examine in depth the vectors that are responsible for transmitting the disease, and the type of behaviour, and dynamics these vectors follow. There is also a need to understand in detail the natural cause of the continuous transmission, and to design more realistic control strategies for vector management at local level.

Malaria control is multi-faceted and a more integrated approach towards malaria control in sub-Saharan Africa may have a greater impact in reducing malaria morbidity and mortality. However, with the increase of human populations, rural to urban migration, urbanization and environmental degradation, there has been an increase in suitable mosquito ponds and a modified ecosystem giving the vector an even greater opportunity to adopt its efficiently in disease transmission. There is a need therefore for more research focusing on improving our understanding of malaria vector population ecology, reducing human vector contact and disease transmission. Vector control has been the means of eradication of malaria in numerous regions of the world, and has dramatically reduced its incidence in some countries. The vector remains the key link in the transmission of malaria, and hence, warrants research and control effort in areas where the disease is still

a public health problem. Historically, success in combating malaria has been attributed to mosquito control, a strategy which has largely failed due to various reasons including the development of insecticide resistance, economic limitations and gaps in the basic biological knowledge of these vectors [95]. For any vector control effort to achieve a reduction in malaria transmission, it is important for control programme staff to have access to adequate information on the local malaria vector ecology, distribution, transmission patterns and the factors affecting transmission in order to design interventions suitable to the area corresponding considered.

Modelling provide interesting tools for experts to validate or improve vector control strategies with a minimal number of field experiments that can be very difficult to conduct and expensive. Most models of malaria transmission and control explain relationships between the number of mosquitoes and malaria transmission in humans while assuming enclosed systems of mosquitoes in which spatial dynamics and movements are not taken into account. These models have limited ability to assess and quantify the distribution of risks and interventions at local scales. Therefore, in order to overcome this limitation, mathematical models that consider the interaction between dispersal behaviour, population dynamics, environmental heterogeneity, and age structures of the mosquito are needed for designing, planning, and management of the control strategies at local scales.

Several studies have demonstrated that remote sensing and geographical information systems (GIS) are powerful tools for understanding mosquito distribution [62, 63, 121] and are suitable for understanding the link between seasonal variations and environmental factors to malaria transmission indicators at large spatial scales. However, these tools remain reliable only at global spatial scales. At local scales, mathematical models provide an alternative way of assessing and quantifying the distribution of risks or assessing interventions. They can also explain the complex dynamics of local populations and dispersal patterns exhibited by mosquitoes. They are also useful tools for capturing spatial characteristics for assisting decisions on mosquito surveillance and malaria prevention [76]. In these models, groups or spatially distributed populations can be linked together across a set of spatial locations.

The concept of modelling mosquito dispersal was highlighted a century ago by Ronald Ross (Ross, 1905). In his model, Ross described distribution of the mosquitoes by distance covered and concluded that mosquitoes movement follows a "centripetal law of random wandering" in which the number of dispersing mosquitoes is high in the vicinity and low far away from their original location. This law is conserved even in situations where the distribution of resources such as hosts and breeding sites is heterogeneous. Although Ross's idea of modelling mosquito dispersal is an important aspect for improving scientific experiments (Ross, 1905), modelling studies has rarely considered it. Other mathematical models of Ronald Ross (Ross, 1915), have long been used to explain relationships between the number of mosquitoes and malaria transmission in humans.

Several mathematical models including different factors have been proposed to understand the distribution of mosquito population and have been used to implement or improve vector managements [46, 105, 104, 131, 15, 2, 48, 1, 108]. The model studied by Anguelov, Esteva and Thomé [2, 46, 131] incorporated sterile insects to assess the effectiveness of the sterile insect technique (SIT) for vector management. The model proposed by Ngwa et al. [105, 104] incorporated human-vector interaction to observe how this interaction could drive mosquito dynamics. The models developed by Abdelrazec and Okuneye [1, 108] incorporated temperature and rainfall in order to assess their effects on mosquitoes abundance. However, these models have always assumed closed systems of mosquitoes in which spatial dynamics and movement are not taken into account. This assumption has enabled many intuitive analyses but has considerable consequences on implementing better strategies for control and evaluation of control interventions in field settings. Some authors have focused on the distribution of mosquitoes including mosquito dispersal. In Lutambi et al. [83], Nourridine et al. [106] and Yakob et al. [154], spatial aspect of mosquito have been modelled in terms of migration between patches in a hypothetical landscape. Likewise, models of spatial dynamics using PDEs have given sufficient conditions to mosquitoes to persist and spread [70, 126, 158, 132, 161]. These modelling studies indicate the need for more explicit models that include vital components of ecological interactions. In response to this need, mathematical models that consider the interaction between dispersal behaviour, population dynamics, environmental heterogeneity, and age distribution of the mosquito are needed for the designing, the planning, and the management of the control strategies at local scales.

Aim and objectives

This thesis aims at providing a mathematical framework to understand the spatial distribution of mosquitoes, which could help to the development and/or improvement of mosquito control strategies. This mathematical framework comprises mathematical models coupled with an appropriate theoretical analysis and thresholding, with adequate schemes for numerical solutions. It is developed in order to address challenges related to what, when and how questions regarding control interventions. The primary objective is to develop spatial mathematical models that capture mosquito dispersal to achieve a broader understanding of mosquito foraging behaviour and its interactions with environmental heterogeneity. To this end, we use two formalisms to capture mosquito dispersal, namely, (1) discrete-space continuous-time approach based on ordinary differential equations and (2) continuous-space continuous-time approach based on partial differential equations.

To address the first objective, we develop a spatial model based on biological and ecological knowledge of mosquitoes. We use a new approach recently introduced to deal with the spread of diseases in ensembles of (local) populations with a complex spatial

arrangement and connected by migration. Such sets of connected populations living in a patchy environment are called metapopulations in ecology. The reaction and diffusion processes modelling the spread of mosquitoes are considered as a two-step process. First, inside each network node, the reaction takes place under the assumption of a homogenous conserving the total number of mosquitoes. In particular, in each node, an individual mosquito is in one of the states of mosquito life cycle. Second, the diffusion term include the outflow of mosquitoes from their current nodes and the inflow of migratory mosquitoes from the nearest nodes. This objective is addressed in chapter 2 of this thesis.

The second objective of this thesis is addressed by constructing an advection-reaction-diffusion model for the dynamics of mosquitoes. To account for specific behaviours, the population is divided into appropriate compartments. We develop a spatial framework that captures mosquito dispersal behaviour in a heterogeneous environment as factors that affect the distribution of mosquitoes in a spatial environment. From modelling perspective, a general functional form of eggs oviposition rate is used including the Verhlust-Pearl logistic, the Hassell and the Maynard-Smith-Slatkin functions. In this work is presented in chapter 3, the dynamics of mosquito population as described on the one hand by a temporal compartmental model which is extended into spatio-temporal model on the other hand.

Outline

In chapter 1 we provide a non exhaustive literature review of mathematical models that concern mosquito population. The goal of this literature review is to properly compare our modelling assumptions as well as our modelling framework with already published models enabling to better discuss the improvements either from modelling or from a mathematical analysis point of view.

In chapter 2, following the classical ordinary differential equation (ODE) modelling framework ([2]), we build and analyse a new mathematical model, which considers the spreading of anopheles mosquito on a complex metapopulation, that is, networks of populations connected by migratory flows which configurations are described in terms of connectivity distribution of nodes (patches) and the conditional probabilities of connections between nodes. The model incorporates age distribution in form of the aquatic and adult stages of the mosquito life cycle and further divides the adult mosquito population into three stages. The metapopulation setting developed in this part, use a recent approach based on statistical mechanics. The spatial characteristics of the model are based on discretisation of space into discrete patches. These patches are assumed to be connected by migration of mosquitoes which move between patches as they search for oviposition sites and blood meals. Local dispersal is modeled by assuming that dispersing adults move from their current locations enter nearest neighboring locations and long-range dispersal

is achieved through repeated movements. The model is based on ordinary differential equations and is replicated across a landscape, a multi-patch system that represents a two-dimensional space. The model is applied to examine the significance of larval habitat connectivity and mosquito dispersal in a homogeneous and a heterogeneous landscapes on the persistence of mosquitoes populations. More precisely, we construct corresponding metapopulation model and perform their qualitative and quantitative analyzes.

In chapter 3, we derive a more general mathematical model for the population dynamics of anopheles mosquitoes that feeds on human blood but breeds outside of the human body at a distinct spatial location, the breeding site away from the human habitat. We develop models that incorporate both intrinsic dynamics and spatial variation of mosquitoes, taking into consideration the dynamics of the human-vector interaction. We will start with a temporal model that allows a general description of the mosquito's growth. This initial model captures the mosquito oviposition cycle as well as its main behavior (which could be useful when one considers chemical or biological control tools, such as SIT or GMM). Moreover, we consider a more general function for egg oviposition rate. Next, we will extend the obtained temporal model to a PDE system by adding both advection and diffusion terms that reflect mosquito's mobility. We study the global well-posedness and the asymptotic behavior of the solutions of this PDE model. Finally, we assess the impact of mosquito dispersal, heterogeneous distribution of mosquito resources (hosts), and other parameters on the spatial distribution, dynamics and persistence of mosquito populations.

Finally, we summarize, discuss and conclude the modeling work presented in the thesis, and suggests directions for future studies.

CHAPTER 1

Contents

VECTORS, THEIRS DISTRIBUTIONS AND MATHEMATICAL MODELING

1.1 Vectors of malaria and their distribution

1.1.1 Vectors of malaria

Mosquito-borne diseases are found in many countries in the world and constitute a major cause of human mortality (morbidity). Mosquitoes transmit some of the world's most relevant parasitic diseases and belong mainly to three genera : Anopheles, Culex and Aedes. Tropical diseases such as malaria, yellow fever, lymphatic filariasis, dengue fever, the West Nile Virus (WNV), Zika virus and other arboviruses are transmitted by mosquitoes. Of these, malaria is the most common and important, transmitted through the bite of a female anopheles mosquito, leading to the infection of humans with either one or more protozoan parasites such as Plasmodium falciparum, P. ovale, P. malariae and P. vivax.

The life cycle of mosquitoes involves aquatic (egg, larva, pupa) and adult stages (see Figure 1.1). The first stage is the egg stage, where eggs are laid on standing water by adult females. The development process of eggs is temperature dependent and eggs are likely to survive low temperatures. The second stage is the larval stage. In this stage, larvae progress through several stages of growth. Their survival depends on climatic conditions and relies very much on standing water providing food in form of organic matters. After the second stage, larvae develop into pupae, the third aquatic stage. It is from this stage mosquitoes emerge as adults. In the fourth stage, emerging adult mosquitoes fly in space. Male and female adults mate rapidly after emerging from the last aquatic stage. The lifespan of males usually is shorter than that of females. After insemination, females disperse to seek a host, possibly resulting in long distance movements and a risk of host defence response. After a blood meal, females mostly remain in a sheltered place during the few days needed for the eggs to mature. Then, females seek for an oviposition site, which may result again in long distance and risky movements. Depending on the species, different sites may be used, from aquatic environments to humid places.

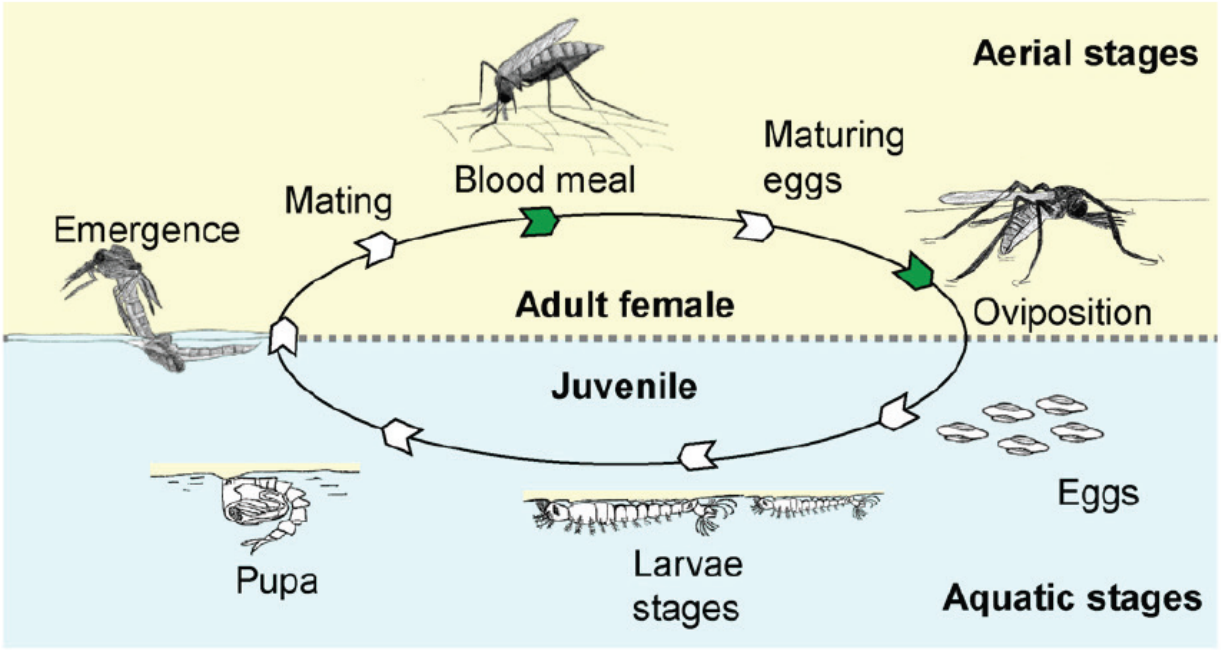

Figure 1.1: An illustration of the mosquito life cycle (P. Ezanno et al. [48])

1.1.2 Distribution of anopheles mosquitoes

Approximately 400 species of anopheles mosquitoes have been identified [95, 133] and out of these, 60 to 80 species have been implicated in malaria transmission, but only 40 are of major importance [147, 95]. In sub-saharan Africa, members of the An. gambiae complex and An. funestus complex are the most efficient vectors of P. falciparum malaria, which is the most important parasite [95]. The importance of each species in malaria transmission however varies from one region to another, as does their geographical distribution.

Mosquito distribution differs in time and space due to seasonal variations and environmental heterogeneity. In areas with favorable environmental factors such as temperature, rainfall and humidity, malaria transmission distribution is highly related to the mosquito abundance. In parts where temperature is not a limiting factor, malaria transmission is highly seasonal. Global maps on the distribution of malaria vectors highlight the present spatial variability of mosquito species across different regions (see for example Figure 1.2). In Africa, for example, An. gambiae, An. arabiensis and An. funestus are prevalent vectors that are responsible for malaria transmission. In Asia and other regions, multiple species co-exists. These differences in species across regions are mainly due to differences in climatic and environmental conditions. These conditions are critical for sustaining the production of resources needed by mosquitoes for survival and reproduction. Since mosquitoes need a variety of resources to survive and reproduce, the distribution of these resources in space affects their distribution and rate of dispersal [121]. This effect contributes to variation in local densities [16, 76, 97, 122], human exposure to vectors, and

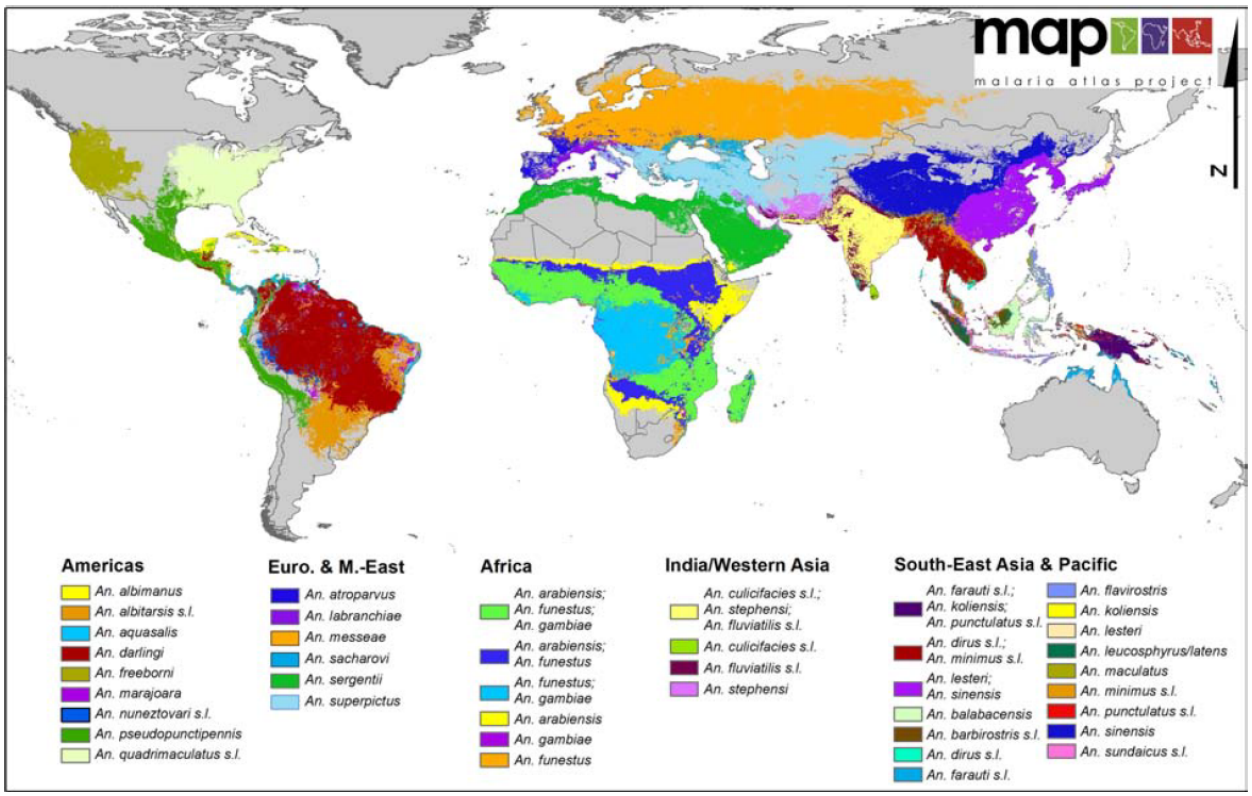

Figure 1.2: A global map of dominant malaria vector species (Sinka et al.[121])

our ability to control disease transmission.

1.1.3 Mosquito dispersal

The planning of future malaria vector control interventions requires information on the vector population, such as vector dispersal and survival. This information is important not only as determinants of the epidemiology of malaria but also for operational malaria vector control activities [71]. The dispersal of mosquito vectors-to find mates, nectar sources, resting sites, oviposition sites, and blood meals-underlies the spatial distribution of vectors, and plays a major role in shaping population structure [120]. Mosquito survivorship and dispersal ability are also critical for understanding malaria transmission risk [18].

Mosquito dispersal is the movement of mosquitoes from one location to another. Mosquito dispersal is a fundamental biological process that operates at multiple temporal and spatial scales, making it an important factor that causes uneven distribution of malaria vectors in local settings. Dispersal may lead to temporary extinction in local settings without driving the population of the whole region to extinction and this is achieved if the population in one or more locations goes to zero. Re-colonization is also possible and can be achieved subsequently through dispersal from other locations.

Studies indicate that the existence of olfactory, visual, and thermal cues play an important role in modifying mosquito flying behaviour [9, 127]. Several experiments have been performed to understand mosquito dispersal [54, 55, 56] and factors such as those

shown in Figure (1.1.3) affect mosquito dispersal at local level. Experiments from capture-

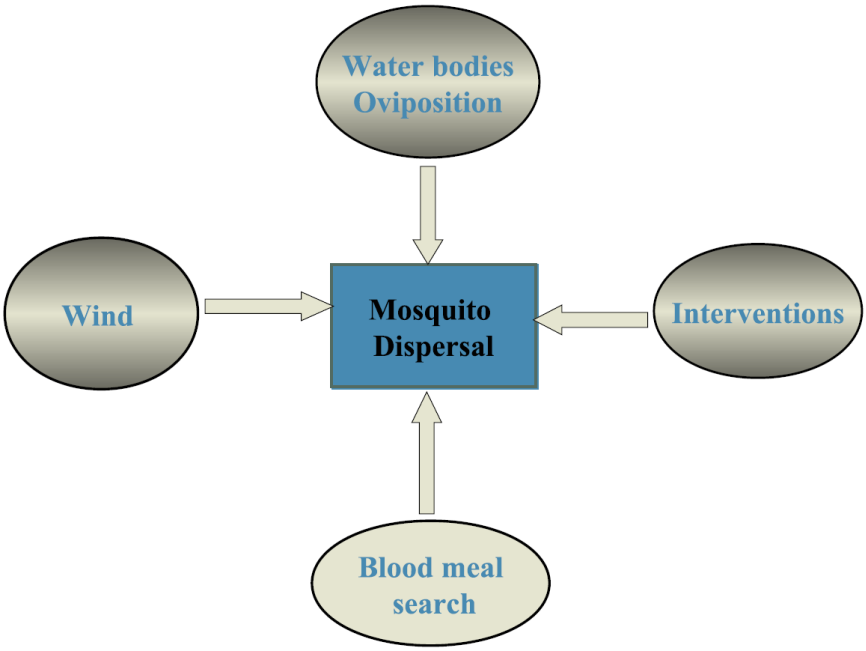

Figure 1.3: Factors affecting dispersal

mark-recapture methods have shown that mosquito dispersal distance is short and variable if driven by search for food, sheltering, and egg laying [120]. These short distances consist in few hundred meters although longer lasting flights of 1 km may be necessary if hosts and oviposition sites are widely separated. The searching strategy may depend on whether mosquitoes rely on information from neighboring areas or from places that are far apart from their present locations. The later can be incrementally achieved by movements made to neighboring locations. The dispersal can be random or unidirectional if facilitated by environmental factors such as wind [120]. Sometimes, long dispersal is likely to be facilitated by human travel.

Dispersal is also affected by vector control interventions. Interventions such as source reduction or environmental management create distances between breeding sites, affecting their spatial distribution. Several studies have shown that there is an association between distance to potential mosquito breeding sites and the variability in the Anopheline density [16] and that availability of hosts and the distribution of larval habitats has an influence on malaria vector abundance [76, 97, 122]. Some interventions divert mosquitoes without killing them (e.g. cream, lotion, soap, and gel, insect proofing of houses, sprays, coils, and local herbs) [98, 115, 118] resulting into local dispersal; others change mosquito densities (e.g. insecticide treated bed-nets) by reducing mosquito population and hence change patterns of mosquito variations among different places. This relationship has a potential effect on the spatial distribution of mosquitoes, and thus of malaria morbidity and mortality.

Mosquito dispersal is directly linked to the population density of mosquitoes, and is the driving force of heterogeneous transmission in local settings. Dispersal and its interaction

with other factors such as population density, interventions, and transmission is complex and has several implications in public health. The effect of dispersal on interventions is two fold. Interventions may appear less effective when evaluated because of mosquito movement between areas under interventions and those not under interventions [71] or may appear beneficial due to the community effects catalyzed by dispersal. The interaction between a heterogeneous environment and movement behaviour of malaria vectors is challenging, requiring different techniques to fight the disease.

1.2 Modelling population dynamics

Population dynamics is the study of the variations in a population size, its structure and/or its distribution with respect to changes in various factors such as time, space, temperature and other environmental factors. The aim of population dynamics is to identify the factors responsible for the growth or decline of a population. Further, it provides a better understanding of the underlying processes that explain how a population interacts with its surrounding environment, for instance, how individuals react to di.erent stimuli. The study of population dynamics has a wide range of useful applications. Studying the spread of a disease, for instance, helps to identify the best periods of intervention to reduce epidemiological risks [34, 172]. In mosquito management, the understanding of the mosquito population dynamics allows to develop appropriate control methods to maintain the population at a low risk level [163]. Population dynamics is also a powerful tool to predict biological invasions [113], by modelling its spreading for instance, and evaluate ecological risks.

Population dynamics can be studied following empirical or theoretical approaches. On the one hand, empirical study of population dynamics is based on observation data obtained via experimentation. A descriptive analysis can be carried out to describe the variations observed in a population in the setting of the experiment. Observation data are useful to establish the behaviour of the population, however, it is typically inherent to the experimental setting and provides very limited information on the general dynamics of a population. On the other hand, theoretical study of population dynamics allows to test various biological hypothesis difficult to assess with direct observations, in particular concerning interactions between the population and its environment, through methods of analysis such as statistical or mathematical modelling. Before going further, I recall what means a mathematical model.

1.2.1 A brief definition of a "Mathematical Model"

A model is a process through which given specific inputs (e.g. time, spatial location or temperature), and specific parameters (e.g. growth rate or dispersal rate), provides an

output which is an approximation of a variable of interest such as the population size. In the essence, a model is a representation of a reality involving some degree of approximation [6, 17, 25]). A model may help to explain natural and artificial phenomena. According to Deutsch et al. [39], other objectives are to test different scenarios and assumptions, to demonstrate that certain ideas should not or cannot be achieved, or to predict for the future. However, if all mechanisms and interactions are included, the resulting mathematical model will have a large number of variables, parameters, constraints leading to complex systems. Paraphrasing Albert Einstein, models should be as simple as possible, but not simpler. Therefore, a major challenge in modelling is to identify key parameters of the physical phenomenon that is to be modelled.

A model is built on biologically/ecologically relevant hypothesis and assumptions to provide an approximation of the population variable of interest, such as the population size, given specific inputs and parameter values. Statistical models are constructed using a specific set of observation data from which the parameter values of the model are estimated in such a way that the output of the model fits as well as possible to the data. Thus, statistical models often provide a good match to the data, but the results are limited by the fact that they are constructed and valid only for the specific setting of the experiment for which the observation data were obtained. Such a model can be used to identify correlations between different variables. However, it does not give information on why such correlations exist. Mathematical models on the other hand, are built on biological and ecological knowledge of the population dynamics, independently from specific observation data. Although the output of mathematical models is not as good in fitting observation data, they offer the possibility to change the settings and simulate various scenarios. This process allows to gain understanding on the underlying mechanisms that govern the dynamics of the population.

Formal models[1] for dynamical systems, in which the set of assumptions about reality is expressed in mathematical (mathematical model) or a computer (simulation model) language, have turned out to be especially useful. Note that not all mathematical models are accessible to mathematical analysis but that all of them can be simulated on a computer. If an analytic solution is available, this may provide a complete characterization of the system dynamics. Many simulation models cannot be described in a coherent mathematical framework in such a way that they become accessible to an analytical mathematical analysis[2]. Those models are to be assessed by means of statistical analysis of large numbers of simulation runs. The choice of a model approach depends on the characteristics of the dynamical system itself and on the aspects of the dynamical system that are emphasized

[1] In contrast to physical models, and pure semantic models, which are mainly used in psychology and social sciences.

[2] For example, agent-based models and models in the framework of artificial life research (Deutsch et al. (2005) [39])

according to the model's purpose [13, 39]. Therefore, interdisciplinary approaches are essential because those who are experts on the structure of the particular application have to work together with those who are experts on the structure of the mathematical modelling approaches. This is particularly true for the designing of ecological/biological systems models, which requires both experimental and mathematical knowledge [39].

In this thesis, I will focus on mathematical models. According to Cobelli et al. [25] a mathematical model is a representation of reality that is expressed in the form of mathematical equations. The process of developing a mathematical model is termed mathematical modeling. Mathematical models are used in many disciplines: natural sciences (such as physics, biology, ecology, meteorology), engineering (such as computer science, artificial intelligence), and social sciences (such as economics, psychology, sociology, political science).

Generally, mathematical modelling is divided into six steps forming a loop as shown in figure 1.2.1. Step 1 Observation of the physical phenomenon (static/dynamic). Step 2 Formulation of hypotheses (formalisation and writing of the mathematical model). Step 3 Mathematical analysis (theory and results). Step 4 Parameter values specification Step 5 Numerical simulations and predictions. Step 6 Testing hypotheses formalised (confirmation/refutation). This last step requires a return to step 1 and possibly the modification of some hypotheses.

Modelling is a useful tool to improve our understanding on the interactions between the population and its environment. Through simulations, modelling enables to vary the parameters and identify the factors of importance in the variation of a population. In the following, we discuss how heterogeneity in a population can be handled considering structured population models. Then, we give an overview on models incorporating the space and time variables, which represent the major interest in this thesis.

1.2.2 Structured population models

Individuals of a population can contribute significantly and differently to the dynamics of the population depending on different aspects, such as their age, stage of development, epidemiological state, spatial position, etc. After we will refer to such aspects as structuring variables. In order to obtain a meaningful model, we structure the population to take into account the heterogeneity of the individual with respect to the mentioned-above aspects. If the structuring variable is discrete assuming a finite number of distinct states, then the model is formulated via a system of equations for which each equation accounts for the dynamics of the population in each state of the structuring variable. Typically the different distinct states are referred to compartments, and the resulting model is called a compartmental model. For example, insects have distinct stages of development, eggs, larvae, pupae and adults, with specific duration, survival rates, exposure to predation,

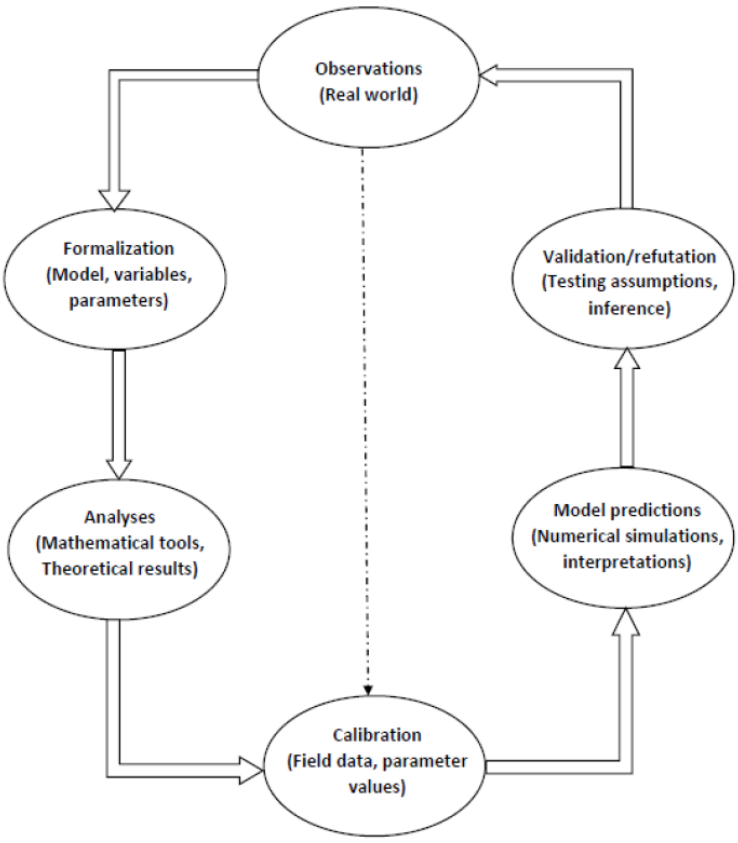

Figure 1.4: An elementary modelling methodology (adapted from Carson and Cobelli (2001)).

behaviour, displacement ranges, etc.

A compartmental model can be discrete or continuous with respect to the time variable. In the discrete case, the state of the population is approximated at specific times $t_0, t_1, \ldots, t_K$, using a relation of the form

$$\mathbf{N}_{k+1} = \mathbf{f}(\mathbf{N}_k), \quad k\{0, 1, \ldots, K\},$$

where $\mathbf{N}_k$ is the vector of each compartments of the population at time t_k and $\mathbf{f}$ is a vector functions which describes the dynamics of each compartment (i.e. demography, interactions between the compartments, etc.).

When the time-variable is continuous, then the state of the population at time t is approximated by a continuous and differentiable vector function $\mathbf{N}(t) \in \mathbb{R}^n$. The resulting model is a system of ODEs formulated as follows

$$\begin{cases} \frac{dN_1}{dt} &= \phi_1(t, N_1, \ldots, N_n), \\ \vdots & \\ \frac{dN_n}{dt} &= \phi_n(t, N_1, \ldots, N_n), \end{cases} \tag{1.1}$$

or equivalently

$$\frac{d\mathbf{N}(t)}{dt} = \phi(\mathbf{N}(t)),$$

where ϕ is a continuous vector function. Each differential equation of (1.1) describes the temporal growth of a specific (homogeneous) compartment and can be modelled using standard temporal population models (exponential, logistic, etc.) and functional and numerical responses.

The model presented in Chapter 3 is of the form of (1.1) and aims at characterizing the asymptotic behavior of this system for some nonlinear birth functions.

1.2.3 Spatio-temporal models

The growth of a population is strongly correlated to its geographic distribution range [74]. A spatio-temporal population model is a structured population model that governs the dynamics a population with respect to changes in time and space. In addition the spatial component makes possible to model population dynamics with more realism taking into account interactions between a species and its habitat. Adding spatial information however makes the model more complex rendering its study more difficult, and simulations more computationally intensive. Therefore a trade-off between the realism of the model and the question it is meant to answer must be kept in mind for its conception. A distinction that can be made among characteristics of spatio-temporal models is on the discrete or continuous nature of the space variable. In discrete-space models, the space is divided in separate areas with an index referring to its position, while continuous-space models use the spatial coordinates of each location. The choice of the model depends on the population as well as on the aim of the model. We now give some examples of commonly used models with applications.

1.2.3.1 Metapopulation models

When the space variable is taken into account implicitly, temporal models at specific locations can be constructed with location-specific parameters and interactions between them, while in the explicit case, the model incorporates a space variable. This is the case of metapopulation models, first formulated by R. Levin in 1969, where the space is discretized in distinct patches with their own specificities on which temporal dynamics are described [59, 60]. The spatio-temporal model is then a coupling of the temporal models on each of the patches with interactions between them. Metapopulation models are discrete in space and continuous in time and are formulated mathematically by ODE or Difference Equations. Considering the migration of populations from a patch i to a patch j, $i, j = 1, 2, \ldots, n$, equation of the population in patch i is given as follows :

$$\frac{du_i(t)}{dt} = f_i(t, u_i) - \left(\sum_{j=1, j\neq i}^{n} m_{ji} \right) u_i(t) + \sum_{j=1, j\neq i}^{n} m_{ij} u_j(t),$$

where $u_i(t)$ represents the population density at time t in patch i, the parameters m_{ji} and m_{ji} are the transfer rate from patch i to patch j, $i \neq j$. The function f is the reaction term.

Metapopulation models have been used, for example, to study host-parasit interactions in patchy environments [61]. They have also been used to study the spread of Malaria in a vector-host population structured according to its infectious state [4, 5]. Another example of application of metapopulation model is to model the dynamics of disease-transmitting vectors in a patchy environment [106].

1.2.3.2 Reaction-Advection-Diffusion models

In the prospect of modelling mosquito population dynamics, a particular attention is given to Reaction-Advection-Diffusion (RAD) models governed by PDEs. These are deterministic mass-interaction models continuous in time and space, thus they account for an average behaviour of the population. In RAD models, the diffusion process accounts for the random dispersal of the individuals of the population, without considering any sort of stimulus to direct their movements [35, 112]. The advection process accounts for directional displacements due to a flow, like wind transport, or attractiveness to a point (feeding site, breeding site, attractive traps...). Finally the reaction process governs the demography. In addition, in order to account for some heterogeneity within the population, the individuals can be grouped according to their age class or development stage. In this case the models becomes a system of coupled RAD equations where the reaction process also accounts for interactions between the different compartments.

RAD models are continuous in space (x) and time (t) and are formulated in terms of partial differential equations. The general form of a RAD equation is given as follows :

$$\frac{\partial u(t,x)}{\partial t} = D\frac{\partial^2 u(t,x)}{\partial x^2} - a\frac{\partial u(t,x)}{\partial x} + f(u(t,x)),$$

where $u(t,x)$ represents the population density at time t and position x, the parameters D and a are respectively the diffusion rate and the advection force, and the function f is the reaction term.

The population RAD models can be derived from random walk processes at the individual level using Taylor's expansions. This derivation is detailed in several publications [10, 107]. Alternatively, it is worth mentioning that the diffusion processes can also be derived using flux considerations instead of random walk processes [44]. In the latter case, the derivation is based on the physics conservation law and the Fick's law of diffusion which connects fluxes of particles to their gradient [29]. The derivation of models from individual level to the population level is a challenge of its own as the dynamics of the individuals are typically more complicated than a simple non-isotropic random walk.

RAD models are particularly useful to study insect dispersal [42, 126, 158, 132] and biological invasion processes. In addition, dispersal abilities of insects is an essential

information to plan efficient control of disease vectors and/or prevent biological invasions. RAD models can be studied analytically to obtain biologically relevant results. For instance, in some cases, we can obtain equilibrium solutions that describe the spatial distribution of the organism as time approaches infinity. Such results are very useful to understand the interaction between spatial heterogeneity and movement, and/or to determine areas where the organisms are most likely to establish. Some theoretical background useful for the mathematical study of RAD models is provided in chapter 3 section 3.3.

1.3 Some mathematical models of mosquito dynamics

In this section, we recall some mathematical models developed for mosquito dynamics. Mosquito models rely on several formalisms that include ordinary differential equations (ODE), partial differential equations (PDE), stochastic differential equations (SDE), etc. Generally, the choice of a modelling formalism is motivated by sake of simplicity and/or realism and/or mathematical tractability.

1.3.1 Mathematical modelling of mosquito dynamics without dispersal

The simplest dynamical population models of mosquitoes and other insect populations are based on ordinary differential equations (ODEs). These are essentially non-spatial dynamical systems, in which the dynamical variables represent the sizes or densities of various sub-populations of the insect species (e.g. eggs, larvae, mature females), tracked by cohort, with the rates of transition between these sub-populations at each step time defined by means of dynamical equations. These equations may be extremely complex, involving many separate biological and physical processes, and are generally dependent on parameters that represent characteristics of the insects (e.g. oviposition rate, mortality) and the habitat (e.g. temperature, number and type of available oviposition sites, predation). The parameters may vary both seasonally and stochastically, though the population dynamics themselves are otherwise intrinsically deterministic [109]. Several models using a system of ordinary differential equations (ODEs) have been proposed to depict and understand mosquito dynamics. In this subsection, we summarize some well known mosquito models in the literature. Some of them are due to the works in [46, 105, 104, 131, 15, 2, 48, 1, 108].

1.3.1.1 The L. Esteva et al. (2005) model [46]

Esteva et al. [46] proposed a mathematical model to assess the effectiveness of the Sterile Insect Technique (SIT) applied to mosquito population. They considered the following compartments : the immature phase of the insects (A), females before mating (I), mating fertilized females (F), mating unfertilized females (U), male insects (M) and sterile

insects (M_T). Their model was given by the following system of ODE :

$$\begin{cases} A' &= \phi\left(1-\frac{A}{C}\right)F-(\gamma+\mu_A)A, \\ I' &= r\gamma A-\frac{\beta MI}{M+M_T}-\frac{\beta_T M_T I}{M+M_T}-\mu_I I, \\ F' &= \frac{\beta MI}{M+M_T}-\mu_F F, \\ U' &= \frac{\beta_T M_T I}{M+M_T}-\mu_U U, \\ M' &= (1-r)\gamma A-\mu_M M, \\ M_T' &= \alpha-\mu_T M_T. \end{cases} \tag{1.2}$$

In order to evaluate the effectiveness of the application of both SIT and insecticide to mosquito population, Thomé et al. [131] used optimal control theory on model (1.7). Their purpose was to find the minimal effort necessary to reduce the fertile female mosquitoes considering the cost of insecticide application, the cost of the production of irradiated mosquitoes and the social cost.

1.3.1.2 The Ngwa et al. (2006, 2010) models [104, 105]

Given that the dynamics of indirectly transmitted infectious diseases of humans is driven, in the most part, by the human biting rate of the vector and based on the idea that the mosquito has a human biting habit, Ngwa et al. [104] derived and studied a simple model for the dynamics of the human malaria vector. One of their objectives was to analyse carefully the dynamics of the human-vector interaction and how this interaction could drive the population dynamics of the vector. In their model, the density of the total mosquito population is divided into three compartments based on the physiological status of the mosquito, namely : (i) the class U, comprising fertilized, well nourished with blood and reproducing female vectors ; (ii) the class W, comprising fertilized but non-reproducing vectors that have left the breeding site and are questing for a blood meal and (iii) the class V, comprising all previously fertilized females at the breeding site that have just laid their eggs but are still resting at the breeding site together with all unfertilized females that are not fed with blood and are not questing for blood but are swarming at the breeding site. In this case, the vector population dynamics in a uniform environment, that may be regarded as a single human habitat site and single vector breeding site, is represented by the following nonlinear system of delay differential equations :

$$\begin{cases} \frac{dU}{dt} &= p\tau HW-(a+\mu)U, \\ \frac{dV}{dt} &= aB(U(t-T))U(t-T)e^{-\mu_e T}+aU-\left(\mu+\frac{bH}{H+K}\right)V, \\ \frac{dW}{dt} &= \left(\frac{bH}{H+K}\right)V-(\mu+\tau H)W, \end{cases} \tag{1.3}$$

where $B(U)$ is the per capita birth rate per reproducing vector of the type U. The function $B : [0, \infty) \longrightarrow \mathbb{R}$, $U \mapsto B(U)$ is assumed to be a non-negative strictly monotone decreasing, continuously-differentiable function. The functional form $B(U) = B_0\left(1 - \frac{U}{L}\right)$ was used there and is commonly know in the literature as the Verhulst-Pearl logistic. The previous model (1.3) originally derived in Ngwa et al. [105] subjected to two birth rate functions :

- the Verhulst-Pearl logistic growth $B(U) = B_0\left(1 - \frac{U}{L}\right)$;
- the Maynard-Smith-Slatkin function $B(U) = \dfrac{B_0}{1 + \left(\frac{U}{L}\right)^n}$, $n > 0$.

The objectives in Ngwa et al. [105] was to : (1) extend the theoretical results of the model (1.3) and (2) study the problem of a suitable functional form for the birth rate function in the population dynamics of mosquitoes.

1.3.1.3 The P. Cailly et al. (2012) model [15]

In order to (1) predict mosquito abundance over several years, (2) identify the main determinants of mosquito population dynamics and (3) assess mosquito control strategies, P. Cailly et al. [15] proposed a general model representing all of the steps of the mosquito life cycle. Ten different stages were considered: 3 aquatic stages (eggs (E), larvae (L), pupae (P)), 1 emerging adult stage (A_{em}), 3 nulliparous stages (A_{1h}, A_{1g}, A_{1o}), and 3 parous stages (A_{2h}, A_{2g}, A_{2o}). Parous females are females that have oviposited at least once, thus including multiparous females. Adults were subdivided regarding their behaviour during the gonotrophic cycle (host-seeking (h), transition from engorged to gravid (g), oviposition site seeking (o)). Their model was based on two systems of ordinary differential equations (ODE), one for the favorable period, during which mosquitoes are active given by

$$\left\{\begin{array}{rcl}
\dot{E} &=& \gamma_{A_o}(\beta_1 A_{1o} + \beta_2 A_{2o}) - (\mu_E + f_E)E, \\
\dot{L} &=& f_E E - (m_L(1 + L/\kappa_L) + f_L)L, \\
\dot{P} &=& f_L L - (m_P + f_P)P, \\
\dot{A}_{em} &=& f_P P \sigma \exp(-\mu_{em}(1 + P/\kappa_P)) - (m_A + \gamma_{A_{em}})A_{em}, \\
\dot{A}_{1h} &=& \gamma_{A_{em}} A_{em} - (m_A + \mu_r + \gamma_{Ah})A_{1h}, \\
\dot{A}_{1g} &=& \gamma_{Ah} A_{1h} - (m_A + f_{Ag})A_{1g}, \\
\dot{A}_{1o} &=& f_{Ag} A_{1g} - (m_A + \mu_r + \gamma_{Ao})A_{1o}, \\
\dot{A}_{2h} &=& \gamma_{Ao}(A_{1o} + A_{2o}) - (m_A + \mu_r + \gamma_{Ah})A_{2h}, \\
\dot{A}_{2g} &=& \gamma_{Ah} A_{2h} - (m_A + f_{Ag})A_{2g}, \\
\dot{A}_{2o} &=& f_{Ag} A_{2g} - (m_A + \mu_r + \gamma_{Ao})A_{2o},
\end{array}\right. \tag{1.4}$$

and one for the unfavorable period, during which diapause occurs given by

$$\begin{cases} \dot{X} &= -Xm_X, \quad \text{for} \quad X \in \{L, P, A_{2h}, A_{2g}, A_{2o}\}, \\ \dot{E} &= -\mu_E E, \\ \dot{A}_{em} &= -(m_A^{dia} + \gamma_{A_{em}})A_{em}, \\ \dot{A}_1 &= \gamma_{A_{em}} A_{em} - m_A^{dia} A_1 \quad \text{with} \quad A_1 = A_{1h} + A_{1g} + A_{1o}. \end{cases} \tag{1.5}$$

Ezanno et al. [48] used and modified the framework proposed by Cailly et al. [15] via the model (1.4) to identify some principal drivers of mosquito population dynamics.

1.3.1.4 The Anguelov-Dumont-Lubuma (2012) models [2]

Anguelov et al. [2] proposed simple mathematical models in which the first model governs the dynamics of anopheles mosquito while the second model deals with the interaction between treated males and wild anopheles. Their purpose was to analyse the impact of the SIT as a measure for the control of the anopheles mosquito population. This model was developed according to the life cycle of a mosquito, which consists of two main stages : aquatic (egg, larvae, pupa) and adult. After emergence from pupa, a female mosquito needs to mate and get a blood meal before it starts laying eggs. Then, the classical Anguelov et al. model is given by the following system

$$\begin{cases} \dot{A} &= \Phi F - (\gamma + \mu_1 + \mu_2 A)A, \\ \dot{Y} &= r\gamma A - (\beta + \mu_Y)Y, \\ \dot{M} &= (1-r)\gamma A - \mu_M M, \\ \dot{F} &= \beta Y - \mu_F F, \end{cases} \tag{1.6}$$

where the population of mosquitoes is divided into the following compartments: population in aquatic stage A; young female not yet laying eggs Y; fertilized and eggs laying females F and males M. Note that in this model, the eggs are laid (at a constant rate ϕ) in the so-called gonotrophic cycle, which consists of taking blood meal, maturation of the eggs and oviposition. Here, the population of aquatic stage was restricted by a density dependent death rate in a different way as in Esteva et al. [46] where this population was restricted by an carrying capacity beyond which no eggs are laid.

In order to take into account of the interaction between treated males and wild anopheles and extend the theoretical results in Esteva et al. [46], the authors modified the model (1.6) and obtained the following SIT model

$$\begin{cases} \dot{A} &= \Phi F - (\gamma + \mu_1 + \mu_2 A)A, \\ \dot{Y} &= r\gamma A - (\beta + \mu_Y)Y, \\ \dot{F} &= \frac{\beta M}{M+M_T} Y - \mu_F F, \\ \dot{U} &= \frac{\beta M_T}{M+M_T} Y - \mu_U U, \\ \dot{M} &= (1-r)\gamma A - \mu_M M, \\ \dot{M}_T &= pq\psi - \mu_T M_T. \end{cases} \tag{1.7}$$

1.3.1.5 The Abdelrazec-Gumel (2017) model [1]

Extending the models of Ngwa et al. [105, 104] by adding the aquatic stages of the mosquito, in order to assess the effect of temperature and rainfall on mosquito abundance, Abdelrazec et al. [1] proposed a stage-structured non-autonomous model. Their model which splits the total mosquito population at time t into mutually exclusive compartments of eggs ($E(t)$), larvae ($L(t)$), pupae ($P(t)$) and female adult mosquitoes ($M(t)$), is given by the following deterministic, non-autonomous system of nonlinear differential equations :

$$\begin{cases} \dot{E} &= MB(M) - [F_E(T,R) + \mu_E(T,R)]E(t), \\ \dot{L} &= F_E E - [F_L(T,R) + \mu_L(T,R) + \delta_L L]L, \\ \dot{P} &= F_L(T,R)L - [F_P(T,R) + \mu_P(T,R)]P, \\ \dot{M} &= \sigma F_P(T,R)P - \mu_M(T)M, \end{cases} \tag{1.8}$$

where $T = T(t)$ and $R = R(t)$ represent temperature and rainfall respectively. The two following functional forms of $B(M)$ were considered in this study, namely :

- the Verhulst-Pearl logistic growth B_L : $B(U) = B_0\left(1 - \frac{U}{L}\right)$;
- the Maynard-Smith-Slatkin function B_S : $B(U) = \frac{B_0}{1 + \left(\frac{U}{L}\right)^n}$, $n > 0$.

1.3.1.6 The Okuneye et al. (2018) model [108]

In order to design a new temperature and rainfall dependent mosquito population model, Okuneye et al. [108] extended the Abdelrazec et al. [1] model's by incorporating four stages for larval development and three different dispersal states (questing for blood meal, fertilized and resting at breeding site) of female adult mosquitoes. Their model, which takes into consideration the human-vector interaction, splits the total immature mosquito population into compartments for eggs (E), four larval stages (L_i, $i = 1,2,3,4$), and pupae (P). To account for the gonotrophic cycle, the population of adult female anopheles mosquitoes was sub-divided into compartments for the class of unfertilized female vectors not questing for blood meal and fertilized female mosquitoes that have laid eggs at the mosquito breeding site (V), the class of fertilized but not producing, female mosquitoes questing for blood meal (W), and the class of fertilized, well-nourished with blood, and reproducing female mosquitoes (U). The Okuneye et al. model is given by the following

deterministic system of nonlinear differential equations.

$$\begin{cases} \frac{dE}{dt} &= \psi_U(T)\left(1-\frac{U}{K_U}\right)U - (\sigma_E(R,T)+\mu_E(T))E, \\ \frac{dL_1}{dt} &= \sigma_E(R,T)E - [\xi_1(R,T)+\mu_L(T)+\delta_L]L_1, \\ \frac{dL_i}{dt} &= \xi_{(i-1)}(R,T)L_{(i-1)} - [\xi_i(R,T)+\mu_L(T)+\delta_L]L_i, \quad i=2,3,4, \\ \frac{dP}{dt} &= \xi_4(R,T)L_4 - [\sigma_P(R,T)+\mu_P(T)]P, \\ \frac{dV}{dt} &= \sigma_P(R,T)P + \gamma_U U - \frac{\eta_V H}{H+F}V - \mu_A(T)V, \\ \frac{dW}{dt} &= \frac{\eta_V H}{H+F}V - [\tau_W H + \mu_A(T)]W, \\ \frac{dU}{dt} &= \alpha\tau_W HW - [\gamma_U + \mu_A(T)]U, \end{cases} \tag{1.9}$$

with $L = L_1 + L_2 + L_3 + L_4$, $R = R(t)$ and $T = T(t)$.

1.3.2 Mathematical modelling of mosquito dynamics with dispersal

The spatial distribution of mosquitoes has shown great potential to affect malaria transmission intensity. The success of some methods for controlling mosquito population is based on taking into account of mosquitoes dispersal ([30, 42]). Mathematical models play an important role in understanding and providing solutions to phenomena which are difficult to measure in the field, but few models have incorporated dispersal or heterogeneity when modelling resource availability. Recently, the spatio-temporal dynamics of mosquito populations have been particularly focused on, either using spatially explicit simulation models [111, 85, 154, 110], or plume models [30]. Some spatial models have used discrete-space continuous-time approach based on ordinary differential equations (ODEs) while another spatial models have used the diffusion approach based on partial differential equations (PDEs), which considers space as a continuous variable. In this subsection, we summarize some well know mosquito models in the literature. Some of them are due to the works in [106, 83, 42, 70, 126, 158, 132, 161].

1.3.2.1 The Nourridine et al. (2011) model [106]

Extending the Ngwa et al. [104] model by including more than one vector-breeding site and more than one host habitat, Nourridine et al. [106] presented and analyzed a deterministic model with spatial consideration for a class of human disease-transmitting vectors. Their goal was to understand how variation in the number of human habitats or variation in the number of breeding sites enhances or affects the interaction between the vector habitat or breeding sites and the host habitat dynamics and how this ultimately affects the dynamics and existence of the vector populations. Their basic model divides the entire vector population into three compartmental classes representing physiological status. These classes are: the class of fed and $reproducing$ vectors returning from human habitats to vector-breeding sites represented by the variable U ; the class of $unfed$ and $resting$ vectors present at vector-breeding sites represented by the variable V ; and the

class of $unfed$ vectors $questing$ (or $foraging$) for food (blood meal) in human habitats represented by the variable W. Each class of vectors is again subdivided into subclasses representing spatial locations. Assuming that there are M human habitats x_i, $i = 1, \cdots, M$ and N vector-breeding sites y_j, $j = 1, \cdots, N$, then the classes of vectors U, V and W are subdivided into subclasses U_i, V_j and W_i, $i = 1, \cdots, M$, $j = 1, \cdots, N$, respectively, where U_i's represents fed vectors returning from location x_i, W_i's represent unfed vectors foraging for food at location x_i and V_j's are unfed and resting vectors resting at the vector-breeding site y_j. Let the density of human population at habitat x_i be $H_i(t)$, then the Nourridine et al. model was given by the following discrete-space-continuous-time mathematical model (metapopulation model) :

$$\begin{cases} \frac{dH_i(t)}{dt} &= C_i - \sum\limits_{j=1, j\neq i}^{M} w_{ij} H_i(t) + \sum\limits_{j=1, j\neq i}^{M} w_{ji} H_j(t) - \mu_{H_i} H_i(t), \quad i = 1, \cdots, M; \\ \frac{dV_j(t)}{dt} &= \sum\limits_{i=1}^{M} a_{ij} \lambda(U_i(t-T)) U_i(t-T) e^{-\mu_e T} - \left(\mu_{V_j} + \sum\limits_{i=1}^{M} b_{ij}\right) V_j(t) \\ &\quad + \sum\limits_{i=1}^{M} a_{ij} U_i(t), \quad j = 1, \cdots, N; \\ \frac{dW_i(t)}{dt} &= \sum\limits_{j=1}^{N} b_{ji} V_j(t) - (\tau_i + \mu_{W_i}) W_i(t), \quad i = 1, \cdots, M; \\ \frac{dU_i(t)}{dt} &= p\tau_i W_i(t) - \left(\mu_{U_i} + \sum\limits_{j=1}^{N} a_{ij}\right) U_i(t), \quad i = 1, \cdots, M, \end{cases} \tag{1.10}$$

where $\lambda : [0, \infty) \to \mathbb{R}$ is a suitable birth rate function for the vectors of type U.

1.3.2.2 The Lutambi et al. (2013) model [83]

Lutambi et al. [83] developed and simulated a discrete-space-continuous-time mathematical model to estimate mosquito dispersal distances and to evaluate the effect of spatial repellents as a vector control strategy. On the one hand, they have developed the following system of differential equations to describe mosquito dynamics without movement :

$$\begin{cases} \frac{dE}{dt} &= b\rho_{A_o} A_o - (\mu_E + \rho_E) E, \\ \frac{dL}{dt} &= \rho_E E - (\mu_{L_1} + \mu_{L_2} L + \rho_L) L, \\ \frac{dP}{dt} &= \rho_L L - (\mu_P + \rho_P) P, \\ \frac{dA_h}{dt} &= \rho_P P + \rho_{A_o} A_o - (\mu_{A_h} + \rho_{A_h}) A_h, \\ \frac{dA_r}{dt} &= \rho_{A_h} A_h - (\mu_{A_r} + \rho_{A_r}) A_r, \\ \frac{dA_o}{dt} &= \rho_{A_r} A_r - (\mu_{A_o} + \rho_{A_o}) A_o, \end{cases} \tag{1.11}$$

which consider six compartments of the mosquito life cycle : eggs (E), larvae (L), pupal (P), host seeking adults (A_h), resting adults (A_r) and oviposition site seeking adults (A_o).

On the other hand, by considering a set of discrete patches and allowing to host seeking and oviposition site searching mosquitoes to move between patches, the model (1.11) was extended in a metapopulation model which incorporate dispersal processes. Then, they

combined the system of equations (1.11) for patch (i, j) and the movement terms

$$\frac{dX_{(i,j)}}{dt} = \left(\sum_{\xi' \in N(i,j)} \beta^H_{\xi'/(i,j)} X_{\xi'}\right) - \left(\sum_{\xi' \in N(i,j)} \beta^H_{(i,j)/\xi'} X_{(i,j)}\right), \quad X \equiv A_h, A_o$$

to form the following system of equations :

$$\begin{cases}
\frac{dE_{(i,j)}}{dt} &= b_{(i,j)}\psi^B_{(i,j)}\rho_{A_o(i,j)}A_{o(i,j)} - (\mu_{E(i,j)} + \rho_{E(i,j)})E_{(i,j)}, \\
\frac{dL_{(i,j)}}{dt} &= \rho_{E(i,j)}E_{(i,j)} - (\mu_{L_1(i,j)} + \mu_{L_2(i,j)}L_{(i,j)} + \rho_{L(i,j)})L_{(i,j)}, \\
\frac{dP_{(i,j)}}{dt} &= \rho_{L(i,j)}L_{(i,j)} - (\mu_{P(i,j)} + \rho_{P(i,j)})P_{(i,j)}, \\
\frac{dA_{h(i,j)}}{dt} &= \rho_{P(i,j)}P_{(i,j)} + \psi^B_{(i,j)}\rho_{A_o(i,j)}A_{o(i,j)} - (\mu_{A_h(i,j)} + \psi^H_{(i,j)}\rho_{A_h(i,j)})A_{h(i,j)} \\
&\quad -\left(\sum_{\xi' \in N(i,j)} \beta^H_{(i,j)/\xi'}\right)A_{h(i,j)} + \left(\sum_{\xi' \in N(i,j)} \beta^H_{\xi'/(i,j)}A_{h\xi'}\right), \\
\frac{dA_{r(i,j)}}{dt} &= \psi^H_{(i,j)}\rho_{A_h(i,j)}A_{h(i,j)} - (\mu_{A_r(i,j)} + \rho_{A_r(i,j)})A_{r(i,j)}, \\
\frac{dA_{o(i,j)}}{dt} &= \rho_{A_r(i,j)}A_{r(i,j)} - (\mu_{A_o(i,j)} + \psi^B_{(i,j)}\rho_{A_o(i,j)})A_{o(i,j)} \\
&\quad -\left(\sum_{\xi' \in N(i,j)} \beta^H_{(i,j)/\xi'}\right)A_{o(i,j)} + \left(\sum_{\xi' \in N(i,j)} \beta^H_{\xi'/(i,j)}A_{o\xi'}\right).
\end{cases} \tag{1.12}$$

1.3.2.3 The Dufourd-Dumont (2013) model [42]

Dufourd et al. [42] developed a mathematical model to simulate the spread of mosquito aedes albopictus taking into account the environment parameters such as wind, temperature and landscape. Their purpose was to investigate the use of sterile insect technique (SIT) which introduces a large number of sterile insects in the environment. Their model, combining ordinary differential equations (ODEs) for the mosquito population and partial differential equation (PDE) for the dispersion of the population, is given by the following system :

$$\begin{cases}
\frac{\partial u_A}{\partial t} &= N_{Egg}\left(1 - \frac{u_A}{K}\right)\mathbf{1}_b u_b(x,t) - (\eta_A + M_A)u_A, \\
\frac{\partial u_Y}{\partial t} &= \nabla(D\nabla u_Y) + V\nabla u_Y - (M_Y + \beta_Y)u_Y + r\eta_A u_A, \\
\frac{\partial u_f}{\partial t} &= \nabla(D\nabla u_f) + V\nabla u_f - \nabla(\nabla C_f(x)u_f) - (M_f + \mu_{fr}\mathbf{1}_f)u_f + u_{bf}\mathbf{1}_b u_b + \beta_Y\left(\frac{u_M + \lambda_s f_s u_{Ms}}{u_M + u_{Ms}}\right)u_Y, \\
\frac{\partial u_r}{\partial t} &= \nabla(D\nabla u_r) + V\nabla u_r - (M_f + \mu_{rb})u_r + \mu_{fr}\mathbf{1}_f u_f, \\
\frac{\partial u_b}{\partial t} &= \nabla(D\nabla u_b) + V\nabla u_b - \nabla(\nabla C_b(x)u_b) - (M_f + \mu_{bf}\mathbf{1}_b)u_b + u_{rb}u_r, \\
\frac{\partial u_M}{\partial t} &= \nabla(D\nabla u_M) + V\nabla u_M - \nabla(\nabla C_f(x)u_M) - \nabla(\nabla C_b(x)u_M) - M_m u_M + (1-r)\eta_A u_A, \\
\frac{\partial u_{Ms}}{\partial t} &= \nabla(D\nabla u_{Ms}) + V\nabla u_{Ms} - \nabla(\nabla C_f(x)u_{Ms}) - \nabla(\nabla C_b(x)u_{Ms}) - M_{ms}u_{Ms}, \\
u_A(x,0) &= u_{A_0}(x), \quad x \in \Omega, \\
u_X(x,0) &= 0, \quad x \in \Omega \text{ with } X \in \{Y, f, b, M, Ms\}, \\
(-D\nabla u_X &+ Vu_X) \cdot n_{in} = 0, \quad \forall x \in \partial\Omega_{in}, \text{ and } t > 0, \text{ with } X \in \{Y, f, b, M, Ms\}, \\
\nabla u_X \cdot n_{out} &= 0, \quad \forall x \in \partial\Omega_{out}, \text{ and } t > 0, \text{ with } X \in \{Y, f, b, M, Ms\}.
\end{cases} \tag{1.13}$$

In this model, seven different compartments were considered : the aquatic stage (u_A), the immature females (u_Y), the matures females (u_f, u_r, u_b), the wild males (u_M) and the

sterilized males (u_{Ms}). This system was numerically studied using the splitting operator approach in order to test different vector control scenarios. However, it is very difficult to analytically study this system. Therefore, some simplifications are needed to investigate the asymptotic behavior and the threshold-type dynamics of this system.

1.3.2.4 The Jiang et al. (2014) model [70]

Jiang et al. [70] considered a system of partial differential equations that describes the interaction of sterile and fertile species undergoing the sterile insect release method (SIRM). Their goal was to derive sufficient conditions for success of the SIRM. The authors considered an SIRM model given by the following system of reaction-diffusion equations :

$$\begin{cases} u_t &= d_1\Delta u + u\left(\frac{a_1 u}{u+n} - a_2\right) - 2\delta u(u+n), \quad x \in \Omega, \\ n_t &= d_2\Delta n + r - a_2 n - 2\delta u(u+n) \quad x \in \Omega, \\ \frac{\partial u}{\partial \nu}\Big|_{\partial\Omega} &= \frac{\partial n}{\partial \nu}\Big|_{\partial\Omega} = 0, \quad t > 0, \\ u(x,0) &= u_0(x) > 0, \;\; n(x,0) = n_0(x) \geq 0, \quad x \in \Omega, \end{cases} \tag{1.14}$$

where $u(t,x)$ and $n(t,x)$ denote the densities of fertile and sterile females respectively. $\frac{\partial}{\partial \nu}$ is the derivative along the outward normal direction.

1.3.2.5 The Takahashi et al. (2005) [126], Yamashita et al. (2017) [158], Tian et al. (2017) [132] and Zhang et al. (2017) [161] models

Takahashi et al. [126] proposed and studied mathematical model mosquito population dispersal by wing and wind. In their attempt to simplify, they considered only two sub-populations of the mosquito : the winged form or matured females (M) and the aquatic forms (eggs, larvae and pupae) denoted by A. The following model was formulated :

$$\begin{cases} \frac{\partial}{\partial t}M(x,t) &= \frac{\partial^2}{\partial x^2}M(x,t) - \nu\frac{\partial}{\partial x}M(x,t) + \frac{\gamma}{k}A(x,t)(1 - M(x,t)) - \mu_1 M(x,t), \\ \frac{\partial}{\partial t}A(x,t) &= k(1 - A(x,t))M(x,t) - (\mu_2 + \gamma)A(x,t). \end{cases} \tag{1.15}$$

This model takes into account the vital aspects of spatial dispersal of the mosquito and, through PDE modelling which was numerically studied, they derived travelling wave solutions for their differential equations.

In the Takahashi et al. model, both invasion along the flow and against the flow scenarios were observed. However, only the first one was studied in details. Yamashita et al. [158] complemented and performed this work (through a rigorous analysis of the model (1.15)) by proving that the invasion against the flow solution also possesses a travelling wave profile.

Since mosquito invasion is an asymptotic process, the habitation of mosquitoes will change with time. In order to describe the dynamics of habitation, Tian et al. [132] assumed that the habitation has a moving free boundary and from model (1.15), they formulated the

free boundary problem as follows :

$$\begin{cases} M_t = DM_{xx} - \nu M_x + \gamma A\left(1 - \frac{M}{k_1}\right) - \mu_1 M, & t > 0, \ \ 0 < x < h(t), \\ M(t,x) = 0, & t > 0, \ \ x \geq h(t), \\ A_t = r\left(1 - \frac{A}{k_2}\right)M - (\mu_2 + \gamma)A, & t > 0, \ \ x > 0, \\ M_x(t,0) = 0, \ \ A_x(t,0) = 0, & t > 0, \\ M(t,h(t)) = 0, \ \ h'(t) = -\mu M_x(t,h(t)), & t > 0, \\ h(0) = h_0, \ \ M(0,x) = M_0(x), & x \in [0,h_0], \\ A(0,x) = A_0(x), & x \in [0,\infty), \end{cases} \tag{1.16}$$

where $M(t,x)$ is the spatial density of the winged mosquitoes at time t and space location x and $A(t,x)$ is the density of the aquatic mosquitoes.

Considering the spatial heterogeneity, based on model (1.16) in order to extend some theoretical results from the above studies, Zhang et al. [161] proposed the following reaction-diffusion-advection problem with free boundaries $x = g(t)$ and $x = h(t)$ to describe the spatial dispersal dynamics of mosquitoes :

$$\begin{cases} M_t = DM_{xx} - \nu M_x + \gamma(x)A\left(1 - \frac{M}{k_1}\right) - \mu_1(x)M, & t > 0, \ \ g(t) < x < h(t), \\ A_t = r(x)\left(1 - \frac{A}{k_2}\right)M - (\mu_2(x) + \gamma(x))A, & t > 0, \ \ g(t) < x < h(t), \\ M(t,x) = A(t,x) = 0, & t > 0, \ \ x = g(t) \ \text{ or } \ x = h(t), \\ g(0) = -h_0, \ \ g'(t) = -\mu M_x(t,g(t)), & t > 0, \\ h(0) = h_0, \ \ h'(t) = -\mu M_x(t,h(t)), & t > 0, \\ M(0,x) = M_0(x), \ \ A(0,x) = A_0(x), & -h_0 \leq x \leq h_0. \end{cases} \tag{1.17}$$

1.4 Conclusion

Altogether, there exists a very large variety of mathematical models designed to study mosquito dynamics. The modelling formalism considered by mosquito modelers included several aspects which are in agreement or not with field observations. The agreement may be also restricted to specific contexts. Moreover, even when a common mechanism of mosquito life cycle is taken into account by different authors, it remains the question of how they translated it in their model ? For example, for mosquito dispersal two modelling frameworks are found, namely, discrete-space continuous-time and continuous-space continuous-time formalisms. Of course, a modelling option has a cost. For example, a non-spatial model using a system of ODEs can lead to a gain in mathematical tractability of the model but also not capture all insights into behavior. Conversely, spatial models using a system of PDEs leads to a gain of realism but it is not always possible to carry out a deep mathematical analysis of such models due to lack of tools. In fact, using diffusion approach, many authors limited their studies to simulations and never investigated qualitative properties of the system. However the mathematical analysis is nevertheless the

essential part of mathematical modeling. Other formalism using discrete-space continuous-time framework has been proposed in [106, 83]. Although these models consider some formalisms to model mosquito dispersal, it is possible to investigate the spatial dynamics of mosquitoes using statistical mechanics of complex networks. Moreover, another formalism using diffusion approach has been proposed in [126, 42, 70, 158, 132, 161]. However, some of them do not take into account all stages of mosquito life cycle while another of them limited their studies to simulations. The aim of my work is to propose and study new spatio-temporal models for mosquito population using two different approaches (continuous and discrete) which incorporate heterogeneity.

1.5 Hypothesis and description of models

In this thesis, we are particularly interested in the spatial dynamics of anopheles mosquitoes. In order to provide a mathematical and modelling framework for the spatial distribution of diseases vectors, we use two different approaches to develop mathematical models that capture mosquito dispersal processes, namely, discrete-space and continuous-space approaches. In the first approach, we use discrete patches as a representation of space to obtain a metapopulation model (see chapter 2), while in the second approach, we use continuous-space model to obtain an advection-reaction-diffusion model (see chapter 3). These models are different from each other and they are presented below.

1.5.1 A metapopulation model for the population dynamics of anopheles mosquito

We make use of an approach based on statistical mechanics which could allow us to identify other breeding-feeding site characteristics and better explain abundance of mosquitoes. We consider the spread of anopheles mosquitoes on complex metapopulations, i.e. networks of populations connected by migratory flows which configurations are described in terms of the conditional probabilities of connections between nodes (see Figure 1.5).

Each nodes of the network represent potential breeding and feeding sites of mosquitoes, around which there are human hosts habitations. The methodology and objectives of this part are : (1) to design a complex network extension of the seminal model in [2] and (2) to analyze and simulate the metapopulation model for the dynamics of anopheles mosquito obtained. The system has four compartments : population in aquatic stage A; young female not yet laying eggs Y; fertilized and eggs laying females F and males M. Using Figure 2.2, we have been able to list some key assumptions of the metapopulation model as follows :

(A_1) The architecture of the network of patches is mathematically encoded by means of the connectivity distribution $p(k)$, where $p(k)$ is the probability that a randomly chosen

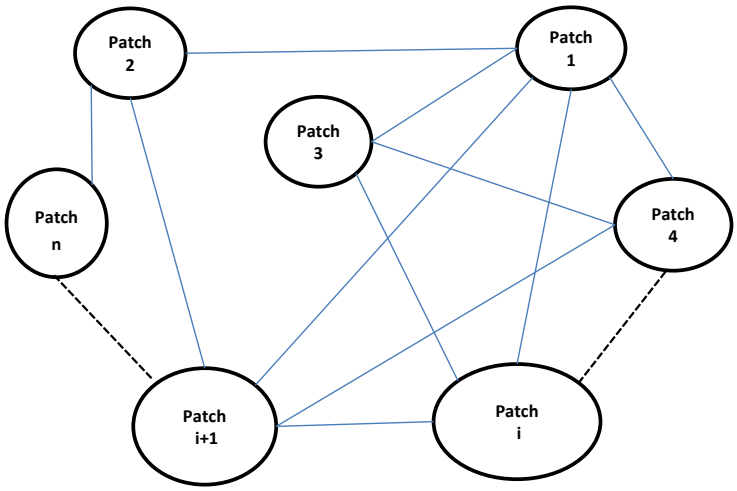

Figure 1.5: A general n-patches network for the population dynamics of anopheles mosquito between n feeding-breeding sites.

patch has degree k. The degree or connectivity of a patch is the number of links connected to this patch.

(A_2) The probability P_k of leaving a patch with degree k is given by

$$P_k = k \sum_{k'} P(k'|k) D_{kk'},$$

where $P(k'|k)$ is the conditional probability that any given edge departing from a node of degree k is pointing to a node of degree k' [27].
In this network, we assume that the degree of the nodes at the end of any given link are independent. In this case, we have

$$P(k'|k) = k' p(k')/\langle k \rangle \quad \text{with} \quad \langle k \rangle = \sum_k k p(k).$$

(A_3) The diffusion rate that mosquito move from a node with degree k to another node with degree k' is given by

$$D_{kk'} = \frac{D_i \psi(d_{kk'})}{k} e^{-\lambda(\overline{H}_k - \overline{H}_{k'})},$$

where D_i is the constant migration rate, $d_{kk'}$ is the cartesian distance between nodes of degree k and k', $\overline{H}_k$ is the proportion of hosts in patch of degree k and $\psi(d_{kk'})$ the distance function. In the case were all patches have similar characteristics, the dispersal parameter is the same for all patches and the diffusion rate is simply equal to $D_{kk'} = \frac{D_i}{k}$.

Following the aforementioned assumptions, the equations governing the spatio-temporal

evolution of anopheles mosquito are given by the system below :

$$\begin{cases} \dot{\rho}_{A,k} &= \Phi\rho_{F,k} - (\gamma + \mu_1 + \mu_2\rho_{A,k})\rho_{A,k}, \\ \dot{\rho}_{Y,k} &= r\gamma\rho_{A,k} - (\beta + \mu_Y)\rho_{Y,k} - P_k\rho_{Y,k} + k\sum_{k'} P(k'|k)D_{k'k}\rho_{Y,k'}, \\ \dot{\rho}_{M,k} &= (1-r)\gamma\rho_{A,k} - \mu_M\rho_{M,k} - P_k\rho_{M,k} + k\sum_{k'} P(k'|k)D_{k'k}\rho_{M,k'}, \\ \dot{\rho}_{F,k} &= \beta\rho_{Y,k} - \mu_F\rho_{F,k} - P_k\rho_{F,k} + k\sum_{k'} P(k'|k)D_{k'k}\rho_{F,k'}. \end{cases} \tag{1.18}$$

System (1.18) consists of three main components. The first component is the continuous-time model that describe the mosquito dynamics. The second component involves the inclusion of the spatial characteristics where the space is discretized into discrete locations to form a patches network. The third component involves the inclusion of the dispersal of adult mosquitoes, which move from one patch to another creating connections between patches. System (1.18) is fully studied in Chapter 2 in the form of the published paper M. L. Mann Manyombe et al. [88]. The advantage of the above discrete-space model is that one can easily assess diseases vector control strategies. Nevertheless, this approach constrains the modeled mosquito movements to follow a limit set of trajectories. To overcome this limitation, we use the continuous-space approach.

1.5.2 A spatio-temporal model for the population ecology of anopheles mosquito

In this part, as an alternative approach to our discrete-space model, we use a partial differential equations (PDE) model for mosquito dispersal. We develop models that incorporate both intrinsic dynamics and spatial variation of mosquitoes, taking into consideration the dynamics of the human-vector interaction. We modify some seminal models [1, 2, 68, 126, 132, 158] by taking into account all stages in the gonotrophic cycle (questing, resting and breeding females). The aquatic stage is reduced to one compartment (A), gathering eggs, larvae and pupae. The adult stage is divided into five compartments including four for females and one for males as follows: immature females (Y), feeding/questing females (Q), resting females (U), breeding females (W) (or more precisely "egg laying females") and males (M). Using Figure 1.6, we list some key assumptions of the model as follows :

(A_4) In the current model, we use a general form of the eggs oviposition function, denoted by $B(W)$. The growth function $B(W)$ depend on the environmental carrying capacity of female adult mosquitoes, which can be related to the availability of breeding sites. In Table 1.1, we have gathered typical examples of function $B(W)$, which are used in the literature.

(A_5) Based on the idea that the mosquito has a human biting habit and since the mating in the most time takes place near the feeding sites [67], questing females successfully obtain blood meals and become resting females at rate $\alpha\varphi H$, where H is the

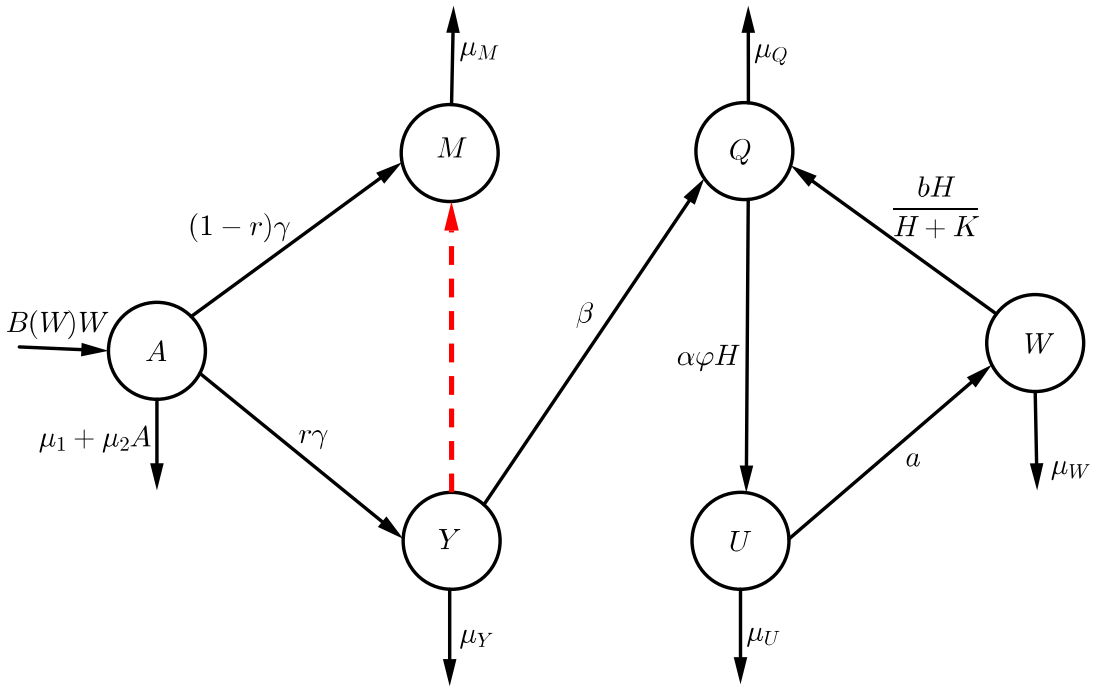

Figure 1.6: Anopheles mosquito simplified life cycle. The dashed arrow indicates the mating between male and immature female mosquitoes.

Table 1.1: Examples of oviposition function $B(W)$ used in the literature.

Names	$B(W)$	Sources
Malthus (B_M)	N_{egg}	[2, 28]
Verhulst-Pearl logistic (B_L)	$N_{egg}\left(1-\frac{W}{L}\right),\ W<L$	[1, 12, 28, 105]
Maynard-Smith-Slatkin (B_S)	$\frac{N_{egg}}{1+\left(\frac{W}{L}\right)^n},\ n>0$	[1, 12, 28, 105]
Hassell (B_H)	$\frac{N_{egg}}{\left(1+\frac{W}{L}\right)^n},\ n>0$	[12]

human population density. After rest, the vector moves to a convenient breeding site. We assume that the breeding females that enter to questing class depend on the proportion of human $\frac{bH}{H+K}$, since breeding females breed outside of the human body at a distinct spatial location, the breeding site away from the human habitat and mosquitoes can adapt their host choice in case of a lower availability of human hosts

[86].

(A_6) Based on the mosquito ability to move [42, 45, 73, 83], we have the following additional assumptions :

- We add advection terms or drift terms, denoted by $\varepsilon_Z \frac{\partial Z}{\partial x}$, $Z = Q, W$, since mosquitoes stimulated by attractants (hosts, breeding sites) move preferably in certain directions.
- We add diffusion terms denoted by $D_Z \frac{\partial^2 Z}{\partial x^2}$, $Z = Y, Q, W$, since mosquitoes not submitted to stimuli, move randomly in any direction ;
- The number of hosts is allowed to differ across the domain introducing heterogeneity. Thus, we assume that the population density of humans $H(x)$ is location-dependent.

Thus, following the aforementioned assumptions, the equations governing the temporal evolution of mosquitoes are given by the system below :

$$\begin{cases} \dot{A} &= B(W)W - [\gamma + \mu_1 + \mu_2 A]A, \\ \dot{Y} &= r\gamma A - [\mu_Y + \beta]Y, \\ \dot{M} &= (1-r)\gamma A - \mu_M M, \\ \dot{Q} &= \beta Y + \dfrac{bH}{H+K}W - [\alpha\varphi H + \mu_Q]Q, \\ \dot{U} &= \alpha\varphi HQ - [a + \mu_U]U, \\ \dot{W} &= aU - \left[\dfrac{bH}{H+K} + \mu_W\right]W, \end{cases} \tag{1.19}$$

The temporal model (1.19) is then extended into an advection-reaction-diffusion model given by the following system :

$$\begin{cases} \dfrac{\partial A}{\partial t} = B(W(t,x))W(t,x) - [\gamma + \mu_1 + \mu_2 A(t,x)]A(t,x), \\ \dfrac{\partial Y}{\partial t} = D_Y \dfrac{\partial^2 Y}{\partial x^2} + r\gamma A(t,x) - [\mu_Y + \beta]Y(t,x), \\ \dfrac{\partial M}{\partial t} = D_M \dfrac{\partial^2 M}{\partial x^2} - \varepsilon_M \dfrac{\partial M}{\partial x} + (1-r)\gamma A(t,x) - \mu_M M(t,x), \\ \dfrac{\partial Q}{\partial t} = D_Q \dfrac{\partial^2 Q}{\partial x^2} - \varepsilon_Q \dfrac{\partial Q}{\partial x} + \beta Y(t,x) + \dfrac{bH(x)}{H(x)+K(x)} W(t,x) - [\alpha\varphi H(x) + \mu_Q]Q(t,x), \\ \dfrac{\partial U}{\partial t} = \alpha\varphi H(x)Q(t,x) - [a + \mu_U]U(t,x), \\ \dfrac{\partial W}{\partial t} = D_W \dfrac{\partial^2 W}{\partial x^2} - \varepsilon_W \dfrac{\partial W}{\partial x} + aU(t,x) - \left[\dfrac{bH(x)}{H(x)+K(x)} + \mu_W\right] W(t,x), \end{cases} \tag{1.20}$$

Here $A(t,x)$, $Y(t,x)$, $Q(t,x)$, $U(t,x)$ and $W(t,x)$ measure the density of mosquitoes at location x and time t. Attractiveness is represented via an advection term taking into account blood meals, breeding sites, wind, etc. We aims to : (1) extend some stability results of the previous works [1, 108], (2) study the global well-posedness and asymptotic behavior of the solution of system (1.20) and (3) assess the impact of host heterogeneity on the spatial distribution of mosquito population in a given region. Systems (1.19) and (1.20) are fully studied in Chapter 3 in the form of the publisher paper M. L. Mann Manyombe et al. (2019)[89].

CHAPTER 2

Contents

A METAPOPULATION MODEL FOR THE POPULATION DYNAMICS OF ANOPHELES MOSQUITO

A more robust assessment of malaria control will come from a better understanding of the distribution and connectivity of breeding and blood feeding sites. Spatial heterogeneity of mosquito resources, such as hosts and breeding sites, affects mosquito dispersal behavior. The main purpose of this chapter is to develop a reaction-diffusion type model to describe the spatial evolution of the anopheles mosquito on a complex metapopulation. The novelty in our work is to make use of an approach based on statistical mechanics of complex networks, that is, networks of populations connected by migratory flows whose configurations are described in terms of connectivity distribution of nodes (patches) and the conditional probabilities of connections between nodes. We examine the impacts of vector dispersal on the persistence and extinction of a mosquito population in both homogeneous and heterogeneous landscapes. For uncorrelated networks in a homogeneous landscape, we derive an explicit formula of the basic offspring number. Using the theory of monotone operators, we obtain sufficient conditions for the global asymptotic stability of equilibria. Precisely, the value one of the basic offspring number is a forward bifurcation for the dynamics of the anopheles mosquito, with the trivial (mosquito-free) equilibrium point being globally asymptotically stable (GAS) when the basic offspring number is less than one, and one stable nontrivial (mosquito-persistent) equilibrium point being born with well determined basins of attraction when the basic offspring number is greater than one. Theoretical results are numerically supported and the impact of the migration of mosquitoes are discussed through global sensitivity analysis and numerical simulations. All the content of this chapter is based on the published paper of Mann Manyombe et al. (2017) [88].

2.1 Introduction

For long, vector-borne diseases among all infectious diseases of human beings, have

constituted a major cause of human mortality and morbidity. Even with the recent advances in biomedical sciences, vector-borne diseases still seriously threaten world health. For example, according to the latest WHO estimates, released in December 2015, there were 214 million cases of malaria in 2015 and 438000 deaths [148]. It is well known that the malaria parasite is transmitted from human-to-human through the anopheles mosquito bites, and that the transmission cycle is essentially driven by the human biting habit of the mosquito [52]. Now, the female anopheles mosquito bites a human being for the sole purpose of harvesting blood that she needs for the development of her eggs. The malaria parasite has exploited the mosquito's life style by adapting its life cycle so that part of it is in the human being and the other part in the mosquito. By so doing, the mosquito can then propagate the parasite from human to human. Transmission of most indirectly transmitted diseases of human being follows the same pattern. The vector (in most cases an insect) interacts with a human being, and depending on the disease status of both organisms, will either infect or be infected. Thus, understanding the population dynamics of mosquitoes, and relationship between mosquitoes and the environment is fundamental to the study of the epidemiology of mosquito-borne diseases. Mosquito abundance is a key determining factor that affects the persistence or resurgence of mosquito-borne diseases in a given region [146]. Hence, it is crucial to study the dynamics of mosquitoes, and devise effective and realistic methods for controlling mosquito population in communities.

The spatial distribution of anopheles vectors has shown great potential to affect malaria transmission intensity [146]. Therefore, a better understanding of the distribution, productivity and connectivity of anopheles breeding sites in order to determine their influence on anopheles distribution could be very useful in malaria control. Several theoretical studies of malaria vector dynamics have emphasized the importance of considering individual larval habitats, but few have addressed the effects of interactions between larval habitat connectivity [146, 154].

Mathematical models play an important role in understanding and providing solutions to natural phenomena which are difficult to measure in the field, and some models have incorporated dispersal or heterogeneity when modeling mosquito population [83, 42, 78]. Spatial models usually used the diffusion approach, which considers space as a continuous variable. Although partial differential equations (PDEs) are a good and classical way of modelling such dispersal [42, 139], their analysis is usually limited and does not incorporate the various factors that affect migrations. However, discrete approaches offer a better and simpler way of modeling heterogeneity [83, 5]. Thus, in areas where resources can be located in patches, mosquito dispersal is more suitably modeled by using a metapopulation approach, in which the population is subdivided into discrete patches. Then, in each patch, the population is subdivided into compartments corresponding to different status. This leads to a multi-patch, multi-compartment system.

Talking about the metapopulation setting, a recent approach based on the formalism

used in statistical mechanics of complex networks is presented in [103, 26, 27, 119]. Under this approach, the structure of the spatial network of patches is encapsulated by means of the connectivity (degree) distribution $p(k)$ defined as the probability that a randomly chosen patch has connectivity k. Note that the degree or connectivity of a patch (node) is the number of links connected to that node (i.e., the number its neighbors). Recent works have shown that it is possible to investigate the dynamics of epidemic spread using statistical mechanics on configuration model networks [11, 114, 137, 138, 140]. Most of the above-mentioned investigations [119, 114, 137, 140] mainly considered epidemic models on networks with no degree correlation (i.e., uncorrelated networks). In such networks, a patch which is only constrained by degree distribution (and hence by the number of neighbors it has), can point to any patch from a pool of the network. However, few recent works [11, 138] have taken into account the degree correlation in complex networks and have conducted comparison studies on the prediction of disease evolution on correlated networks.

Many other works have focused on a metapopulation approach to model the mosquito population [154, 83]. In their work in [154], the authors presented a stochastic network model not governed by a dynamical system and did not consider all main stages of the mosquito life cycle to analyze the significance of the productivity of breeding sites. The work in [83] considered a set of discrete hexagonal patches to investigated the effects of mosquito dispersal on its dynamics.

In this work, we intend to fill in some of the gaps mentioned above in order to better take into account the heterogeneity in the connectivity of the nodes of network. To fulfill our goal, we make use of an approach based on statistical mechanics which could allow us to identify other breeding site characteristics which could best explain the distribution and abundance of mosquitoes. The methodology and objectives of this paper are (1) to design a complex network extension of the seminal model in [2], (2) to analyze and simulate a mathematical model for the spatio-temporal dynamics of anopheles mosquito using the alternative approach based on a statistical mechanics. This extension is inspired by the works [154, 83, 26, 27, 119] and some references therein. We consider the spread of anopheles mosquitoes on complex metapopulations, i.e., networks of populations connected by migratory flows whose configurations are described in terms of the conditional probabilities of connections between nodes. Note that nodes of the network represent potential breeding and feeding sites of mosquitoes, around which are human hosts habitations.

From the modelling perspective, the model proposed in this manuscript is a substantial extension of the basic model in [2] by incorporating the dispersal of mosquitoes. It also extends and enriches the work in [154, 83] by considering: (i) all the stages of the mosquito life cycle and (ii) heterogeneity in the connectivity of patches. From the theoretical and numerical perspectives, we examine the significance of larval habitat connectivity and mosquito dispersal in a homogeneous and a heterogeneous landscapes

on the persistence of mosquitoes populations. More precisely, we construct corresponding metapopulation models and perform their qualitative and quantitative analyzes. Specifically, for the mathematical tractability, uncorrelated networks in a homogeneous landscape are considered and the following investigations are highlighted:

- The bifurcation/threshold parameter (basic offspring number) is explicitly computed.
- The sensitivity analysis of the threshold parameter, the model variables with respect to model parameters is given.
- A simple and digestive proof based on the Hethcote-Thieme fixed point theorem [65], of a unique nontrivial equilibrium point is provided.
- Contrary to the few existing works where, Lyapunov-LaSalle techniques are usually used, the monotone operator theory [124] is the main ingredient here for the establishment of global asymptotic stability of both trivial and nontrivial equilibrium points.

Moreover for both homogeneous and heterogeneous landscapes, the effects of dispersal/migration and patch heterogeneity on the mosquito population are numerically investigated. Finally, the comparison of metapopulation models in homogeneous and heterogeneous landscapes are presented through numerical simulations. The rest of the paper is organized as follows. After the presentation of the basic model without mosquito dispersal in Section 2, we formulate metapopulation models for both homogeneous and heterogeneous landscapes in Section 3. Their qualitative and quantitative analyzes are further presented. Theoretical results and the role of dispersal, patch connectivities and migration are investigated through numerical simulations in Section 4. The summary of the main results of our work and its possible extensions conclude the paper in Section 5.

2.1.1 Mosquito dynamics in a single patch without dispersal

We consider the classical Anguelov-Dumont-Lubuma model [2]:

$$\begin{cases} \dot{A} &= \Phi F - (\gamma + \mu_1 + \mu_2 A)A, \\ \dot{Y} &= r\gamma A - (\beta + \mu_Y)Y, \\ \dot{M} &= (1-r)\gamma A - \mu_M M, \\ \dot{F} &= \beta Y - \mu_F F. \end{cases} \tag{2.1}$$

This model was developed according to the following biological and entomological facts recalled hereafter. The life cycle of mosquitos consists of two main stages: aquatic (egg, larva, pupa) and adult. After its emergence from pupa, a female mosquito needs to mate and get a blood meal before it starts laying eggs. Depending on the condition, this takes about a week. Then, every 4-5 days she will take a blood meal and lay 100-150 eggs at

different places (10-15 per place). Mathematically, the population of mosquitoes is then divided into the following compartments: population in aquatic stage A; young female not yet laying eggs Y; fertilized and eggs laying females F and males M. This description was depicted in [2] by the flowchart in Fig. 2.1.

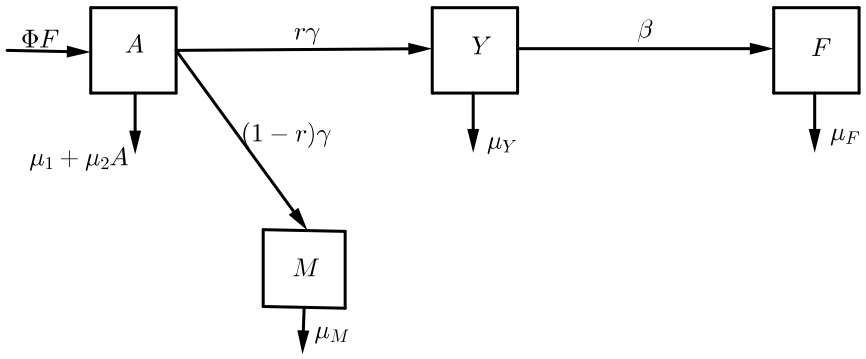

Figure 2.1: Wild mosquito flow chart.

Note that the first equation of system (2.1) can be combined as logistic population with harvesting. A female needs to mate successfully only once. The eggs are laid in the so-called gonotrophic cycle, which consists of taking blood meal, maturation of the eggs and oviposition. Before a female begins to lay eggs, two essential events need to take place, mating and taking a blood meal, occurring in varying order.

A female mosquito is considered to be in the Y-compartment since its emergence from pupa until her gonotrophic cycle has began, that is the time needed to mate and take the first blood meal, which takes typically 3-4 days. The death rate during that period reflects essentially only death from predators and adverse climatic conditions. Therefore, it is generally lower than the death rate for the F-compartment. Typically, the male mosquitoes are (depending on the temperature) about half or 40 percent of the total population.

In the model, the fraction of the emerging female mosquitoes is denoted by r, with $(1-r)$ being the fraction of emerging male mosquitoes. A male mosquito can mate practically through all its life. Since a female needs one successful mating, there is an overabundance of males. Therefore, in general, it is reasonable to assume that the waiting time for mating does not depend on the number of males (M) in the sense that, if M is increased further this rate remains the same. For the model, this means that the transfer rate β from compartment Y to compartment F is independent of M. Mathematically, this means that the third equation of system (2.1) can be decoupled from the system. Sometimes β is referred to as "mating rate", which, as explained above, can be abetted misleading and does not define clearly the boundary between compartments Y and F. The model under derivation clearly fixed boundary at the beginning of the first gonotrophic cycle of female, that is immediately after the mating and first blood meal. Then, the rate (per day) of laying eggs in the breeding sites is ϕF, where ϕ is the average amount of eggs laid per fertilized female per day. In the model, the size of the population is restricted by a density dependent

Table 2.1: Numerical values for the parameters of system (2.1) [2].

Parameter	Description	Value
r	Fraction of the emerging female mosquitoes (per day)	0.5
γ	Maturation rate from larvae to adult (per day)	0.1
β	Transfer rate from the compartment Y to F (per day)	0.25
$1/\mu_M$	Average lifespan of male mosquitoes (in days)	7
$1/\mu_F$	Average lifespan of female mosquitoes (in days)	10
$1/\mu_Y$	Average lifespan of adult female mosquitoes (in days)	20
Φ	Number of eggs at each deposit per capita (per day)	variable
μ_1	Mortality rate of the aquatic stage (per day)	0.25
μ_2	Density mortality rate of the aquatic stage (per day)	10^{-5}

death rate similar to [21, 22]. However, the density dependent death rate is used only for the aquatic stage. The reason is that in a typical environment the size of the mosquito population is also restricted mainly by the available breeding sites. In [46], the size of the population is also restricted only in the aquatic stages but in a different way by an explicit carrying capacity beyond which no egg is laid. In equation (2.1), the parameters μ_1 and μ_2 denote the density independent and the density dependent death rates of the aquatic stage, respectively. In all equations of model (2.1), μ with respective index refers to the death rate for the specific compartment (which is density independent).

The parameter values of model (2.1) used for simulations are given in Table 2.1 and the analytical results for this model can be found in [2]. However, for an easier readability of our work, we recall without proof the main results. System (2.1) has two equilibria: the trivial equilibrium $Q_0 = (0, 0, 0, 0)$ and the nontrivial equilibrium $Q^* = (A^*, Y^*, F^*, M^*)^T$ where A^*, Y^*, F^* and M^* are defined as follows:

$$\begin{aligned} A^* &= \frac{(\gamma+\mu_1)(\mathcal{R}_0-1)}{\mu_2}, \qquad Y^* = \frac{r\gamma(\gamma+\mu_1)(\mathcal{R}_0-1)}{\mu_2(\beta+\mu_Y)}, \\ F^* &= \frac{\beta r\gamma(\gamma+\mu_1)(\mathcal{R}_0-1)}{\mu_F\mu_2(\beta+\mu_Y)} \qquad \text{and} \qquad M^* = \frac{(1-r)\gamma(\gamma+\mu_1)(\mathcal{R}_0-1)}{\mu_2\mu_M}, \end{aligned} \tag{2.2}$$

where $\mathcal{R}_0$ is given by

$$\mathcal{R}_0 = \frac{r\gamma\beta\Phi}{(\gamma+\mu_1)(\beta+\mu_Y)\mu_F}. \tag{2.3}$$

The nontrivial equilibrium Q^* has a biological meaning if and only if $\mathcal{R}_0 \geq 1$. The threshold quantity $\mathcal{R}_0$ is the basic offspring number for the population of anopheles mosquitoes in a single patch model [2]. It is the average number of the newly anopheles mosquitoes generated by a single fertilized and eggs laying female anopheles mosquito during her life when she is introduced into a population of male anopheles mosquitoes in the absence of any given intervention strategies.

The following result summarizes the asymptotic behavior of model (2.1) as shown in [2].

Theorem 2.1.1. System (2.1) is a dissipative dynamical system in $\Omega = \mathbb{R}^4_+ = \{(S, Y, F, M) \in \mathbb{R}^4 \ / \ S, Y, F, M \geq 0\}$. Moreover,

(i) If $\mathcal{R}_0 \leq 1$, then the trivial (mosquito-free) equilibrium Q_0 is globally asymptotically stable on Ω.

(ii) If $\mathcal{R}_0 > 1$, then the system has two equilibria Q_0 and Q^* on Ω where Q^*(the mosquito-persistent equilibrium) is stable with basin of attraction $\Omega \setminus \{(A, Y, M, F) \in \mathbb{R}^4_+, \ A = Y = F = 0\}$ and Q_0 is unstable with the nonnegative M-axis being a stable manifold.

2.2 Metapopulation models in complex networks

2.2.1 A generic reaction-diffusion model in a complex network

Herein, we extend model (2.1) to incorporate the diffusion/migration process. Mosquitoes disperse while searching for hosts or breeding sites [154]. We consider the dynamical evolution of the population of anopheles mosquitoes in heterogeneous metapopulation. The model consists of n patches. We recall that these patches represent breeding-feeding sites around which are potential human habitats and between which mosquitoes move creating links between these nodes. A given fraction of adult mosquitoes searching for hosts and a fraction of adult mosquitoes searching for breeding sites leave their current patches of residence, while the remaining fraction is motionless. We assume that the architecture of the network of patches (nodes) where local populations live is mathematically encoded by means of the connectivity (degree) distribution $p(k)$. Typically, $p(k)$ is defined as the probability that a randomly chosen path has degree k. We recall that the degree or connectivity of a patch is the number of links connected to that patch. At any given time, in each patch, an individual mosquito is in one of the following states: population in aquatic stage ($\rho_{A,k}$), young female not yet laying eggs ($\rho_{Y,k}$), fertilized and eggs laying females ($\rho_{F,k}$), male mosquitoes ($\rho_{M,k}$). The total variable population size in patches of degree k at time t is given by $\rho_k(t) = \rho_{A,k}(t) + \rho_{Y,k}(t) + \rho_{F,k}(t) + \rho_{M,k}(t)$. Note again that, we focus in this part on the migration of mosquitoes from patch to patch (that is the case of connected patches). A reasonable assumption is that, mosquitoes in aquatic phase can not move out of their residence patch, while those in adult phase can migrate.

In Fig. 2.2, we give an example of a n-patches network: each patch here is breeding-feeding site. Without loss of generality, we suppose that in each patch, the population dynamics of anopheles mosquitoes is governed by the basic system (2.1). Mosquitoes move from a patch with degree k to another with degree k' with a diffusion rate $D_{kk'}$ that

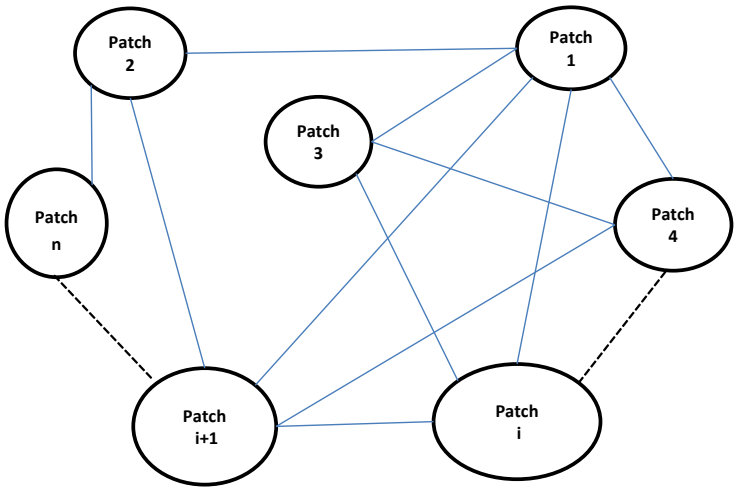

Figure 2.2: A general n-patches network for the population dynamics of anopheles mosquito between n feeding-breeding sites.

depends on the degrees of the origin and destination patches. The probability P_k of leaving a patch with degree k is then given by

$$P_k = k \sum_{k'} P(k'|k) D_{kk'}, \tag{2.4}$$

where $P(k'|k)$ is the conditional probability that any given edge departing from a node of degree k is pointing to a node of degree k' [27].

Under this generic type of diffusion, the equations governing the spatio-temporal evolution of anopheles mosquitoes are giving by the system below :

$$\begin{cases} \dot{\rho}_{A,k} &= \Phi\rho_{F,k} - (\gamma + \mu_1 + \mu_2\rho_{A,k})\rho_{A,k}, \\ \dot{\rho}_{Y,k} &= r\gamma\rho_{A,k} - (\beta + \mu_Y)\rho_{Y,k} - P_k\rho_{Y,k} + k\sum_{k'} P(k'|k) D_{k'k}\rho_{Y,k'}, \\ \dot{\rho}_{M,k} &= (1-r)\gamma\rho_{A,k} - \mu_M\rho_{M,k} - P_k\rho_{M,k} + k\sum_{k'} P(k'|k) D_{k'k}\rho_{M,k'}, \\ \dot{\rho}_{F,k} &= \beta\rho_{Y,k} - \mu_F\rho_{F,k} - P_k\rho_{F,k} + k\sum_{k'} P(k'|k) D_{k'k}\rho_{F,k'}. \end{cases} \tag{2.5}$$

As in classical reaction-diffusion processes, system (2.5) expresses the time variation of the subpopulations of mosquitoes in aquatic phase, young female not yet laying eggs, fertilized and eggs laying females and males mosquitoes as the sum of two independent contributions: reaction and diffusion. In particular, the diffusion term includes the outflow of mosquitoes (diffusing particles) from patches of degree k and the inflow of migratory mosquitoes from the nearest patches of degree k'. In general, with n different patches of corresponding degrees $k_1, k_2, ..., k_n$ in the network, Eq. (2.5) is a $4 \times n$ system of differential equations. The solutions of system (2.5) remain nonnegative in $\mathbb{R}_+^{4n}$ because the out movement always stops when the corresponding patch is emptied. This latter assertion is mathematically established in the following result.

Theorem 2.2.1. If system (2.5) with initial condition in $\mathbb{R}_+^{4n}$ has a solution, then the latter solution remains in $\mathbb{R}_+^{4n}$ (i.e. nonnegative) for all times.

Proof: It suffices to show that system (2.5) can written in the following form:

$$\dot{X} = \mathcal{M}(X)X, \tag{2.6}$$

where $\mathcal{M}(X)$ is a $4n \times 4n$ cooperative (Metzler) matrix, and X a $4n$ column matrix to be determined below. To this end, system (2.5) rewrites:

$$\begin{cases} \dot{\rho}_{A,k_i} &= \Phi\rho_{F,k_i} - (\gamma + \mu_1 + \mu_2\rho_{A,k_i})\rho_{A,k_i}, \\ \dot{\rho}_{Y,k_i} &= r\gamma\rho_{A,k_i} - (\beta + \mu_Y)\rho_{Y,k_i} - P_{k_i}\rho_{Y,k_i} + k_i \sum_{j=1}^{n} P(k_j|k_i)D_{k_jk_i}\rho_{Y,k_j}, \\ \dot{\rho}_{M,k_i} &= (1-r)\gamma\rho_{A,k_i} - \mu_M\rho_{M,k_i} - P_{k_i}\rho_{M,k_i} + k_i \sum_{j=1}^{n} P(k_j|k_i)D_{k_jk_i}\rho_{M,k_j} \qquad i = \{1,2,...,n\}, \\ \dot{\rho}_{F,k_i} &= \beta\rho_{Y,k_i} - \mu_F\rho_{F,k_i} - P_{k_i}\rho_{F,k_i} + k_i \sum_{j=1}^{n} P(k_j|k_i)D_{k_jk_i}\rho_{F,k_j}. \end{cases} \tag{2.7}$$

Now, let

$$X_A = (\rho_{A,k_1}, \rho_{A,k_2}, \ldots, \rho_{A,k_n})^T, \quad X_Y = (\rho_{Y,k_1}, \rho_{Y,k_2}, \ldots, \rho_{Y,k_n})^T,$$

$$X_M = (\rho_{M,k_1}, \rho_{M,k_2}, \ldots, \rho_{M,k_n})^T, \quad X_F = (\rho_{F,k_1}, \rho_{F,k_2}, \ldots, \rho_{F,k_n})^T,$$

$$Q_1 = \text{diag}(P_{k_1}, \cdots, P_{k_n}), \quad Q_2 = \left(k_i P\left(k_j|k_i\right) D_{k_jk_i}\right)_{(i,j)}, \quad M_A = -(\gamma + \mu_1)I_n - \mu_2\text{diag}(X_A),$$

$$M_Y = -(\beta + \mu_Y + Q_1)I_n + Q_2, \quad M_M = -(\mu_M + Q_1)I_n + Q_2 \quad M_F = -(\mu_F + Q_1)I_n + Q_2,$$

and

$$\mathcal{M}(X) = \begin{pmatrix} M_A & O_n & O_n & \Phi I_n \\ r\gamma I_n & M_Y & O_n & O_n \\ (1-r)\gamma I_n & O_n & M_M & O_n \\ O_n & \beta I_n & O_n & M_F \end{pmatrix},$$

where I_n and O_n denote the $n \times n$ identity and null matrices, respectively. Since the entries of Q_1 and Q_2 are nonnegative, it is straightforward that M_A, M_Y, M_M, M_F are Metzler matrices, so is $\mathcal{M}(X)$. Finally, let

$$X = (X_A,\ X_Y,\ X_M,\ X_F)^T,$$

then model (2.7) becomes

$$\dot{X} = \mathcal{M}(X)X.$$

This achieves the proof. □

In the following subsections we study special cases of system (2.5) depending on the type of diffusion processes by considering diffusion rates that are inherent to the traffic characteristics of each node. Typically there are two distinguishable landscapes with different features which must retain our attention.

2.2.2 The metapopulation model in a homogeneous landscape

A landscape is homogeneous when all its patches have similar characteristics. Thus, in such landscapes, it is reasonable to assume that the mosquitoes have the same dispersal/diffusion rate between patches. The mosquitoes searching for breeding sites to lay their eggs are attracted by the availability of breeding sites [97]. Therefore they move randomly in any breeding sites to lay their eggs. Mosquitoes can detect host odor, but it is unclear whether they have the learning capacity they would need to enable them to return to particular hosts or breeding sites [83, 72]. In the case where all patches have similar characteristics (i.e. homogeneous landscape), the mosquitoes disperse equally between the patches and the dispersal parameter is the same for all patches. In this case, the diffusion rate along any given link of a node with degree k is simply equal to

$$D_{kk'} = \frac{D_i}{k}, \quad i = Y, M, F. \tag{2.8}$$

For the sake of brevity, we consider strictly positive diffusion rates $D_Y, D_F, D_M > 0$. Thus, assuming that distance has no bearing on the probability of mosquito flying between breeding sites and, using the fact that $\sum_k P(k|k') = 1$, the dynamics of free-flying mosquitoes in a patch of degree k is

$$\begin{cases} \dot{\rho}_{A,k} &= \Phi\rho_{F,k} - (\gamma + \mu_1 + \mu_2\rho_{A,k})\rho_{A,k}, \\ \dot{\rho}_{Y,k} &= r\gamma\rho_{A,k} - (\beta + \mu_Y)\rho_{Y,k} - D_Y\rho_{Y,k} + kD_Y \sum_{k'} P(k'|k)\frac{\rho_{Y,k'}}{k'}, \\ \dot{\rho}_{M,k} &= (1-r)\gamma\rho_{A,k} - \mu_M\rho_{M,k} - D_M\rho_{M,k} + kD_M \sum_{k'} P(k'|k)\frac{\rho_{M,k'}}{k'}, \\ \dot{\rho}_{F,k} &= \beta\rho_{Y,k} - \mu_F\rho_{F,k} - D_F\rho_{F,k} + kD_F \sum_{k'} P(k'|k)\frac{\rho_{F,k'}}{k'}, \end{cases} \tag{2.9}$$

Note that, since the number of links emanating from nodes of degree k to nodes of degree k' must be equal to the number of links emanating from nodes of degree k' to nodes of degree k in non-directed graphs, we have the following relationship between $p(k)$ and $P(k'|k)$ [11]:

$$kP(k'|k)p(k) = k'P(k|k')p(k'). \tag{2.10}$$

For networks with a connectivity pattern defined by a set of conditional probabilities $P(k'|k)$, we define the elements of the connectivity matrix C as

$$C_{kk'} = \frac{k}{k'}P(k'|k). \tag{2.11}$$

Note that these elements are the average number of mosquitoes that patches of degree k receive from neighboring patches of degree k' assuming that one mosquito leaves each of these patches by choosing at random one of the k' connections [119]. On the other hand, for those degrees k that are not present in the network, one must have $P(k'|k) = 0$, $\forall k'$. Hereafter in this paper, when talking about degrees, we implicitly mean those degrees

that are present in the network. Furthermore, the case where all patches have the same connectivity is excluded from our consideration because, under the present approach, the model equations reduce to those of a single patch model.

In order to obtain further analytical results about the metapopulation dynamics of anopheles mosquitoes, we need to be precise about the form of $P(k'|k)$. As in most network models, the easiest and usual assumption is to restrict ourselves to uncorrelated networks.

(a) Uncorrelated networks

In these networks, the degrees of the nodes at the end of any given link are independent. In other words, there is no degree-degree correlation between the connected nodes. Therefore, we have

$$P(k'|k) = k'p(k')/\langle k\rangle, \tag{2.12}$$

which corresponds to the degree distribution of nodes (patches) that arrive at by following a randomly chosen link [103]. Using Eqs. (2.10), (2.11), (2.12), $\sum_k P(k|k') = 1$ and change the order of summations in system (2.7), one obtains the following equations for the time evolution of anopheles mosquitoes in metapopulations described by uncorrelated networks:

$$\begin{cases} \dot{\rho}_{A,k} &= \Phi\rho_{F,k} - (\gamma + \mu_1 + \mu_2\rho_{A,k})\rho_{A,k}, \\ \dot{\rho}_{Y,k} &= r\gamma\rho_{A,k} - (\beta + \mu_Y)\rho_{Y,k} - D_Y\left(\rho_{Y,k} - \dfrac{k}{\langle k\rangle}\rho_Y\right), \\ \dot{\rho}_{M,k} &= (1-r)\gamma\rho_{A,k} - \mu_M\rho_{M,k} - D_M\left(\rho_{M,k} - \dfrac{k}{\langle k\rangle}\rho_M\right), \\ \dot{\rho}_{F,k} &= \beta\rho_{Y,k} - \mu_F\rho_{F,k} - D_F\left(\rho_{F,k} - \dfrac{k}{\langle k\rangle}\rho_F\right), \end{cases} \tag{2.13}$$

where

$$\langle k\rangle = \sum_k kp(k) \quad \text{and} \quad \rho_j(t) = \sum_k p(k)\rho_{j,k}, \quad j = A, Y, M, F.$$

$\langle k\rangle$ is defined as the average network degree. ρ_A, ρ_Y, ρ_F and ρ_M, represent the average number of population in aquatic stage, young females and eggs laying females, and population of males mosquitoes in each patch at time t, respectively. In this case, the diffusion term is simply given by the difference between the outflow of young females not yet laying eggs ($D_Y\rho_{Y,k}$), fertilized and eggs laying females ($D_F\rho_{F,k}$) and male mosquitoes ($D_M\rho_{M,k}$) in patches of connectivity k and the total inflow of young females not yet laying eggs ($D_Y\rho_Y/\langle k\rangle$), fertilized and eggs laying females ($D_F\rho_F/\langle k\rangle$) and male mosquitoes ($D_M\rho_M/\langle k\rangle$) in patches of connectivity k, respectively; across all their k connections, which is k times the average flow of mosquitoes across a connection in the network. Note that this average flow across a connection does not depend on the degree k of the considered patch because we have assumed that the architecture of the metapopulation is described by an uncorrelated network. In these network configurations, the elements of the connectivity

matrix C are simply

$$C_{kk'} = \frac{kp(k')}{\langle k \rangle}. \tag{2.14}$$

Clearly, C is a rank-one matrix and the vector v, whose components $v_k = k$, is its eigenvector corresponding to its unique non-zero eigenvalue 1. Thus, if there are (as assumed above) n different patches in the network, then the eigenvalues of the said connectivity matrix are $\lambda = 0$ (with algebraic multiplicity $n-1$) and $\lambda = 1$ (which is a simple eigenvalue). This latter remark will be used to prove the stability of equilibria of the model. For the way forward, we first "vectorialize" system (2.13), using the following set of vectors as formerly defined:

$$X_A = (\rho_{A,k_1}, \rho_{A,k_2}, \ldots, \rho_{A,k_n})^T, \quad X_Y = (\rho_{Y,k_1}, \rho_{Y,k_2}, \ldots, \rho_{Y,k_n})^T,$$
$$X_M = (\rho_{M,k_1}, \rho_{M,k_2}, \ldots, \rho_{M,k_n})^T, \quad X_F = (\rho_{F,k_1}, \rho_{F,k_2}, \ldots, \rho_{F,k_n})^T.$$

Remind that, if $X \in \mathbb{R}^n$ is a vector, diag(X) denotes the $n \times n$ diagonal matrix whose entries are given by the respective components of X. With these notations, system (2.13) becomes

$$\begin{cases} \dot{X}_A = f_1(X) &= \Phi X_F - [\gamma + \mu_1 + \mu_2 \text{diag}(X_A)]\, X_A, \\ \dot{X}_Y = f_2(X) &= r\gamma X_A - [\beta + \mu_Y + D_Y]\, X_Y + D_Y C X_Y, \\ \dot{X}_M = f_3(X) &= (1-r)\gamma X_A - [\mu_M + D_M]\, X_M + D_M C X_M, \\ \dot{X}_F = f_4(X) &= \beta X_Y - [\mu_F + D_F]\, X_F + D_F C X_F, \end{cases} \tag{2.15}$$

where C is the connectivity matrix defined in Eq. (2.14).

Notice that, in the case where the parameters Φ, γ, β, μ_1, μ_2, μ_Y, μ_M and μ_F are not the same for all patches, they are replaced in system (2.15) by nonnegative diagonal blocs matrices and this does not change the fundamental structure of the system.

(b) Basic offspring number

System (2.15) has a trivial (mosquito-free) equilibrium $\mathcal{P}_0 = (\mathbf{0}, \mathbf{0}, \mathbf{0}, \mathbf{0})$ with $\mathbf{0}$ standing for the zero vector of dimension n when there is no fertilized and eggs laying females in each patch. We calculate the basic offspring number, $\mathcal{R}_0^{(m)}$ (where the subscript "m" stands for "metapopulation" and simply differentiate it with the single patch basic offspring number $\mathcal{R}_0$), using the next generation approach developed in [40]. Let

$$\mathcal{F} = \begin{pmatrix} \Phi X_F \\ \mathbf{0} \\ \mathbf{0} \end{pmatrix} \quad \text{and} \quad \mathcal{V} = \begin{pmatrix} \gamma X_A + (\mu_1 + \mu_2 \text{diag}(X_A)) X_A \\ -r\gamma X_A + (\mu_Y + \beta) X_Y + D_Y X_Y - D_Y C X_Y \\ -\beta X_Y + \mu_F X_F + D_F X_F - D_F C X_F \end{pmatrix}.$$

The Jacobian matrices of $\mathcal{F}$ and $\mathcal{V}$ at the trivial equilibrium $\mathcal{P}_0$ are

$$F = \begin{bmatrix} F_{11} & F_{12} \\ F_{21} & F_{22} \end{bmatrix} \quad \text{and} \quad V = \begin{bmatrix} (\gamma + \mu_1) I_n & \mathbf{0} & \mathbf{0} \\ -r\gamma I_n & (\beta + \mu_Y + D_Y - D_Y C) I_n & \mathbf{0} \\ \mathbf{0} & -\beta I_n & (\mu_F + D_F - D_F C) I_n \end{bmatrix},$$

where

$$F_{11} = \mathbf{0}, \qquad F_{12} = \begin{bmatrix} \mathbf{0}, & \Phi \end{bmatrix}, \qquad F_{21} = \begin{bmatrix} \mathbf{0} \\ \mathbf{0} \end{bmatrix} \qquad \text{and} \qquad F_{22} = \begin{bmatrix} \mathbf{0} & \mathbf{0} \\ \mathbf{0} & \mathbf{0} \end{bmatrix}.$$

To compute V^{-1}, denote

$$V = \begin{bmatrix} V_1 & V_2 \\ V_3 & V_4 \end{bmatrix}, \quad \text{where} \quad V_1 = (\gamma + \mu_1) I_n, \quad V_2 = \begin{bmatrix} \mathbf{0} & \mathbf{0} \end{bmatrix}, \quad V_3 = \begin{bmatrix} -r\gamma I_n \\ \mathbf{0} \end{bmatrix}$$

and

$$V_4 = \begin{bmatrix} (\beta + \mu_Y + D_Y - D_Y C) I_n & \mathbf{0} \\ -\beta I_n & (\mu_F + D_F) I_n - D_F C \end{bmatrix}.$$

We emphasize that, since V is a M-matrix and $-V$ is stable, $V^{-1} \geq 0$. Let the inverse matrix of V be written in the following form:

$$V^{-1} = \begin{bmatrix} W_{11} & W_{12} \\ W_{21} & W_{22} \end{bmatrix},$$

where W_{11} and W_{22} are square matrices of dimension $(2n \times 2n)$ and $(n \times n)$, respectively. With this in mind, one has

$$FV^{-1} = \begin{bmatrix} \mathcal{A} & \mathcal{B} \\ \mathbf{0} & \mathbf{0} \end{bmatrix},$$

where $\mathcal{A} = F_{12} W_{21}$ and $\mathcal{B} = F_{12} W_{22}$. Then following [40], the basic offspring number $\mathcal{R}_0^{(m)}$ is defined as the spectral radius of the next generation matrix, FV^{-1}. Precisely,

$$\mathcal{R}_0^{(m)} = \rho(FV^{-1}) = \rho\left(F_{12} W_{21}\right). \tag{2.16}$$

To obtain an explicit expression of the basic offspring number, we only need to compute W_{21}. The following lemma is instrumental :

Lemma 2.2.1. Let N be a square block matrix of the following form:

$$N = \begin{bmatrix} N_1 & N_2 \\ N_3 & N_4 \end{bmatrix},$$

where N_1 and N_4 are square matrices.
If N_1 and $D = N_4 - N_3 N_1^{-1} N_2$ are invertible, then the inverse matrix of N is given by

$$N^{-1} = \begin{bmatrix} N_1^{-1} + N_1^{-1} N_2 D^{-1} N_3 N_1^{-1} & -N_1^{-1} N_2 D^{-1} \\ -D^{-1} N_3 N_1^{-1} & D^{-1} \end{bmatrix}.$$

Proof. Note that the matrix N can be written as

$$N = \begin{bmatrix} N_1 & N_2 \\ N_3 & N_4 \end{bmatrix} = \begin{bmatrix} N_1 & \mathbf{0} \\ N_3 & I \end{bmatrix} \begin{bmatrix} I & N_1^{-1} N_2 \\ \mathbf{0} & D \end{bmatrix}.$$

Then, one can deduce that

$$N^{-1} = \begin{bmatrix} I & N_1^{-1}N_2 \\ \mathbf{0} & D \end{bmatrix}^{-1} \begin{bmatrix} N_1 & \mathbf{0} \\ N_3 & I \end{bmatrix}^{-1} = \begin{bmatrix} I & -N_1^{-1}N_2 D^{-1} \\ \mathbf{0} & D^{-1} \end{bmatrix} \begin{bmatrix} N_1^{-1} & \mathbf{0} \\ -N_3N_1^{-1} & I \end{bmatrix},$$

$$= \begin{bmatrix} N_1^{-1} + N_1^{-1}N_2D^{-1}N_3N_1^{-1} & -N_1^{-1}N_2D^{-1} \\ -D^{-1}N_3N_1^{-1} & D^{-1} \end{bmatrix}.$$

This ends the proof. □

Notice that V defined above has the same form as N defined in Lemma 2.2.1 (with: $N_1 = V_1$, $N_2 = V_2$, $N_3 = V_3$ and $N_4 = V_4$). Moreover, it is easy to check that V satisfies all the assumptions in Lemma 2.2.1. Thus, applying Lemma 2.2.1, V^{-1} is given by

$$V^{-1} = \begin{bmatrix} V_1^{-1} & \mathbf{0} \\ -V_4^{-1}V_3V_1^{-1} & V_4^{-1} \end{bmatrix},$$

from which one can extract $W_{21} = -V_4^{-1}V_3V_1^{-1}$. Thus, computing W_{21} amounts to compute V_4^{-1} since V_3 is given and V_1^{-1} is obvious. Notice also that V_4 has the same form as N in Lemma 2.2.1 (with $N_1 = (\beta+\mu_Y+D_Y-D_YC)I_n$, $N_2 = 0$, $N_3 = -\beta I_n$ and $N_4 = (\mu_F+D_F)I_n-D_FC$). Hence, another application of Lemma 2.2.1 yields

$$V_4^{-1} = \begin{bmatrix} N_1^{-1} & \mathbf{0} \\ -N_4^{-1}N_3N_1^{-1} & N_4^{-1} \end{bmatrix}.$$

From the above expressions, it appears that to obtain an explicit expressions of V_4^{-1}, we need to compute the inverse matrices of N_1^{-1} and N_4^{-1}. These shall be done using another instrumental lemma, stated below.

Lemma 2.2.2. Let $G = U + KWZ$ be an $n \times n$ invertible matrix. Assume the matrices U, W and $W^{-1} + ZU^{-1}K$ are invertible. Then the inverse matrix of G is given by

$$G^{-1} = U^{-1} - U^{-1}K[W^{-1} + ZU^{-1}K]^{-1}ZU^{-1}. \tag{2.17}$$

Proof. It suffices to verified that $GG^{-1} = I_n$. Indeed, one has

$$\begin{aligned} GG^{-1} &= UU^{-1} - K\left[W^{-1} + ZU^{-1}X\right]^{-1}ZU^{-1} + KWZU^{-1} \\ &- KWZU^{-1}K\left[W^{-1} + ZU^{-1}K\right]^{-1}ZU^{-1}, \\ &= I_n - K\left[\left[W^{-1} + ZU^{-1}K\right]^{-1} + W - WZU^{-1}K\left[W^{-1} + ZU^{-1}K\right]^{-1}\right]ZU^{-1}, \\ &= I_n - KW\left[W^{-1}\left[W^{-1} + ZU^{-1}K\right]^{-1} - I_n + ZU^{-1}K\left[W^{-1} + ZU^{-1}K\right]^{-1}\right]ZU^{-1}, \\ &= I_n - KW\left[\left[W^{-1} + ZU^{-1}K\right]\left[W^{-1} + ZU^{-1}K\right]^{-1} - I_n\right]ZU^{-1}, \\ &= I_n - KW(I_n - I_n)ZU^{-1}, \\ &= I_n. \end{aligned}$$

This concludes the proof. □

Now, we can explicitly calculate N_1^{-1} and N_4^{-1}. We shall use recursively Lemma 2.2.2 and the fact that $C^m = C, \forall m \in \mathbb{N}^*$.

Note that $N_4 = (\mu_F + D_F)I_n - D_F C$ has the form of the matrix G with

$$U = (\mu_F + D_F)I_n, \qquad K = (k_1, ..., k_n)^T, \qquad W = I_n \qquad \text{and}$$

$$Z = \frac{-D_F}{\langle k \rangle} (P(k_1), ..., P(k_n)) .$$

With this in mind and using Lemma 2.2.2, it is straightforward that

$$\begin{aligned} N_4^{-1} &= \frac{I_n}{(\mu_F + D_F)} - \frac{I_n}{(\mu_F + D_F)} \begin{pmatrix} k_1 \\ \vdots \\ k_n \end{pmatrix} \left[I_n - \frac{D_F}{\mu_F + D_F} \right]^{-1} \\ &\times \frac{-D_F}{\langle k \rangle (\mu_F + D_F)} (P(k_1), ..., P(k_2)), \\ &= \frac{I_n}{(\mu_F + D_F)} + \frac{I_n}{(\mu_F + D_F)} \frac{D_F C}{\mu_F} = \frac{1}{(\mu_F + D_F)} \left[I_n + \frac{D_F}{\mu_F} C \right]. \end{aligned}$$

Now, let us compute $N_1 = (\beta + \mu_Y + D_Y - D_Y C)I_n$. One can also observe that N_1 has the form of G in Lemma 2.2.2, with

$$U = (\beta + \mu_Y + D_Y)I_n, \qquad K = (k_1, ..., k_n)^T, \qquad W = I_n \qquad \text{and}$$

$$Z = \frac{-D_Y}{\langle k \rangle} (P(k_1), ..., P(k_n)) .$$

Thus, another application of Lemma 2.2.2 yields

$$N_1^{-1} = \frac{1}{(\beta + \mu_Y + D_Y)} \left[I_n + \frac{D_Y}{\beta + \mu_Y} C \right].$$

Using the expressions of N_1^{-1} and N_4^{-1}, one has

$$N_4^{-1} N_3 N_1^{-1} = \frac{-\beta}{(\mu_F + D_F)(\beta + \mu_Y + D_Y)} \left(I_n + \frac{D_Y C}{\beta + \mu_Y} + \frac{D_F C}{\mu_F} + \frac{D_F D_Y C}{\mu_F (\beta + \mu_Y)} \right).$$

Thus,

$$F_{12} W_{21} = \frac{r\beta\gamma\Phi}{(\gamma + \mu_1)(\mu_F + D_F)(\beta + \mu_Y + D_Y)} \left[I_n + \frac{D_Y C}{\beta + \mu_Y} + \frac{D_F}{\mu_F} C + \frac{D_F D_Y}{\mu_F (\beta + \mu_Y)} C \right].$$

The basic offspring number is therefore

$$\begin{aligned} \mathcal{R}_0^{(m)} &= \rho(F_{12} W_{21}), \\ &= \rho \left[\Gamma (a_0 I_n + (b_0 + c_0 + d_0) C) \right], \end{aligned} \tag{2.18}$$

where

$$a_0 = 1, \quad b_0 = \frac{D_Y}{\beta + \mu_Y}, \quad c_0 = \frac{D_F}{\mu_F}, \quad d_0 = \frac{D_F D_Y}{\mu_F (\beta + \mu_Y)} \quad \text{and} \quad \Gamma = \frac{r\beta\gamma\Phi}{(\gamma + \mu_1)(\mu_F + D_F)(\beta + \mu_Y + D_Y)}.$$

Since the rank of C is one and $\lambda = 1$ is its unique non-zero and positive eigenvalue, the largest eigenvalue of the matrix $\Gamma[a_0 I_n + (b_0 + c_0 + d_0)C)$ is $\Gamma(a_0 + b_0 + c_0 + d_0) > 0$. Thus, $\mathcal{R}_0^{(m)}$ for system (2.13) is

$$\mathcal{R}_0^{(m)} = \frac{r\beta\gamma\Phi}{(\gamma + \mu_1)(\mu_F + D_F)(\beta + \mu_Y + D_Y)}\left[1 + \frac{D_Y}{\beta + \mu_Y} + \frac{D_F}{\mu_F} + \frac{D_F D_Y}{\mu_F(\beta + \mu_Y)}\right]. \tag{2.19}$$

Remark 2.2.1. The relevance of the above techniques (Lemma 2.2.1 and Lemma 2.2.2) used to compute $\mathcal{R}_0^{(m)}$ lies in that it enables us to obtain an explicit formula of the basic offspring number for a complex metapopulation model. More importantly, it gives an easy interpretable expression of the basic offspring number. In metapopulation settings, this kind of result is quite rare (or does not exist at all). It is worth pointing out that, this achievement has been probably made possible thanks to the "statistical" modelling approach used in this work.

(c) Sensitivity analysis

We carried out sensitivity analysis to determine the model robustness to parameter values [87, 90]. This amounts to single out the most influential parameters on $\mathcal{R}_0^{(m)}$ and mosquito subpopulation dynamics. A Latin Hypercube Sampling (LHS) scheme [90] samples 1000 values for each input parameter using a uniform distribution over the range of biologically realistic values, listed in Table 2.3 with descriptions and references given in Table 2.1 and Table 2.2. Using system (2.15), 1000 model simulations are performed by randomly pairing sampled values for all LHS parameters. Outcome measures are calculated for each run : the basic offspring number ($\mathcal{R}_0^{(m)}$), the average number of population in aquatic stage (ρ_A), young females (ρ_Y) and fertilized females (ρ_F) for a network of five patches. Partial Rank Correlation Coefficients (PRCC) and corresponding p-values are computed. An output is assumed sensitive to an input if the corresponding PRCC is less than -0.50 or greater than $+0.50$, and the corresponding p-values is less than 5%.

Parameter	Range	Parameter	Range	Parameter	Range
r	[0.49 , 0.51]	μ_2	$[10^{-6}, 10^{-4}]$	μ_F	[0.05 , 0.2]
γ	[0.05 , 0.2]	β	[0.05 , 0.35]	D_Y	$[10^{-2}, 1]$
Φ	[0.5 , 50]	μ_Y	[0.01 , 0.2]	D_M	$[10^{-2}, 1]$
μ_1	[0.1 , 0.5]	μ_M	[0.05 , 0.2]	D_F	$[10^{-2}, 1]$

Table 2.2: Parameter value ranges of model (2.15) used as input for the LHS method.

Table 2.3 suggests that parameter Φ has the highest influence on the offspring number $\mathcal{R}_0^{(m)}$, following in decreasing order by the parameters μ_F, μ_1, γ, μ_Y and β. One can also observe that, for the values of ρ_A, ρ_Y and ρ_F, the parameters with more influence are D_Y,

Parameter	$\mathcal{R}_0^{(m)}$	ρ_A	ρ_Y	ρ_F
r	0.0831	0.0003	0.0325	0.0593
γ	**0.6617**	0.3648	0.2364	0.4401
Φ	**0.9281**	0.4003	**0.5414**	**0.5079**
μ_1	**-0.7047**	−0.0565	−0.0123	−0.0520
μ_2	−−	−0.3327	−0.4112	−0.3789
β	**0.5329**	0.2586	0.2033	0.1317
μ_Y	**-0.5770**	−0.2008	−0.1530	−0.1389
μ_M	−−	0.0874	−0.0066	−0.1577
μ_F	**-0.7959**	−0.3169	−0.2749	−0.1873
D_Y	0.0136	**0.9103**	**0.8641**	**0.8411**
D_M	−−	−0.0237	0.0283	0.0231
D_F	0.0402	**-0.9058**	**-0.8712**	**-0.8547**

Table 2.3: PRCCs between $\mathcal{R}_0^{(m)}$, ρ_A, ρ_Y, ρ_F and each parameter: The (⋆)'s indicate the most influential parameters. Precisely, (⋆) indicates a parameter whose sensitivity level (in absolute value) is between 0.5 and 0.65. The (⋆⋆) indicates a parameter whose sensitivity level (in absolute value) is between 0.66 and 0.8. The (⋆⋆⋆) indicates a parameter whose sensitivity level (in absolute value) is above 0.84.

D_F and Φ. This suggests that the migration of female mosquitoes between the patches may play a dominant role on the persistence of the mosquito's population.

(d) Global stability of the trivial (mosquito-free) equilibrium point

Using Theorem 2 in [40], the following result is straightforward.

Lemma 2.2.3. The trivial (mosquito-free) equilibrium point $\mathcal{P}_0$ of system (2.15) is locally asymptotically stable whenever $\mathcal{R}_0^{(m)} < 1$, and unstable if $\mathcal{R}_0^{(m)} > 1$.

Biologically speaking, Lemma 3.2.1 implies that mosquitoes can be eliminated in all breeding sites (when $\mathcal{R}_0^{(m)} < 1$) if the initial sizes of the population of anopheles mosquitoes are in the basin of attraction of the trivial equilibrium point $\mathcal{P}_0$.

System (2.15) can be written in the form $\dot{X} = f(X)$, where $X = (X_A, X_Y, X_M, X_F)^T$ and $f(X) = (f_1(X), f_2(X), f_3(X), f_4(X))^T$. It is straightforward that system (2.15) is cooperative on $\Omega = \mathbb{R}_+^{4n}$ because the jacobian matrix of (2.15) is a Metzler matrix. Furthermore, f is continuous on Ω and the vector field defined by f is directed inwards on the border $\partial\Omega$ of Ω. Thus, Theorems 2, 5 and 6 in [2] can be applied to extend the local result in Lemma 3.2.1 to a global one on Ω as follows:

Theorem 2.2.2. System (2.15) defines a dissipative dynamical system on $\Omega = \mathbb{R}_+^{4n}$. Moreover, if $\mathcal{R}_0^{(m)} \leq 1$ then the trivial (mosquito-free) equilibrium point $\mathcal{P}_0$ is globally asymptotically stable on Ω.

Proof. It hinges basically on the monotone properties of model (2.15). The inequalities

$$\frac{4\mathcal{R}_0^{(m)} k_i p(k_i) + 4\Gamma \sum_{j=1, j\neq i}^{n} k_j p(k_j)}{\langle k \rangle} < \frac{\gamma + \mu_1 + \mu_2 \rho_{A,k_i}}{\gamma + \mu_1}, \quad i = 1, 2, \cdots, n, \tag{2.20}$$

hold for all sufficiently large X_A. Let $m = (m_1, m_2, \cdots, m_n) > 0$ and let X_{A_m} be so large that in addition to (2.20) the following inequalities also hold :

$$X_{A_m} \geq m, \tag{2.21}$$

$$X_{F_m} := \frac{(\gamma + \mu_1 + \mu_2 \text{diag}(X_{A_m}))X_{A_m}}{2\Phi} \geq m, \tag{2.22}$$

$$X_{Y_m} := \frac{(\mu_F I_n + D_F I_n - D_F C)X_{F_m}}{2\beta} \geq m, \tag{2.23}$$

$$X_{M_m} := \frac{2(1-r)\gamma}{\mu_M + D_M}\left[I_n + \frac{D_M}{\mu_M} C\right] X_{A_m} \geq m. \tag{2.24}$$

Let $b_m = (X_{A_m}, X_{Y_m}, X_{F_m}, X_{M_m})^T$. Then, one has

$$f_1(b_m) = -\Phi X_{F_m} < 0; \quad f_3(b_m) = -(1-r)\gamma X_{A_m} < 0; \quad f_4(b_m) = -\beta X_{Y_m} < 0;$$

$$\begin{aligned} f_2(b_m) &= r\gamma\left[I_n - \frac{(N_1^{-1})^{-1}(N_4^{-1})^{-1}[\gamma + \mu_1 + \mu_2 \text{diag}(X_{A_m})]}{4\beta\Phi r\gamma}\right] X_{A_m}, \\ &= r\gamma\left[I_n - \frac{(a_0 I_n + (b_0 + c_0 + d_0)C)^{-1}}{4\Gamma}\frac{[\gamma + \mu_1 + \mu_2 \text{diag}(X_{A_m})]}{\gamma + \mu_1}\right] X_{A_m}, \\ &< 0 \quad \text{if} \quad 4\Gamma(a_0 I_n + (b_0 + c_0 + d_0)C) < \frac{\gamma + \mu_1 + \mu_2 \text{diag}(X_{A_m})}{\gamma + \mu_1}, \end{aligned}$$

i.e.

$$f_2(b_m) < 0 \quad \text{if} \quad \frac{4\mathcal{R}_0^{(m)} k_i p(k_i) + 4\Gamma \sum_{j=1, j\neq i}^{n} k_j p(k_j)}{\langle k \rangle} < \frac{\gamma + \mu_1 + \mu_2 \rho_{A,k_i}}{\gamma + \mu_1}, \quad i = 1, 2, \cdots, n.$$

So, $f(b_m) = (f_1(b_m), f_2(b_m), f_3(b_m), f_4(b_m))^T < 0$. Applying Theorem 6 in [2] with $a = 0$ and $b = b_m$, we obtain that (2.15) defines a dynamical system on $[0, b_m]$. However, b_m can be selected larger than any $X \in \mathbb{R}_+^{4n}$. Thus, (2.15) defines a dynamical system on $\Omega = \mathbb{R}_+^{4n}$. The only equilibrium point in Ω is the trivial equilibrium $\mathcal{P}_0$. It follows from Theorem 6 in [2] that $\mathcal{P}_0$ is globally asymptotically stable on $[0, b_m]$ for any $m > 0$, and therefore is globally asymptotically stable on $\Omega = \mathbb{R}_+^{4n}$. □ □

(e) Nontrivial (mosquito-persistent) equilibrium point and its stability

In this paragraph, we begin by showing that system (2.15) has a unique nontrivial equilibrium point when $\mathcal{R}_0^{(m)} > 1$. To achieve our goal, we reformulate the problem in terms of fixed point problem and use Theorem 2.1 in [65] for the existence and uniqueness of a positive fixed point of a multi-variable function. To be self contained, Theorem 2.1 in [65] is recalled hereafter.

Theorem 2.2.3 ([65], Theorem 2.1)**.** Let $F(x)$ be a continuous, monotone non-decreasing, strictly sublinear, bounded function which maps the non-negative orthant $\mathbb{R}_+^n$ into itself. Let $F(0) = 0$ and $F'(0)$ exists and be irreducible. Then $F(x)$ does not have a nontrivial fixed point on the boundary of $\mathbb{R}_+^n$. Moreover, $F(x)$ has a positive fixed point iff $\rho(F'(0)) > 1$. If there is a positive fixed point, then it is unique.

An equilibrium point $\mathcal{P}^* = (X_A^*, X_Y^*, X_M^*, X_F^*)$ for system (2.15) satisfies the following system of equations

$$\begin{cases} \Phi X_F^* - \left[\gamma + \mu_1 + \mu_2 \text{diag}(X_A^*)\right] X_A^* = 0, \\ r\gamma X_A^* - \left[(\beta + \mu_Y) + D_Y\right] X_Y^* + D_Y C X_Y^* = 0, \\ (1-r)\gamma X_A^* - \left[\mu_M + D_M\right] X_M^* + D_M C X_M^* = 0, \\ \beta X_Y^* - \left[\mu_F + D_F\right] X_F^* + D_F C X_F^* = 0. \end{cases} \tag{2.25}$$

Solving (2.25) yields

$$\begin{aligned} X_F^* &= \frac{[\gamma + \mu_1 + \mu_2 \text{diag}(X_A^*)]X_A^*}{\Phi}, \\ X_Y^* &= \frac{(\mu_F I_n + D_F I_n - D_F C)[\gamma + \mu_1 + \mu_2 \text{diag}(X_A^*)]X_A^*}{\beta\Phi}, \\ X_M^* &= \frac{(1-r)\gamma}{\mu_M + D_M}\left[I_n + \frac{D_M}{\mu_M} C\right] X_A^*. \end{aligned} \tag{2.26}$$

Replacing (2.26) in the second equation of system (2.25), one obtain

$$r\gamma\left[I_n - \frac{N_1 N_4[\gamma + \mu_1 + \mu_2 \text{diag}(X_A^*)]}{\beta\Phi r\gamma}\right] X_A^* = 0.$$

Hence, the existence of the nontrivial equilibrium point is reformulated as the following fixed point problem: Find a unique positive X_A^*, such that $X_A^* = F(X_A^*)$, where

$$F(X_A^*) = r\beta\gamma\Phi\left[\gamma + \mu_1 + \mu_2 \text{diag}(X_A^*)\right]^{-1} N_4^{-1} N_1^{-1} X_A^*.$$

Notice that F is a continuous, bounded function that maps $\mathbb{R}_+^n$ into itself and it is infinitely differentiable.

Let us prove that F is strictly sublinear in $\mathbb{R}_+^n$ i.e. $F(\nu X_A^*) > \nu F(X_A^*)$, for any $X_A^* \in \mathbb{R}_+^n$ with $X_A^* > 0$, and $\nu \in (0,1)$. Direct, but lengthly calculations give

$$\nu F(X_A^*)[F(\nu X_A^*)]^{-1} = \text{diag}\left(\frac{\gamma + \mu_1 + \nu\mu_2\rho_{A,k_1}}{\gamma + \mu_1 + \mu_2\rho_{A,k_1}}, \cdots, \frac{\gamma + \mu_1 + \nu\mu_2\rho_{A,k_n}}{\gamma + \mu_1 + \mu_2\rho_{A,k_n}}\right).$$

Since $\nu \in (0,1)$, we have

$$\frac{\gamma + \mu_1 + \nu\mu_2\rho_{A,k_i}}{\gamma + \mu_1 + \mu_2\rho_{A,k_i}} < 1, \qquad i = 1, 2, \cdots, n.$$

Thus, $\nu F(X_A^*)[F(\nu X_A^*)]^{-1} < I_n$ i.e. $\nu F(X_A^*) < F(\nu X_A^*)$. Hence, F is strictly sublinear.

One can easily check that the off-diagonal elements $a_{i,j}$ $(i \neq j)$ of the matrix $F'(X_A^*)$ is

$$a_{ij} = \frac{\Gamma(b_0 + c_0 + d_0)k_i p(k_j)}{\langle k \rangle(\gamma + \mu_1 + \mu_2\rho_{A,k_i})} > 0, \quad \forall i \neq j \in \{1, 2, \cdots, n\}.$$

Thus, F is a monotone non-decreasing function. We have also that $F(0) = 0$ and $F'(0) = \Gamma(a_0 I_n + (b_0 + c_0 C + d_0)C)$. Therefore $\rho(F'(0)) = \mathcal{R}_0^{(m)} > 1$ iff $\mathcal{R}_0^{(m)} > 1$. Thanks to the graph theory and the irreducibility of the matrix C, $F'(0)$ is irreducible because its associated graph is strongly connected. Thus, we have established the following theorem :

Theorem 2.2.4. If $\mathcal{R}_0^{(m)} \leq 1$, the only equilibrium point of the system is the trivial equilibrium $\mathcal{P}_0$. If $\mathcal{R}_0^{(m)} > 1$ there also exists a unique nontrivial (mosquito-persistent) equilibrium point $\mathcal{P}^*$ in int(Ω).

By Lemma 3.2.1, the trivial equilibrium point $\mathcal{P}_0$ is unstable whenever $\mathcal{R}_0^{(m)} > 1$. We terminate this section by proving the following result which establishes the global stability of the nontrivial equilibrium.

Theorem 2.2.5. If $\mathcal{R}_0^{(m)} > 1$, the nontrivial (mosquito-persistent) equilibrium $\mathcal{P}^*$ of the system (2.15) is GAS on Ω.

Proof. Since $\mathcal{R}_0^{(m)} > 1$, the inequalities

$$\frac{\gamma + \mu_1 + \mu_2\rho_{A,k_i}}{\gamma + \mu_1} < \frac{\mathcal{R}_0^{(m)} k_i p(k_i) + \Gamma \sum_{j=1, j\neq i}^{n} k_j p(k_j)}{\sqrt{\mathcal{R}_0^{(m)}}\,\langle k \rangle}, \quad i = 1, 2, \cdots, n, \tag{2.27}$$

hold for all sufficiently small values X_A. Let $\varepsilon = (\varepsilon_1, \varepsilon_2, \cdots, \varepsilon_n) > 0$ and let X_{A_ε} be so small that in addition to (2.27) the following inequalities also hold :

$$X_{A_\varepsilon} \leq \varepsilon, \tag{2.28}$$

$$X_{F_\varepsilon} := \frac{\sqrt[4]{\mathcal{R}_0^{(m)}}\,(\gamma + \mu_1 + \mu_2 \mathrm{diag}(X_{A_\varepsilon}))X_{A_\varepsilon}}{\Phi} \leq \varepsilon, \tag{2.29}$$

$$X_{Y_\varepsilon} := \frac{\sqrt[4]{\mathcal{R}_0^{(m)}}\,(\mu_F I_n + D_F I_n - D_F C)X_{F_\varepsilon}}{\beta} \leq \varepsilon, \tag{2.30}$$

$$X_{M_\varepsilon} := \frac{(1-r)\gamma}{\sqrt[4]{\mathcal{R}_0^{(m)}}\,(\mu_M + D_M)}\left[I_n + \frac{D_M}{\mu_M}C\right]X_{A_\varepsilon} \leq \varepsilon. \tag{2.31}$$

Let $a_\varepsilon = (X_{A_\varepsilon}, X_{Y_\varepsilon}, X_{F_\varepsilon}, X_{M_\varepsilon})^T$. Then, one has

$$f_1(a_\varepsilon) = \left(1 - \frac{1}{\sqrt[4]{\mathcal{R}_0^{(m)}}}\right)\Phi X_{F_\varepsilon} > 0; \quad f_3(a_\varepsilon) = \frac{(\sqrt{\mathcal{R}_0^{(m)}} - 1)(1-r)\gamma}{\sqrt{\mathcal{R}_0^{(m)}}} X_{A_\varepsilon} > 0;$$

$$\begin{aligned} f_4(a_\varepsilon) &= \left(1 - \frac{1}{\sqrt[4]{\mathcal{R}_0^{(m)}}}\right)\beta X_{Y_\varepsilon} > 0; \\ f_2(a_\varepsilon) &= r\gamma\left[I_n - \frac{\sqrt{\mathcal{R}_0^{(m)}}(N_1^{-1})^{-1}(N_4^{-1})^{-1}[\gamma + \mu_1 + \mu_2 \mathrm{diag}(X_{A_m})]}{\beta\Phi r\gamma}\right]X_{A_m}, \\ &= r\gamma\left[I_n - \frac{\sqrt{\mathcal{R}_0^{(m)}}(a_0 I_n + b_0 I_n C + c_0 I_n C + d_0 I_n C)^{-1}}{\Gamma}\frac{[\gamma + \mu_1 + \mu_2 \mathrm{diag}(X_{A_m})]}{\gamma + \mu_1}\right]X_{A_m} \\ &> 0 \quad \text{if} \quad \frac{\Gamma(a_0 I_n + b_0 I_n C + c_0 I_n C + d_0 I_n C)}{\sqrt{\mathcal{R}_0^{(m)}}} > \frac{\gamma + \mu_1 + \mu_2 \mathrm{diag}(X_{A_m})}{\gamma + \mu_1}, \end{aligned}$$

i.e.

$$f_2(a_\varepsilon) > 0 \quad \text{if} \quad \frac{\gamma + \mu_1 + \mu_2 \rho_{A,k_i}}{\gamma + \mu_1} < \frac{\mathcal{R}_0^{(m)} k_i p(k_i) + \Gamma \sum_{j=1, j\neq i}^{n} k_j p(k_j)}{\sqrt{\mathcal{R}_0^{(m)}}\,\langle k\rangle}, \quad i = 1, 2, \cdots, n.$$

Thus, $f(a_\varepsilon) = (f_1(a_\varepsilon), f_2(a_\varepsilon), f_3(a_\varepsilon), f_4(a_\varepsilon))^T > 0$. Applying once again Theorem 6 in [2] (with $a = a_\varepsilon$ and $b = b_m$), we obtain that the nontrivial equilibrium point $\mathcal{P}^*$ is globally asymptotically stable on $[a_\varepsilon, b_m]$. Since a_ε can be selected to be smaller than any $X > 0$ and b_m can be selected to be larger than any $X > 0$, we obtain that $\mathcal{P}^*$ is asymptotically stable on $\Omega = \mathbb{R}_+^{4n}$ with basin of attraction being at least the interior of Ω. □

2.2.3 The metapopulation model in a heterogeneous landscape

Differences in the distribution of resources create heterogeneity on the network, since patches may have different degrees of attractiveness to mosquitoes. According to [83] we describe how heterogeneity and differences in patch attractiveness to mosquitoes during movement is incorporated. Here, each patch represent a potential breeding-feeding site. The number of hosts is allowed to differ between patches across the local network, introducing heterogeneity. Heterogeneity of breeding sites is incorporated here by taking different values for parameter μ_2 in each patch. In this case, the carrying capacities of breeding sites would be different.

Let H be the total population of hosts in the network and H_k the population of hosts in patches of degree k. The proportion of hosts in patches of degree k is

$$\overline{H}_k = \frac{H_k}{H}, \quad \text{with} \quad \sum_k \overline{H}_k = 1. \tag{2.32}$$

Mosquitoes are attracted by odors released by hosts, this leads to mosquitoes being less likely to leave the patch if their current patch is a home with many hosts and more likely to move out of the patch if there are few hosts [72, 100]. As in [83], we mimic this phenomenon by using a decreasing exponential function to model the movement rate. We assume that heterogeneity of hosts also influence the males dispersal because females go to the hosts for blood-meal and males go to meet females [24]. Note that immature females are not subjected to the attraction of hosts, they diffuse randomly in any direction. We also incorporate the spatial proximity of patches by using a decreasing linear function, since mosquitoes have a limited mobility. Hence, we can define the diffusion rate along any given link of a patch of degree k to a patch of degree k' as

$$D_{kk'} = \frac{D_Y \psi(d_{kk'})}{k} \quad \text{and} \quad D_{kk'} = \frac{D_i \psi(d_{kk'})}{k} e^{-\lambda(\overline{H}_k - \overline{H}_{k'})}, \quad i = M, F, \tag{2.33}$$

where λ is a constant parameter for the decay function, $d_{kk'} = \sqrt{(x_k - x_{k'})^2 + (y_k - y_{k'})^2}$ is the cartesian distance between a node of degree k and a node of degree k'; ψ the distance function defined as

$$\psi(d_{kk'}) = \begin{cases} \dfrac{d_{max} - d_{kk'}}{d_{max}} & \text{if} \quad d_{kk'} < d_{max}, \\ 0 & \text{else}, \end{cases} \tag{2.34}$$

with d_{max} the maximal mobility distance.

Thus, the equations governing the spatio-temporal evolution of anopheles mosquitoes in this case for a n-patches in an uncorrelated network are giving by the system below:

$$\begin{cases} \dot{\rho}_{A,k} &= \Phi_k \rho_{F,k} - (\gamma_k + \mu_{1k} + \mu_{2k}\rho_{A,k})\rho_{A,k}, \\ \dot{\rho}_{Y,k} &= r\gamma_k \rho_{A,k} - (\beta_k + \mu_{Y_k})\rho_{Y,k} - \dfrac{D_Y}{\langle k \rangle}\left(\sum_{k'} k' p(k') \psi(d_{kk'})\right)\rho_{Y,k} + \dfrac{kD_Y}{\langle k \rangle}\sum_{k'} p(k')\psi(d_{kk'})\rho_{Y,k'}, \\ \dot{\rho}_{M,k} &= (1-r)\gamma_k \rho_{A,k} - \mu_{M_k}\rho_{M,k} - \dfrac{D_M}{\langle k \rangle}\left(\sum_{k'} e^{-\lambda(\overline{H}_k - \overline{H}_{k'})} k' p(k') \psi(d_{kk'})\right)\rho_{M,k} \\ &\quad + \dfrac{kD_M}{\langle k \rangle}\sum_{k'} e^{-\lambda(\overline{H}_{k'} - \overline{H}_k)} p(k')\psi(d_{kk'})\rho_{M,k'}, \\ \dot{\rho}_{F,k} &= \beta_k \rho_{Y,k} - \mu_{F_k}\rho_{F,k} - \dfrac{D_F}{\langle k \rangle}\left(\sum_{k'} e^{-\lambda(\overline{H}_k - \overline{H}_{k'})} k' p(k') \psi(d_{kk'})\right)\rho_{F,k} \\ &\quad + \dfrac{kD_F}{\langle k \rangle}\sum_{k'} e^{-\lambda(\overline{H}_{k'} - \overline{H}_k)} p(k')\psi(d_{kk'})\rho_{F,k'}, \end{cases} \tag{2.35}$$

From Theorem 2.2.1 above, one can easily see that (2.35) is a dynamical system in $\mathbb{R}_+^{4n}$. A patch of degree k is at a mosquito-free equilibrium point if $\rho_{A,k} = \rho_{Y,k} = \rho_{M,k} = \rho_{F,k} = 0$.

However, given the complexity of the equations, we do not perform further theoretical analysis for model (2.35). We shall rather focus on numerical analysis in the next section.

2.3 Numerical simulations

To illustrate the various theoretical results of the previous sections, we consider a metapopulation network with five patches and the following connectivities: $k_1 = 2$; $k_2 = 3$; $k_3 = 4$; $k_4 = 1$ and $k_5 = 2$ (see Figure 2.3). Since we do not know what trajectories

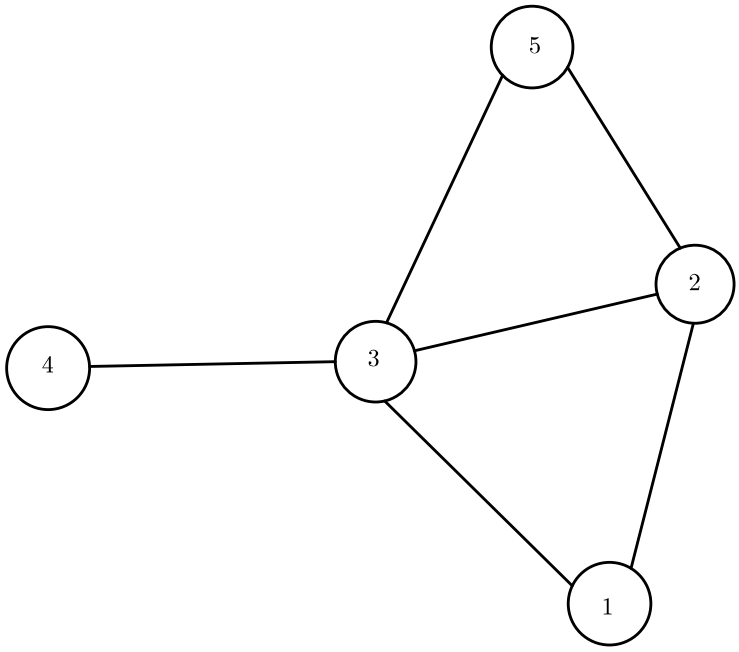

Figure 2.3: An example of a network with five patches.

mosquitoes adopt in reality, we use strategies such as Levy-flight (which are comprised of random sequences of movement-segments with lengths l drawn from a probability distribution function having a power-law tail $p(l) \sim l^{-\mu}$ where $1 < \mu \leq 3$) to optimize foraging efficiency [116]. Thus, we consider an architecture network given by the distribution $p(k) \sim k^{-3}$ [27, 119].

Models (2.15) and (2.35) are both simulated by using data from recent works. These data are summarized in Table 2.1. As far as mosquito dispersal is concerned, some studies have shown that daily flights range from 200 to 400 m, where the maximum distance recorded is 661 m [95]. We run all simulations with the following initial conditions: the total number mosquitoes in aquatic stages is 1500, 1000 young mosquitoes are females not yet laying eggs, 1000 are males, while 1250 are fertilized and eggs laying females. They are evenly distributed across the network.

2.3.1 General dynamics

In this subsection, we numerically illustrate the asymptomatic behavior of model (2.15). For that, we consider a network of metapopulation with five patches. The dynamics of all compartments are very similar to each other. Hence, only the graphs of mosquitoes at the aquatic stage and total flying mosquito population (that is, $Y + M + F$) are presented here.

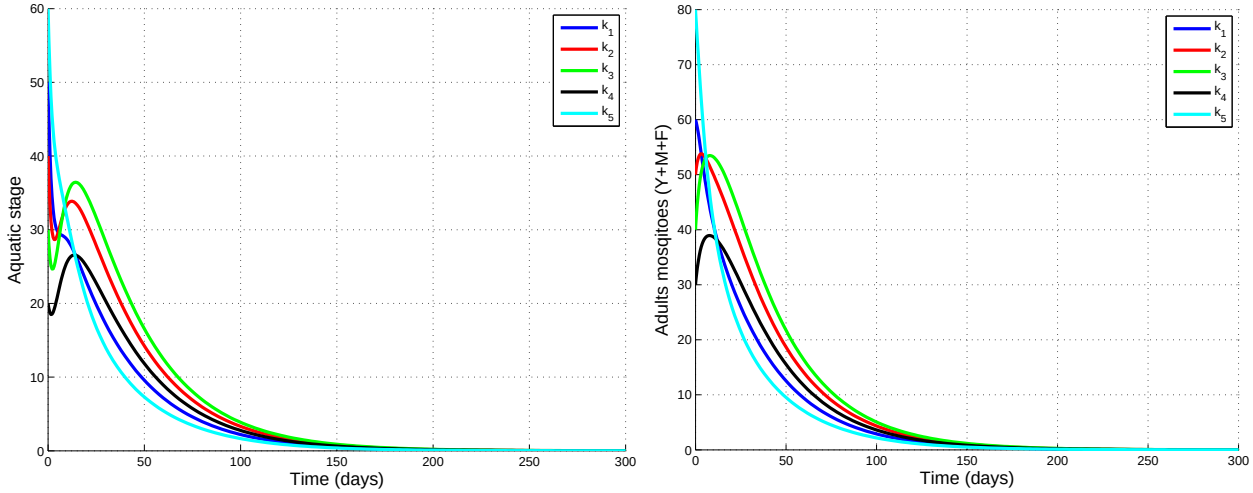

Figure 2.4: Simulation results showing the GAS of the trivial equilibrium $\mathcal{P}_0$ for the basic model when $\Phi = 0.5$, $D_Y = D_M = D_F = 0.1$ and $\mathcal{R}_0^{(m)} \leq 1$. All other parameters are as in Table 2.1.

Figure 2.4 presents the trajectories of model (2.15) for all patches when $\Phi = 0.5$, $D_Y = D_M = D_F = 0.1$ and the basic offspring number $\mathcal{R}_0^{(m)}$ is less than one ($\mathcal{R}_0^{(m)} = 0.6531$). From this figure, we can see that the mosquito populations die out in all patches. Thus, the trajectories converge to the trivial equilibrium as shown in Theorem 2.2.2.

Figure 2.5 plots the trajectories of system (2.15) when $\Phi = 10$, $D_Y = D_M = D_F = 0.1$ and the basic offspring number $\mathcal{R}_0^{(m)}$ is greater than one ($\mathcal{R}_0^{(m)} = 13.0612$). This illustrates the fact that the mosquitoes are always present in all patches and the trajectories converge to the nontrivial equilibrium as established in Theorem 2.2.5.

2.3.2 Impact of dispersal on population dynamics

To evaluate the impact of dispersal on population dynamics, we carry out in Figure 2.6 numerical simulations (when $\Phi = 10$) on system (2.15) both without and with dispersal. This figure shows that persistence of mosquito population is more important in the presence of dispersal than in the case without dispersal, especially in high-degree patches.

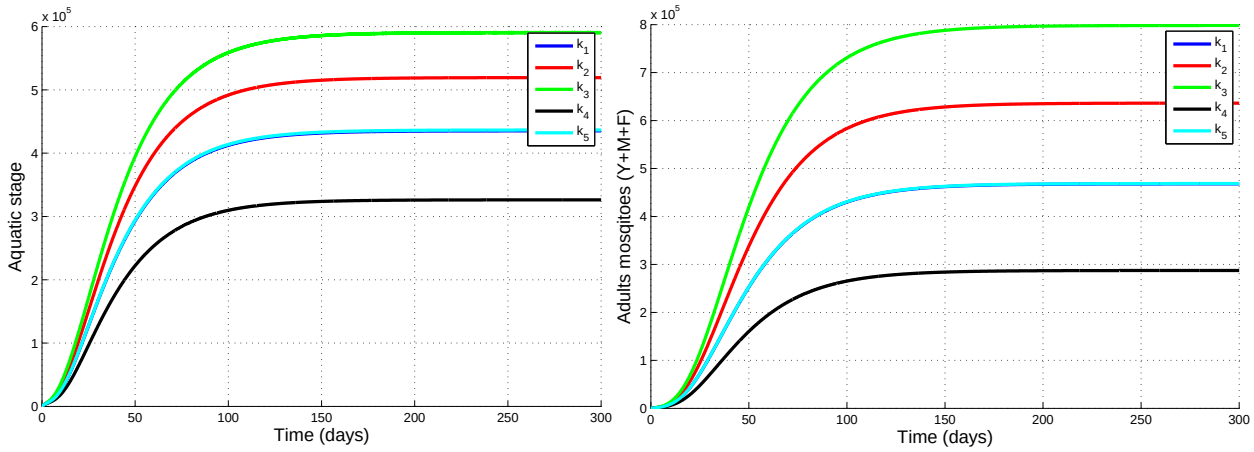

Figure 2.5: Simulation results showing the GAS of the nontrivial equilibrium $\mathcal{P}^*$ when $\Phi = 10$, $D_Y = D_M = D_F = 0.1$ and $\mathcal{R}_0^{(m)} > 1$. All other parameters are as in Table 2.1.

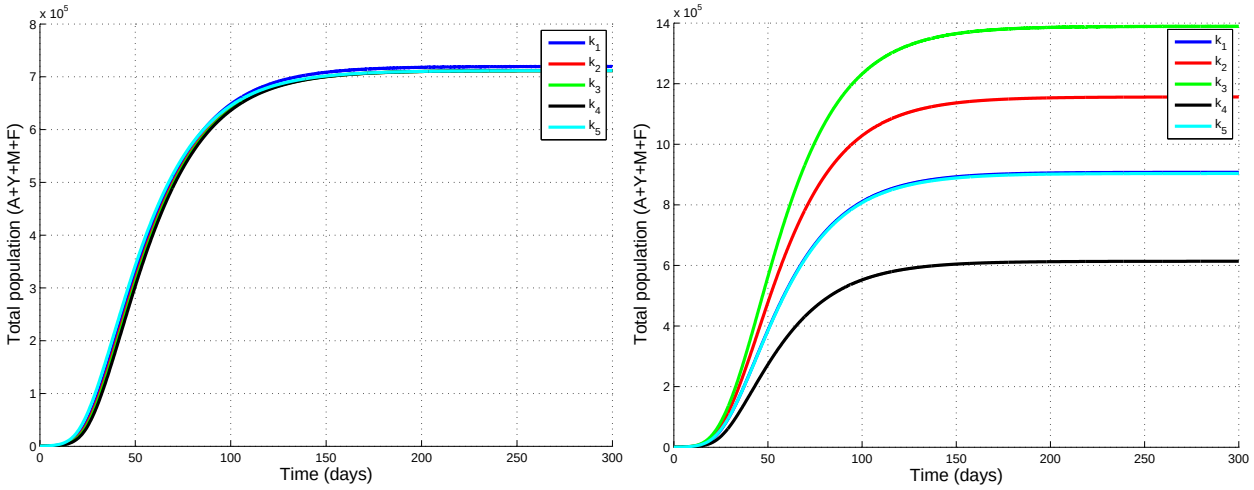

Figure 2.6: Trajectories plots of model (2.15) without dispersal (left) and with dispersal (right) when $\Phi = 10$: the total mosquito population increases as the diffusion coefficients increase.

2.3.3 Impact of the heterogeneous connectivity of patches on population dynamics

To investigate the significance of heterogeneous connectivity of patches on vector population dynamics, system (2.15) is simulated in Figure 2.7 with variable degrees of patches.

Figure 2.7 illustrates the fact that, with the same diffusion coefficients ($D_M = D_Y = D_F$), the total mosquito population increases as the connectivity of the patch increases. This suggests that the heterogeneous connectivity of patches play an important role on vector population dynamics. This heterogeneity may come from the daily productivity and

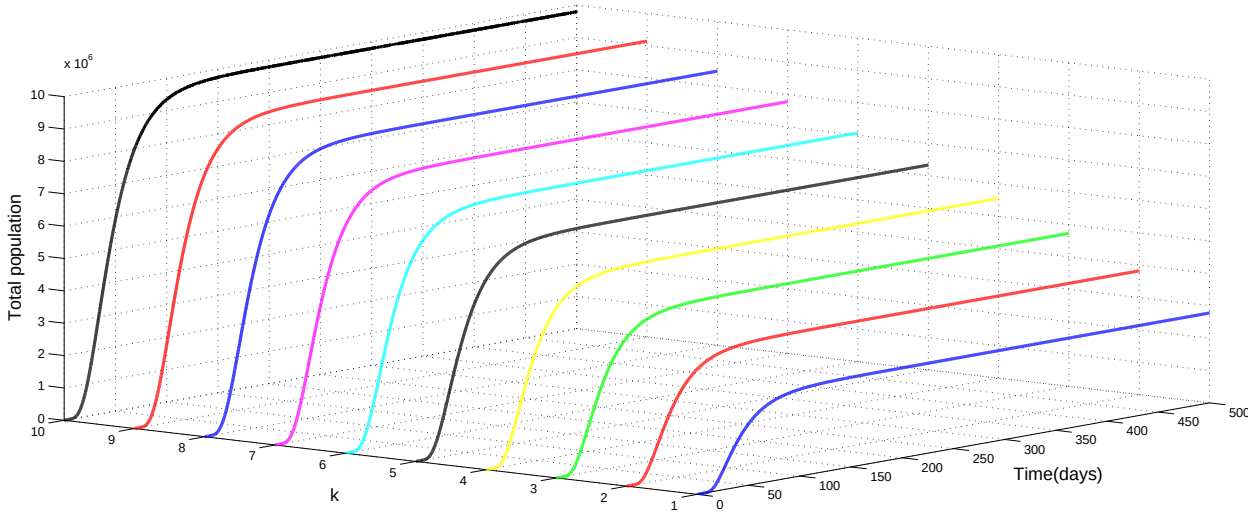

Figure 2.7: Mosquito population in patches of degree $k = 1, 2, ..., 10$, when $\Phi = 10$ and $D_M = D_Y = D_F = 0.1$: the total mosquito population increases as the patch connectivity increases.

destruction of some breeding sites, since small pools of water are continually destroyed and reformed [154].

2.3.4 Impact of migration and heterogeneity on mosquito spread

In this section, numerical simulations are carried out to investigate the role of dispersal/diffusion and heterogeneity on mosquito spread. Models (2.15) and (2.35) are both simulated with different values of Φ in each patch. In order to observe more effects of the migration on the dynamics of model (2.15) and (2.35), we consider the hypothetical scenario where the mosquito-persistent equilibrium is GAS in the patch of minimal degree (patch 4) and unstable in the other patches (patch 1, 2, 3, 5). Model (2.35) is simulated with $\overline{H}_{k_1} = 0.6$, $\overline{H}_{k_2} = 0.07$, $\overline{H}_{k_3} = 0.06$, $\overline{H}_{k_4} = 0.03$, $\overline{H}_{k_5} = 0.24$, $d_{\max} = 661$ m and $\lambda = 0.5$. Let $\mathcal{R}_0^{(i)}$, $i = 1, 2, 3, 4, 5$, denotes the basic offspring number for the local population of anopheles mosquito in patch i as defined in (2.3). Choose $\Phi_1 = \Phi_2 = \Phi_3 = \Phi_5 = 0.5$, $\Phi_4 = 10$ so that $\mathcal{R}_0^{(1)} = \mathcal{R}_0^{(2)} = \mathcal{R}_0^{(3)} = \mathcal{R}_0^{(5)} = 0.5714 < 1$ and $\mathcal{R}_0^{(4)} = 11.4286 > 1$. It is observed from Figure 2.8 that, in the absence of migration/diffusion (i.e. $D_M = D_Y = D_F = 0$), the mosquito-persistent equilibrium point is unstable in patches 1, 2, 3, 5 and stable in the fourth patch, as expected.

Figures 2.9-2.12 present the mosquito spread from an mosquito-persistent patch (patch 4) to mosquito-free patches (patches 1, 2, 3, 5) under different scenario when $D_M = D_Y = D_F = 0.1$.

Observing these latter figures, one can see that in the presence of dispersal, mosquitoes moving out of an mosquito-persistent patch (patch 4) migrate into the mosquito-free patches

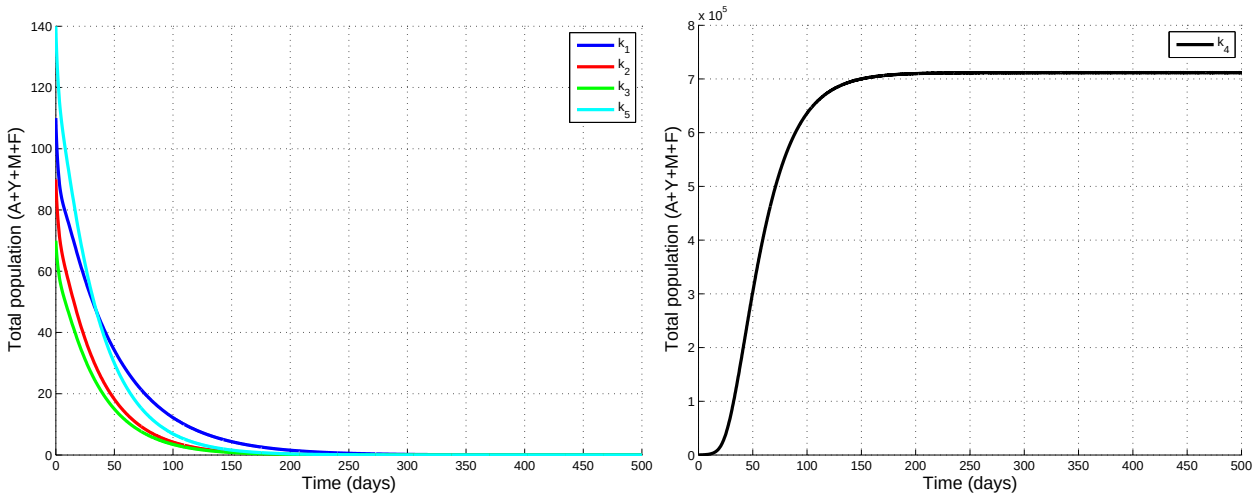

Figure 2.8: Simulation results of systems (2.15) and (2.35) showing the mosquito population in mosquito-free patches (left) and mosquito-persistent patch (right) in absence of migration. $\mathcal{R}_0^{(i)} < 1, i = 1, 2, 3, 5$ and $\mathcal{R}_0^{(4)} > 1$. All other parameters are as in Table 2.1.

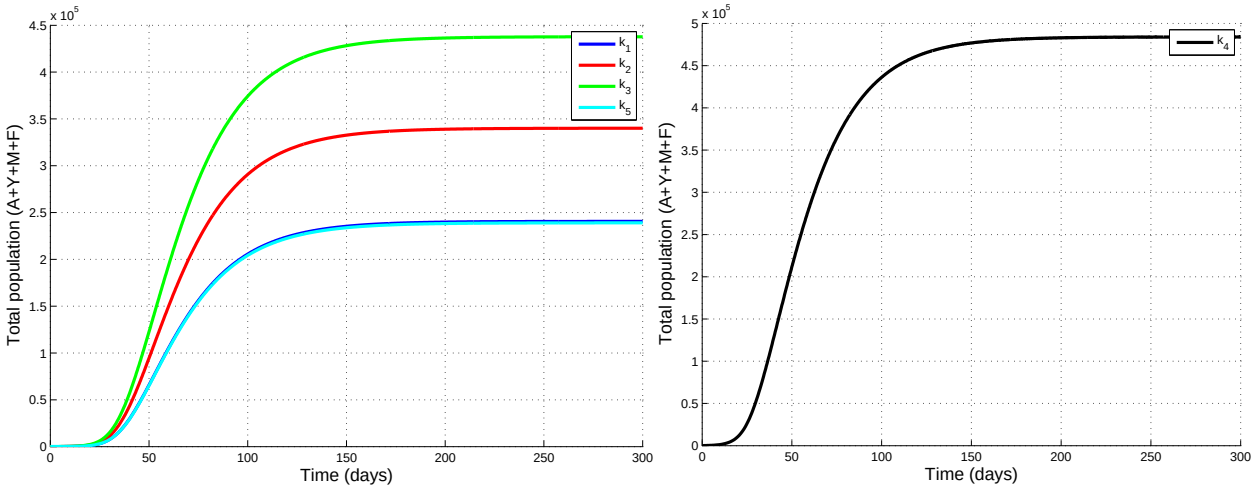

Figure 2.9: Simulation result showing the mosquito spread from mosquito-persistent patch (right) to mosquito-free patches (left) in a homogeneous landscape (Eq. 2.15) with $D_M = D_Y = D_F = 0.1$ and all other parameters are as in Table 2.1. $\mathcal{R}_0^{(i)} < 1, i = 1, 2, 3, 5$ and $\mathcal{R}_0^{(4)} > 1$.

(patches 1, 2, 3, 5). This illustrates the fact that mosquito dispersal could lead to a larger presence of mosquitoes in all patches and, shows the important effects of dispersal and connectivity of patches on population spread. However, this diffusion varies according to the type of landscape.

(a) Dispersal in a homogeneous landscape

Figure 2.9 presents the trajectories of the mosquito spread from mosquito-persistent patch (right) to mosquito-free patches (left) in a homogeneous landscape (Eq. (2.15)).

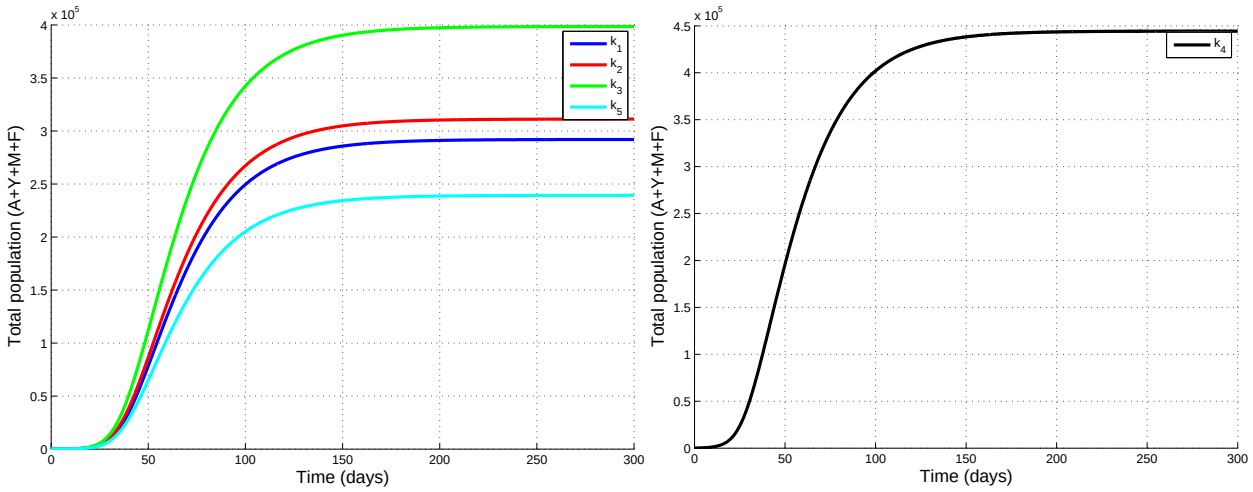

Figure 2.10: Simulation results showing the mosquito spread from mosquito-persistent patch (right) to mosquito-free patches (left) in a heterogeneous landscape (heterogeneity of hosts and homogeneity of breeding sites) with $\psi(d_{kk'}) = 1, \forall k, k', D_M = D_Y = D_F = 0.1$ and all other parameters are as in Table 2.1. $\mathcal{R}_0^{(i)} < 1, i = 1, 2, 3, 5$ and $\mathcal{R}_0^{(4)} > 1$.

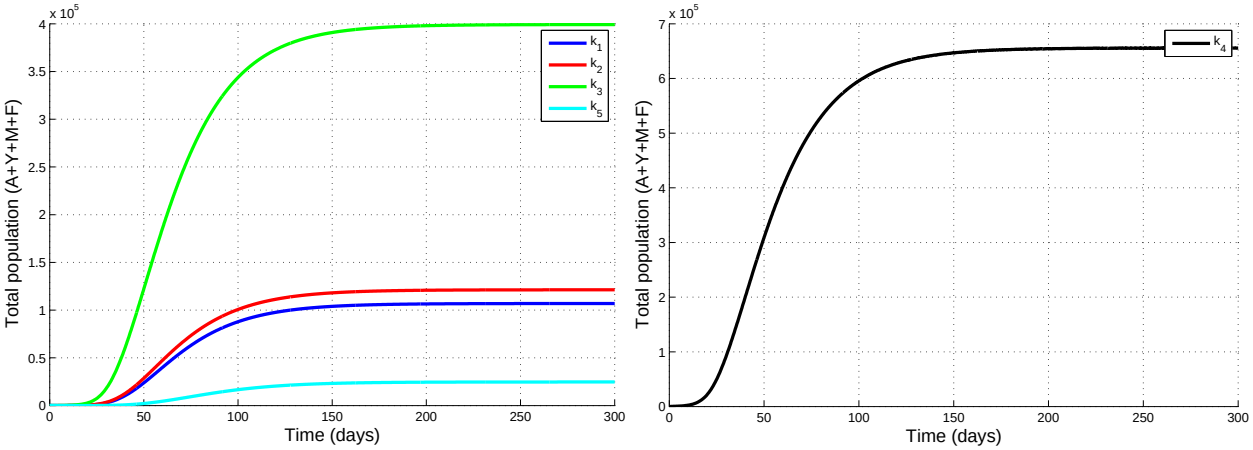

Figure 2.11: Simulation results showing the mosquito spread from mosquito-persistent patch (right) to non mosquito-persistent patches (left) in a heterogeneous landscape (heterogeneity of hosts and homogeneity of breeding sites) with $\psi(d_{kk'})$ as in (2.34), $D_M = D_Y = D_F = 0.1$ and all other parameters are as in Table 2.1. $\mathcal{R}_0^{(i)} < 1, i = 1, 2, 3, 5$ and $\mathcal{R}_0^{(4)} > 1$.

We observe in this case that mosquitoes coming from mosquito-persistent patch (patch 4) migrate more to the high-degree patches (see patches 3 and 2) and equitably to the patches with equal degree (see patches 1 and 5).

(b) Dispersal in a heterogeneous landscape

Figure 2.10 gives numerical solutions of model (2.35), depicting the mosquito spread from mosquito-persistent patch (right) to non mosquito-persistent patches (left) in a heterogeneous landscape (heterogeneity of hosts and homogeneity of breeding sites), when

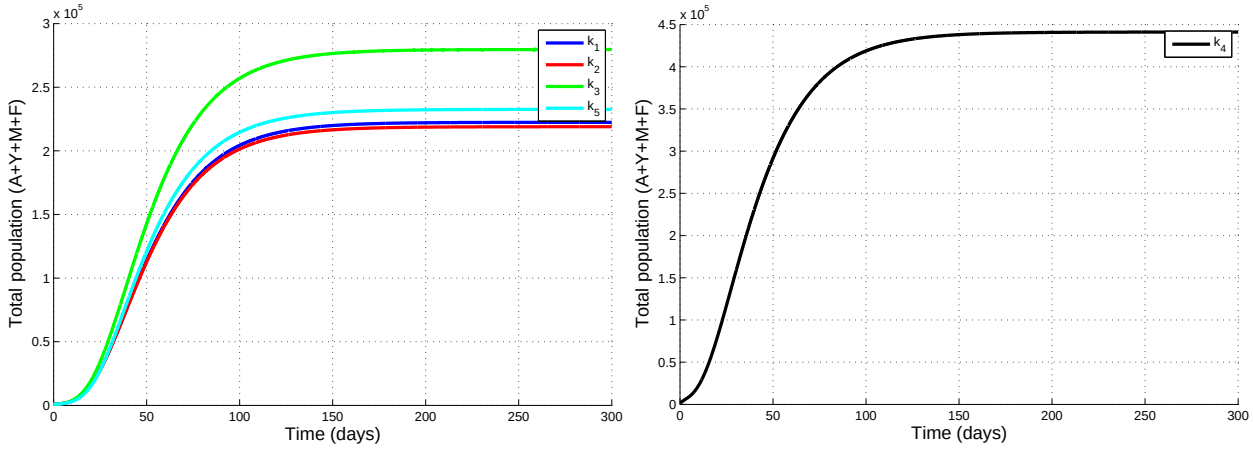

Figure 2.12: Simulation result showing the mosquito spread from mosquito-persistent patch (right) to non mosquito-persistent patches (left) in a heterogeneous landscape (heterogeneous hosts and breeding sites) with $\psi(d_{kk'}) = 1$, $\forall k, k'$, $\mu_{21} = 10^{-4}$, $\mu_{22} = 10^{-3}$, $\mu_{23} = 10^{-2}$, $\mu_{24} = 10^{-5}$, $\mu_{25} = 10^{-5}$ and $D_M = D_Y = D_F = 0.1$ $D_M = D_Y = D_F = 0.1$. $\mathcal{R}_0^{(i)} < 1$, $i = 1, 2, 3, 5$ and $\mathcal{R}_0^{(4)} > 1$.

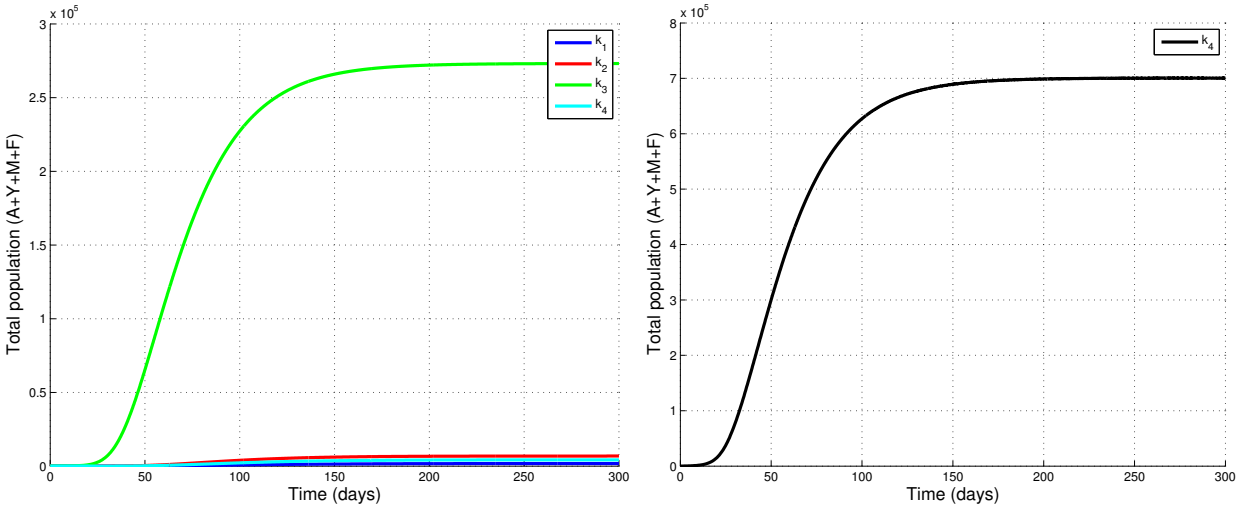

Figure 2.13: Simulation result showing the mosquito spread from mosquito-persistent patch (right) to non mosquito-persistent patches (left) (heterogeneity of hosts and homogeneity of breeding sites) with $\psi(d_{kk'})$ as in (2.34), when distances between patches 1, 2, 3, 5 are large.

distance has no effect on mosquito flights (i.e. $\psi(d_{kk'}) = 1$, $\forall k, k'$). Even though a great number of mosquitoes moves into the patches of high degree, the dispersal becomes more important in the patches with more hosts.

Figure 2.11 simulates the solutions of model (2.35) and displays the mosquito spread from mosquito-persistent patch (right) to non mosquito-persistent patches (left) in a heterogeneous landscape (heterogeneity of hosts and homogeneity of breeding sites), when distance affects mosquito dispersal (i.e. $\psi(d_{kk'})$ as in (2.34), with $d_{k_3k_4} = 300$ m, $d_{k_5k_1} = 370$

m, $d_{k_3k_1} = 361$ m, $d_{k_3k_2} = 361$ m, $d_{k_3k_5} = 400$ m, $d_{k_2k_5} = 380$ m). As in the latter Figure 2.10, similar result is observed, with the difference in that the mosquito dispersal from mosquito-persistent patch (patch 4) to mosquito-free patches (patches 1, 2, 3 and 5) is less important in this case.

Figure 2.12 presents the simulation results of model (2.35), showing the mosquito spread from mosquito-persistent patch (right) to mosquito-free patches (left) in a heterogeneous landscape (heterogeneity of hosts and breeding sites), with $\mu_{21} = 10^{-4}$, $\mu_{22} = 10^{-3}$, $\mu_{23} = 10^{-2}$, $\mu_{24} = 10^{-5}$, $\mu_{25} = 10^{-5}$ and $\psi(d_{kk'}) = 1$, $\forall k, k'$. From this figure, it is noticeable that heterogeneity of hosts and breeding sites greatly influences the mosquito dispersal and their spatial distribution. This suggests that the heterogeneous connectivity of patches and heterogeneous distribution of hosts and breeding sites may play an important role on the spatial distribution of mosquitoes.

Figure 2.13 simulates model (2.35) and shows that the mosquito spread from mosquito-persistent patch (right) to mosquito-free patches (left) in a heterogeneous landscape (heterogeneity of hosts and homogeneity of breeding sites), with $\psi(d_{kk'})$ as in (2.34) when patches are highly distanced from each other and close to the maximal distance d_{max} between nodes ($d_{k_3k_4} = 500$ m, $d_{k_5k_1} = 510$ m, $d_{k_3k_1} = 589$ m, $d_{k_3k_2} = 539$ m, $d_{k_3k_5} = 400$ m, $d_{k_2k_5} = 539$ m). From this figure, one observes that mosquito migration rate to distant patches is very low. This is coherent with the known preference of the mosquito dispersal: indeed, according to [45] the dispersal of adult mosquitoes can be classified into long-range and short-range dispersals. Long-range dispersal is often unintentional and aided by wind or human transport while short-range dispersal is often intentional. Furthermore, Figure 2.13 shows that the availability and abundance of sites have a strong influence on the distance that individual adult female mosquitoes need to fly in order to lay their eggs, since spatial distance between patches is large when breeding sites are eliminated from neighborhoods of hosts or are not available in most patches. Similar findings were obtained in [22]. Thus, more efforts to reduce breeding sites in close proximity to houses (mechanical control) is needed and can be very efficient as a vector control strategy.

Our simulations results in homogeneous landscape (Eq. 2.15) and heterogeneous landscape (Eq. 2.35) reveal that the heterogeneous connectivity of patches plays an important role on the spatial distribution of mosquito population. Simulations in a homogeneous landscape indicate that there is a linear relationship between connectivity of patches and mosquitoes distribution (see Figures 2.6 and 2.9). However, when there are heterogeneities in the network (hosts, distances), this linear relationship is perturbed and induces a strong influence on spatial distribution and population dynamics of mosquitoes (see Figures 2.10-2.13).

2.4 Conclusion and perspectives

In this paper, we have developed a reaction-diffusion type model to describe the spatial evolution of the anopheles mosquito in heterogeneous complex metapopulations and assess the influences of larvae habitats (breeding-feeding sites) connectivity and vector on the spatial distribution and populations dynamics of mosquitoes. We have focused on the migration of mosquitoes from one patch to another in both homogeneous and heterogeneous landscapes. The spatial configuration was given by the degree $p(k)$ and the conditional probabilities $P(k'/k)$.

For uncorrelated networks in a homogeneous landscape, we have derived an explicit formula for the basic offspring number, $\mathcal{R}_0^{(m)}$, which has been proven to be a sharp threshold parameter for our model. The most influential parameter on the expression for $\mathcal{R}_0^{(m)}$ is the number of eggs at each deposit Φ. Using the theory of monotone operators, we have established the global stability of equilibrium points. Precisely, we have shown that the mosquito-free equilibrium is GAS whenever $\mathcal{R}_0^{(m)} \leq 1$ and unstable otherwise. In the case where $\mathcal{R}_0^{(m)} > 1$, we have shown that there exists a unique mosquito-persistent equilibrium, which is GAS.

For uncorrelated networks in a heterogeneous landscape, we have only carried out numerical studies. Comparing our simulation results in Figures 2.6 - 2.12, we have concluded that numerous factors considered in our models play important roles in spatial distribution of mosquitoes and could lead to a larger amount of mosquitoes. Further, our sensitivity analysis results have revealed that an efficient strategy to reduce the amount of mosquitoes in all patches could be to control the production of eggs (by mechanical control for example) and minimize the migration of female mosquitoes.

To summarize our contributions in few words, the methodology and results we have obtained are as follows:

• From the modelling perspective, we have extended to a complex network of patches the single patch models in [154, 2] by incorporating the dispersal of mosquitoes and patch connectivity.

• From the theoretical and numerical perspectives, we have examined the impacts of larval habitat connectivity and mosquito dispersal in a homogeneous and a heterogeneous landscapes on the persistence of mosquitoes populations.

• From the qualitative and quantitative aspects for uncorrelated networks have obtained the following analytical results:

1. The bifurcation/threshold parameter (basic offspring number) has been explicitly computed.

2. The sensitivity analysis of the threshold parameter has been performed.

3. A simple and digestive proof based on Hethcote-Thieme fixed point theorem [65], of a unique mosquito-persistent equilibrium has been provided.

4. Contrary to the few existing works where, Lyapunov-LaSalle techniques are usually used, the monotone operator approach [124] has been the main ingredient here, for the establishment of the global asymptotic stability of both mosquito-free and mosquito-persistent equilibria.

The advantage of the above discrete-space model is that one can easily assess diseases vector control strategies, because the discrete space enables easy representation of interventions that cover sets houses or villages. Nevertheless, this approach constrain the modeled mosquito movements to follow a limit set of trajectories. As immediate possible extension of this work, we use the continuous-space approach to capture mosquito dispersal.

CHAPTER 3

Contents

MATHEMATICAL ANALYSIS OF A SPATIO-TEMPORAL MODEL FOR THE POPULATION ECOLOGY OF ANOPHELES MOSQUITO

In this chapter, I propose a novel model for the population dynamics of mosquitoes by considering the dispersal states of female mosquitoes of oviposition's cycle and spatial variations. From the modelling perspective, a general functional form of eggs oviposition rate is used including the Malthusian, the Verhlust-Pearl logistic, the Hassell and the Maynard-Smith-Slatkin functions. From the theoretical and numerical perspectives, the study is done in two steps using the more realistic birth Maynard-Smith-Slatkin function. Firstly, we consider an ordinary differential equations model and show that the mosquito-free equilibrium (MFE) is globally asymptotically stable whenever the basic offspring number of the ODE model is less than unity. Using a fluctuation argument, we prove that the unique mosquito-persistent equilibrium (MPE) is globally attractive, whenever the basic offspring number of the ODE model exceeds the unity. Moreover, the temporal model undergoes a Hopf bifurcation in the absence of density-dependent mortality in the aquatic stage of mosquitoes. Secondly, the temporal model is extended into an advection-reaction-diffusion model in order to account for the movement of mosquitoes and their spatial source of heterogeneity. We establish the uniform persistence and the existence of at least one positive steady state whenever the spatial basic offspring number of the PDE model is greater than unity. Finally, for the case study of malaria vector agent (Anopheles mosquito), we construct a nonstandard finite difference scheme which is dynamically consistent with the features of the continuous model to illustrate our results, including the spatial heterogeneity of mosquito resources.

3.1 Introduction

Among all infectious diseases of humans, vector-borne diseases (VBDs) constitute a major cause of human mortality and morbidity. They account for 17% of the estimated global burden of all infectious diseases [149, 150]. Mosquitoes are the best known vectors

of such diseases. They are responsible for many diseases throughout the world such as malaria, yellow fever, chikungunya, west Nile virus, dengue fever, Zika virus and other arboviruses [3, 101]. These diseases are transmitted from human-to-human through effective mosquito bites. The transmission cycle is essentially driven by the human bite habit of the mosquito [104]. Typically, the vector interacts with a human being. Then depending on the disease status of both organisms, they will either infect or be infected.

Due to the significant burden caused by mosquitoes on human health, specifically as reflected through the persistence and/or resurgence of vector-borne diseases, mosquitoes have become a target of medical, veterinary and conservation research since the nineteenth century [108]. In order to devise effective control and realistic control methods, it is crucial and essential to study the mosquitoes population dynamics, their interaction with their biotope and subsequently the epidemiology of mosquito-borne diseases [88, 146].

Like many other insect species, mosquitoes can move and disperse in any direction for various reasons such as searching for resource availability. At local scales (i.e. from 100 m to 1 km), mosquito behavior and ecology play an important role in determining the distribution of transmission [83]. The spatial distribution of the anopheles has shown great potential to affect malaria transmission intensity [146, 162]. The success and optimal impact of methods for controlling mosquito population (e.g. sterile insect technique (SIT), genetically modified mosquitoes (GMM) or mechanical control) are based on a good knowledge of the biology and the behavior of mosquitoes, as well as on an accurate modelling of their dispersal. Thus, to achieve a high level of effectiveness in reducing the mosquito population, control interventions should consider mosquito location and its ability to move.

In view of the challenge and high costs to conduct field experiments, mathematical modeling add value to validate and improve vector control strategies. Mathematical models have proven to be useful in gaining insights into the interactive dynamics and control of mosquito populations [1, 2, 14, 46, 104, 105, 108], as well as into the influence of mosquito mobility and dispersal [30, 42, 41, 68, 83, 88, 126, 132, 158].

Partial differential equations (PDEs) constitute a classical setting to model real-life situations such as dispersal [145, 162, 163]. For linear PDEs, the theory and the corresponding constructive treatment by numerical methods are well developed (see for instance the famous books [31, 32, 33, 34]). However, the complexity of biological processes and particularly the strong nonlinearity in the transmission dynamics of diseases in time and space lead to mathematical challenging nonlinear PDEs, which include advection-reaction-diffusion equations and cross-diffusion equations [102, 125]. It is therefore not surprising that the authors could identify only very few PDEs models on mosquito population dynamics that have investigated the well-posedness and the asymptotic behavior of the solutions [41, 42, 68, 126, 132, 158]. A metapopulation setting has been used in [83, 88] for anopheles mosquito population dynamics as an intermediate approach between tem-

poral and spatio-temporal modeling. To explore the temporal and spatial dispersal of the mosquitoes, the authors in [68, 126, 132, 158] proposed advection-reaction-diffusion models where the mosquito population is divided into two stages: aquatic and adult female stages. These studies gave sufficient conditions for mosquitoes to persist and spread or to vanish. However, the oviposition/gonotrophic cycle has been recognized as an important feature that may determine population levels, distribution and biting behavior of mosquitoes. Thus, it is necessary to take into account all stages in the gonotrophic cycle (questing, resting and breeding females) for the adult female mosquitoes in order to get insights into the behavior and dynamics of mosquitoes. The ultimate purpose of this paper is to extend works in [68, 126, 132, 158], as well as the temporal models in [1, 2, 108] into an advection-reaction-diffusion system in which spatial heterogeneity is taken into consideration explicitly.

We develop models that incorporate both intrinsic dynamics and spatial variation of mosquitoes, taking into consideration the dynamics of the human-vector interaction. We will start with a temporal model that allows a general description of the mosquito's growth. This initial model captures the mosquito oviposition cycle as well as its main behavior (which could be useful when one considers chemical or biological control tools, such as SIT or GMM). Moreover, unlike the works in [2, 42, 88], where a constant generating rate was used for the population in the aquatic stage, we consider a more general function for egg oviposition rate. Next, we will extend the obtained temporal model to a PDE system by adding both advection and diffusion terms that reflect the mosquito's mobility. We study the global well-posedness and the asymptotic behavior of the solutions of this PDE model. Finally, we assess the impact of mosquito dispersal, heterogeneous distribution of mosquito resources (hosts), and other parameters on the spatial distribution, dynamics and persistence of mosquito populations. As mentioned earlier, the nonlinearity of the ODE model and its extended PDE counterpart results in challenging mathematical equations. This necessitates the use of a variety of techniques, methods and approaches including Lyapunov-Lasalle techniques, monotone dynamical systems approach, semigroup applications, fluctuation method and spectral theory approach.

The paper is organized as follows. In Section 3.2, we present a compartmental temporal model, which is analyzed quantitatively (e.g. existence/uniqueness of positive solutions, existence of equilibria points, etc...) and qualitatively (e.g. global stability of equilibria, existence of Hopf bifurcation). In Section 3.3, we extend the temporal model to an advection-reaction-diffusion system of equations, the global well-posedness, the asymptotic behavior and the threshold-type dynamics of which are investigated. In Subsection 3.3.4, a case study is handled, namely malaria which is the world's most devastating parasitic infectious disease caused by anopheles mosquitoes as vector agents. We develop a nonstandard finite difference (NFSD) scheme, which is dynamically consistent with the continuous model as illustrated by numerical simulations in which parameters relevant

to the population biology of adult female anopheles mosquitoes are used. Concluding remarks that show how our findings fit in the literature and a brief discussion are provided in Section 3.4.

3.2 Temporal model

3.2.1 Model formulation

It is well known that there are two main stages in the development of mosquitoes represented by the aquatic and the adult stages. The aquatic stage, reduced to one compartment (A), gathers eggs, larvae and pupae [2, 42]. The adult stage is divided into five compartments including four for females and one for males as follows: immature females (Y), feeding/questing females (Q), resting females (U), breeding females (W) (or more precisely "egg laying females") and males (M). We assume that there is no sex differences for mosquitoes in the aquatic stage. Moreover, after emergence, mosquitoes are distributed between the immature female and the male compartments. We denote by r the sex ratio of emerging females. According to [37], r can be set to $\frac{1}{2}$ in the case when the number of emerging females and males are balanced. We further assume that, a female mates only once with a male during her lifespan. After mating, immature females start their gonotrophic cycle by entering the feeding female compartment [7]. The gonotrophic cycle starts with a blood meal and ends with the first laid egg [7]. Then, after blood meals, females progress to the resting compartment, allowing egg maturation. Afterward, they pass into the breeding compartment, seeking for a breeding site to deposit eggs. Once eggs are deposited, these females start a new gonotrophic cycle. The eggs laid by the breeding females supply the aquatic stage. Note that unlike female mosquitoes where four sub-compartments are considered due to their involvement in the gonotrophic cycle, we only consider one compartment for the males.

At time t, and following [28, 105], we assume that the population in the aquatic stage is generated from breeding females by a decreasing, continuously differentiable and positive function which is a general form of the eggs oviposition. The population in the aquatic stage is decreased by maturation to adult mosquitoes (at the rate γ), density-independent mortality (at the rate μ_1), and density-dependent mortality (at the rate μ_2). After mating with males, immature females exit breeding sites and arrive at the human resource where they become feeding/questing females Q. The number of matings that occur per unit of time is β (mating rate). Actually, β can be regarded as the product of the likelihood of a mating producing eggs, the (fixed) proportion of the population that is female, the likelihood that an appropriate place can be found so that, when the eggs are laid they will certainly hatch. Also, when the number of males is large, we expect that immature females will have

no difficulty finding a mate [2, 42]. Thus, immature females become feeding females at rate β. Resting females die at rate μ_U. At the human habitat, questing females interact with humans by mass action contact, during which they can either survive to reproduce or get killed [104, 105]. Questing females that feed successfully become resting females at rate $\alpha\varphi H$, where φ is the biting rate of questing females, α ($\alpha \in [0,1]$) is the probability of successfully taking a blood meal, and H is a parameter representing the density of human habitats. Questing females die at rate μ_Q. Once settled, resting females become breeding females at rate a. The compartment of breeding females is affected by a mortality rate μ_W. After laying eggs, breeding females will begin to search blood meals and we assume that they are attracted to humans and enter the questing class at rate $\frac{bH}{H+K}$, where $\frac{H}{H+K}$ represents the proportion of resting females that take human blood as opposed to those that feed on other animals [52, 105, 108]. K is a positive constant representing a constant alternative food source for the site, and b is a positive constant representing the rate at which breeding females leave the site to restart their gonotrophic cycle.

The above mentioned biological and entomological descriptions lead to the following deterministic and autonomous system of nonlinear differential equations whose flow diagram, state variables and parameters are given in Figure 3.1 and in Table 3.2, respectively:

$$\begin{cases} \dot{A} &= B(W)W - [\gamma + \mu_1 + \mu_2 A]A, \\ \dot{Y} &= r\gamma A - [\mu_Y + \beta]Y, \\ \dot{M} &= (1-r)\gamma A - \mu_M M, \\ \dot{Q} &= \beta Y + \dfrac{bH}{H+K}W - [\alpha\varphi H + \mu_Q]Q, \\ \dot{U} &= \alpha\varphi HQ - [a + \mu_U]U, \\ \dot{W} &= aU - \left[\dfrac{bH}{H+K} + \mu_W\right]W, \end{cases} \tag{3.1}$$

In this study, $B(W)$ is the general form of the eggs oviposition function. It is assumed that function $B(W)$ is strictly non-negative, continuously-differentiable and satisfies the following conditions:

- $B(0) = N_{egg}$,
- $B'(W) \leq 0,\ \forall W \geq 0$, (3.2)
- $B(W)W$ is monotone or bounded by $N_{egg}L$,

where, N_{egg} is the average number of eggs laid per fertilized female per day, and $L > 0$ is the environmental carrying capacity of fertilized females.

Let $\mathcal{R}_0^{ode}$ denote the basic offspring number of model (3.1) and $F_{\mathcal{R}_0^{ode}}$ the function given by

$$F_{\mathcal{R}_0^{ode}}(s) = \nu_1 \mathcal{R}_0^{ode} B\left(\frac{\nu_1 \mathcal{R}_0^{ode}}{N_{egg}} s\right) - N_{egg}(\nu_1 + \mu_2 s), \ \forall\ s \geq 0, \tag{3.3}$$

where ν_1 is defined below in (3.5). We further assume that the general egg oviposition function B is such that

$$F_{\mathcal{R}_0^{ode}}(0) F_{\mathcal{R}_0^{ode}}(+\infty) < 0, \text{ when } \mathcal{R}_0^{ode} > 1. \tag{3.4}$$

In Table 3.1, we have gathered typical examples of function $B(W)$, which are used in the literature.

Table 3.1: Examples of oviposition function $B(W)$ used in the literature which satisfy (3.2)-(3.4).

Names	$B(W)$	$B(0)$	Sources
Malthus (B_M)	N_{egg}	N_{egg}	[2, 28]
Verhulst-Pearl logistic (B_L)	$N_{egg}\left(1 - \frac{W}{L}\right),\ W < L$	N_{egg}	[1, 12, 28, 105]
Maynard-Smith-Slatkin (B_S)	$\frac{N_{egg}}{1+\left(\frac{W}{L}\right)^n},\ n > 0$	N_{egg}	[1, 12, 28, 105]
Hassell (B_H)	$\frac{N_{egg}}{\left(1+\frac{W}{L}\right)^n},\ n > 0$	N_{egg}	[12]

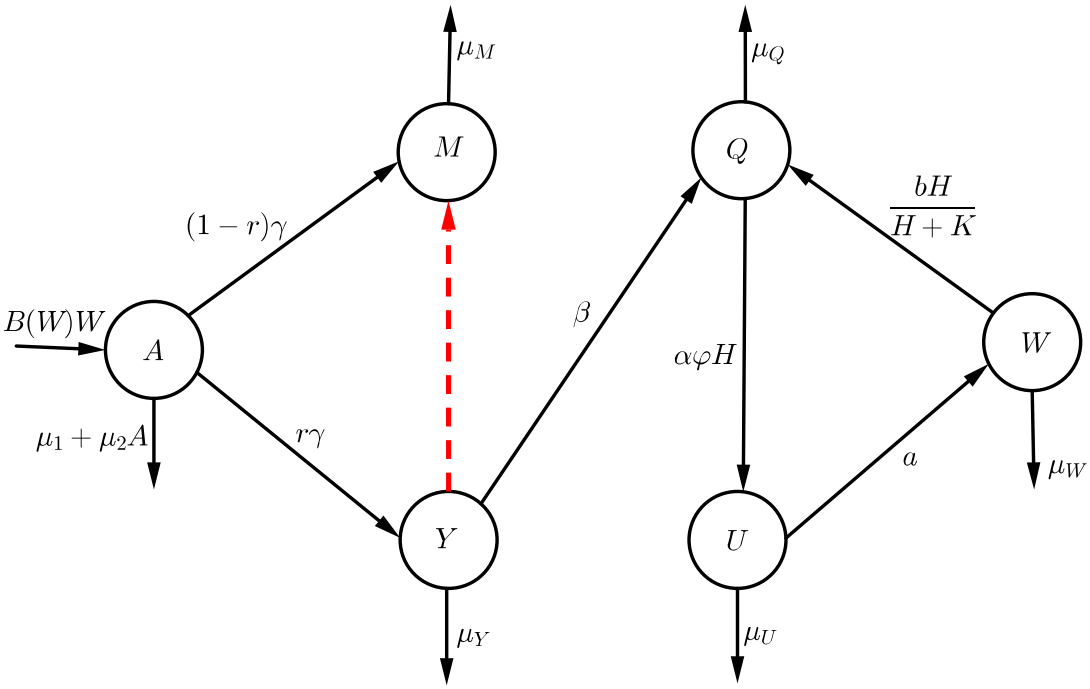

Figure 3.1: Anopheles mosquito simplified life cycle. The dashed arrow indicates the mating between male and immature female mosquitoes.

We point out that the model (3.1) extends some of the existing models in many respects. Unlike [1, 2, 88], it incorporates the gonotrophic cycle of adult female mosquito

Table 3.2: Description of state variables and parameters of model (3.1).

Variables	Description
A	Population in the aquatic stage (eggs, larvae, pupae).
Y	Population of immature females not yet laying eggs.
M	Population of males.
Q	Population of feeding females.
U	Population of resting females.
W	Population of breeding females.
Parameters	**Description**
r	Fraction of the emerging female mosquitoes.
γ	Rate of emerging mosquitoes from the aquatic stage.
N_{egg}	Number of eggs at each deposit per capita.
L	Environmental carrying capacity of female adult mosquitoes.
β	Transfer rate (mating rate) from the compartment Y to Q
μ_2	Density-dependent mortality rate in the aquatic stage.
μ_1	Mortality rate in the aquatic stage.
μ_M	Mortality rate of male mosquitoes.
μ_Y	Mortality rate of immature females.
μ_Q	Mortality rate of questing females.
μ_U	Mortality rate of resting females.
μ_W	Mortality rate of breeding females.
φ	Biting rate of feeding females.
α	Probability of successfully taking a blood meal.
H	Constant population density of humans at human resource sites.
K	Constant alternative of blood meal for vectors.
b	Rate at which breeding females leave the site to restart their gonotrophic cycle.
a	Rate at which resting females become breeding females.

population. It further extends the model in [1, 2, 88, 108] by incorporating the more general egg oviposition function (a new birth rate function for modeling mosquito oviposition is proposed).

Remark 3.2.1. From the ecological point of view, it is well known that the Maynard-Smith-Slatkin oviposition function is more suitable to model the mosquito oviposition rate, compared to the Malthus and Verhulst-Pearl logistic functions [1, 105]. Therefore, the latter function will be our focus throughout the theoretical and numerical investigations in this work, with one of the main target of solving the opened problem in [1, 108] regarding the global asymptotic stability of the MPE. However, our results can readily apply to the

Hassell oviposition function [12], whereas, for Malthus and Verhulst-Pearl functions, we refer the reader to [1, 2, 104, 105].

3.2.2 Basic properties

In this section, the basic properties of model (3.1) are explored. Model (3.1) takes the matrix form $\dot{X} = \mathcal{A}(X)X$, where $X(t) = (A(t), Y(t), M(t), Q(t), U(t), W(t))^T$,

$$\mathcal{A}(X) = \begin{pmatrix} -[\nu_1 + \mu_2 A] & 0 & 0 & 0 & 0 & B(W) \\ r\gamma & -\nu_2 & 0 & 0 & 0 & 0 \\ (1-r)\gamma & 0 & -\mu_M & 0 & 0 & 0 \\ 0 & \beta & 0 & -\nu_3 & 0 & b_1 \\ 0 & 0 & 0 & \alpha\varphi_1 & -\nu_4 & 0 \\ 0 & 0 & 0 & 0 & a & -\nu_5 \end{pmatrix},$$

and

$$\nu_1 = \gamma + \mu_1,\ \nu_2 = \mu_Y + \beta,\ \varphi_1 = \varphi H,\ \nu_3 = \alpha\varphi_1 + \mu_Q,\ b_1 = \frac{bH}{H+K},\ \nu_4 = a + \mu_U,\ \nu_5 = \mu_W + b_1. \tag{3.5}$$

Since all the parameters are positive, the right-hand side of system (3.1)-(3.2) is locally Lipschitz continuous, there exists a local solution. Furthermore, for all $X \in \mathbb{R}^6_+$, $\mathcal{A}(X)$ is a Metzler matrix. Thus, the analysis of the model can be carried out in the following invariant region

$$\Gamma = \Big\{(A, Y, M, Q, U, W) \in \mathbb{R}^6 \ :\ A(t), Y(t), M(t), Q(t), U(t), W(t) \geq 0\Big\}.$$

The invariance of Γ implies that all solutions of (3.1) with non-negative initial data remain non-negative for all $t \geq 0$. To be more precise, one has the following result.

Theorem 3.2.1. Denote $\mu_v = \min\Big\{\mu_1, \mu_Y, \mu_M, \mu_Q, \mu_U, \mu_W\Big\}$. Then the model (3.1) is a dynamical system in the region

$$\Gamma_L = \left\{(A, Y, M, Q, U, W) \in \Gamma :\ V(t) \leq \frac{N_{egg}L}{\mu_v}\right\}.$$

Proof. Define the total mosquito population

$$V(t) = A(t) + Y(t) + M(t) + Q(t) + U(t) + W(t).$$

Add all the terms on the right-hand side of (3.1). Then, it follows that

$$\dot{V}(t) \leq B(W)W - \mu_v V(t). \tag{3.6}$$

Using assumption (3.2), one has $B(W)W \leq N_{egg}L$, which yields

$$\dot{V}(t) \leq N_{egg}L - \mu_v V(t).$$

Thus,

$$\limsup_{t\to\infty}(A(t)+Y(t)+M(t)+Q(t)+U(t)+W(t)) \leq \frac{N_{egg}L}{\mu_v}.$$

We conclude that every solution of (3.1) is bounded and consequently, the initial value problem associated with system (3.1) has a unique solution defined for all $t > 0$. □

Theorem 3.2.1 implies that system (3.1) is mathematically and ecologically well-posed.

3.2.3 The MFE and basic offspring number $\mathcal{R}_0^{ode}$

Model (3.1) has a trivial equilibrium or mosquito-free equilibrium (MFE) $\mathcal{T}_0 = (0,0,0,0,0,0)$, which is obtained by setting the right-hand side of (3.1) to zero. Following [40], the next generation approach is used to calculate the basic offspring number $\mathcal{R}_0^{ode}$. Let

$$\mathcal{F} = \begin{pmatrix} B(W)W \\ 0 \\ 0 \\ 0 \\ 0 \end{pmatrix} \quad \text{and} \quad \mathcal{V} = \begin{pmatrix} (\nu_1+\mu_2 A)A \\ -r\gamma A + \nu_2 Y \\ -\beta Y - b_1 W + \nu_3 Q \\ -\alpha\varphi_1 Q + \nu_4 U \\ -aU + \nu_5 W \end{pmatrix},$$

be the vector of new generated mosquitoes and the vector of transfers between compartments, respectively. The Jacobian matrices of $\mathcal{F}$ and $\mathcal{V}$ at the MFE $\mathcal{T}_0$ are

$$F = \begin{bmatrix} 0 & 0 & 0 & 0 & N_{egg} \\ 0 & 0 & 0 & 0 & 0 \\ 0 & 0 & 0 & 0 & 0 \\ 0 & 0 & 0 & 0 & 0 \\ 0 & 0 & 0 & 0 & 0 \end{bmatrix} \quad \text{and} \quad V = \begin{bmatrix} \nu_1 & 0 & 0 & 0 & 0 \\ -r\gamma & \nu_2 & 0 & 0 & 0 \\ 0 & -\beta & \nu_3 & 0 & -b_1 \\ 0 & 0 & -\alpha\varphi_1 & \nu_4 & 0 \\ 0 & 0 & 0 & -a & \nu_5 \end{bmatrix}.$$

Thanks to [40], the associated basic offspring number $\mathcal{R}_0^{ode}$ of (3.1) is the spectral radius of the next generation matrix FV^{-1}. That is

$$\mathcal{R}_0^{ode} = \frac{N_{egg} r\gamma\beta\alpha\varphi_1 a}{\nu_1\nu_2 m_1}, \tag{3.7}$$

where, for notational convenience, we have set

$$m_1 = a\alpha\varphi_1\mu_W + \nu_5\left[\alpha\varphi_1\mu_U + \mu_Q\nu_4\right]; \quad m_2 = \nu_1\nu_2 m_1\left(1 - \frac{1}{\mathcal{R}_0^{ode}}\right). \tag{3.8}$$

Remark 3.2.2. The threshold quantity $\mathcal{R}_0^{ode}$ measures the average expected number of new adult female offsprings produced by a single female mosquito during its lifespan. It can be ecologically interpreted as the product of the fraction of mosquitoes in aquatic stage that survived to become immature female mosquitoes $\left(\frac{N_{egg}r\gamma}{\nu_1}\right)$, the fraction of immature females that survived and start their gonotrophic cycle by entering the questing female compartment $\left(\frac{\beta}{\nu_2}\right)$, and the fraction of fertilized adult females that survived and completed their gonotrophic cycle $\left(\frac{\alpha\varphi_1 a}{m_1}\right)$.

Following Theorem 2 in [40], one has:

Lemma 3.2.1. The trivial equilibrium or MFE $\mathcal{T}_0$ of system (3.1) is locally asymptotically stable (LAS) whenever $\mathcal{R}_0^{ode} < 1$, and unstable otherwise.

Ecologically speaking, Lemma 3.2.1 implies that mosquitoes can be eliminated if the initial sizes of the population of anopheles mosquitoes are in the basin of attraction of the MFE $\mathcal{T}_0$. Thus, the mosquito population can be effectively controlled if $\mathcal{R}_0^{ode} < 1$. To ensure that the effective control of the mosquito population is independent of the initial size of the mosquito population, a global asymptotic stability result must be established for the trivial equilibrium.

Theorem 3.2.2. The MFE $\mathcal{T}_0$ of system (3.1) is globally asymptotically stable (GAS) in Γ, whenever $\mathcal{R}_0^{ode} \leq 1$.

Proof. Thanks to the boundedness of solutions, we use the reduction theorem by Vidyasagar [135]. Denote $y(t) = (A(t), Y(t), Q(t), U(t), W(t))^T$ and $z(t) = M(t)$. Then system (3.1) takes the form

$$\begin{cases} \dfrac{dy}{dt} &= f(y), \\ \dfrac{dz}{dt} &= g(y,z). \end{cases} \tag{3.9}$$

Let us first show that the equilibrium $\mathbf{0_5} = (0,0,0,0,0)$ is GAS for the subsystem $\frac{dy}{dt} = f(y)$. Consider the Lyapunov function

$$V_0(y) = \frac{1}{\nu_1}\left[r\gamma A + \nu_1 Y\right] + \frac{\nu_2}{\beta\alpha\varphi_1}\left[\alpha\varphi_1 Q + \nu_3 U\right] + \frac{\nu_2\nu_3\nu_4}{a\beta\alpha\varphi_1} W.$$

It is obvious that $V_0(0) = 0$, and $V_0(y) > 0$, for all $y > 0$. Moreover,

$$\begin{aligned} \dot{V}_0(y) &= \frac{1}{\nu_1}\left[r\gamma\dot{A} + \nu_1\dot{Y}\right] + \frac{\nu_2}{\beta\alpha\varphi_1}\left[\alpha\varphi_1\dot{Q} + \nu_3\dot{U}\right] + \frac{\nu_2\nu_3\nu_4}{a\beta\alpha\varphi_1}\dot{W}, \\ &= \frac{1}{\nu_1}\left[r\gamma B(W)W - \nu_1\nu_2 Y - r\gamma\mu_2 A^2\right] + \frac{\nu_2}{\beta\alpha\varphi_1}\left[\alpha\varphi_1\beta Y + b_1\alpha\varphi_1 W - \nu_3\nu_4 U\right] \\ &\quad + \frac{\nu_2\nu_3\nu_4}{a\beta\alpha\varphi_1}\left[aU - \nu_5 W\right], \\ &= \left[\frac{r\gamma}{\nu_1}B(W)W + \frac{\nu_2 b_1}{\beta} - \frac{\nu_2\nu_3\nu_4\nu_5}{a\beta\alpha\varphi_1}\right]W - \frac{r\gamma\mu_2}{\nu_1}A^2, \\ &= -\frac{r\gamma N_{egg}}{\nu_1\mathcal{R}_0^{ode}}\left[1 - \frac{\mathcal{R}_0^{ode}}{N_{egg}}B(W)\right]W - \frac{r\gamma\mu_2}{\nu_1}A^2. \end{aligned}$$

Since, $\max_W B(W) \leq N_{egg}$ and $\mathcal{R}_0^{ode} \leq 1$, we have $\dfrac{\mathcal{R}_0^{ode}}{N_{egg}}B(W) < 1$. Hence, $\dot{V}(y) \leq 0$. On the other hand, let $\mathcal{H}$ be the largest invariant set such that $\mathcal{H} \subset \{(A,Y,Q,U,W) \in \mathbb{R}_+^5 / \dot{V}_0(y) = 0\}$. Then $\mathcal{H} = \{\mathbf{0_5}\}$. Thus, by the LaSalle Invariance Principle, we deduce that $\mathbf{0_5}$ is GAS in $\mathbb{R}_+^5$ for system $\dfrac{dy}{dt} = f(y)$. Finally, using the fact 0 is GAS in $\mathbb{R}_+$ for system $\dfrac{dz}{dt} = g(\mathbf{0_5}, z)$, we conclude that $\mathcal{T}_0$ is GAS in Γ. This completes the proof. □

3.2.4 The non-trivial equilibrium or MPE

(a) Existence and uniqueness

The existence and stability of a MPE of the system (3.1) are addressed. Let such a MPE be denoted by $\mathcal{T}^* = (A^*, Y^*, M^*, Q^*, U^*, W^*)^T$. Then $A^*, Y^*, M^*, Q^*, U^*, W^*$ are

$$\begin{cases} Y^* = \dfrac{r\gamma}{\nu_2}A^*, \quad M^* = \dfrac{(1-r)\gamma}{\mu_M}A^*, \quad Q^* = \dfrac{\nu_1\nu_4\nu_5\mathcal{R}_0^{ode}}{aN_{egg}\alpha\varphi_1}A^*, \\ U^* = \dfrac{\nu_1\nu_5\mathcal{R}_0^{ode}}{aN_{egg}}A^*, \quad W^* = \dfrac{\nu_1\mathcal{R}_0^{ode}}{N_{egg}}A^*, \end{cases} \tag{3.10}$$

where A^* is a positive solution of the equation $F_{\mathcal{R}_0^{ode}}(A^*) = 0$, where the function $F_{\mathcal{R}_0^{ode}}$ is given in Eq. (3.3). Notice that $F_{\mathcal{R}_0^{ode}}(0) = \nu_1 N_{egg}(\mathcal{R}_0^{ode} - 1) > 0$ whenever $\mathcal{R}_0^{ode} > 1$, $F_{\mathcal{R}_0^{ode}}(+\infty) = -\infty$, and $F_{\mathcal{R}_0^{ode}}$ is continuous and strictly decreasing on interval $]0; +\infty[$. Thus, by the intermediate value theorem, $F_{\mathcal{R}_0^{ode}}$ vanishes exactly once in $]0; +\infty[$. This proves the existence and uniqueness of a positive A^* when $\mathcal{R}_0^{ode} > 1$. Replacing the value of A^* in (3.10) yields the existence and uniqueness of $\mathcal{T}^*$. This result is summarized as follows.

Theorem 3.2.3. Model (3.1) has a unique MPE $\mathcal{T}^*$ whenever $\mathcal{R}_0^{ode} > 1$. Moreover, for the special case B_S and in the absence of density dependent mortality (i.e. $\mu_2 = 0$), the unique solution of $F_{\mathcal{R}_0^{ode}}(A^*) = 0$ is explicitly given by

$$A^* = \frac{N_{egg}L}{\nu_1\mathcal{R}_0^{ode}}\left(\mathcal{R}_0^{ode} - 1\right)^{\frac{1}{n}}. \tag{3.11}$$

Remark 3.2.3. Similar to [75], it can be easily proved that: (1)-the GAS of $\mathcal{T}_0$ given in Theorem 3.2.2, (2-) the instability of $\mathcal{T}_0$ shown in Lemma 3.2.1, (3)-the existence of a unique MPE $\mathcal{T}^*$ established by Theorem 3.2.3 whenever $\mathcal{R}_0^{ode} > 1$ and (4)-the fact that $\mathcal{T}_0 \in \partial\Gamma$, imply the uniform persistence of system (3.1).

(b) Local stability and existence of Hopf bifurcation for the special case where $\mu_2 = 0$

Theorem 3.2.4. Consider model (3.1), with $\mu_2 = 0$. Then, there exists two thresholds n_0^* and n_0^{**} such that:
(i)-The MPE $\mathcal{T}^*$ is LAS in $\Gamma \setminus \{\mathcal{T}_0\}$ whenever $\mathcal{R}_0^{ode} > 1$ and $1 < n < \min\{n_0^*, n_0^{**}\}$.
(ii)-The system (3.1) undergoes a Hopf bifurcation whenever n crosses the critical value n_0^{**}.

Proof. This will be done in two steps. In the first, we prove the local asymptotic stability. The second is devoted to the proof of the existence of Hopf bifurcation.

Step 1: The LAS of $\mathcal{T}^*$ is explored using the properties of Bézout matrices. To that end, let us recall the following instrumental results.

Lemma 3.2.2 (Theorem 2.6,[64]). Let A be a $n \times n$ complex matrix, and let E_k be the sum of all the principal minors of A of order k, $k \in \langle n \rangle = \{1, 2, ..., n\}$. Let $\Omega(A)$ be the $n \times n$ Hurwitz matrix of A and assume that $\Omega(A)$ is real. Then A is stable if and only if all the leading principal minors of $\Omega(A)$ are positive.

Definition 3.2.1 (Definition 2.7,[64]). Let $a(x)$ and $b(x)$ be two polynomials with real coefficients of degree n and m ($n \geq m$), respectively. The Bézoutiant defined by $a(x)$ and $b(x)$ is the bilinear form

$$\frac{a(x)b(y) - a(y)b(x)}{x - y} = \sum_{i,k=0}^{n-1} b_{i,k} x^i y^k.$$

The symmetric matrix $(b_{i,k})_0^{n-1}$ associated with this bilinear form is called the Bézout matrix and is denoted by $B_{a,b}$.

Lemma 3.2.3 (Theorem 2.8,[64]). Let $f(x) = x^n - a_n x^{n-1} - \cdots - a_1$ be a polynomial with real coefficients, and let $a_{n+1} = -1$. Define the polynomials

$$h(u) = -a_1 - a_3 u - \cdots, \quad \text{and} \quad g(u) = -a_2 - a_4 u - \cdots.$$

The polynomial $f(x)$ is negative stable if and only if the Bézout matrix $B_{h,g}$ is positive definite and $a_i < 0$ for all $i \in \langle n \rangle$.

Lemma 3.2.4 (Sylvester's Criterion,[50]). A real, symmetric matrix is positive definite if and only if all its principal minors are positive.

We consider the model (3.1) in the absence of density-dependent mortality in aquatic stage (i.e. $\mu_2 = 0$). Evaluating the Jacobian matrix at $\mathcal{T}^*$ gives

$$\mathcal{J}(\mathcal{T}^*) = \begin{pmatrix} -\nu_1 & 0 & 0 & 0 & 0 & B(W^*) + W^* \dfrac{dB(W^*)}{dW} \\ r\gamma & -\nu_2 & 0 & 0 & 0 & 0 \\ (1-r)\gamma & 0 & -\mu_M & 0 & 0 & 0 \\ 0 & \beta & 0 & -\nu_3 & 0 & b_1 \\ 0 & 0 & 0 & \alpha\varphi_1 & -\nu_4 & 0 \\ 0 & 0 & 0 & 0 & a & -\nu_5 \end{pmatrix}.$$

The eigenvalues of $\mathcal{J}(\mathcal{T}^*)$ are the roots of the polynomial

$$P(\lambda) = (\lambda + \mu_M)\left[\lambda^5 + b_4\lambda^4 + b_3\lambda^3 + b_2\lambda^2 + b_1\lambda + b_0\right], \tag{3.12}$$

where

$$\begin{cases} b_4 &= \nu_5 + \nu_4 + \nu_3 + \nu_2 + \nu_1, \\ b_3 &= \nu_5(\nu_4 + \nu_3 + \nu_2 + \nu_1) + \nu_4(\nu_3 + \nu_2 + \nu_1) + \nu_3(\nu_2 + \nu_1) + \nu_2\nu_1, \\ b_2 &= m_1 + \nu_5\nu_4(\nu_1 + \nu_2) + \nu_5\nu_3(\nu_1 + \nu_2) + \nu_5\nu_2\nu_1 + \nu_4\nu_3(\nu_1 + \nu_2) \\ &\quad + \nu_4\nu_2\nu_1 + \nu_3\nu_2\nu_1, \\ b_1 &= m_1(\nu_1 + \nu_2) + \nu_5\nu_4\nu_2\nu_1 + \nu_5\nu_3\nu_2\nu_1 + \nu_4\nu_3\nu_2\nu_1, \\ b_0 &= \nu_1\nu_2 m_1 - a\alpha\varphi_1 r\beta\gamma\left[B(W^*) + W^* \dfrac{dB(W^*)}{dW}\right]. \end{cases} \tag{3.13}$$

Now, define

$$h(u) = b_0 + b_2u + b_4u^2 \text{ and } g(u) = b_1 + b_3u + u^2.$$

It follows from Definition 3.2.1 that the corresponding Bézout matrix $B_{h,g}(P)$ of $P(\lambda)$ given by (3.12) is

$$B_{h,g}(P) = \begin{pmatrix} b_{0,0} & b_{0,1} \\ b_{0,1} & b_{1,1} \end{pmatrix},$$

where $b_{0,0} = b_2b_1 - b_3b_0$, $b_{0,1} = b_4b_1 - b_0$ and $b_{1,1} = b_4b_3 - b_2$.
Since $B_{h,g}(P)$ is symmetric, it suffices by Theorem 3.2.4, to show that the k^{th} leading principal minor Δ_k of $B_{h,g}(P)$, is positive. Since $\mathcal{R}_0^{ode} > 1$, we have $b_0 = n\nu_1\nu_2m_1\left(1 - \frac{1}{\mathcal{R}_0^{ode}}\right) = nm_2 > 0$.
The first leading principal minor of $B_{h,g}(P)$, $\Delta_1 = b_{0,0} = b_2b_1 - b_3b_0$, is positive whenever

$$n < n_0^*, \quad \text{where} \quad n_0^* = \frac{b_2b_1}{b_3m_2}.$$

The second leading principal minor of $B_{h,g}(P)$,

$$\Delta_2 = b_{1,1}b_{0,0} - b_{0,1}^2 = b_{1,1}b_2b_1 - (b_4b_1)^2 + m_2(2b_1b_4 - b_{1,1}b_3)n - m_2^2n^2,$$

is positive whenever

$$n < n_0^{**}, \quad \text{where} \quad n_0^{**} = \frac{b_{1,1}\sqrt{b_3^2 - 4b_1} + 2b_1b_4 - b_{1,1}b_3}{2m_2} > 0.$$

We conclude by choosing the integer n such that $1 < n < \min\{n_0^*, n_0^{**}\}$.

Step 2: Consider the model (3.1) with $\mathcal{R}_0^{ode} > 1$. A Hopf bifurcation can occur when the Jacobian matrix $\mathcal{J}(\mathcal{T}^*)$ of (3.1), evaluated at $\mathcal{T}^*$, has a pair of purely imaginary eigenvalues. Note that when the rank of the Bézout matrix $B_{h,g}(P)$ is reduced by exactly one, then the characteristic polynomial P has a pair of purely imaginary eigenvalues [113]. Thus to prove the existence of Hopf bifurcation, it suffices to verify the transversality condition [23].

Let $n = n_0^{**}$ be a bifurcation parameter. Let's fix all other parameters of model (3.1). Then, by Theorem 3.2.4, $\Delta_1 > 0$. Hence, $\Delta_2(n) = 0$ if and only if $n = n_0^{**}$. Moreover,

$$\left.\frac{d\Delta_2(n)}{dn}\right|_{n=n_0^{**}} = -m_2b_{1,1}\sqrt{b_3^2 - 4b_1} < 0.$$

□

Remark 3.2.4. One should note that, the stability analysis of the temporal model (3.1) subject to the newly considered Hassell oviposition function B_H, as well as the stability results with respect of the existing works are summarized in Table 3.3. Note that, $\mathcal{R}_0^{\mathcal{L}}$, n_1^*, n_1^{**} $b_0, b_1, ..., b_4$ and $b_{1,1}$ are computed similarly to the proof Theorem 3.2.4 above such that:

(i) For $B(W)$ given by B_L, $b_0 = \nu_1\nu_2m_1(\mathcal{R}_0^{ode} - 1) > 0$ and $\mathcal{R}_0^{\mathcal{L}} = 1 + \frac{b_{1,1}\sqrt{b_3^2 - 4b_1} + 2b_1b_4 - b_{1,1}b_3}{2\nu_1\nu_2m_1}$.

(ii) For $B(W)$ given by B_H, $b_0 = nv_1v_2m_1\left(1 - \frac{1}{(\mathcal{R}_0^{ode})^{\frac{1}{n}}}\right) > 0$. Thus, $n_{1*} = \min\{n_1^*, n_1^{**}\}$ where n_1^* and n_1^{**} are the positive roots of the equations $\Delta_1(n) = 0$ and $\Delta_2(n) = 0$, respectively.

Theorem 3.2.4 is numerically illustrated by Figure 3.2. The LAS of $\mathcal{T}^*$ is depicted in Figure 3.2**(A)** and shows that, without competition in the aquatic stage (i.e. $\mu_2 = 0$), the mosquito population will persist as long as $\mathcal{R}_0^{ode} > 1$ and $1 < n < \min\{n_0^*, n_0^{**}\}$. On the other hand, the Hopf bifurcation shown by Figure 3.2**(B)** proves that, sustained oscillations are possible when $\mu_2 = 0$. Moreover, Figure 3.2**(B)** suggests that, if competition is negligible in the aquatic stage (i.e. $\mu_2 = 0$), the solutions of model (3.1) converge to a periodic solution, whenever $n > n_0^{**}$. This is in agreement with the studies in [1, 105, 108].

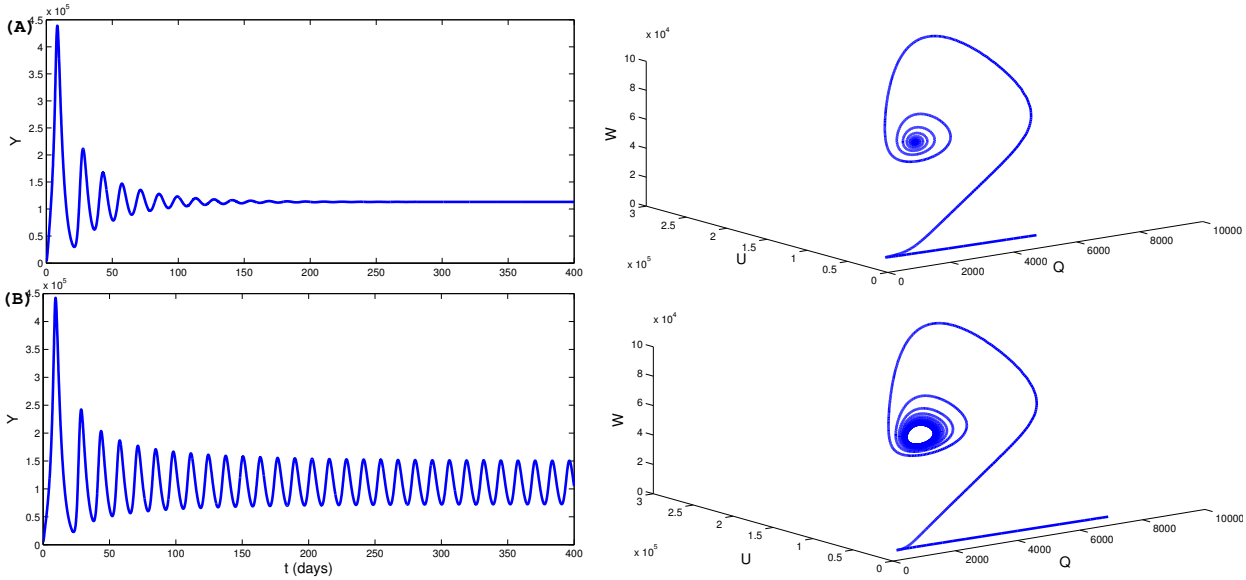

Figure 3.2: **(A)** LAS of $\mathcal{T}^*$ for model (3.1) with $\mu_2 = 0$, $n = 10$ and $N_{egg} = 25$ (so that $\mathcal{R}_0^{ode} = 13.9399 > 1$ and $n_0^{**} = 12.4606$).
(B) Hopf bifurcation in model (3.1) around of the MPE $\mathcal{T}^*$ with $\mu_2 = 0$, $n = 13$ and $N_{egg} = 25$ (so that $\mathcal{R}_0^{ode} = 13.9399 > 1$ and $n_0^{**} = 12.4606$). All other parameters are as in Table 3.4.

(c) Global stability

We explore the global asymptotic property of the MPE $\mathcal{T}^*$ of model (3.1) with density dependent mortality in the aquatic stage (i.e. $\mu_2 > 0$).

Theorem 3.2.5. Consider the system (3.1) subject to the Maynard-Smith-Slatkin oviposition function with $n = 1$. Then, the MPE $\mathcal{T}^*$ is GAS in $\Gamma \setminus \{\mathcal{T}_0\}$ whenever $\mathcal{R}_0^{ode} > 1$.

The proof of Theorem 3.2.5 can be cheaply done thanks to the monotone (cooperative) properties of system (3.1). It can also be proven by Lyapunov-LaSalle techniques, with the construction of a suitable Lyapunov function of Goh-Volterra type. The latter proof is provided below.

Proof. Suppose $\mathcal{R}_0^{ode} > 1$ in system (3.1). Let us first show that the equilibrium $\mathcal{T}^* = (A^*, Y^*, Q^*, U^*, W^*)^T$ is globally asymptotically stable for system $\frac{dx}{dt} = f(x)$. To this end, consider the non-linear Lyapunov function of Goh-Volterra type as follows (see also proof of Theorem 4.3 in [87])

$$V_1(x) = a_1(A - A^* \ln A) + a_2(Y - Y^* \ln Y) + a_3(Q - Q^* \ln Q) + a_4(U - U^* \ln U) + a_5(W - W^* \ln W),$$

where,

$$a_1 = \frac{r\gamma\beta a\alpha\varphi_1 N_{egg}}{\nu_1\nu_2\nu_3\nu_4 B(W^*)\mathcal{R}_0^{ode}}, \quad a_2 = \frac{\beta a\alpha\varphi_1}{\nu_2\nu_3\nu_4}, \quad a_3 = \frac{a\alpha\varphi_1}{\nu_3\nu_4}, \quad a_4 = \frac{a}{\nu_4}, \quad \text{and} \quad a_5 = 1.$$

At the steady state $\mathcal{T}^*$, the following relations hold:

$$\begin{aligned} &B(W^*)W^* = (\nu_1 + \mu_2 A^*)A^* = \nu_1\mathcal{R}_0\tfrac{B(W^*)}{N_{egg}}A^*, \quad \nu_3 Q^* = \beta Y^* + b_1 W^*, \\ &r\gamma A^* = \nu_2 Y^*, \alpha\varphi_1 Q^* = \nu_4 U^* \quad \text{and} \quad aU^* = \nu_5 W^*. \end{aligned} \tag{3.14}$$

The time derivative of $V_1(x)$ is

$$\begin{aligned} \dot{V}_1(x) &= a_1\left(1 - \frac{A^*}{A}\right)\dot{A} + a_2\left(1 - \frac{Y^*}{Y}\right)\dot{Y} + a_3\left(1 - \frac{Q^*}{Q}\right)\dot{Q} + a_4\left(1 - \frac{U^*}{U}\right)\dot{U} + a_5\left(1 - \frac{W^*}{W}\right)\dot{W}, \\ &= a_1\left[B(W)W - (\nu_1 + \mu_2 A)A - \frac{B(W)WA^*}{A} + (\nu_1 + \mu_2 A)A^*\right] + a_2\left[r\gamma A - \nu_2 Y\right. \\ &\quad \left. - \frac{r\gamma AY^*}{Y} + \nu_2 Y^*\right] + a_3\left[\beta Y + b_1 W - \nu_3 Q - \frac{\beta YQ^*}{Q} - b_1\frac{WQ^*}{Q} + \nu_3 Q^*\right] \\ &\quad + a_4\left[\alpha\varphi_1 Q - \nu_4 U - \frac{\alpha\varphi_1 QU^*}{U} + \nu_4 U^*\right] + a_5\left[aU - \nu_5 W - \frac{aUW^*}{W} + \nu_5 W^*\right]. \end{aligned} \tag{3.15}$$

Using (3.14), Eq. (3.15) becomes

$$\begin{aligned} \dot{V}_1(x) &= a_1\mu_2 A^* A\left(2 - \frac{A}{A^*} - \frac{A^*}{A}\right) + a_1 B(W^*)W^* + a_2\nu_2 Y^* + a_3\nu_3 Q^* + a_4\nu_4 U^* + a_5\nu_5 W^* \\ &\quad - a_1\frac{B(W)WA^*}{A} - a_2\frac{r\gamma AY^*}{Y} - a_3\frac{\beta YQ^*}{Q} - a_3 b_1\frac{WQ^*}{Q} - a_4\frac{\alpha\varphi_1 QU^*}{U} - a_5\frac{aUW^*}{W}, \end{aligned}$$

and the relations

$$\begin{aligned} &a_1 B(W^*)W^* = a_2\nu_2 Y^* = a_3\beta Y^* = a_2 r\gamma A^* \; ; \; a_5\nu_5 W^* = a_2 r\gamma A^* + a_3 b_1 W^* \\ &a_3\nu_3 Q^* = a_4\nu_4 U^* = a_4\alpha\varphi_1 Q^* = a_5 aU^* = a_2 r\gamma A^* + a_3 b_1 W^* \end{aligned} \tag{3.16}$$

are satisfied. Substituting the expressions in Eq. (3.16) yields

$$\begin{aligned}
\dot{V}_1(x) &= a_1\mu_2 A^* A\left(2-\frac{A}{A^*}-\frac{A^*}{A}\right)+6a_2r\gamma A^*+3a_3b_1W^*-a_2r\gamma A^*\left(\frac{B(W)WA^*}{B(W^*)W^*A}\right.\\
&\left.+\frac{AY^*}{A^*Y}+\frac{YQ^*}{Y^*Q}+\frac{QU^*}{Q^*U}+\frac{UW^*}{U^*W}+\frac{B(W^*)}{B(W)}\right)-a_3b_1W^*\left(\frac{WQ^*}{W^*Q}+\frac{QU^*}{Q^*U}+\frac{UW^*}{U^*W}\right)\\
&+a_2r\gamma A^*\left(\frac{B(W^*)}{B(W)}-1\right)+\left(\frac{\nu_3\nu_4\nu_5-b_1\alpha\varphi_1 a}{\nu_3\nu_4}\right)\left(\frac{B(W)}{B(W^*)}-1\right)W\\
&= a_1\mu_2 A^* A\left(2-\frac{A}{A^*}-\frac{A^*}{A}\right)+a_2r\gamma A^*\left(6-\frac{B(W)WA^*}{B(W^*)W^*A}-\frac{AY^*}{A^*Y}-\frac{YQ^*}{Y^*Q}\right.\\
&\left.-\frac{QU^*}{Q^*U}-\frac{UW^*}{U^*W}-\frac{B(W^*)}{B(W)}\right)+a_3b_1W^*\left(3-\frac{WQ^*}{W^*Q}-\frac{QU^*}{Q^*U}-\frac{UW^*}{U^*W}\right)\\
&+a_2r\gamma A^*\left(\frac{B(W)}{B(W^*)}-1\right)\left(\frac{W}{W^*}-\frac{B(W^*)}{B(W)}\right). \qquad (3.17)
\end{aligned}$$

In Eq. (3.17), the terms between the brackets are Volterra-type functions. These functions are positive definite. For $B(W)$ with $n=1$, we have

$$\frac{B(W)}{B(W^*)}-1=\frac{W^*-W}{L+W} \quad \text{and} \quad \frac{W}{W^*}-\frac{B(W^*)}{B(W)}=\frac{(W-W^*)L}{W^*(L+W^*)}.$$

Hence,

$$\left(\frac{B(W)}{B(W^*)}-1\right)\left(\frac{W}{W^*}-\frac{B(W^*)}{B(W)}\right)=-\frac{(W^*-W)^2L}{W^*(L+W)(L+W^*)}<0.$$

Thus, using the arithmetic-geometric means inequality, it follows that $\dot{V}_1\leq 0$. The proof follows by the conclusion in the proof of Theorem 3.2.2 as well. □

Unfortunately, for the case $n>1$, none of these latter theories can easily apply. This owing to high nonlinearity, the system (3.1) is neither cooperative, nor amenable for Lyapunov-LaSalle techniques. Alternatively, to prove the global attractivity of $\mathcal{T}^*$ when $n>1$, we shall adopt a generic approach (which can also apply for $n=1$) based on a fluctuation argument [77, 80, 82, 152]. We shall construct two monotone convergent sequences such that one is the upper bound and the other the lower bound of the constant solution $\mathcal{T}^*$. Moreover, the constructed sequences must share the same limit.

Before the implementation of the above mentioned approach, let us give some useful preliminaries.

For two vectors $a,b\in\mathbb{R}^5$, we write: $a\geq b$ if $a_i\geq b_i$; $a>b$ if $a\geq b$ and $a\neq b$ and $a\gg b$ if $a_i>b_i$.

Let $y=(A,Y,Q,U,W)^T=(y_1,y_2,y_3,y_4,y_5)^T\in\mathbb{R}^5_+$, $g\geq 0$ be any nonnegative quantity and

$$F(y,g)=\begin{pmatrix} gW-(\nu_1+\mu_2A)A\\ r\gamma A-\nu_2Y\\ \beta Y+b_1W-\nu_3Q\\ \alpha\varphi_1Q-\nu_4U\\ aU-\nu_5W\end{pmatrix}.$$

Consider the system

$$\frac{dy}{dt} = F(y, g). \tag{3.18}$$

One can easily verify that the function F satisfies the following conditions:

(1) F is cooperative on $\mathbb{R}^5_+$ and $DF(y, g)$ is irreducible for every $y \in \mathbb{R}^5_+$;

(2) $F(0, g) = 0$ and $F_i(y, g) \geq 0$ for all $y \in \mathbb{R}^5_+$ with $y_i = 0$, $i = 1, 2, \ldots, 5$;

(3) F is strictly sublinear on $\mathbb{R}^5_+$.

Thus, thanks to [159] (Corollary 3.2), the following result holds.

Lemma 3.2.5. Consider the system (3.18). Denote $s(DF(0, g)) = s(F'_y(0, g)) = \max\{Re\lambda : det(\lambda I_5 - DF(0, g)) = 0\}$, the stability modulus of the matrix $DF(0, g)$. Then,

(i) If $s(DF(0, g)) \leq 0$, then $y = 0$ is GAS in $\mathbb{R}^5_+$.

(ii) If $s(DF(0, g)) > 0$, then $\frac{dy}{dt} = F(y, g)$ admits a unique positive equilibrium $y^*(g)$ which is GAS in $\mathbb{R}^5_+ \setminus \{0\}$.

To stress the dependence of $\mathcal{T}^*$ on the oviposition function $B(W)$, we denote $\mathcal{T}^* = \mathcal{T}^*(B(W^*))$.

Remark 3.2.5. In the case when $s(DF(0, g)) > 0$, the positive equilibrium $y^*(g)$ is an increasing function of g, that is $g_1 > g_2$ implies $y^*(g_1) \gg y^*(g_2)$. Indeed, by the comparison principle, we prove that $y^*(g_1) \geq y^*(g_2)$, and use condition (1) above to conclude (since F is strongly monotone [124]) that $y^*(g_1) \gg y^*(g_2)$. Furthermore, by setting $g = B(0) = N_{egg}$, Theorem 3.2.5 with $B(W)$ replaced by $B(0) = N_{egg}$ and item (ii) of Lemma 3.2.5 imply that, for $\mathcal{R}_0^{ode} > 1$ (or equivalently, $s(DF(0, B(0))) > 0$), there is a MPE $y^*(B(0)) = \mathcal{T}^*(B(0))$ which is GAS for the system $\frac{dy}{dt} = F(y, B(0))$.

Denote

$$x^{(1)} = \mathcal{T}^*(B(0)) = y^*(B(0)) = \left(x_1^{(1)}, x_2^{(1)}, x_3^{(1)}, x_4^{(1)}, x_5^{(1)}\right)^T.$$

Using Eq. (3.10), the fifth coordinate of $x^{(1)}$ is

$$x_5^{(1)} = W^*(B(0)) = \frac{\mathcal{R}_0^{ode}}{N_{egg}} \frac{\nu_1^2}{\mu_2} \left(\mathcal{R}_0^{ode} - 1\right).$$

Clearly $x^{(1)}$ is the MPE of system (3.1) when $B(W)$ is replaced by $B(0) = N_{egg}$.
The following result proves the global attractivity of $\mathcal{T}^*$ when $n > 1$ and $\mathcal{R}_0^{ode} > 1$.

Theorem 3.2.6. Suppose $\mathcal{R}_0^{ode} > 1$ and $s(DF(0, B(x_5^{(1)}))) > 0$. Then the MPE $\mathcal{T}^*$ of system (3.1) for $B(W)$ with $n > 1$ is globally attractive.

Proof. We prove this theorem by implementing the fluctuation method in two steps as mentioned earlier in the introduction section.

Step 1 : Construction of two monotone sequences $\{z^{(m)}\}_{m=1}^{\infty}$ and $\{x^{(m)}\}_{m=1}^{\infty}$.

If $y \in \mathbb{R}_+^5$ be any solution of system (3.1). Since $\frac{dA}{dt} \leq B(0)W - (\nu_1 + \mu_2 A)A$, then system (3.1) is bounded from above by the cooperative system

$$\frac{d\tilde{y}}{dt} = F(\tilde{y}, B(0)), \quad \text{where} \quad \tilde{y} = y = (A, Y, Q, U, W)^T.$$

It follows from the global stability of $\mathcal{T}^*(B(0))$ and the comparison principle that, for any $\epsilon = (\epsilon_1, \epsilon_2, \epsilon_3, \epsilon_4, \epsilon_5)^T \gg 0$, there exists a $t_1 > 0$ such that

$$y(t) \leq \mathcal{T}^*(B(0)) + \epsilon = x^{(1)} + \epsilon, \quad \forall t > t_1.$$

Since $s(DF(0, B(x_5^{(1)}))) > 0$, we can choose ϵ small enough such that $s(DF(0, B(x_5^{(1)} + \epsilon_5))) > 0$. It follows from Lemma 3.2.5 that there exists a unique positive equilibrium

$$y^*(B(x_5^{(1)} + \epsilon_5)) = \mathcal{T}^*(B(x_5^{(1)} + \epsilon_5)) \quad \text{for} \quad \frac{d\bar{y}}{dt} = F(\bar{y}, B(x_5^{(1)} + \epsilon_5)),$$

with $\bar{y} = y = (A, Y, Q, U, W)^T$, which is globally asymptotically stable in $\mathbb{R}_+^5 \setminus \{0\}$. Denote

$$z^{(1)} = \mathcal{T}^*(B(x_5^{(1)} + \epsilon_5)), \text{ and } z_5^{(1)} = W^*(B(x_5^{(1)} + \epsilon_5)) \text{ the fifth coordinate of } z^{(1)}.$$

Since $W(t) \leq x_5^{(1)} + \epsilon_5$, $\forall t > t_1$, we have

$$B(W(t)) \geq B(x_5^{(1)} + \epsilon_5) \quad \text{for} \quad t > t_1.$$

Hence,

$$\frac{dA}{dt} \geq B(x_5^{(1)} + \epsilon_5)W - (\nu_1 + \mu_2 A)A, \quad \forall t > t_1.$$

Therefore, the system (3.1) is bounded from below by cooperative system

$$\frac{d\bar{y}}{dt} = F(\bar{y}, B(x_5^{(1)} + \epsilon_5)), \quad \forall t > t_1.$$

Thus, the global stability of $z^{(1)} = \mathcal{T}^*(B(x_5^{(1)} + \epsilon_5))$ and the comparison principle imply that for any $\epsilon > 0$, with $z^{(1)} - \epsilon \gg 0$, there exists $t_2 > t_1$ such that $y(t) \geq z^{(1)} - \epsilon$, $\forall t > t_2$.
Using Remark 3.2.5, we have $z^{(1)} \ll x^{(1)}$.

Iterating this process, we construct two vectors

$$x^{(2)} = \mathcal{T}^*(B(z_5^{(1)} - \epsilon_5)) \quad \text{and} \quad z^{(2)} = \mathcal{T}^*(B(x_5^{(2)} + \epsilon_5)) \quad \text{with} \quad x_5^{(2)} = W^*(B(z_5^{(1)} - \epsilon_5)),$$

and subsequently find $t_3 > t_2$ such that $y(t) \leq x^{(2)} + \epsilon$, $\forall t > t_3$ and $t_4 > t_3$ such that $y(t) \geq z^{(2)} - \epsilon$, $\forall t > t_4$. Hence,

$$z^{(2)} - \epsilon \leq y(t) \leq x^{(2)} + \epsilon, \quad \forall t > t_4.$$

Furthermore, the relationship $z^{(1)} \ll z^{(2)} \ll x^{(2)} \ll x^{(1)}$ is verified. Indeed,

$$\text{since } B(z_5^{(1)} - \epsilon_5) < B(0), \text{ we have } \quad x^{(2)} = \mathcal{T}^*(B(z_5^{(1)} - \epsilon_5)) \ll \mathcal{T}^*(B(0)) = x^{(1)}.$$

Similarly, since $B(x_5^{(2)} + \epsilon_5) > B(x_5^{(1)} + \epsilon_5)$, we have

$$z^{(2)} = \mathcal{T}^*(B(x_5^{(2)} + \epsilon_5)) \gg \mathcal{T}^*(B(x_5^{(1)} + \epsilon_5)) = z^{(1)}.$$

Since $B(z_5^{(1)} - \epsilon_5) > B(x_5^{(1)} + \epsilon_5)$, we have

$$x^{(2)} = \mathcal{T}^*(B(z_5^{(1)} - \epsilon_5)) \gg \mathcal{T}^*(B(x_5^{(1)} + \epsilon_5)) = z^{(1)}.$$

Hence, $B(x_5^{(2)} + \epsilon_5) < B(z_5^{(1)} - \epsilon_5)$, and consequently,

$$z^{(2)} = \mathcal{T}^*(B(x_5^{(2)} + \epsilon_5)) \ll \mathcal{T}^*(B(z_5^{(1)} - \epsilon_5)) = x^{(2)}.$$

Therefore, $z^{(1)} \ll z^{(2)} \ll x^{(2)} \ll x^{(1)}$.

Repeating the above arguments, we get two monotone sequences of vectors $\{z^{(m)}\}_{m=1}^{\infty}$ and $\{x^{(m)}\}_{m=1}^{\infty}$ such that

$$0 \ll z^{(1)} \ll z^{(2)} \ll \cdots \ll z^{(m)} \ll x^{(m)} \ll \cdots \ll x^{(2)} \ll x^{(1)},$$

with $F(z^{(m)}, B(x_5^{(m)} + \epsilon_5)) = 0$ and $F(x^{(m)}, B(z_5^{(m)} - \epsilon_5)) = 0$, $\forall m \geq 2$. Moreover, there exists $t_{2m} > 0$ such that

$$z^{(m)} - \epsilon \leq y(t) \leq x^{(m)} + \epsilon, \forall t > t_{2m}.$$

Hence, there exist two positive vectors X^* and Z^* with $X \geq Z$ such that

$$\lim_{m\to\infty} z^{(m)} = Z^* \quad \text{and} \quad \lim_{m\to\infty} x^{(m)} = X^*.$$

Furthermore, $Z^* \leq \mathcal{T}^* \leq X^*$.

Step 2 : Passage to the limit.

For any $y_0 \neq 0$, the omega limit set $w(y_0) \in [Z^*, X^*]$ because the ordered interval $[Z^*, X^*]$ is positively invariant.

- If $Z^* = X^*$, then we have proved that $Z^* = X^* = \mathcal{T}^*$ and $\mathcal{T}^*$ is globally attractive.
- If $Z^* \neq X^*$, that is $Z^* < X^*$, then it is easy to see that $Z^* \ll X^*$. Moreover, by the uniform persistence in Remark 3.2.3, there exists $\eta > 0$ such that $w(y_0) \in [Z^*, X^*]$ with $Z_5^* + \eta \leq w_5(y_0) \leq X_5^* - \eta$, where $w_5(y_0)$ is the fifth coordinate of $w(y_0)$. By repeating the previous process, we can construct two vectors $Z^{*(1)}$ and $X^{*(1)}$ such that for any nonzero point y_0,

$$Z^* \ll Z^{*(1)} \ll \mathcal{T}^* \ll X^{*(1)} \ll X^* \quad \text{and} \quad w(y_0) \in [Z^{*(1)}, X^{*(1)}].$$

- If $Z^{*(1)} = X^{*(1)}$ then $Z^{*(1)} = X^{*(1)} = \mathcal{T}^*$ and $\mathcal{T}^*$ is globally attractive.
- If not, $Z^{*(1)} < X^{*(1)}$, then $Z^{*(1)} \ll X^{*(1)}$. Repeating the procedure, we can construct two sequences $Z^{*(m)}$ and $X^{*(m)}$ such that

$$Z^{*(1)} \ll Z^{*(2)} \ll \cdots \ll Z^{*(m-1)} \ll Z^{*(m)} \leq \mathcal{T}^* \leq X^{*(m)} \ll X^{*(m-1)} \ll X^{*(m-2)} \ll \cdots \ll X^{*(2)} \ll X^{*(1)}$$

and

$$\lim_{m\to\infty} Z^{*^{(m)}} = \lim_{m\to\infty} X^{*^{(m)}} = \mathcal{T}^*,$$

which implies that the omega limit set of every nonzero point y is $\mathcal{T}^*$ and thus $\mathcal{T}^*$ is globally attractive. □

Ecologically speaking, Theorem 3.2.5 and Theorem 3.2.6 imply that, mosquitoes will persist in the community whenever the associated conditions for the global stability/attractivity of $\mathcal{T}^*$ hold. These theorems are numerically supported by simulating the model (3.1) using; $n = 1$ for Figure 3.3(a) and $n = 13$ for Figure 3.3(b). Figure 3.3(b) show that, in the presence of density dependent mortality in the aquatic stage (i.e. $\mu_2 \neq 0$), the solutions of model (3.1) converge to $\mathcal{T}^*$ even if the conditions of Theorem 3.2.4 are satisfied. This suggests that, the phenomenon of Hopf bifurcation can be ruled out in the system by addicting a positive density dependent mortality rate $\mu_2 > 0$ in the aquatic stage of the mosquitoes.

In Table 3.3 below, we summarize the long run behavior of the solutions of the ODE model (3.1) subject to either of the four egg oviposition functions given in Table 3.1. The expressions of $\mathcal{R}_0^{\mathcal{L}}$ and n_{1*} are specified in Remark 3.2.4.

Table 3.3: Stability properties of the model (3.1). † denotes a result established exclusively in this paper.

$B(W)$	n and μ_2	$\mathcal{R}_0^{ode}$	$\mathcal{T}_0$	$\mathcal{T}^*$	Stable limit cycle	Source
B_M	$\mu_2 \geq 0$	$\mathcal{R}_0^{ode} \leq 1$	GAS	No	No	[2, 88]
	$\mu_2 > 0$	$\mathcal{R}_0^{ode} > 1$	Unstable	GAS	No	[2, 88]
B_L	$\mu_2 \geq 0$	$\mathcal{R}_0^{ode} \leq 1$	GAS	No	No	[108]
	$\mu_2 = 0$	$1 < \mathcal{R}_0^{ode} \leq \mathcal{R}_0^{\mathcal{L}}$	Unstable	LAS	No	[108]
	$\mu_2 = 0$	$\mathcal{R}_0^{ode} > \mathcal{R}_0^{\mathcal{L}}$	Unstable	Unstable	Yes	[108]
	$\mu_2 > 0$	$\mathcal{R}_0^{ode} > 1$	Unstable	GAS	No	†
B_S	$n > 0, \mu_2 \geq 0$	$\mathcal{R}_0^{ode} \leq 1$	GAS	No	No	†
	$1 < n < n_0^{**}, \mu_2 = 0$	$\mathcal{R}_0^{ode} > 1$	Unstable	LAS	No	†
	$n > n_0^{**}, \mu_2 = 0$	$\mathcal{R}_0^{ode} > 1$	Unstable	Unstable	Yes	†
	$n > 0, \mu_2 > 0$	$\mathcal{R}_0^{ode} > 1$	Unstable	GAS	No	†
B_H	$n > 0, \mu_2 \geq 0$	$\mathcal{R}_0^{ode} \leq 1$	GAS	No	No	†
	$1 < n < n_{1*}, \mu_2 = 0$	$\mathcal{R}_0^{ode} > 1$	Unstable	LAS	No	†
	$n > n_{1*}, \mu_2 = 0$	$\mathcal{R}_0^{ode} > 1$	Unstable	Unstable	Yes	†
	$n > 0, \mu_2 > 0$	$\mathcal{R}_0^{ode} > 1$	Unstable	GAS	No	†

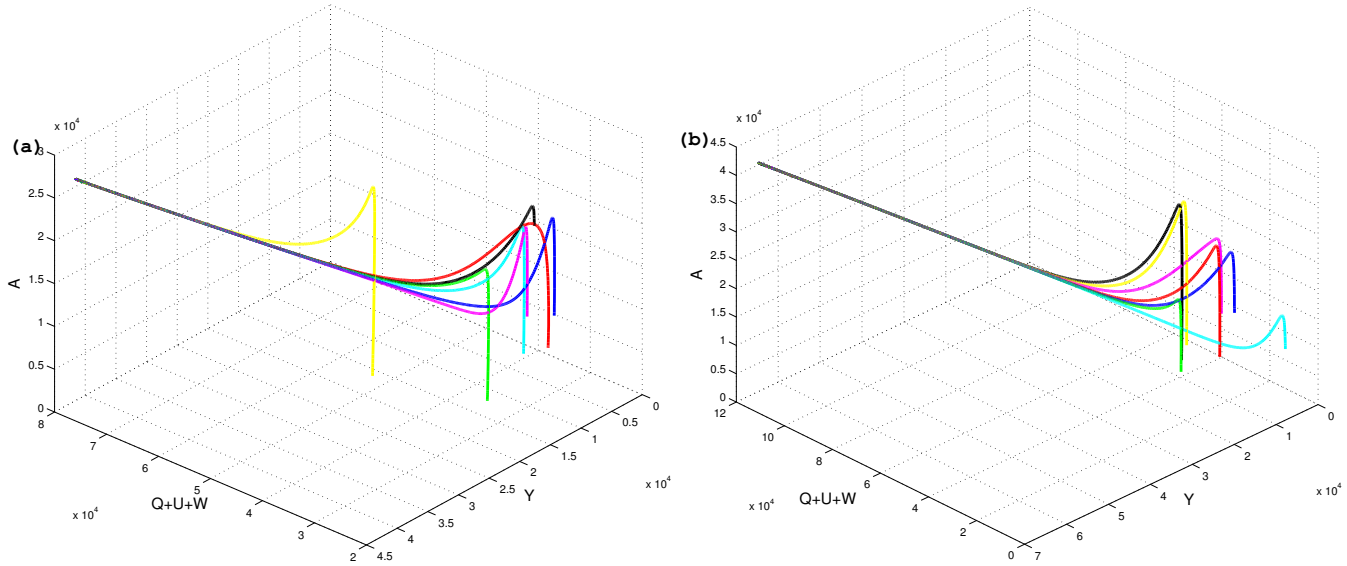

Figure 3.3: GAS of the MPE $\mathcal{T}^*$ for model (3.1). $\mu_2 = 0.0004$, $N_{egg} = 25$ and all other parameters are as in Table 3.4 (so that $\mathcal{R}_0^{ode} = 13.9399 > 1$): **(a)** $n = 1$. **(b)** $n = 13$.

3.2.5 Sensitivity analysis

We carried out sensitivity analysis to determine the model robustness to parameter values [8, 88]. This is a tool to identify the most influential parameters in determining mosquito dynamics. A latin hypercupe Sampling (LHS) scheme [90] samples 1000 values for each input parameter using a uniform distribution over the range of ecologically realistic values is given in Figures 3.4 and 3.5 with descriptions and references given in Table 3.4. Using the system of differential equations that describe (3.1) for $B(W)$ with $n = 1$, 5000 model simulations are performed by randomly pairing sampled values for all LHS parameters. Partial Rank Correlation Coefficients (PRCC) and corresponding p-values between $\mathcal{R}_0^{ode}$ and each parameter are computed. An output is assumed sensitive to an input if the corresponding PRCC is less than -0.50 or greater than $+0.50$, and the corresponding p-value is less than 5%.

From Figure 3.4 and Figure 3.5, we can identify five parameters that strongly influence the population dynamics and dispersal of the mosquito, namely the natural mortality rate of immature females (μ_Y), the natural mortality rate of the aquatic stage (μ_1), the natural mortality rate of breeding females (μ_W), the transfer rate (β) (also referred to as mating rate), the maturation rate (γ) and the deposit rate of eggs by females (N_{egg}). Thus, from this sensitivity analysis, the following suggestions are made:

(i) The mechanical control (such as removal of stagnant waters) could be an effective control measure against the growing of mosquitoes because the value of N_{egg} and the population size of mosquitoes are minimized;

Table 3.4: Values and ranges of the parameters of the model (3.1).

Parameters	Baseline Value	Range	Source
r	0.5		
γ	0.8/day	$0.5 - 0.89$	[38]
N_{egg}	50/day	$10 - 100$	[38, 108]
L	40000	$50 - 3 \times 10^6$	[108]
β	0.2/day	$0.05 - 0.35$	
μ_2	0.04/ml	$0.02 - 0.06$	[108]
μ_1	0.51/day	$0.28 - 0.76$	[38]
μ_M	0.14/day	$0.02 - 0.2$	[2, 88]
μ_Y	0.05/day	$0.01 - 0.2$	[2, 88]
μ_Q	0.18/day	$0.125 - 0.233$	[20]
μ_U	0.0043/day	$0.0034 - 0.01$	[20]
μ_W	0.41/day	$0.41 - 0.56$	[20]
φ_1	16	$12 - 20$	[104]
α	0.86	$0.75 - 0.95$	[104]
b_1	0.8/day	$0.46 - 0.92$	[104, 105]
a	0.43	$0.30 - 0.56$	[20]

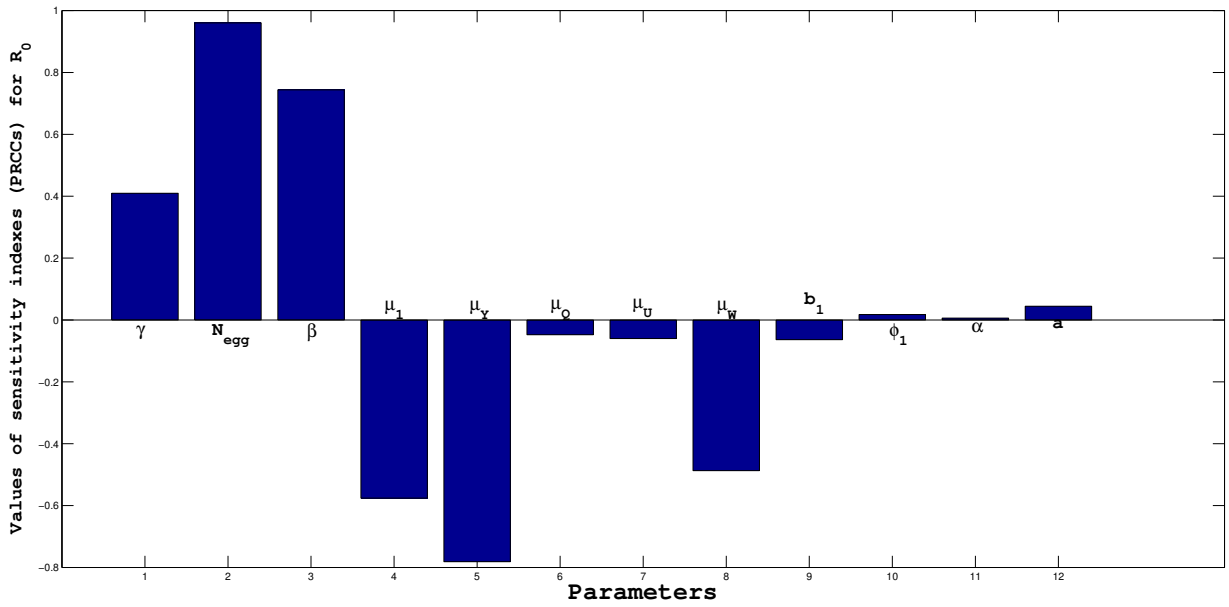

Figure 3.4: Sensitivity analysis between $\mathcal{R}_0^{ode}$ and each parameter.

(ii) The use of larvicides and removal of mosquito breeding sites seem to be important control measures against the mosquitoes because they increase in the value of μ_1 and reduce the value of γ;

(iii) The use of insecticides is potentially another good control tool against mosquito

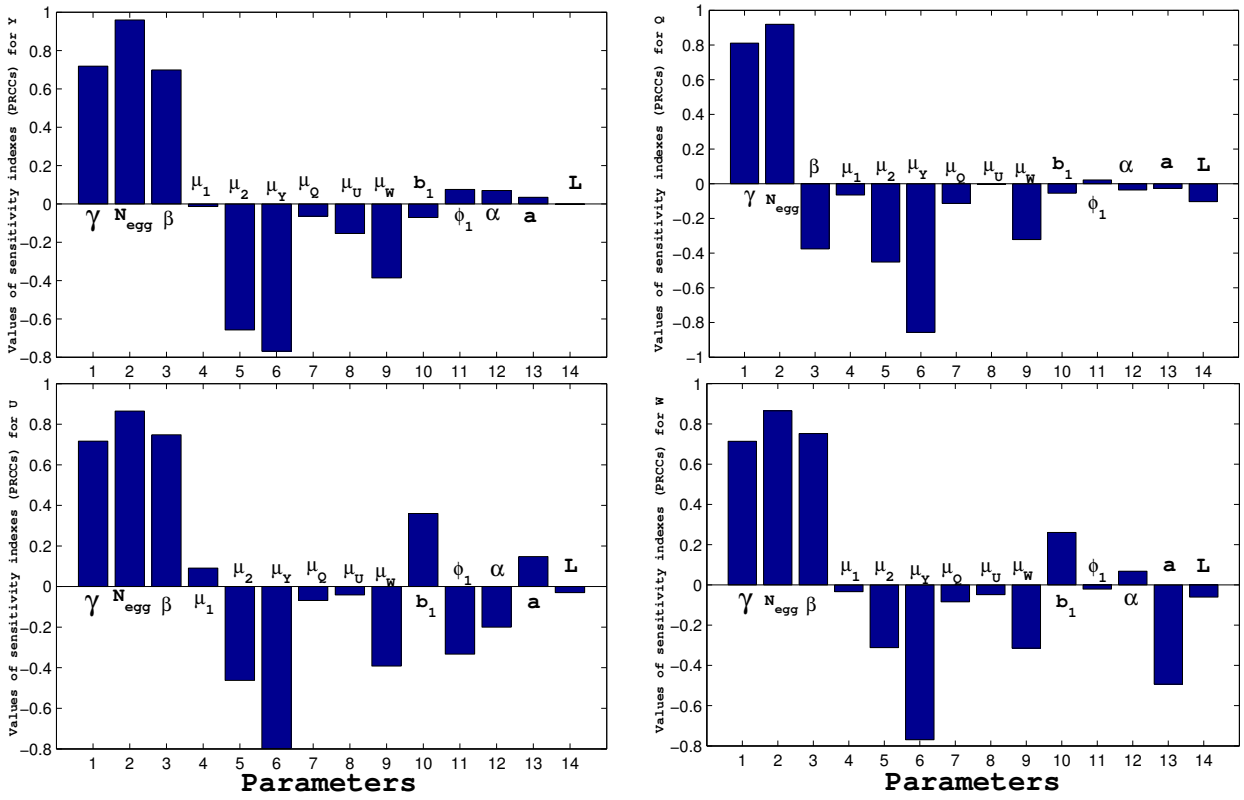

Figure 3.5: Sensitivity analysis between Y, Q, U, W and each parameter.

population because it helps increasing the values of μ_Y and μ_W;

(iv) The use of sterile insect technique (SIT) and genetically modified mosquitoes (GMM) may play an important role in minimizing the size of mosquito population by reducing the transfer rate (β) and maturation rate (γ).

3.3 Spatio-temporal model

3.3.1 Modeling framework

In order to assess the influence of mobility on the spread of mosquitoes, we extend model (3.1) by taking into account the spatial component. In this new setting, we give additional assumptions based on the mosquito ability to move, knowing that the mosquitoes in the aquatic stage often live in closed habitats such as unattended water containers. Therefore, it is reasonable to assume that resting females mosquitoes, as well as mosquitoes in the aquatic stage do not move. The remaining classes of adult mosquitoes disperse while searching for hosts for blood meals or breeding sites for reproduction [154]. The movements of adult mosquitoes can be classified into long-range and short-range dispersals. Long-range dispersal is often unintentional and aided by wind or human transport while short-range dispersal is often intentional and can be divided into non-oriented flights or oriented flights towards sites [45]. Mosquitoes follow odors and carbon dioxide carried by

the wind, which gives their main direction of migration [53]. Therefore, we add advection or drift terms to account for the fact that, when mosquitoes are stimulated by attractants (e.g. wind, hosts, breeding sites), they move preferably in certain directions [30, 42]. We use ε_M, ε_Q and ε_W to denote the constant velocity fluxes (migration coefficients) of males, questing females and breeding females, respectively. When mosquitoes are not submitted to stimuli, it is possible to assume that they move randomly in any direction [35, 42]. For simplicity, to describe the random movement of mosquitoes, we use diffusion to model it according to Fick's law. We denote D_Y, D_M, D_Q and D_W the diffusion coefficients for immature females, males, questing females and breeding females, respectively.

To make it simple, we concentrate on one dimensional spatial habitat $\Omega = (0, l),\ l > 0$ and assume that the mosquitoes are confined in that line segment all the time. The number of hosts is allowed to differ across Ω, introducing heterogeneity. Thus, the population density of humans $H(x)$ is location-dependent, implying that the parameters $\varphi_1(x)$, $b_1(x)$, $\nu_3(x)$ and $\nu_5(x)$ are location-dependent as well.

According to the above description, we propose the following spatio-temporal model

$$\begin{cases} \dfrac{\partial A}{\partial t} = B(W(t,x))W(t,x) - [\nu_1 + \mu_2 A(t,x)]A(t,x), \\ \dfrac{\partial Y}{\partial t} = D_Y \dfrac{\partial^2 Y}{\partial x^2} + r\gamma A(t,x) - \nu_2 Y(t,x), \\ \dfrac{\partial Q}{\partial t} = D_Q \dfrac{\partial^2 Q}{\partial x^2} - \varepsilon_Q \dfrac{\partial Q}{\partial x} + \beta Y(t,x) + b_1(x)W(t,x) - \nu_3(x)Q(t,x), \\ \dfrac{\partial U}{\partial t} = \alpha\varphi_1(x)Q(t,x) - \nu_4 U(t,x), \\ \dfrac{\partial W}{\partial t} = D_W \dfrac{\partial^2 W}{\partial x^2} - \varepsilon_W \dfrac{\partial W}{\partial x} + aU(t,x) - \nu_5(x)W(t,x), \end{cases} \tag{3.19}$$

Here $A(t,x)$, $Y(t,x)$, $Q(t,x)$, $U(t,x)$ and $W(t,x)$ measure the density of mosquitoes at location x and time t. Note that the equation for the density of male mosquitoes $M(t,x)$ is

$$\frac{\partial M}{\partial t} = D_M \frac{\partial^2 M}{\partial x^2} - \varepsilon_M \frac{\partial M}{\partial x} + (1-r)\gamma A(t,x) - \mu_M M(t,x). \tag{3.20}$$

We discard Eq. (3.20) from system (3.19) because the unknown $M(t,x)$ can be determined if $A(t)$ is known. Indeed, once $A(t)$ is found, (3.20) is a scalar advection-diffusion-reaction equation. Thereafter, it is well known that, along the characteristics $x \to x - t\varepsilon_M$, is transformed into a scalar reaction-diffusion equation that can be solved in a classical manner [79]. System (3.19) is appended with the initial conditions

$$\begin{cases} A(0,x) = \phi_1(x), \quad Y(0,x) = \phi_2(x), \quad Q(0,x) = \phi_3(x), \\ U(0,x) = \phi_4(x), \quad W(0,x) = \phi_5(x), \quad x \in \Omega, \end{cases} \tag{3.21}$$

the Neumann boundary conditions

$$\frac{\partial Y}{\partial x}(t,0) = \frac{\partial Y}{\partial x}(t,l) = 0, \tag{3.22}$$

and the Robin boundary conditions

$$D_Z \frac{\partial Z}{\partial x}(t,0) - \varepsilon_Z Z(t,0) = \frac{\partial Z}{\partial x}(t,l) = 0, \quad Z = Q, W, \tag{3.23}$$

where each ϕ_i $(i = 1,2,3,4,5)$ is assumed to be nonnegative and continuous in the space variable x.

3.3.2 Existence of positive solutions

The aim here is to give the preliminary results for the well-posedness of system (3.19)-(3.23). These results include the existence of the unique maximal bounded semiflow associated with (3.19)-(3.23).

Let $u(t,x) = (A(t,x), Y(t,x), Q(t,x), U(t,x), W(t,x)) = (u_1(t,x), u_2(t,x), u_3(t,x), u_4(t,x), u_5(t,x))$ denote a solution for (3.19) corresponding to the initial condition $\phi = (\phi_1, \phi_2, \phi_3, \phi_4, \phi_5)$. Let $X := C(\overline{\Omega}, \mathbb{R}^5) = \prod_{i=1}^5 X_i$, $X_i := C(\overline{\Omega}, \mathbb{R})$, $i = 1, ..., 5$ be the Banach space of $\mathbb{R}^5$-valued functions continuous in $x \in \overline{\Omega}$ equipped with the usual sup norm $\|u\|_X = \sum_{i=1}^5 \|u_i\|_{X_i}$, $X^+ := C(\overline{\Omega}, \mathbb{R}^5_+) = \prod_{i=1}^5 X_i^+$, where $X_i^+ := C(\overline{\Omega}, \mathbb{R}_+)$ the positive cone of X_i.

Denote by $\mathbb{I}$ the identity operator on X_i. Let $T_i(t) : X_i \longrightarrow X_i$, $t \geq 0$, $i = 2,3,5$, be the semigroups associated with the operators $D_Y \partial^2_{xx} - \nu_2 \mathbb{I}$, $D_Q \partial^2_{xx} - \varepsilon_Q \partial_x - \nu_3(\cdot)\mathbb{I}$ and $D_W \partial^2_{xx} - \varepsilon_W \partial_x - \nu_5(\cdot)\mathbb{I}$, respectively, subject to the Neumann and Robin boundaries conditions. It follows from [124] that $T_i(t)$, $i = 2,3,5$ is compact. Moreover, according to Definition A.1.5 in Appendix and thanks to Corollary 7.2.3 in [124], $T_i(t)$, $i = 2,3,5$ is strongly positive. We also define

$$(T_1(t)\phi_1)(x) = e^{-\nu_1 t}\phi_1(x) \quad \text{and} \quad (T_4(t)\phi_4)(x) = e^{-\nu_4 t}\phi_4(x),$$

for any $\phi_i \in X_i$, $i = 1,4$, $t \geq 0$. Then,

$$T(t) = (T_1(t), T_2(t), T_3(t), T_4(t), T_5(t)) : X \longrightarrow X, \quad \forall t \geq 0 \tag{3.24}$$

defines a C_0-semigroup (see e.g. [134]).

Define $F = (F_1, F_2, F_3, F_4, F_5) : X^+ \longrightarrow X$ by

$$F(\phi)(x) := \begin{pmatrix} B(\phi_5)\phi_5 - \mu_2\phi_1^2 \\ r\gamma\phi_1 \\ \beta\phi_2 + b_1(x)\phi_5 \\ \alpha\varphi_1(x)\phi_3 \\ a\phi_4 \end{pmatrix}, \ \forall x \in \overline{\Omega} \quad \text{and} \quad \phi = (\phi_1, \phi_2, \phi_3, \phi_4, \phi_5) \in X^+. \tag{3.25}$$

Then, system (3.19)-(3.23) can be rewritten as the following integral equation

$$u(t) := T(t)\phi + \int_0^t T(t-s)F(u(s))ds, \tag{3.26}$$

whose solution is called mild solution (see Definition A.1.4). The following result guaranties the local well-posedness of (3.19)-(3.23) on X^+.

Theorem 3.3.1. For all $\phi \in X^+$, the system (3.19)-(3.23) has a unique mild solution $u(t,\cdot,\phi) := (u_1(t,\cdot), u_2(t,\cdot), u_3(t,\cdot), u_4(t,\cdot), u_5(t,\cdot))$ on the interval of existence $[0,\sigma_\phi)$ with $u(0,\cdot,\phi) = \phi$, where $\sigma_\phi \leq \infty$. Furthermore for $t \in [0,\sigma_\phi)$, $u(t,\cdot,\phi) \in X^+$ and $u(t,\cdot,\phi)$ is a classical solution of (3.19)-(3.23).

Proof. By Corollary 4 in [91] and Theorem 7.3.1 in [124], it suffices to show that for any $\phi \in X^+$,

$$\lim_{h\to 0^+} dist(\phi + hF(\phi), X^+) = 0. \tag{3.27}$$

Let $\tilde{b}_1 = \min_{x\in\overline{\Omega}}\{b_1(x)\}$ and $\tilde{\varphi}_1 = \min_{x\in\overline{\Omega}}\{\varphi_1(x)\}$. Then for any $\phi \in X^+$ and $h \geq 0$, we have

$$\phi + hF(\phi) = \begin{pmatrix} \phi_1 + h[B(\phi_5)\phi_5 - \mu_2\phi_1^2] \\ \phi_2 + hr\gamma\phi_1 \\ \phi_3 + h[\beta\phi_2 + b_1(x)\phi_5] \\ \phi_4 + h\alpha\varphi_1(x)\phi_3 \\ \phi_5 + ha\phi_4 \end{pmatrix} \geq \begin{pmatrix} \phi_1[1 - h\mu_2\phi_1] \\ \phi_2 + hr\gamma\phi_1 \\ \phi_3 + h[\beta\phi_2 + \tilde{b}_1\phi_5] \\ \phi_4 + h\alpha\tilde{\varphi}_1\phi_3 \\ \phi_5 + ha\phi_4 \end{pmatrix}.$$

The above inequalities imply that (3.27) holds, this complete the proof. □

In order to state and establish the global well-posedness result for (3.19)-(3.23), the following result, established in [156], which extends Lemma 1 in [82] in the presence of advection, is instrumental.

Lemma 3.3.1 ([156], Proposition 1)**.** Consider in a spatial domain with $x \in \overline{\Omega}$, the following scalar reaction-advection-diffusion equation

$$\begin{cases} \partial_t w(t,x) = \overline{D}\partial^2_{xx} w(t,x) - \overline{\varepsilon}\partial_x w(t,x) + g(x) - \lambda w(t,x),\ t > 0, \\ \overline{D}\partial_x w(t,x) - \overline{\varepsilon} w(t,x) = 0, \quad x \in \partial\Omega,\ t > 0, \\ w(0,x) = \psi(x), \quad x \in \overline{\Omega}, \end{cases} \tag{3.28}$$

where $\overline{D} > 0$, $\lambda > 0$, $\overline{\varepsilon} \geq 0$, and $g(x) > 0$ is a continuous function. Then, for all $\psi \in C(\overline{\Omega}, \mathbb{R}_+)$, there exists a unique positive steady state w^* which is globally attractive in $C(\overline{\Omega}, \mathbb{R})$. Moreover, in the case $\overline{\varepsilon} = 0$ and $g(x) \equiv g$, it holds that $w^* = \dfrac{g}{\lambda}$.

Now we are in a position to show that solutions of the system (3.19)-(3.23) exist globally for $t \in [0,\infty)$ in X^+.

Theorem 3.3.2. For any $\phi \in X^+$, system (3.19)-(3.23) admits a unique solution $u(t,x,\phi)$ defined on $[0,\infty)$ with $u(0,\cdot,\phi) = \phi$ and a semiflow $\Phi_t := \Phi(t) : X^+ \longrightarrow X^+$ is generated by (3.19)-(3.23) which is defined by

$$\Phi(t)\phi = u(t,\cdot,\phi), \quad t \geq 0. \tag{3.29}$$

Furthermore $\Phi_t := \Phi(t) : X^+ \longrightarrow X^+$ is point dissipative.

Proof. For any $\phi \in X^+$, we denote by $u(t,x,\phi)$ the unique solution of system (3.19)-(3.23) satisfying $u(0,x) = u_0(x) = \phi(x)$ with the maximal interval of existence $[0,\sigma)$ for some $\sigma > 0$. By Theorem 3.3.1, we have $u(t,x,\phi) \geq 0$. Having in mind that $B(W)W$ is bounded above by $N_{egg}L$, it comes that

$$\partial_t A(t,x) \leq N_{egg}L - \nu_1 A, \quad \forall t \geq 0, \quad x \in \overline{\Omega}.$$

This implies that there exists $t_1 = t_1(\phi) > 0$ such that $A(t,x) \leq \dfrac{N_{egg}L}{\nu_1}$, $\forall t \geq t_1$, $x \in \overline{\Omega}$.

Next, from Eq. (3.19), one has

$$\partial_t Y(t,x) \leq D_Y \partial^2_{xx} Y + r\gamma M_0 - \nu_2 Y, \quad \forall t \geq t_1.$$

The comparison principle (see [49] or [125], Theorem 10.1) and Lemma 3.3.1 with $\overline{D} = D_Y$, $\overline{\varepsilon} = 0$, $g(x) = r\gamma M_0$, $\lambda = \nu_2$, imply that there exists $t_2 = t_2(\phi) > t_1 > 0$ large enough so that

$$Y(t,x) \leq \frac{r\gamma M_0}{\nu_2} := M_1, \quad \forall t \geq t_2, \quad x \in \overline{\Omega}.$$

Let $V := Q + U + W$, then from (3.19) we have

$$\partial_t V(t,x) \leq D_0 \partial^2_{xx} V - \varepsilon_0 \partial_x V + \beta M_1 - \mu_0 V, \quad \forall t > t_2,$$

where $D_0 = \max\{D_Q, D_W\}$, $\varepsilon_0 = \min\{\varepsilon_Q, \varepsilon_W\}$ and $\mu_0 = \min\{\mu_Q, \mu_U, \mu_W\}$. Another application of the comparison principle and Lemma 3.3.1 with $\overline{\varepsilon} = \varepsilon_0 > 0$, $\overline{D} = D_0$, $g(x) = \beta M_1$, $\lambda = \mu_0$, yields $t_3 = t_3(\phi) > t_2 > 0$ large enough so that

$$Q(t,x) + U(t,x) + W(t,x) \leq \frac{\beta M_1}{\mu_0} := M_2, \quad \forall t \geq t_3, \quad x \in \overline{\Omega}.$$

Hence, the solutions of (3.19)-(3.23) are ultimately bounded with respect to the maximum norm. Therefore, the latter results, combined with the local existence in Theorem 3.3.1, yields the global existence of the solution $u(t,x,\phi)$ in $[0,\infty)$. It follows that the solution semiflow Φ_t is point dissipative. □

Since the first and the fourth equation in (3.19) have no diffusion term, the solution map Φ_t is no compact. In order to overcome this problem, we introduce the Kuratowski measure κ (see [36]), which is defined by

$$\kappa(B) := \inf\{r_1 : B \text{ has a finite cover of diameter} < r_1\}, \tag{3.30}$$

for any bounded set B. We set $\kappa(B) = \infty$ whenever B is unbounded. It is easy to see that B is precompact (i.e. $\overline{B}$ is compact) if and only if $\kappa(B) = 0$. Then the solution map Φ_t has some partial compactness in the following sense.

Lemma 3.3.2. Φ_t is κ-contracting in the sense that

$$\lim_{t\to\infty} \kappa(\Phi(t)B) = 0 \quad \text{for any bounded} \quad B \subset X^+.$$

Proof. For convenience, we let $\mathbf{u} := (Y, Q, W)$, $\mathbf{v} := (A, U)$, $\mathbf{D} = \text{diag}(D_Y, D_Q, D_W)$, $\varepsilon = \text{diag}(0, \varepsilon_Q, \varepsilon_W)$ and define

$$m(t,x,\mathbf{u},\mathbf{v}) = \begin{pmatrix} r\gamma A - \nu_2 Y \\ \beta Y + b_1(x)W - \nu_3(x)Q \\ aU - \nu_5(x)W \end{pmatrix} \quad \text{and} \quad g(t,x,\mathbf{u},\mathbf{v}) = \begin{pmatrix} B(W)W - (\nu_1 + \mu_2 A)A \\ \alpha\varphi_1(x)Q - \nu_4 U \end{pmatrix}.$$

Then system (3.19)-(3.23) can be rewritten as

$$\begin{cases} \dfrac{\partial \mathbf{u}}{\partial t} = \mathbf{D}\dfrac{\partial^2 \mathbf{u}}{\partial x^2} - \varepsilon\dfrac{\partial \mathbf{u}}{\partial x} + m(t,x,\mathbf{u},\mathbf{v}), \\ \dfrac{\partial \mathbf{v}}{\partial t} = g(t,x,\mathbf{u},\mathbf{v}), \quad x \in \overline{\Omega},\ t > 0, \\ \mathbf{D}\dfrac{\partial \mathbf{u}}{\partial x}(t,0) - \varepsilon\mathbf{u}(t,0) = \dfrac{\partial \mathbf{u}}{\partial x}(t,l) = 0 \\ \mathbf{u}(0,x) = \phi, \quad \mathbf{v}(0,x) = \psi. \end{cases}$$

Then, for any $(\mathbf{u}, \mathbf{v}) \in X^+$, we have

$$\mathbf{x}^T \mathcal{M}(\mathbf{u},\mathbf{v})\mathbf{x} \le -r_1 \mathbf{x}^T\mathbf{x}, \quad \forall \mathbf{x} \in \mathbb{R}^2, \tag{3.31}$$

where

$$\mathcal{M}(\mathbf{u},\mathbf{v}) = \frac{\partial g(t,x,\mathbf{u},\mathbf{v})}{\partial \mathbf{v}} = \begin{pmatrix} -\nu_1 - 2\mu_2 A & 0 \\ 0 & -\nu_4 \end{pmatrix} \quad \text{and} \quad r_1 = \min\{\nu_1; \nu_4\}.$$

Let B be a given bounded subset in X^+. We first show that Φ_t is asymptotically compact on B in the sense that for any sequences $\varphi_n \in B$ and $t_n \to \infty$, there exist subsequences φ_{n_k} and $t_{n_k} \to \infty$ such that $\Phi_{t_{n_k}}(\varphi_{n_k})$ converges in X^+ as $k \to \infty$. Note that the family of functions $\{\Phi_{t_n}(\varphi_n)(x)\}_{n\ge1}$ is uniformly bounded on $\overline{\Omega}$ for all $n \ge 1$. In view of the Arzela-Ascoli Theorem, it suffices to prove that $\{\Phi_{t_n}(\varphi_n)(x)\}_{n\ge1}$ is equicontinuous in $x \in \overline{\Omega}$ for all $n \ge 1$.

Let $(\mathbf{u}_n(t,x), \mathbf{v}_n(t,x)) = \Phi_t(\varphi_n)(x)$, $\forall \varphi_n \in X^+$, $t \ge 0$, $x \in \overline{\Omega}$. For simplicity, we define

$$\overline{\mathbf{u}}_n(t,x) := \mathbf{u}_n(t + t_n, x) \quad \text{and} \quad \overline{\mathbf{v}}_n(t,x) := \mathbf{v}_n(t + t_n, x), \quad \forall t \ge -t_n,\ x \in \overline{\Omega}.$$

Clearly, $(\overline{\mathbf{u}}_n(0,x), \overline{\mathbf{v}}_n(0,x)) = \Phi_{t_n}(\varphi_n)(x)$, $\forall n \ge 1$, $x \in \overline{\Omega}$. Note that $\overline{\mathbf{u}}_n(t,x)$ and $\overline{\mathbf{v}}_n(t,x)$ are uniformly bounded, $\forall n \ge 1$, $x \in \overline{\Omega}$, $t \ge 0$.

By a direct computation, we see that for all $t \ge -t_n$, $x, y \in \overline{\Omega}$, there holds

$$\begin{aligned} \frac{\partial}{\partial t}\Big[(\overline{\mathbf{v}}_n(t,x) - \overline{\mathbf{v}}_n(t,y))^T \cdot (\overline{\mathbf{v}}_n(t,x) - \overline{\mathbf{v}}_n(t,y))\Big] &= 2(\overline{\mathbf{v}}_n(t,x) - \overline{\mathbf{v}}_n(t,y))^T \cdot \frac{\partial}{\partial t}(\overline{\mathbf{v}}_n(t,x) - \overline{\mathbf{v}}_n(t,y)) \\ &= 2(\overline{\mathbf{v}}_n(t,x) - \overline{\mathbf{v}}_n(t,y))^T \cdot \Big[g(t+t_n, x, \overline{\mathbf{u}}_n(t,x), \overline{\mathbf{v}}_n(t,x)) \\ &\quad - g(t+t_n, y, \overline{\mathbf{u}}_n(t,y), \overline{\mathbf{v}}_n(t,y))\Big]. \end{aligned} \tag{3.32}$$

Moreover,

$$\begin{aligned}
&\Big[g(t+t_n,x,\overline{\mathbf{u}}_n(t,x),\overline{\mathbf{v}}_n(t,x))-g(t+t_n,y,\overline{\mathbf{u}}_n(t,y),\overline{\mathbf{v}}_n(t,y))\Big]\\
&=\Big[g(t+t_n,x,\overline{\mathbf{u}}_n(t,x),\overline{\mathbf{v}}_n(t,x))-g(t+t_n,x,\overline{\mathbf{u}}_n(t,x),\overline{\mathbf{v}}_n(t,y))\Big]\\
&+\Big[g(t+t_n,x,\overline{\mathbf{u}}_n(t,x),\overline{\mathbf{v}}_n(t,y))-g(t+t_n,y,\overline{\mathbf{u}}_n(t,y),\overline{\mathbf{v}}_n(t,y))\Big]\\
&=\left[\int_0^1\frac{\partial g(t+t_n,x,\overline{\mathbf{u}}_n(t,x),\overline{\mathbf{v}}_n(t,x)+\eta(\overline{\mathbf{v}}_n(t,x)-\overline{\mathbf{v}}_n(t,y))}{\partial\mathbf{v}}d\eta\right]\cdot[(\overline{\mathbf{v}}_n(t,x)-\overline{\mathbf{v}}_n(t,y))]\\
&+\Big[g(t+t_n,x,\overline{\mathbf{u}}_n(t,x),\overline{\mathbf{v}}_n(t,y))-g(t+t_n,y,\overline{\mathbf{u}}_n(t,y),\overline{\mathbf{v}}_n(t,y))\Big].
\end{aligned}\tag{3.33}$$

Set

$$\mathbf{H}_n(t,x,y):=\|g(t+t_n,x,\overline{\mathbf{u}}_n(t,x),\overline{\mathbf{v}}_n(t,y))-g(t+t_n,y,\overline{\mathbf{u}}_n(t,y),\overline{\mathbf{v}}_n(t,y))\|.$$

It then follows from (3.31), (3.32) and (3.33) that there exists a real number $N>0$ such that

$$\frac{\partial}{\partial t}\|\overline{\mathbf{v}}_n(t,x)-\overline{\mathbf{v}}_n(t,y)\|^2\le -2r_1\|\overline{\mathbf{v}}_n(t,x)-\overline{\mathbf{v}}_n(t,y)\|^2+N\mathbf{H}_n(t,x,y),\tag{3.34}$$

for all $t\ge -t_n$, $x,y\in\overline{\Omega}$.

By the constant variation formula and the comparison argument, we obtain

$$\|\overline{\mathbf{v}}_n(t,x)-\overline{\mathbf{v}}_n(t,y)\|^2\le e^{-2r_1(t-s)}\|\overline{\mathbf{v}}_n(s,x)-\overline{\mathbf{v}}_n(s,y)\|^2+N\int_s^t e^{-2r_1(t-\theta)}\mathbf{H}_n(\theta,x,y)d\theta,\tag{3.35}$$

for all $t\ge s\ge -t_n$. Letting $t=0$ and $s=-t_n$ in (3.35), we further have

$$\|\overline{\mathbf{v}}_n(0,x)-\overline{\mathbf{v}}_n(0,y)\|^2\le e^{-2r_1t_n}\|\overline{\mathbf{v}}_n(-t_n,x)-\overline{\mathbf{v}}_n(-t_n,y)\|^2+N\int_{-t_n}^0 e^{2r_1\theta}\mathbf{H}_n(\theta,x,y)d\theta,$$

and hence,

$$\|\mathbf{v}_n(t_n,x)-\mathbf{v}_n(t_n,y)\|^2\le e^{-2r_1t_n}\|\mathbf{v}_n(0,x)-\mathbf{v}_n(0,y)\|^2+N\int_{-t_n}^0 e^{2r_1\theta}\mathbf{H}_n(\theta,x,y)d\theta,\tag{3.36}$$

for all $n\ge 1$, $x,y\in\overline{\Omega}$.

Note that $(\mathbf{u}_n(0,x),\mathbf{v}_n(0,x))=\varphi_n$ and $\varphi_n\in B$, for all $n\ge 1$ and $x\in\overline{\Omega}$, and that $\{\mathbf{u}_n(t_n,x)\}_{n\ge1}$ is equicontinuous on $\overline{\Omega}$ for all $n\ge1$. Thus, it suffices to prove that $\{\mathbf{v}_n(t_n,x)\}_{n\ge1}$ is equicontinuous on Ω for all $n\ge1$ in the sense that for any $\epsilon>0$, there exists $\delta>0$ such that

$$\|\mathbf{v}_n(t_n,x)-\mathbf{v}_n(t_n,y)\|<\epsilon,\ \ \forall n\ge1,\ \ \forall x,y\in\overline{\Omega}\ \text{ with }\ |x-y|<\delta.$$

Suppose, by contradiction, that there exist an $\epsilon_0>0$, $n_k\to\infty$, $x_k,y_k\in\overline{\Omega}$ with $|x_k-y_k|<\frac{1}{k}$ such that $\|\mathbf{v}_{n_k}(t_{n_k},x_k)-\mathbf{v}_{n_k}(t_{n_k},y_k)\|\ge\epsilon_0$, $\forall k\ge1$. Letting $x=x_k$, $y=y_k$ and $n=n_k$ in (3.36), we then obtain

$$\epsilon_0^2\le\limsup_{k\to\infty}\|\mathbf{v}_{n_k}(t_{n_k},x_k)-\mathbf{v}_{n_k}(t_{n_k},y_k)\|^2\le N\cdot\limsup_{k\to\infty}\int_{-t_{n_k}}^0 e^{2r_1\theta}\mathbf{H}_{n_k}(\theta,x_k,y_k)d\theta.\tag{3.37}$$

Note that for each $\theta \leq 0$, there exists a large integer $n_0 > 0$ such that the sequence of functions $\{\overline{\mathbf{u}}_n(\theta, x) = \mathbf{u}_n(\theta + t_n, x)\}_{n \geq n_0}$ is equicontinuous on $\overline{\Omega}$, and that $g(t, x, \mathbf{u}, \mathbf{v})$ is uniformly continuous in $(t, x, \mathbf{u}, \mathbf{v}) \in [0, \infty) \times \overline{\Omega} \times \mathcal{H}$, where $\mathcal{H}$ is any given compact subset of $\mathbb{R}^5_+$. Since $\lim_{k\to\infty} \|\overline{\mathbf{u}}_{n_k}(\theta, x_k) - \overline{\mathbf{u}}_{n_k}(\theta, y_k)\| = 0$, it follows that for any given $\theta \leq 0$, we have $\lim_{k\to\infty} \mathbf{H}_{n_k}(\theta, x_k, y_k) = 0$. Using Fatou's lemma in (3.37), we then obtain

$$\epsilon_0^2 \leq N \cdot \int_{-\infty}^{0} e^{2r_1\theta} \limsup_{k\to\infty} \mathbf{H}_{n_k}(\theta, x_k, y_k) d\theta = 0,$$

a contradiction. Consequently, Φ_t is asymptotically compact on B.

Now we consider the omega limit set of B for the Poincaré map Φ_t on X^+, which is defined as

$$\omega(B) = \{\varphi \in X^+ \,:\, \lim_{k\to\infty} \Phi_{t_{n_k}}(\varphi_k) = \varphi \text{ for some sequences } \varphi_k \in B \text{ and } n_k \to \infty\}.$$

From what we proved for Φ_t, we easily see that $\Phi_{t_n}, \forall n \geq 0$ is asymptotically compact on B in the sense that for any sequences $\varphi_k \in B$ and $n_k \to \infty$, there exists subsequences, which we label as φ_k and $n_k \to \infty$, such that $\Phi_{t_{n_k}}(\varphi_k)$ converges in X as $k \to \infty$. It then follows that $\omega(B)$ is a nonempty, compact and invariant set for Φ_t in X^+, and $\omega(B)$ attracts B. In view of Lemma 2.1 (b) in [84], we have

$$\kappa(\Phi(t)B) \leq \kappa(\omega(B)) + \delta(\Phi(t)B, \omega(B)) = \delta(\Phi(t)B, \omega(B)) \to 0 \text{ as } t \to \infty.$$

This completes the proof. □

Now we are ready to show that solutions of system (3.19) converge to a compact attractor in X^+.

Theorem 3.3.3. $\Phi(t)$ admits a connected global attractor on X^+.

Proof. By Theorem 3.3.2 and Lemma 3.3.2, it follows that $\Phi(t)$ is point dissipative and κ-contracting on X^+. From the proof of Theorem 3.3.2, we also know that the positive orbits of bounded subsets of X^+ for $\Phi(t)$ are uniformly bounded. By Theorem 2.6 in [84], $\Phi(t)$ has a global attractor that attracts every bounded set in X^+. □

3.3.3 Threshold dynamics of model (3.19)

In order to define the basic offspring ratio $\mathcal{R}_0^{pde}$ for system (3.19)-(3.23), we first observe that system (3.19) has a spatially homogeneous trivial equilibrium $\mathcal{T}_0 = (0, 0, 0, 0, 0)$. Note that, while a huge number of works deals with the threshold dynamics for ODE models, very few such studies are devoted to PDE models. This is probably due to the fact that the concept of basic reproduction number has just recently been extended to PDE models such as reaction-diffusion and reaction-convection-diffusion epidemic models with mixed boundary conditions [129, 141, 142, 144]. The definition of $\mathcal{R}_0^{pde}$ in this work follows the

approach developed in [129]. That is, $\mathcal{R}_0^{pde} = r(\mathcal{L})$ is the spectral radius of the operator $\mathcal{L} := -\mathcal{G}\mathcal{S}^{-1}$, where

$$\mathcal{S} = \text{diag}\Big(-\nu_1, D_Y\partial_{xx}^2 - \nu_2, D_Q\partial_{xx}^2 - \varepsilon_Q\partial_x - \nu_3(.), -\nu_4, D_W\partial_{xx}^2 - \varepsilon_W\partial_x - \nu_5(.)\Big),$$

being the infinitesimal generator of the semigroup $T(t)$ defined in Eq. (3.24) and $\mathcal{G}$ defined by

$$\mathcal{G}(x) = \begin{pmatrix} 0 & 0 & 0 & 0 & N_{egg} \\ r\gamma & 0 & 0 & 0 & 0 \\ 0 & \beta & 0 & 0 & b_1(x) \\ 0 & 0 & \alpha\varphi_1(x) & 0 & 0 \\ 0 & 0 & 0 & a & 0 \end{pmatrix},$$

such that, for all $\psi \in X$, and $x \in \Omega$,

$$\mathcal{L}(\psi)(x) = (-\mathcal{G}\mathcal{S}^{-1}\psi)(x) = \mathcal{G}(x)(-\mathcal{S}^{-1}\psi)(x) = \mathcal{G}(x)\int_0^\infty T(t)(\psi(x))dt.$$

Let us recall some important results on which our proof will heavily rely.

Lemma 3.3.3 ([129], Theorem 3.12)**.** Let Ψ be the generator of a C_0-semigroup P on an ordered Banach space X with a normal and generating cone X^+. Then Ψ is resolvent-positive if and only if P is a positive semigroup i.e. $P(t)X^+ \subset X^+$, $\forall t \geq 0$.

Lemma 3.3.4 ([129], Theorem 3.5)**.** Let Ψ be a resolvent-positive operator in X, $s(\Psi) < 0$ and $\Theta = \Phi + \Psi$ be a positive perturbation of Ψ. If Θ is resolvent-positive, then $s(\Theta)$ has the same sign as $r(-\Phi\Psi^{-1}) - 1$.

The result below establishes the global attractivity of $\mathcal{T}_0$.

Theorem 3.3.4. Consider the model (3.19)-(3.23). Then, the spatially homogeneous trivial equilibrium $\mathcal{T}_0$ is globally attractive whenever $\mathcal{R}_0^{pde} < 1$.

Proof. Linearizing system (3.19)-(3.23) around $\mathcal{T}_0$, we obtain the linear cooperative system

$$\begin{cases} \frac{\partial A}{\partial t} = N_{egg}W(t,x) - \nu_1 A(t,x), \\ \frac{\partial Y}{\partial t} = D_Y\frac{\partial^2 Y}{\partial x^2} + r\gamma A(t,x) - \nu_2 Y(t,x), \\ \frac{\partial Q}{\partial t} = D_Q\frac{\partial^2 Q}{\partial x^2} - \varepsilon_Q\frac{\partial Q}{\partial x} + \beta Y(t,x) + b_1(x)W(t,x) - \nu_3(x)Q(t,x), \\ \frac{\partial U}{\partial t} = \alpha\varphi_1(x)Q(t,x) - \nu_4 U(t,x), \\ \frac{\partial W}{\partial t} = D_W\frac{\partial^2 W}{\partial x^2} - \varepsilon_W\frac{\partial W}{\partial x} + aU(t,x) - \nu_5(x)W(t,x), \\ \partial_x Y(t,0) = \partial_x Y(t,l) = 0, \\ D_Z\partial_x Z(t,0) - \varepsilon_Z Z(t,0) = \partial_x Z(t,l) = 0, \quad Z = Q, W. \end{cases} \tag{3.38}$$

Substituting $(A, Y, Q, U, W) = (e^{\lambda t}\psi_1(x), e^{\lambda t}\psi_2(x), e^{\lambda t}\psi_3(x), e^{\lambda t}\psi_4(x), e^{\lambda t}\psi_5(x))$ in (3.38), with $\lambda \in \mathbb{C}$, yields the eigenvalue problem

$$\begin{cases} \lambda\psi_1 = N_{egg}\psi_5 - \nu_1\psi_1, \\ \lambda\psi_2 = D_Y\partial^2_{xx}\psi_2 + r\gamma\psi_1 - \nu_2\psi_2, \\ \lambda\psi_3 = D_Q\partial^2_{xx}\psi_3 - \varepsilon_Q\partial_x\psi_3 + \beta\psi_2 + b_1(x)\psi_5 - \nu_3(x)\psi_3, \\ \lambda\psi_4 = \alpha\varphi_1(x)\psi_3 - \nu_4\psi_4, \\ \lambda\psi_5 = D_W\partial^2_{xx}\psi_5 - \varepsilon_W\partial_x\psi_5 + a\psi_4 - \nu_5(x)\psi_5, \\ \partial_x\psi_2(t,0) = \partial_x\psi_2(t,l) = 0, \\ D_Z\partial_x\psi_i(t,0) - \varepsilon_Z\psi_i(t,0) = \partial_x\psi_i(t,l) = 0, \quad i = 3,5, \quad Z = Q, W. \end{cases} \tag{3.39}$$

The right-hand side of first five equations of eigenvalue problem (3.39) takes the form

$$\Theta\psi := (\mathcal{S} + \mathcal{G})\psi, \text{ where, } \psi = (\psi_1, \psi_2, ..., \psi_5)^T. \tag{3.40}$$

Note that $\mathcal{G}$ is a positive and cooperative. Thanks to the graph theory, $\mathcal{G}$ is also irreducible. Moreover, $\mathcal{S}$ and $\mathcal{G}$ are both generators of positive C_0-semigroups. Hence, by Lemma 3.3.3, $\mathcal{S}$ and $\mathcal{G}$ are both resolvent-positive (see Definition A.1.6 in Appendix A). Following the arguments in [124] or [157], one can prove that the spectral bound $s(\mathcal{S})$ of $\mathcal{S}$ is negative. In fact, let us consider the system

$$\begin{cases} \partial_t Z = D_Z\partial^2_{xx}Z - \varepsilon_Z\partial_x Z, \\ D_Z\partial_x Z(t,0) - \varepsilon_Z Z(t,0) = \partial_x Z(t,l) = 0, \quad Z = Q, W. \end{cases} \tag{3.41}$$

The substitution of $P = e^{\lambda t}\zeta(x)$ in (3.41) gives

$$\begin{cases} \lambda\zeta(x) = D\partial^2_{xx}\zeta - \varepsilon\partial_x\zeta. \\ D_Z\partial_x\zeta(t,0) - \varepsilon_Z\zeta(t,0) = \partial_x\zeta(t,L_1) = 0, \quad Z = Q, W. \end{cases} \tag{3.42}$$

The asymptotic behavior of solutions to (3.41) is determined by that of the eigenvalue problem (3.42). Theorem 7.6.1 in [124] and Remark **??** imply that the eigenvalue problem (3.42) has a real principal eigenvalue λ_0 and a corresponding eigenvector $\zeta_0(x) > 0$ for all $x \in \Omega$. We claim that $\lambda_0 < 0$. Indeed, if $\boldsymbol{Q}_1(\zeta) := D_Z\partial^2_{xx}\zeta - \varepsilon_Z\partial_x\zeta$ denotes the differential operator on the right hand side of (3.42), then integration by parts yields

$$\begin{aligned} \lambda_0 \int_\Omega |\zeta_0(x)|^2 dx &= \int_\Omega (\boldsymbol{Q}_1(\zeta_0))(x)\zeta_0(x)dx \\ &= \int_0^l [D_Z\partial^2_{xx}\zeta_0 - \varepsilon_Z\partial_x\zeta_0]\zeta_0(x)dx, \\ &= -\tfrac{\varepsilon_Z}{2}[\zeta_0^2(0) + \zeta_0^2(l)] - D_Z\int_0^l |\partial_x\zeta_0(x)|^2 dx < 0. \end{aligned}$$

Since $\zeta_0(x) > 0$ for all $x \in \overline{\Omega}$, we have $\lambda_0 < 0$.

One can prove that an eigenvalue of $\boldsymbol{Q}_1$, is also an eigenvalue of $\partial_t Z = D_Z\partial^2_{xx}Z - \varepsilon_Z\partial_x Z - \nu_i(x)Z$, with $i = 3, 5$. Indeed, the operator $\boldsymbol{Q}_{1,i} = D_Z\partial^2_{xx} - \varepsilon_Z\partial_x - \nu_i(x)$ is a sum of $\boldsymbol{Q}_1$ and the

linear operator M_i defined by: $M_i(Z)(x) = -\nu_i(x)Z$, with $\nu_i(x) > 0$. Thus, using Theorem 7.6.1 in [124], there exists a real principal eigenvalue λ^* and an associated eigenfunction $\zeta^* > 0$ such that

$$\lambda^*\zeta^* = D_Z\partial^2_{xx}\zeta^* - \varepsilon_Z\partial_x\zeta^* - \nu_i(x)\zeta^* \quad \text{or} \quad (\lambda^* + \nu_i(x))\zeta^* = D_Z\partial^2_{xx}\zeta^* - \varepsilon_Z\partial_x\zeta^*. \tag{3.43}$$

Since the eigenvalue problem (3.42) has eigenvalues λ_n, $n \geq 0$, then the eigenvalues of (3.43) are $\lambda_n - \nu_i(x)$, $n \geq 0$. Hence, $\lambda^* = \lambda_0 - \nu_i(x) < 0$ because $\lambda_0 < 0$, $\nu_i(x) > 0$. Therefore, $s(\mathcal{S}) < 0$. It follows from Lemma 3.3.4 that the spectral bound $s(\Theta)$ of $\Theta = \mathcal{S} + \mathcal{G}$, has the same sign as $r(-\mathcal{G}\mathcal{S}^{-1}) - 1 = \mathcal{R}_0^{pde} - 1$. That is, $\mathcal{R}_0^{pde} - 1$ and the principal eigenvalue of Θ, $\lambda = \lambda(\mathcal{T}_0)$, have same sign. Since $\mathcal{R}_0^{pde} < 1$, we have $\lambda(\mathcal{T}_0) < 0$ and $\lim_{\epsilon\to 0}\lambda(\mathcal{T}_0 + \epsilon) = \lambda(\mathcal{T}_0) < 0$. Thus, there is an $\epsilon_0 > 0$ such that $\lambda_{\epsilon_0} = \lambda(\mathcal{T}_0 + \epsilon_0) < 0$. Fixing $\epsilon_0 > 0$, and using the fact that A is nonnegative gives the existence of t_0 such that for all $t \geq t_0$, $x \in \overline{\Omega}$, $A(t,x) \geq \epsilon_0$. Thus, from (3.2), we have $\partial_t A \leq N_{egg}W - (\nu_1 + \mu_2\epsilon_0)A$, $\forall t \geq t_0$, $x \in \overline{\Omega}$. Finally, we consider the linear system.

$$\begin{cases} \frac{\partial v_1}{\partial t} = N_{egg}v_5 - (\nu_1 + \mu_2\epsilon_0)v_1, \\ \frac{\partial v_2}{\partial t} = D_Y\frac{\partial^2 v_2}{\partial x^2} + r\gamma v_1 - \nu_2 v_2, \\ \frac{\partial v_3}{\partial t} = D_Q\frac{\partial^2 v_3}{\partial x^2} - \varepsilon_Q\frac{\partial v_3}{\partial x} + \beta v_2 + \overline{b}_1 v_5 - \widetilde{\nu}_3 v_3, \\ \frac{\partial v_4}{\partial t} = \alpha\overline{\varphi}_1 v_3 - \nu_4 v_4, \\ \frac{\partial v_5}{\partial t} = D_W\frac{\partial^2 v_5}{\partial x^2} - \varepsilon_W\frac{\partial v_5}{\partial x} + a v_4 - \widetilde{\nu}_5 v_5, \end{cases} \tag{3.44}$$

where $\overline{b}_1 = \max_{x\in\overline{\Omega}} b_1(x)$, $\overline{\varphi}_1 = \max_{x\in\overline{\Omega}} \varphi_1(x)$, $\widetilde{\nu}_3 = \min_{x\in\overline{\Omega}} \nu_3(x)$ and $\widetilde{\nu}_5 = \min_{x\in\overline{\Omega}} \nu_5(x)$.

Notice that system (3.44) controls system (3.19) from above. Moreover, similar arguments as in Theorem 2.2 in [130] yield the following result.

Lemma 3.3.5. The problem (3.44) has a principal eigenvalue $\overline{\lambda}_{\epsilon_0}$ with a positive eigenfunction ψ_0, and $\overline{\lambda}_{\epsilon_0}$ has the same sign as λ_0.

Since $\lambda_0 < 0$, we have $\overline{\lambda}_{\epsilon_0} < 0$ and system (3.44) admits a positive solution

$$v(t,x) = e^{\overline{\lambda}_{\epsilon_0}(t-t_0)}\psi_0(x), \quad t \geq t_0.$$

For any $\phi \in X^+$, there exists some $\eta > 0$ sufficiently large such that

$$u(t,\cdot,\phi) \leq \eta v(t,\cdot), \quad t \geq t_0.$$

Since the reaction term F^+ of system (3.44) is cooperative, we conclude by the comparison principle (see Theorem 7.3.4 in [124]) that,

$$\Big(A(t,x,\phi), Y(t,x,\phi), Q(t,x,\phi), U(t,x,\phi), W(t,x,\phi)\Big)^T \leq \eta e^{\overline{\lambda}_{\epsilon_0}(t-t_0)}\psi_0(x), \ \forall t \geq t_0.$$

Hence, $\lim_{t\to\infty}\Big(A(t,x,\phi), Y(t,x,\phi), Q(t,x,\phi), U(t,x,\phi), W(t,x,\phi)\Big)^T = 0$, uniformly for $x \in \overline{\Omega}$. This achieves the proof of Theorem 3.3.4. □

The ecologically implication of Theorem 3.3.4 is that the mosquito population can be effectively controlled (or eliminated) in a given bounded region as long as the associated spatial offspring number $\mathcal{R}_0^{pde}$, can be brought (and kept) to a value less than or equal to unity.

In order to prove the uniform persistence of the mosquito population, we need to show that $\mathcal{T}_0$ is a weak repeller. That is:

Lemma 3.3.6. If $\mathcal{R}_0^{pde} > 1$, then there exists $\delta > 0$ such that for any $\phi \in X^+$ with $\phi_i(0) \not\equiv 0$, $i = 1, 2, 3, 4, 5$, the solution $u(t, \cdot, \phi)$ of system (3.19)-(3.23) satisfies

$$\limsup_{t\to\infty} \|u(t, \cdot, \phi) - \mathcal{T}_0\|_X \geq \delta. \tag{3.45}$$

Proof. Since $\mathcal{R}_0^{pde} > 1$, by the proof of Theorem 3.3.4, the principal eigenvalue $\lambda(\mathcal{T}_0)$ of $\Theta = \mathcal{S} + \mathcal{G}$, is positive. Assume, by contradiction that there exists some $\phi \in X^+$ with $\phi_i(0) \not\equiv 0$, $i = 1, 2, 3, 4, 5$ such that for every $\delta > 0$, $\limsup_{t\to\infty} \|u(t, \cdot, \phi) - \mathcal{T}_0\|_X < \delta$. Then, there exists $t_1 = t_1(\phi) > 0$ sufficiently large such that $A(t, x) \leq \delta$ and $W(t, x) \leq \delta$, $\forall t \geq t_1$, $x \in \overline{\Omega}$. Since $B'(W) \leq 0$ for all $W \geq 0$, it follows that $B(W) \geq B(\delta)$. Hence, we have

$$\partial_t A(t, x) \geq B(\delta)W(t, x) - (\nu_1 + \mu_2\delta)A(t, x), \forall t \geq t_1, x \in \overline{\Omega}.$$

Consider the following linear system.

$$\begin{cases} \frac{\partial w_1}{\partial t} = B(\delta)w_5 - (\nu_1 + \mu_2\delta)w_1, \\ \frac{\partial w_2}{\partial t} = D_Y\frac{\partial^2 w_2}{\partial x^2} + r\gamma w_1 - \nu_2 w_2, \\ \frac{\partial w_3}{\partial t} = D_Q\frac{\partial^2 w_3}{\partial x^2} - \varepsilon_Q\frac{\partial w_3}{\partial x} + \beta w_2 + \widetilde{b}_1 w_5 - \overline{\nu}_3 w_3, \\ \frac{\partial w_4}{\partial t} = \alpha\widetilde{\varphi}_1 w_3 - \nu_4 w_4, \\ \frac{\partial w_5}{\partial t} = D_W\frac{\partial^2 w_5}{\partial x^2} - \varepsilon_W\frac{\partial w_5}{\partial x} + a w_4 - \overline{\nu}_5 w_5, \end{cases} \tag{3.46}$$

where $\widetilde{b}_1 = \min_{x\in\overline{\Omega}} b_1(x)$, $\widetilde{\varphi}_1 = \min_{x\in\overline{\Omega}} \varphi_1(x)$, $\overline{\nu}_3 = \max_{x\in\overline{\Omega}} \nu_3(x)$ and $\overline{\nu}_5 = \max_{x\in\overline{\Omega}} \nu_5(x)$.

It is straightforward that (3.46) controls system (3.19) from below. Another application of Lemma 3.3.5, yields a principal eigenvalue $\overline{\lambda}_\delta$ of (3.46) associated with a strongly positive eigenvector $w_0(x)$. Moreover, $\overline{\lambda}_\delta$ and $\lambda(\mathcal{T}_0)$ have the same sign. Thus, system (3.46) has a positive solution $w(t, x) = e^{\overline{\lambda}_\delta(t-t_1)}w_0(x)$, $t \geq t_1$, $x \in \overline{\Omega}$. For any $\phi \in X^+$ with $\phi_i(0) \not\equiv 0$, $i = 1, 2, 3, 4, 5$, it follows from the parabolic maximum principle that

$$A(t, x) > 0,\ Y(t, x) > 0,\ Q(t, x) > 0,\ U(t, x) > 0,\ W(t, x) > 0,\ \forall t > 0,\ x \in \overline{\Omega}. \tag{3.47}$$

Therefore, we can choose a sufficiently small number $\eta_0 > 0$ such that

$$\Big(A(t_1, x, \phi), Y(t_1, x, \phi), Q(t_1, x, \phi), U(t_1, x, \phi), W(t_1, x, \phi)\Big) \geq \eta_0 w_0(x).$$

Since the reaction term F^- of system (3.46) is cooperative, another application of the comparison principle [124] lead us to

$$\Big(A(t, x, \phi), Y(t, x, \phi), Q(t, x, \phi), U(t, x, \phi), W(t, x, \phi)\Big) \geq \eta_0 e^{\overline{\lambda}_\delta(t-t_1)}w_0(x),\ \forall t \geq t_1,\ x \in \overline{\Omega}.$$

Therefore, since $\overline{\lambda}_\delta > 0$, one has $\eta_0 e^{\overline{\lambda}_\delta(t-t_1)} w_0(x) \to \infty$ as $t \to \infty$. This implies $(A, Y, Q, U, W)(t, x, \phi)$ is unbounded, which is a contradiction, and the proof of Lemma 3.3.6 is achieved. □

We are now in a position to state and prove the uniform persistence result, which indicates that $\mathcal{R}_0^{pde}$ is a threshold for mosquito persistence.

Theorem 3.3.5. If $\mathcal{R}_0^{pde} > 1$, then there exists $\delta_1 > 0$ such that any nonnegative solution $u(t, x, \phi)$ of (3.19)-(3.23) with $\phi_i(0) \not\equiv 0$ satisfies

$$\liminf_{t\to\infty} u_i(t, x, \phi) \geq \delta_1, \quad \forall i = 1, 2, 3, 4, 5, \tag{3.48}$$

uniformly for all $x \in \overline{\Omega}$.

Proof. For $\mathcal{R}_0^{pde} > 1$, we use the persistence theory developed in [123]. To that end, set

$$\mathbb{D}_0 := \{\phi = (\phi_1, \phi_2, \phi_3, \phi_4, \phi_5) \in X^+ : \phi_i(0) \not\equiv 0\}.$$

Clearly, we have

$$\partial\mathbb{D}_0 := X^+ \backslash \mathbb{D}_0 = \{\phi \in X^+ : \phi_1(0) \equiv 0 \text{ or } \phi_2(0) \equiv 0 \text{ or } \phi_3(0) \equiv 0 \text{ or } \phi_4(0) \equiv 0 \text{ or } \phi_5(0) \equiv 0\},$$

and $\Phi_t(\mathbb{D}_0) \subset \mathbb{D}_0$, $\forall t \geq 0$. If $\phi \in \mathbb{D}_0$, then, from (3.47), one has $u(t, x, \phi) \gg 0$, $\forall x \in \overline{\Omega}$, $t > 0$. Define

$$K_\partial := \{\phi \in \partial\mathbb{D}_0 \ : \ \Phi_t(\phi) \in \partial\mathbb{D}_0, \ \forall t \geq 0\},$$

and let $\omega(\phi)$ be the ω-limit set of the positive orbit $\gamma^+(\phi) := \{\Phi_t(\phi)\}_{t\geq 0}$.

We claim that

$$\bigcup_{\phi\in K_\partial} \omega(\phi) = \{\mathcal{T}_0\}.$$

Indeed, for any given $\phi \in K_\partial$, we have $\Phi_t(\phi) \in \partial\mathbb{D}_0$, $\forall t \geq 0$. Thus, for every $t \geq 0$, either $A(t, \phi) \equiv 0$ or $Y(t, \phi) \equiv 0$ or $Q(t, \phi) \equiv 0$ or $U(t, \phi) \equiv 0$ or $W(t, \phi) \equiv 0$. In the case where $A(t, \phi) \equiv 0$, we see from the first equation of (3.19) that $\lim_{t\to\infty} W(t, x) = 0$ uniformly for $x \in \overline{\Omega}$. From the second, third and fourth equations in (3.19), and thanks to the theory of asymptotically autonomous semiflows [128], we have; $\lim_{t\to\infty} Y(t, x) = 0$, $\lim_{t\to\infty} Q(t, x) = 0$ and $\lim_{t\to\infty} U(t, x) = 0$ uniformly for $x \in \overline{\Omega}$. If $Y(t, \phi) \equiv 0$, $\forall t \geq 0$, the second equation in (3.19) yields $\lim_{t\to\infty} A(t, x) = 0$ uniformly for $x \in \overline{\Omega}$. Similar arguments show that $\lim_{t\to\infty} W(t, x) = 0$, $\lim_{t\to\infty} Q(t, x) = 0$ and $\lim_{t\to\infty} U(t, x) = 0$ uniformly for $x \in \overline{\Omega}$. Similar arguments and conclusions hold for the cases where $Q(t, \phi) \equiv 0$, $U(t, \phi) \equiv 0$ and $W(t, \phi) \equiv 0$. Therefore, in either case, the ω-limit set of $\gamma^+(\phi)$ for $\phi \in K_\partial$ is $\{\mathcal{T}_0\}$. Hence the claim.

Now, we define the function $p : X^+ \longrightarrow \mathbb{R}_+$ by

$$p(\phi) = \min\left\{\min_{x\in\overline{\Omega}} \phi_i(x), \ i = 1, 2, 3, 4, 5\right\}.$$

It is straightforward that $p^{-1}((0,\infty)) \subset \mathbb{D}_0$. Suppose $p(\phi) = 0$ and $\phi \in \mathbb{D}_0$. Then we have $\phi_i(\cdot) \not\equiv 0$, $i = 1,2,3,4,5$. By (3.47), one has $\min\left\{\min_{x\in\overline{\Omega}} u(t,x,\phi)\right\} > 0$, $\forall t > 0$, which implies that $p(\Phi_t(\phi)) > 0$, $\forall t > 0$. Thus, p is a generalized distance function for the semiflow $\Phi_t : X^+ \longrightarrow X^+$ (see [123]). Note that, by the above claim, any positive orbit of $\Phi(t)$ in K_∂ converges to $\mathcal{T}_0$. In view of Lemma 3.3.6, we conclude that $\{\mathcal{T}_0\}$ is an isolated invariant set in X^+, and that $W^s(\mathcal{T}_0) \cap \mathbb{D}_0 = \varnothing$, where $W^s(\mathcal{T}_0)$ is the stable manifold of $\mathcal{T}_0$. Therefore, making use of Theorem 3.3.2, we conclude that there exists $\delta_1 > 0$ such that $\min\{p(\psi) : \psi \in \omega(\phi)\} > \delta_1$ for any $\phi \in \mathbb{D}_0$. This implies that $\liminf_{t\to\infty} u_i(t,x,\phi) \geq \delta_1$, $\forall \phi \in \mathbb{D}_0$. □

3.3.4 Numerical simulations: case study of anopheles mosquitoes, the malaria vector agent

This section deals with numerical simulations for system (3.19). Our main objective here, is to investigate through numerical simulations, the impacts of dispersal and heterogeneity on the dynamics and persistence of mosquitoes, as well as illustrating some of our theoretical results. To make it simple, we concentrate on one dimensional domain Ω. Model (3.19) is simulated by using data from recent works, who are summarized in Table 3.4. We choose $D_Y = D_Q = D_W = D_M = 0.04\, m^2/s$ and $\varepsilon_Q = \varepsilon_W = 0.1\, m/s$. To describe the spatial heterogeneity, we assume that the hosts are unevenly distributed. In order to capture the fact that, the more people leave villages and farms to cities, the faster the distribution of human density changes, and the more the urbanization have impact on mosquito distribution [73, 82], we choose the location-dependent parameters as follows:

$$\varphi_1(x) = 16(1 + p\cos(2x)),\ b_1(x) = 0.8(1 + p\cos(2x)),$$

where, $p \in [0,1]$ is the magnitude of host's heterogeneity. Note that when $p = 0$, humans distribute evenly in space (homogeneity in human's distribution). With this set of parameters, the spatial average of $\varphi_1(x)$ and $b_1(x)$ remain 16 and 0.8, respectively.

(a) A nonstandard numerical scheme for the system (3.19)-(3.23)

In this subsection, we consider the full discretisation of model (3.19)-(3.23). This is achieved by the nonstandard finite difference (NSFD) approach, which has shown great potential in providing reliable numerical schemes that replicate the dynamics of continuous models in Mathematical Biology [93, 94, 57]. The construction in the papers [19, 96] is appropriate for the case under consideration.

Let $dt > 0$ and $dx > 0$ be the time and space step-size respectively. We denote by u_j^n, an approximation of $u(t,x)$ at the grid point $t_n = ndt$ and $x_j = jdx$, for $n = 1,2,\ldots$, $j = 1,2,\ldots,N_e$. The challenge in the approximation of the model equations (3.19)-(3.20)

arises from the fact that it consists of three types of equations. These are: **(1)** ordinary system of differential equations (i.e. $(3.19)_1$, $(3.19)_4$) ; **(2)** reaction-diffusion equation (i.e. $(3.19)_2$) ; **(3)** advection-reaction-diffusion equations (i.e. $(3.19)_3$, $(3.19)_5$ and (3.20)). The ODE equations $(3.19)_1$ and $(3.19)_4$ are approximated by

$$\begin{cases} \dfrac{A_j^{n+1} - A_j^n}{\rho(dt)} = B(W_j^n)W_j^n - [\nu_1 + \mu_2 A_j^n]A_j^{n+1}, \\ \dfrac{U_j^{n+1} - U_j^n}{\rho(dt)} = \alpha\varphi_1(x_j)Q_{j-1}^n - \nu_4 U_j^{n+1}, \end{cases} \tag{3.49}$$

where the complex denominator function ρ is given by

$$\rho(dt) = \frac{1 - e^{-p_0 dt}}{p_0}, \quad \text{with} \quad p_0 = \max\{\nu_1, \nu_2, \nu_3, \nu_4, \nu_5, \mu_M\}.$$

The reaction-diffusion equation $(3.19)_2$ is approximated by

$$\frac{Y_j^{n+1} - Y_j^n}{\rho(dt)} = D_Y \frac{Y_{j+1}^{n+1} - 2Y_j^{n+1} + Y_{j-1}^{n+1}}{dx^2} + r\gamma A_j^{n+1} - \nu_2 Y_j^{n+1}. \tag{3.50}$$

For the advection-reaction-diffusion equations, we assume for simplicity that the advection coefficients are the same i.e. $\varepsilon_0 = \varepsilon_Q = \varepsilon_W = \varepsilon_M$. We impose the functional relation $dx = \varepsilon_0 dt$ between the step sizes. Then the advection-reaction-diffusion equations $(3.19)_3$, $(3.19)_5$ and (3.20) are approximated by

$$\begin{cases} \dfrac{Q_j^{n+1} - Q_{j-1}^n}{\rho(dt)} = D_Q \dfrac{Q_{j+1}^{n+1} - 2Q_j^{n+1} + Q_{j-1}^{n+1}}{dx^2} + \beta Y_j^{n+1} + b_1(x_j)W_{j-1}^n - \nu_3(x_j)Q_{j-1}^n, \\ \dfrac{W_j^{n+1} - W_{j-1}^n}{\rho(dt)} = D_W \dfrac{W_{j+1}^{n+1} - 2W_j^{n+1} + W_{j-1}^{n+1}}{dx^2} + aU_j^{n+1} - \nu_5(x_j)W_{j-1}^n, \\ \dfrac{M_j^{n+1} - M_{j-1}^n}{\rho(dt)} = D_M \dfrac{M_{j+1}^{n+1} - 2M_j^{n+1} + M_{j-1}^{n+1}}{dx^2} + (1-r)\gamma A_j^{n+1} - \mu_M M_j^{n+1}. \end{cases} \tag{3.51}$$

It should be noted that the left hand side of (3.51) is a discretisation of the continuous advection term. Indeed,

$$\frac{\partial Z}{\partial t} + \varepsilon_0 \frac{\partial Z}{\partial x} \approx \frac{Z_j^{n+1} - Z_j^n}{\rho(dt)} + \varepsilon_0 \frac{Z_j^n - Z_{j-1}^n}{\varepsilon_0 \rho\left(\dfrac{dx}{\varepsilon_0}\right)} \quad \text{where} \quad Z = Q, W, M.$$

Grouping (3.49)-(3.51), we obtain the following NSFD scheme which by construction pre-

serves the conservation laws associated with the continuous model:

$$\begin{cases} \dfrac{A_j^{n+1}-A_j^n}{\rho(dt)} = B(W_j^n)W_j^n - [\nu_1+\mu_2 A_j^n]A_j^{n+1}, \\ \dfrac{Y_j^{n+1}-Y_j^n}{\rho(dt)} = D_Y\dfrac{Y_{j+1}^{n+1}-2Y_j^{n+1}+Y_{j-1}^{n+1}}{dx^2} + r\gamma A_j^{n+1} - \nu_2 Y_j^{n+1}, \\ \dfrac{Q_j^{n+1}-Q_{j-1}^n}{\rho(dt)} = D_Q\dfrac{Q_{j+1}^{n+1}-2Q_j^{n+1}+Q_{j-1}^{n+1}}{dx^2} + \beta Y_j^{n+1} + b_1(x_j)W_{j-1}^n - \nu_3(x_j)Q_{j-1}^n, \\ \dfrac{U_j^{n+1}-U_j^n}{\rho(dt)} = \alpha\varphi_1(x_j)Q_{j-1}^n - \nu_4 U_j^{n+1}, \\ \dfrac{W_j^{n+1}-W_{j-1}^n}{\rho(dt)} = D_W\dfrac{W_{j+1}^{n+1}-2W_j^{n+1}+W_{j-1}^{n+1}}{dx^2} + aU_j^{n+1} - \nu_5(x_j)W_{j-1}^n, \\ \dfrac{M_j^{n+1}-M_{j-1}^n}{\rho(dt)} = D_M\dfrac{M_{j+1}^{n+1}-2M_j^{n+1}+M_{j-1}^{n+1}}{dx^2} + (1-r)\gamma A_j^{n+1} - \mu_M M_j^{n+1}. \end{cases} \tag{3.52}$$

However, for computational purposes, it is preferable to work with the NSFD scheme (3.52) in the Gauss-Seidel-type and sequential order (3.49), (3.50) and (3.51) which leads to an explicit scheme as explained below. It is clear from (3.49) that

$$A_j^{n+1} = \frac{A_j^n + \rho(dt)B(W_j^n)W_j^n}{1+\rho(dt)[\nu_1+\mu_2 A_j^n]} \quad \text{and} \quad U_j^{n+1} = \frac{U_j^n + \rho(dt)\alpha\varphi_1(x_j)Q_{j-1}^n}{1+\rho(dt)\nu_4}.$$

Eq. (3.50) is equivalent to

$$-D_Y\frac{\rho(dt)}{dx^2}Y_{j+1}^{n+1} + \left(1+\rho(dt)\nu_2 + 2D_Y\frac{\rho(dt)}{dx^2}\right)Y_j^{n+1} - D_Y\frac{\rho(dt)}{dx^2}Y_{j-1}^{n+1} = Y_j^n + \rho(dt)r\gamma A_j^{n+1}. \tag{3.53}$$

This takes the equivalent vector form

$$\mathcal{M}_1\underline{\mathbf{Y}}^{n+1} = \underline{\mathbf{N}}^{1,n} \geq 0,$$

where the matrix $\mathcal{M}_1$, in which boundary values are incorporated, is an M-matrix because it is strictly diagonally dominant and has positive diagonal entries. Thus,

$$\underline{\mathbf{Y}}^{n+1} = \mathcal{M}_1^{-1}\underline{\mathbf{N}}^{1,n}.$$

The first equation in (3.51) is equivalent to

$$\begin{aligned} -D_Q\frac{\rho(dt)}{dx^2}Q_{j+1}^{n+1} + \left(1+2D_Q\frac{\rho(dt)}{dx^2}\right)Q_j^{n+1} - D_Q\frac{\rho(dt)}{dx^2}Q_{j-1}^{n+1} &= Q_{j-1}^n + \rho(dt)\beta Y_j^{n+1} + \rho(dt)b_1(x_j)W_{j-1}^n \\ &\quad -\rho(dt)\nu_3(x_j)Q_{j-1}^n. \end{aligned}$$

This takes the equivalent vector form

$$\mathcal{M}_2\underline{\mathbf{Q}}^{n+1} = \underline{\mathbf{N}}^{2,n},$$

where as in the previous case $\mathcal{M}_2$ is an M-matrix. Note that the vector $\underline{\mathbf{N}}^{2,n}$ is nonnegative because $1 - \rho(dt)\nu_3(x_j) \geq 0$ by the choice of $\rho(dt)$. Thus,

$$\underline{\mathbf{Q}}^{n+1} = \mathcal{M}_2^{-1}\underline{\mathbf{N}}^{2,n}.$$

In a similar manner, one obtains that the second and last equations in (3.51) have the equivalent vector form

$$\mathcal{M}_3\underline{\mathbf{W}}^{n+1} = \underline{\mathbf{N}}^{3,n} \geq 0, \quad \mathcal{M}_4\underline{\mathbf{M}}^{n+1} = \underline{\mathbf{N}}^{4,n} \geq 0,$$

so that

$$\underline{\mathbf{W}}^{n+1} = \mathcal{M}_3^{-1}\underline{\mathbf{N}}^{3,n} \quad \text{and} \quad \underline{\mathbf{M}}^{n+1} = \mathcal{M}_4^{-1}\underline{\mathbf{N}}^{4,n}.$$

At this stage, a comment is made in order to explain how the boundary values are actually incorporated in the matrices M_k $(k = 1, 2, 3, 4)$. To illustrate the process for the matrix $\mathcal{M}_1$, put $j = 0$ and $j = N_e$ in Eq. (3.53). From the known data $\dfrac{\partial Y}{\partial x}(t_{n+1}, 0)$ and $\dfrac{\partial Y}{\partial x}(t_{n+1}, l)$, we can use the approximations

$$\frac{\partial Y}{\partial x}(t_{n+1}, 0) \simeq \frac{Y_1^{n+1} - Y_{-1}^{n+1}}{2dx} \quad \text{and} \quad \frac{\partial Y}{\partial x}(t_{n+1}, l) \simeq \frac{Y_{N_e+1}^{n+1} - Y_{N_e}^{n+1}}{dx}.$$

We can then take

$$Y_{-1}^{n+1} = Y_1^{n+1} - 2dx\frac{\partial Y}{\partial x}(t_{n+1}, 0) \quad \text{and} \quad Y_{N_e+1}^{n+1} = Y_{N_e}^{n+1} + dx\frac{\partial Y}{\partial x}(t_{n+1}, l).$$

We then replace Y_{-1}^{n+1} an $Y_{N_e+1}^{n+1}$ with these expressions in the scheme (3.53).

(b) General dynamics

The long run behavior of system (3.19) is simulated using $\Omega = [0, 10]$. Figures 3.6 and 3.8 show the numerical plots of the female mosquito compartments $Y(t, x)$, $Q(t, x)$, $U(t, x)$ and $W(t, x)$, with the initial conditions $A(0, x) = 500 - \cos(2x)$, $Y(0, x) = 75 - \sin(2x)$, $Q(0, x) = 50 - \cos(2x)$, $U(0, x) = 50 - \cos(2x)$ and $W(0, x) = 75 - \cos(2x)$.

Figure 3.6 depicts the solutions of model (3.19) when $p = 0$ (i.e. with homogeneity in hosts' distribution) while, Figures 3.7, 3.8, 3.9 and 3.10 show the solutions of model (3.19) in a landscape with heterogeneity in hosts distribution $(p > 0)$. These figures illustrate the persistence of mosquito population as established in Theorem 3.3.5. Although mosquito population persists, its distribution in the domain is not the same. Figure 3.6 show that spatial distribution of mosquitoes is homogeneous in the domain when the hosts density is too, while Figure 3.7 show a drastic change in the spatial distribution of mosquitoes in gonotrophic cycle when the hosts density is heterogeneous.

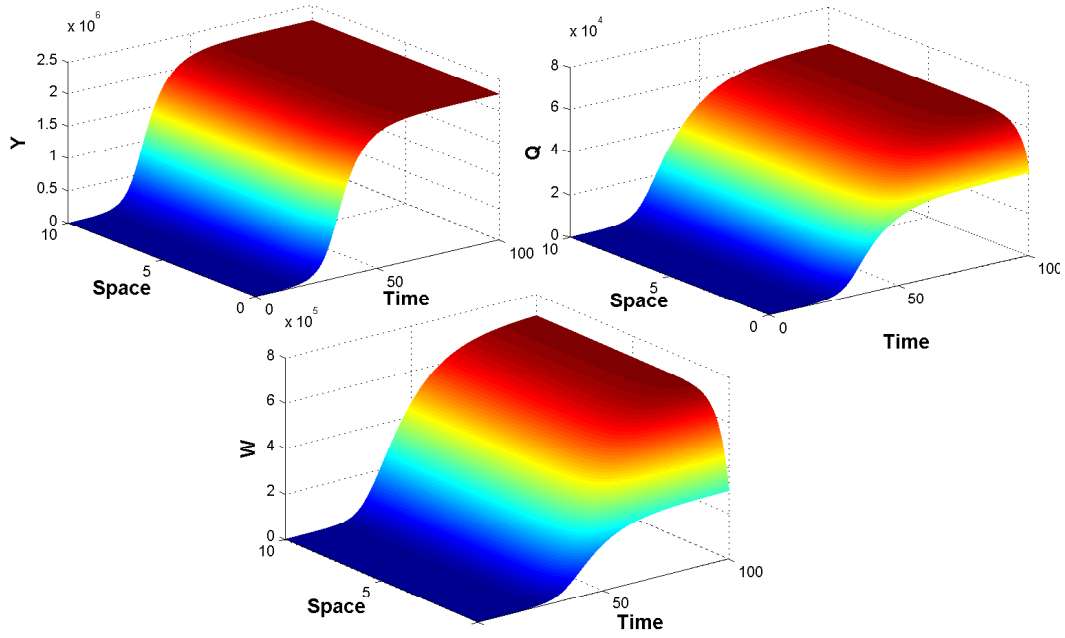

Figure 3.6: Distribution of mature females in a domain with homogeneous distribution of humans ($p = 0$). $n = 1$ and all other parameters as in Table 3.4

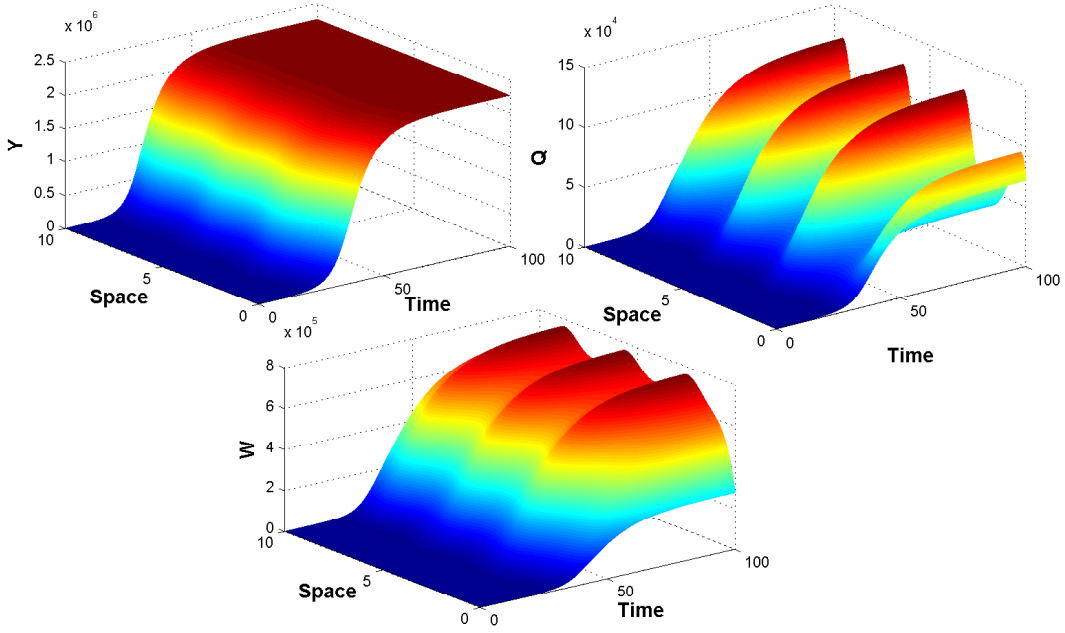

Figure 3.7: Distribution of mature females in a domain with heterogeneous distribution of humans ($p = 0.5$). $n = 1$ and all other parameters as in Table 3.4

(c) Impact of spatial heterogeneity on mosquito spread

To investigate the spatial heterogeneity effect on the mosquito dynamics, we take the variation of human distribution.

Figures 3.8, 3.9 and 3.10 show the influence of the spatial heterogeneity of hosts on the dynamics of female mosquitoes. From these figures, one observe that spatial distribution of females in gonotrophic cycle is strongly influenced by the hosts density. Moreover, when

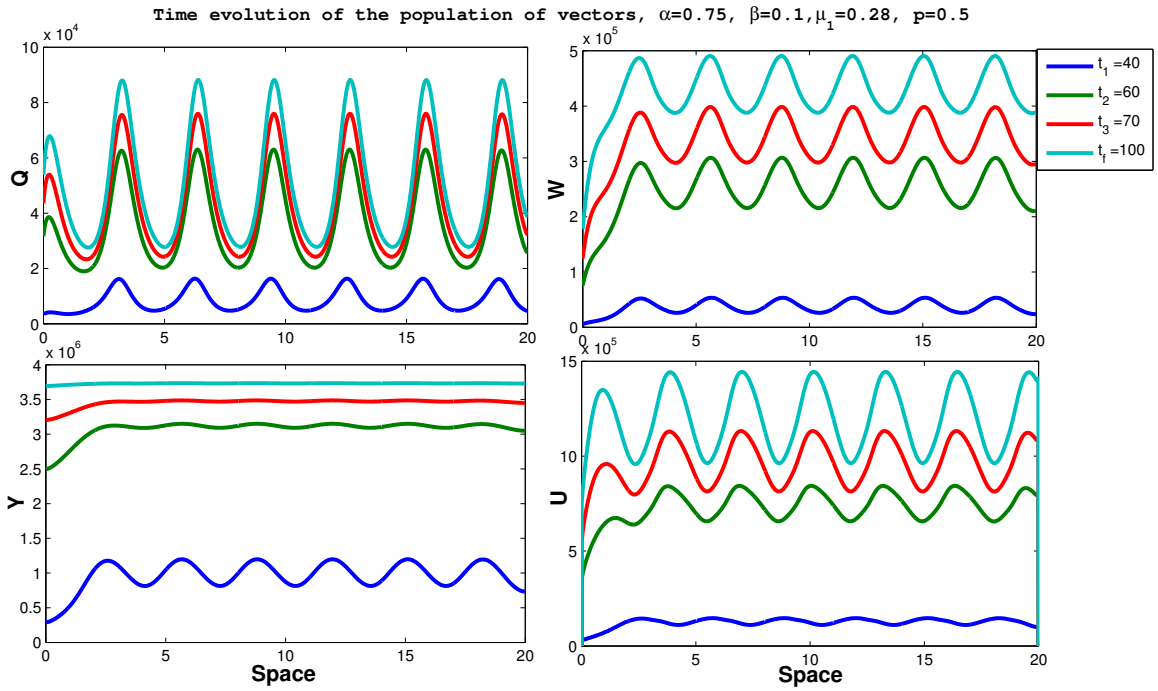

Figure 3.8: Distribution of mature females in a domain with heterogeneous distribution of humans ($p = 0.5$). $n = 1$ and all other parameters as in Table 3.4

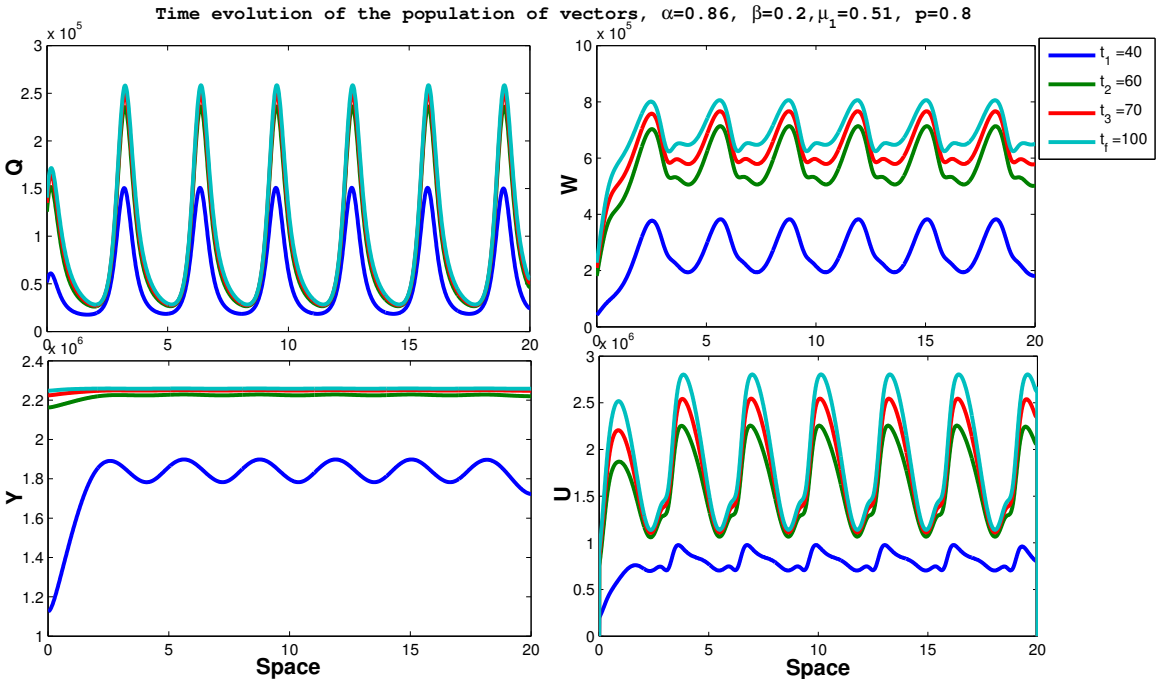

Figure 3.9: Distribution of mature females in a domain with heterogeneous distribution of humans ($p = 0.8$). $n = 1$ and all other parameters as in Table 3.4.

p increases from 0 to 1, an increase on the heterogeneity is observed in spatial distribution of female mosquitoes. Note that, the larger the value of p, the higher the heterogeneity of spatial density of hosts. It follows that the population distribution is strongly dependent on the distribution of hosts. Thus, we can conclude that urbanization strongly influence the

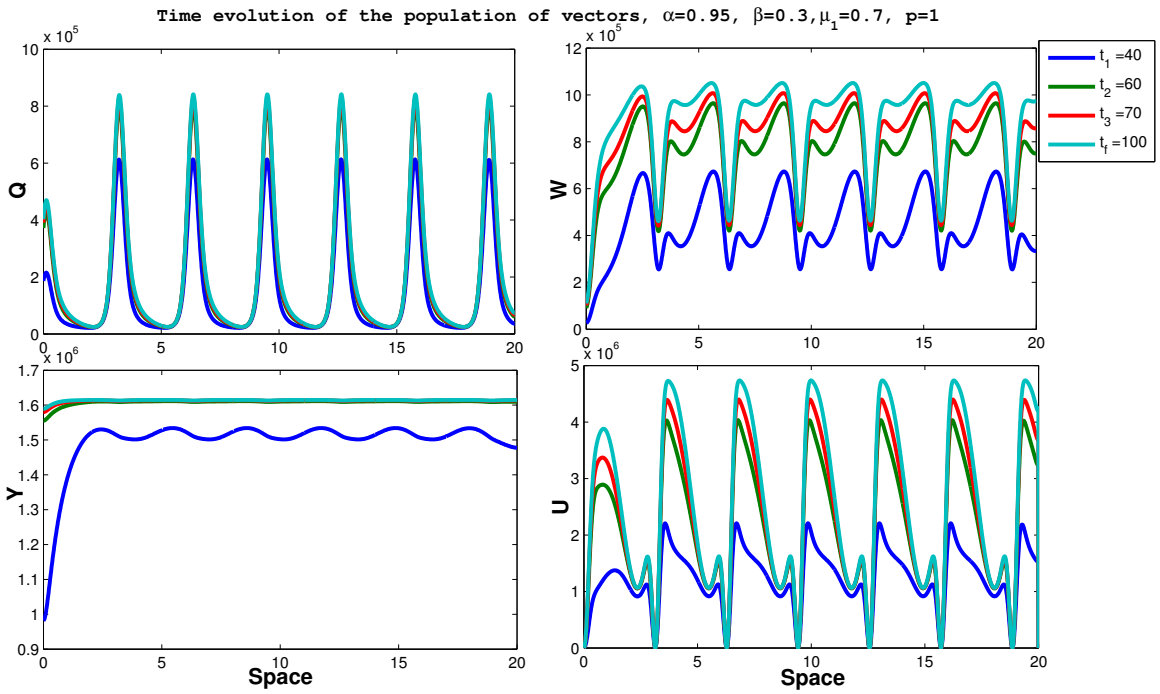

Figure 3.10: Distribution of mature females in a domain with heterogeneous distribution of humans ($p = 1$). $n = 1$ and all other parameters as in Table 3.4.

mosquito dynamics, and therefore increases or decreases malaria risk depending on the range of the remaining model parameters.

Altogether, the above plotted figures show that landscape really play an important role in the dispersal of mosquitoes. From a practical point of view, it may be useful to know how mosquitoes are distributed on a domain, in order to determine where they are likely to gather, before conducting vector control. Our simulations show that, when we consider a homogeneous distribution of hosts, the distribution of mature females is homogeneous on the domain (see Figure 3.6). But, when we consider a heterogeneous distribution of hosts, we observe a drastic change in the distribution (see Figures 3.8-3.10). This indicates that there exists a linear relationship between hosts density and mosquitoes distribution when there is homogeneity (i.e. $p = 0$). However, when there is heterogeneity (i.e. $p > 0$), this relationship is perturbed and induces a strong influence on spatial distribution.

3.4 Conclusion and discussion

In this paper, we have assessed the impact of dispersal and the spatial heterogeneity on the distribution of mosquito population. To achieve our goal, we have described the spatial evolution of anopheles mosquito by developing a temporal model subject to a general form of the oviposition function and extended it to a spatio-temporal one. Our models have been rigorously analyzed using, among others, the more realistic Maynard-Smith-Slatkin oviposition function. However, our results remain valid even if the latter oviposition function

is replaced by any function drawn from Table 3.1, including the Hassell function which was considered for the first time in this work. Our models have been investigated in many aspects.

From the modelling point of view, we have extended some recent ODE models [1, 2, 87, 108] by: (a) incorporating the gonotrophic cycle (Q, U and W) of adult female mosquitoes and considering a general egg oviposition function ; (b) taking into account the mating behavior and human-vector interaction ; (c) including a spatial component in order to taking into account movement of vectors and spatial heterogeneity of mosquito resources. Moreover, our PDE model have extended some recent dispersal models [68, 126, 132, 158] by incorporating the gonotrophic cycle of adult female mosquitoes, by considering a general egg oviposition function and by including the spatial heterogeneity of mosquito resources.

From the theoretical perspective, due to the high nonlinearity of the ODE model and its extended PDE counterpart, we made use of a variety techniques and approaches, including and not limited to: Lyapunov-Lasalle techniques, monotone dynamical systems approach, semigroup application and spectral theory approach. The main results read as follows:

- For the temporal model (3.1), we have derived the basic offspring number $\mathcal{R}_0^{ode}$, and through a sensitivity analysis, we have realized that, the natural mortality rate of immature females μ_Y, the mating rate β and the deposit rate of eggs by females N_{egg} are the top three more influential parameters on the dynamics of mosquito population. The trivial equilibrium of the temporal model is GAS whenever $\mathcal{R}_0^{ode}$ is less than unity. In the case where $\mathcal{R}_0^{ode}$ exceeds unity, there exists a unique non-trivial equilibrium, which is GAS for $n = 1$ and globally attractive for $n > 1$. When there is no density-dependent mortality in the aquatic stage (i.e. $\mu_2 = 0$), the model exhibits the Hopf bifurcation phenomenon. These results hold for the Verhlust-Pearl logistic and Hassell oviposition functions. For the remaining four oviposition functions in Table 3.1, we have summarized the long run behavior of the solutions of their corresponding ODE model (3.1) in in Table 3.3.

- For the spatio-temporal model (3.19), we have given the formula for the basic offspring ratio $\mathcal{R}_0^{pde}$ for the PDE model. On the one hand, we have shown that spatio-temporal model has a spatially homogeneous trivial equilibrium, which is globally attractive whenever $\mathcal{R}_0^{pde}$ is less than unity. On the other hand, the persistence theory have been used to show that, the mosquito population persists whenever the $\mathcal{R}_0^{pde}$ exceeds unity.

From the computational aspect, we have used ODE45 in Matlab and perform numerical simulations of the ODE model to illustrate our theoretical results. Precisely, the Hopf bifurcation occurrence and GAS of the MPE have been illustrated, sensitivity analysis for

$\mathcal{R}_0^{ode}$ and sensitivity indices have been calculated. In the presence of density-dependent mortality in the aquatic stage (i.e. $\mu_2 > 0$), we have extended the global stability results for the ODE models in [1, 108] by establishing the global attractivity of the MPE whenever the basic offspring number is above unity. Though, it is still challenging to theoretically prove the local asymptotic stability of the non-trivial equilibrium of the model (3.1) in the presence of density-dependent mortality in the aquatic stage; alternatively, numerical simulations were used to conjecture it (Figure 3.3). Together with the latter conjecture, our global attractivity result conjecture the global asymptotical stability of the MPE of the model (3.1) in presence of the density-dependent mortality in the aquatic stage whenever $\mathcal{R}_0^{ode}$ exceeds unity.

Unlike the temporel model (3.1), where a standard numerical scheme (i.e., Runge-Kutta of order 4) has been used, for spatio-temporal PDE model, we have constructed a dynamical consistent (with respect to the positivity and boundeness) nonstandard difference scheme, using the Maynard-Smith-Slatkin oviposition function and the parameters associated with the anopheles species to show that the spatial heterogeneity of mosquito resources (humans) strongly influences the spatial distribution of adult female mosquitoes (Figures 3.6-3.10).

As far as future investigations are concerned, we are planning to perform a sensitivity analysis and tackle the existence of travelling fronts for the spatial model. On the one hand, it is well known that seasonality and climatic changes, such as temperature, rainfall, affect the life-cycle of mosquitoes. Thus, a possible extension of this manuscript, on which we are already working, is to incorporate these latter features in our models in order to assess the impact of temperature and rainfall on the abundance of mosquitoes. On the other hand, the comparison with real experiments in order to validate, modified or adapt the models is another challenge we intend to face in the near future. To better reflect the details of spatial variation, an equally challenging problem will be to consider the situation where the diffusion and convection coefficients, as well as other parameters depend on a two dimensional spatial variable.

♣ General conclusion ♣

The interaction between a heterogeneous environment and ecological behavior of malaria vectors requires novel modeling approaches that can investigate these complex relationships. Much of knowledge on the mosquito can be obtained via field observations, typically collected via trapping, that are usually costly and time consuming and provide information in the specific setting of the experiment. In order to gain understanding on the biological processes observed in the field in a more generic manner and test various hypothesis, mathematical modelling is a very useful tool. This thesis contributes to this investigation by developing mathematical models for local mosquito dispersal to understand vector ecological behaviors, distribution of mosquitoes, and their interactions with malaria vector control interventions. These models set up a framework for use in understanding, assessing, and evaluating the malaria intervention programs. We developed and studied several mathematical models either discrete-space or continuous-space, models that were simulated and applied to explain some properties of heterogeneity, and to answer specific questions concerning the spatial distribution of mosquitoes. In this work continuous and discrete space modelling are addressed. This research work encompasses two parts and each of them has its peculiar features.

Models studied and contributions

In the first part (chapter 2), the model developed was a reaction-diffusion type model to describe the spatial evolution of the anopheles mosquito using statistical mechanics of complex networks i.e. networks of populations connected by migratory flows whose configurations are described in terms of the conditional probabilities of connections between nodes. This model categorizes the life of a mosquito into four compartments, namely, population in aquatic stage, young female not yet laying eggs, fertilized and eggs laying females and males. It consists of three main components. The first component is the continuous time model based on ordinary differential equations that describe the mosquito dynamics. This dynamics is driven by the birth, the mortality and, the development rates from one compartment to another. The second component of this metapopulation model involves the inclusion of the spatial characteristics. The space is discretized into discrete locations (patches) to form a patches network. Each nodes of the network represent

potential breeding and feeding sites of mosquitoes, around which there are human hosts habitations. The third component of the model is modeling dispersal of adult mosquitoes which move from one patch to another in search of hosts and breeding sites, creating connectivity between these patches. The model incorporates two key features : spatial heterogeneity and mosquito dispersal. The spatial heterogeneity was included on the one hand by different connectivities of the patches, and on the other hand by allowing hosts and breeding sites (resources) to differ between patches across the network. Mosquito dispersal was modelled on the formalism used in statistical mechanics where dispersal of adult mosquitoes searching for hosts or breeding sites depend on the degrees of the origin and destination patches, and conditional probability that any given edge departing from a patch is pointing to another patch. Here, dispersal of mosquitoes from one patch to other patch is also affected by hosts density and distance between patches. The theoretical study of this model was done using the theory of monotone dynamical systems recalled in appendix. This study allowed to identify threshold values that ensure an effective control of the population. The model has several contributions to science and to public health. The coupling of the compartments of each mosquito stage and the spatial network patches of the model makes it comprehensive but simple model that explicitly captures mosquito behavioural and ecological features that are often neglected. From mathematical point of view, the dispersal model was analyzed further to gain mathematical insight. The computation of the basic offspring number for the whole domain help to understand the effects of dispersal on the overall total population of mosquitoes and its implication on the maintaining disease risk. Our results reveal that the connectivity of breeding-feeding sites strongly influence the spatial distribution of mosquitoes. The advantage of the metapopulation model (discrete space) developed in this work is that one can easily assess vector control strategies, because the discrete space enables easy representation of interventions that cover sets of house holds or villages. The metapopulation model, together with field data, can be used to determine areas of high transmission within local settings, evaluate the community effect of interventions, and assist to develop possible and efficient vector control strategies, which can optimize the allocation of scarce resources.

In the second part (chapter 3), an alternative approach to metapopulation model was developed using PDEs for mosquito dispersal. Some seminal models was modified by taking account all stages in the gonotrophic cycle (questing, resting and breeding female). We have presented here a framework for studying the dynamics of the mosquito populations by interpreting its life cycle. The model developed in this part categorize the life of a mosquito into six stages, namely, aquatic stage, young females, males, questing females, resting females and breeding females. A general form of the eggs oviposition function was used and the dynamics of the human-vector interactions was took into account based on the idea that mosquito has a human biting rate. The last three compartments of the model (questing females, resting females and breeding females)

provide an opportunity to study the life style of the adult mosquito and assess the impact of urbanization process on the distribution of the mosquitoes. They also offer direct opportunity to assess the impact of interventions specifically targeting a certain state to reduces contacts between mosquitoes and human hosts. Mosquito dispersal was modelled using PDEs where advection and diffusion terms was added. The diffusion term accounts for random movements of mosquitoes when they are not responding to any stimulus, while advection term governs the attraction of the mosquitoes towards breeding-feeding sites. To describe the spatial heterogeneity, urbanization process was used to capture the fact that hosts was unevenly distributed in the domain. A deep theoretical study of this model was carried out using a variety techniques and approaches including : Lyapunov-LaSalle techniques, monotone dynamical systems theory, fluctuation method and spectral theory approach. On the one hand, we have used several approaches to prove global stability of equilibria and for some nonlinear birth functions, we have characterized the asymptotic behavior of our model. Our results on stability study show that, in absence of density-dependent mortality, Hopf bifurcation phenomenon can occur at the mosquito-persistent equilibrium while in the presence of density-dependent mortality, the mosquito-persistent equilibrium is always asymptotically stable. In the other hand, a special emphasis of this part was the role played by the spatial component and variation of human distribution on mosquitoes distribution. Our study indicates that there is a relationship between hosts density and mosquitoes distribution, and this relationship has far-reaching effects on spatial distribution of mosquitoes. Through numerical simulations, this work suggests that spatial variation of human distribution strongly influences the spatial distribution of adult female mosquitoes. When the index describing urbanization process, varies from zero to one, the distribution of females in the gonotrophic cycle is strongly disturbed. This shows that urbanization may increase or decrease malaria risk in regions where this disease is endemic. With regard to control measure, a probably efficient strategy for the containment of anopheles mosquito could be the mitigation of human-mosquito contact. It is well known that so far that a sustainable and efficient method of reducing this human-mosquito contact remains the use of mosquito bed nets, and it should be noted that, the consideration of such measure alongside with the spatial effects (as in this work) on mosquito population dynamics will bring further interesting and challenging modelling and mathematical questions.

Throughout this thesis, the importance of models that incorporate dispersal and environmental heterogeneity was shown. Crucial to assessing disease transmission spatial variations, this work shows that alongside patterns of heterogeneity, mosquito dispersal should be considered when designing intervention strategies. Spatially-explicit dispersal models integrated with environmental heterogeneity allow predictions to capture ecological behaviour of mosquitoes, the main source of variations in malaria risk at local spatial scales. These predictions vary in space but provide more information than predictions of

models that assume enclosed systems without taking into account the underlying heterogeneity of the landscape. Such predictions can assist not only in determining risk areas for targeted control, but also in determining optimal strategies for deploying interventions to assist achieving malaria elimination goals. The findings concerning different impacts of heterogeneity have important implications for the development of control strategies. In addition, the models can be used to explore the implications of the resulting multiplicity of combinations of different environments with intervention strategies in understanding malaria epidemiology and control. The knowledge gained from the models allow informed decisions on designing the most effective intervention strategies in the area. At local level, transmission appears to be shaped by the availability of resources (Smith et al., 2004 [122]) because mosquitoes movement between places is often related to the distribution of resources. Thus, routine movement play a key role in spread diseases at local spatial scales. This finding has important implications for malaria prevention, challenging the appropriateness of current approaches to vector control. The argument is that assessment of current approaches and sampling methods used in vector control should consider vector dispersal. This will lead to improvements in preventing transmission.

Based on the results, the models will stimulate dialogue and future modelling directions in response to the results generated by this study and field research for valuable resource management and rational decisions about strategies for local malaria control. Mathematical analysis is an essential tool for assessing the true impact of each parameter and to provide evidence for interventions that aim at reducing mosquito abundance. The translation of the knowledge gained from models to the field will improve our understanding of ecological processes such as dispersal and interactions among populations. The models developed in this thesis and the results emerging from its application are essential for implementation of better malaria vector control programs. Together with field data, these models could help determine better ways of spatially distributing interventions in local settings to optimize the allocation of scarce resources available especially when country economies do not allow high coverage levels.

Future work

The models developed in this thesis have some limitations but also are capable of accommodating further extensions which could improve its performance qualities to enable further investigations.

The development times of each stage of the mosquito, particularly the aquatic stages highly dependent on the environmental conditions. Since the model structured the mosquito into its life stages, incorporating environmental and seasonal effects such as rainfall, temperature is possible (Abdelrazec et al. (2017) [1] ; Depinay et al. (2004) [38] ; Mordecai et al. (2013) [99] ; Okuneye et al. (2018) [108]). These environment-dependent

parameters include the mosquito recruitment or birth rate, the mosquito mortality rates, and the development rates. The seasonal effects could be modelled by making some of these parameters periodic functions of time. However, these environmental effects have implications on the analytical results of the model. Analyzing periodical models with changes in the mosquito population reproductive number and steady states is complex but could provide more information on the spatial distribution of mosquitoes over time and its implications on the distribution of vector control interventions. Thus, a possible extension of this thesis is to incorporate the seasonality and climate changes in our spatial models in order to assess the impact of temperature and rainfall on the abundance of mosquitoes. To better reflect the details of spatial variation, an equally challenging problem will be to consider the situation where the diffusion and convection coefficients, as well as other parameters depend on a two dimensional spatial variable.

The control of diseases vector is a matter of main environmental and health concern. Control programs of mosquitoes aim at developing control strategies in order to maintain the mosquito population at a low-impact level while satisfying environmentally respectful requirements. In this context, more and more attention is given to specific methods such as mechanical control, biological control, involving SIT control, and/or behavioral methods. Thus, since we take into account the male dispersal, another possible extension would be to incorporate a compartment of sterile males insects in our models, in order to assess the impact of Sterile Insect Technique (SIT) control. The classical SIT consists of mass releases of males sterilized by ionizing radiation. The released sterile males transfer their sterile sperms to wild females, which results in a progressive decay of the targeted population.

In the field, the models could be validated by applying it to an area which is endemic to malaria. Using data from mark-recapture studies, parameter values specific to particular locations could be used as input values in the model, and simulations of the effects of host and breeding sites distribution on the distribution of mosquitoes could be made with and without interventions. The present work gives a mathematical framework to model the spatial dynamics of the mosquitoes. Although the models presented here can be made more realistic by adding complexity, their relative simplicity allowed to carry out theoretical mathematical studies and simulations providing biologically relevant and applicable results useful for the development of mosquito control tool satisfying the requirements of control programs.

ANNEXE

CHAPTER A

Contents

MATHEMATICAL TOOLS

A.1 General setting for the models

The models presented in chapter 2 and 3 are dynamical systems. A dynamical system describes the evolution in time of the different states of a system. The set of states is often referred to as the phase space and it can be of different nature depending on the formulation of the problem. For instance, the phase space of a dynamical system defined via an ODE representing the evolution of a population size can be a subset of $\mathbb{R}$. When the population is divided into compartments, then its dynamics are governed by a system of ODEs, and then, the states of its dynamical system are vectors of $\mathbb{R}^n$ giving the size of each compartment. The states of a dynamical system can also be functions or vector of functions. When we deal with spatio-temporal models governed by PDEs (resp. systems of PDEs), then the phase space of the corresponding dynamical system becomes the space of $\mathbb{R}$-valued functions (resp. $\mathbb{R}^n$-valued functions). Dynamical systems can be categorized according to the nature of its parameter (time), its phase space and its evolution rule. The time as well as the phase space can be continuous or discrete. Further, the evolution rule can be deterministic or stochastic. When the evolution rule is deterministic, it takes each state of the system to a unique subsequent state, which is not the case when the evolution rule is stochastic. The models presented in chapters 2 and 3 describe continuous deterministic dynamical systems, thus we only focus on this case. In more precise terms the definition of dynamical system is given as follows [66] :

Definition **A.1.1.** Let $\mathcal{D}$ be a topological space. A dynamical system is a C^1 map $\varphi : \mathbb{R}_+ \times \mathcal{D} \to \mathcal{D}$ such that $\varphi_t \equiv \varphi(t, \cdot) : \mathcal{D} \to \mathcal{D}$ satisfies the following properties :

(i) $\varphi_0 = Id$,

(ii) $\varphi_{t+s} = \varphi_t \circ \varphi_s, \quad \forall t, s \geq 0.$

The operator φ is called a semigroup or semiflow operator, since from (i) and (ii), it follows that $\{\varphi_t, \ t \geq 0\}$ is a semigroup with respect to composition.

The models presented in chapter 2 and 3 are formulated via ODEs and PDEs. In all cases, the model can be formulated in the following operator form

$$\begin{cases} \dfrac{du}{dt} &= \Psi u(t) + F(t,u), \quad t > 0, \\ u(0) &= u_0, \end{cases} \tag{A.1}$$

where $u(t) \in \mathbb{R}^n$ when the model is given as a system of ODEs and where u is a mapping $u : [0,\infty) \to X$, X being a functional space, when the model is formulated by PDEs. Then, we have that $u(t) = \varphi_t(u_0)$ is a solution of (A.1).

In the following we recall some useful definitions.

Definition A.1.2 (pg 1, 4, [134]). Let X be a Banach space. A family $(T(t))_{t\geq 0}$ of bounded linear operators such that $T(t) : X \to X$ for all $t \geq 0$, is a strongly continuous semigroup of bounded linear operators if the following conditions hold:

(i) $T(0) = id_X$;

(ii) $T(t+s) = T(t)T(s)$, $\forall t, s \geq 0$;

(iii) $\forall x \in X$, $t \longmapsto T(t)x$ is continuous at 0.

A strongly continuous semigroup of bounded linear operators on X will be called a C_0-semigroup.

Definition A.1.3 (pg 1, [134]). The linear operator Ψ defined by

$$\Psi x = \lim_{t\to 0^+} \frac{T(t)x - x}{t}, \quad \text{for} \quad x \in D(\Psi),$$

is called the infinitesimal generator of the semigroup $(T(t))_{t\geq 0}$, where

$$D(\Psi) = \left\{ x \in X : \lim_{t\to 0^+} \frac{T(t)x - T(0)x}{t-0} \ \text{ exists} \right\},$$

is called the domain of Ψ.

Definition A.1.4 (pg 105, [134]). Let $u : [0,T] \longrightarrow X$ be a function.

(i) The function $u \in C([0,T], X)$ given by

$$u(t) = T(t)u_0 + \int_0^t T(t-s)F(s,u(s))ds, \quad 0 \leq t \leq T,$$

with $x \in X$ and $F \in L^1([0,T]; X)$ is called mild solution of (A.1) on $[0,T]$.

(ii) u is a classical solution of (A.1) if u is continuous on $[0,T]$ and $u(t) \in D(A)$, for $0 < t \leq T$ satisfies (A.1).

Definition A.1.5. Let X be an ordered Banach with positive cone X^+ such that $int(X^+) \neq \emptyset$. A linear operator A on X is said to be positive if $A(X^+) \subset X^+$, strongly positive if $A(X^+ \setminus \{0\}) \subset int(X^+)$.

Definition A.1.6. For a closed linear operator $\Theta : D(\Theta) \longrightarrow X$, $\lambda \in \mathbb{C}$ is a resolvent value of Θ if $\lambda I - \Theta$ has a bounded inverse operator that is defined on the entire X. The set of resolvent values of Θ is called the resolvent set of Θ and is denoted by $\rho(\Theta)$. The set $\sigma(\Theta) := \mathbb{C} \setminus \rho(\Theta)$ is called the spectrum of Θ. A closed operator Θ in X is called resolvent-positive if the resolvent set of Θ, $\rho(\Theta)$ contains a ray (η, ∞) and $(\lambda I - \Theta)^{-1}$ is a positive operator $\forall \lambda > \eta$.

Definition A.1.7. A linear operator $\Phi : Y \longmapsto X$, defined on a linear subspace Y of X, is called positive if $\Phi(x) \in X^+$, $\forall x \in Y \cap X^+$ and Φ is not the zero operator. If Ψ is a resolvent-positive operator and $\Phi : D(\Psi) \mapsto X$ is a positive linear operator, then $\Theta = \Psi + \Phi$ is called a positive perturbation of Ψ.

We recall the spectral radius $r(\Theta)$ of a square matrix Θ is defined by

$$r(\Theta) := \sup\{|\lambda| \ : \ \lambda \in \sigma(\Theta)\},$$

where $\sigma(\Theta)$ is the spectrum of Θ. Its spectral bound $s(\Theta) := \sup\{Re\lambda \ : \ \lambda \in \sigma(\Theta)\}$.

In many cases, it is not possible to find an explicit formulation for a solution to such problems. In order to study PDE or ODE problems, we typically investigate the *well-posedness* of the problem. A problem is said to be well-posed (in the sense of Hadamard) when it satisfies the following conditions: (i) there exists a solution to the problem ; (ii) this solution is unique ; (iii) the solution depends continuously on the data of the problem.

In sections A.2 and A.3, we give some mathematical background in the appropriate settings to show that the problems describe well-posed dynamical systems. For the model of chapter 2, we consider the setting of monotone dynamical systems. For the advection-diffusion model presented in chapter 3 formulated by PDEs, we consider the setting of the dissipative dynamical systems in order to give global behavior of the system. In the following, we recall some fundamental results which will be used in our further analysis.

A.2 Dissipative dynamical systems

We present concepts of limit sets and attractors and some fundamental theorems such as the LaSalle invariance principle, the asymptotic fixed point theorem, and the global attractor theorems.

A.2.1 Limits sets and global attractors

Let X be a complete metric space with metric d and $\Phi : X \longrightarrow X$ a continuous map. For a nonempty invariant set M (i.e. $\Phi(M) = M$), the set

$$W^s(M) = \{x \in X \ : \ \lim_{n\to\infty} d(\Phi^n(x), M) = 0\}$$

is called the stable set of M. The omega limit set of x is defined in the usual way as

$$\omega(x) = \{y \in X \ : \ \Phi^{n_k}(x) \to y, \text{ for some } n_k \to \infty\}.$$

Thanks to Lemma 2.1.2 in [58], If the positive orbit of x, $\gamma^+(x) = \{\Phi^n(x)\ n \geq 0\}$ is precompact (i.e., it is contained in a compact set), then $\omega(x)$ is nonempty, compact, and invariant.

Let $x^* \in X$ be a fixed point of Φ (i.e. $\Phi(x^*) = x^*$). Recall that x^* is said to be stable for Φ if for each $\epsilon > 0$ there exists $\delta > 0$ such that for any $x \in X$ with $d(x, x^*) < \delta$, we have $d(\Phi^n(x), x^*) < \epsilon$, $\forall n \geq 0$. The following simple observation is useful in proving the convergence of a precompact positive orbit to a fixed point.

Lemma A.2.1 (Lemma 1.1.1 in [160])**.** Let x^* be a stable fixed point and $\gamma^+(x)$ a precompact positive orbit for $\Phi : X \to X$. If $x^* \in \omega(x)$, then $\omega(x) = \{x^*\}$.

Definition A.2.1. Let G be a closed subset of X. A continuous function $V : G \to \mathbb{R}$ is said to be a Liapunov function on G of the map $\Phi : G \to G$, if $\dot{V}(x) = V(\Phi(x)) - V(x) \leq 0$ for all $x \in G$.

Theorem A.2.1 (Theorem 1.1.1 in [160] (LaSalle Invariance Principle))**.** Assume that V is a Liapunov function on G of Φ, and that $\gamma^+(x)$ is a precompact orbit of Φ and $\gamma^+(x) \subset G$. Then $\omega(x) \subset M \cap V^{-1}(c)$ for some $c = c(x)$, where M is the largest invariant set in $E := \{x \in G \ : \ \dot{V}(x) = 0\}$, and $V^{-1}(c) := \{x \in G \ : \ V(x) = c\}$.

Recall that a set U in X is said to be a neighborhood of another set V provided that V is contained in the interior int(U) of U. For any subsets $A, B \subset X$ and any $\epsilon > 0$, we define

$$d(x, A) := \inf_{y\in A} d(x, y), \quad \delta(B, A) := \sup_{x\in B} d(x, A).$$

The Kuratowski measure of noncompactness, κ, is defined by

$$\kappa(B) := \inf\{r : B \text{ has a finite cover of diameter } < r\},$$

for any bounded set B of X. We set $\kappa(B) = \infty$ whenever B is unbounded. The following lemma is straightforward.

Lemma A.2.2 (Lemma 1.1.2. in [160])**.** The following statements are valid :

(i) Let $I \subset [0, \infty)$ be unbounded, and $\{A_t\}_{t\in I}$ be a nonincreasing family of nonempty closed subsets (i.e., $t \leq s$ implies $A_s \subset A_t$). Assume that $\kappa(A_t) \to 0$ as $t \to \infty$. Then $A_\infty = \bigcap_{t\geq 0} A_t$ is nonempty and compact, and $\delta(A_t, A_\infty) \to 0$ as $t \to \infty$.

(ii) For each $A \subset X$ and $B \subset X$, we have $\kappa(B) \leq \kappa(A) + \delta(B, A)$.

For a subset $B \subset X$, let

$$\gamma^+(B) := \bigcup_{m \geq 0} \Phi^m(B) \quad \text{and} \quad \omega(B) := \bigcap_{n \geq 0} \overline{\bigcup_{m \geq n} \Phi^m(B)},$$

be the positive orbit of B for Φ and the omega limit set of B, respectively. A subset $A \subset X$ is positively invariant for Φ if $\Phi(A) \subset A$. We say that a subset $A \subset X$ attracts a subset $B \subset X$ for Φ if $\lim_{n \to \infty} \delta(\Phi^n(B), A) = 0$. It is easy to see that B is precompact (i.e. $\overline{B}$ is compact) if and only if $\kappa(B) = 0$. A continuous mapping $\Phi : X \to X$ is said to be compact (completely continuous) if Φ maps any bounded set to a precompact set in X.

The theory of attractors is based on the following fundamental result.

Lemma A.2.3 (Lemma 1.1.3. in [160])**.** Let B be a subset of X and assume that there exist a compact subset C of X which attracts B for Φ. Then $\omega(B)$ is nonempty, compact, invariant for Φ and attracts B.

Definition A.2.2. A continuous mapping $\Phi : X \to X$ is said to be

(i) point (compact, bounded) dissipative if there is a bounded set B_0 in X such that B_0 attracts each point (compact set, bounded set) in X ;

(ii) κ-contracting if $\lim_{n \to \infty} \kappa(\Phi^n(B)) = 0$ for any bounded set $B \subset X$;

(iii) asymptotically smooth if for any nonempty closed bounded set $B \subset X$ for which $\Phi(B) \subset B$, there is a compact set $J \subset B$ such that J attracts B.

Remark A.2.1. By Lemma A.2.2, it follows that $\Phi : X \to X$ is asymptotically smooth if and only if $\lim_{n \to \infty} \kappa(\Phi^n(B)) = 0$ for any nonempty closed bounded subset $B \subset X$ for which $\Phi(B) \subset B$. This implies that any κ-contracting map is asymptotically smooth.

Definition A.2.3. A nonempty, compact and invariant set $A \subset X$ is said to be

(i) an attractor for Φ if A attracts some open neighborhood of itself ;

(ii) a global attractor for Φ if A is an attractor that attracts every point in X ;

(iii) a strong global attractor for Φ if A attracts every bounded subset of X.

The following result gives the existence of a global attractor for Φ.

Theorem A.2.2 (Theorem 1.1.2 in [160] (Global attractors))**.** Let $\Phi : X \to X$ be a continuous map. Assume that

(a) Φ is point dissipative and asymptotically smooth ;

(b) positive orbits of compact subsets of X for Φ are bounded.

Then Φ has a global attractor $A \subset X$. Moreover, if a subset B of X admits the property that $\gamma^+(\Phi^k(B))$ is bounded for some $k \geq 0$, then A attracts B for Φ.

A.2.2 Uniform persistence

Uniform persistence is an important concept in population dynamics, since it characterizes the long-term survival of some or all interacting species in an ecosystem. Looked at abstractly, it is the notion that a closed subset of the state space is repelling for the dynamics on the complementary set, and then it gives a uniform estimate for omega limit sets, which sometimes is essential to obtain a more detailed global dynamics.

Let $\Phi : X \to X$ be a continuous map and $X_0 \subset X$ an open set. Define

$$\partial X_0 := X \setminus X_0, \quad \text{and} \quad M_\partial := \{x \in \partial X_0 \ : \ \Phi^n(x) \in \partial X_0,\ n \geq 0\},$$

which may be empty. Note that ∂X_0 need not be the boundary of X_0 as the notation suggests. This peculiar notation has become standard in persistence theory. We assume that every positive orbit of Φ is precompact.

Definition A.2.4. Let $A \subset X$ be a nonempty invariant set. We call A internally chain transitive if the following stronger condition holds : For any $a, b \in A$ and any $\epsilon > 0$, there is a finite sequence $x_1, \cdots, x_m$ in A with $x_1 = a$, $x_m = b$ such that $d(\Phi(x_i), x_{i+1}) < \epsilon$, $1 \leq i \leq m-1$. The sequence $\{x_1, \cdots, x_m\}$ is called an ϵ-chain in A connecting a and b.

The following result give an example of internally chain transitive sets.

Lemma A.2.4 (Lemma 1.2.1 in [160])**.** Let $\Phi : X \to X$ be a continuous map. Then the omega limit set of any precompact positive orbit is internally chain transitive.

Definition A.2.5. A lower semicontinuous function $p : X \to \mathbb{R}_+$ is called a generalized distance function for $\Phi : X \to X$ if for every $x \in (X_0 \cap p^{-1}(0)) \cup p^{-1}(0, \infty)$, we have $p(\Phi^n(x)) > 0$, $\forall n \geq 1$.

Theorem A.2.3 (Theorem 1.3.2. in [160])**.** Let p be a generalized distance function for continuous map $\Phi : X \to X$. Assume that

($P1$): Φ has a global attractor A ;

($P2$): There exists a finite sequence $M = \{M_1, \ldots, M_k\}$ of disjoint, compact,and isolated invariant sets in ∂X_0 with the following properties :

(a) $\cup_{x \in M_\partial} \omega(x) \subset \cup_{i=1}^{k} M_i$;

(b) no subset of M forms a cycle in ∂X_0 ;

(c) M_i is isolated in X ;

(d) $W^s(M_i) \cap p^{-1}(0, \infty) = \varnothing$ for each $1 \leq i \leq k$.

Then there exists $\delta > 0$ such that for any compact chain transitive set L with $L \not\subset M_i$ for all $1 \leq 1 \leq k$, we have $\min_{x \in L} p(x) > \delta$.

Definition A.2.6. A function $\Phi : X \to X$ is said to be uniformly persistent with respect to $(X_0, \partial X_0)$ if there exists $\eta > 0$ such that

$$\liminf_{n\to\infty} d(\Phi^n(x), \partial X_0) \geq \eta \quad \text{for all} \quad x \in X_0.$$

If "inf" in this inequality is replaced with "sup", then Φ is said to be weakly uniformly persistent with respect to $(X_0, \partial X_0)$.

Definition A.2.7. Let p be a generalized distance function for a continuous map $\Phi : X \to X$. Then Φ is said to be uniformly persistent with respect to $(X_0, \partial X_0, p)$ if there exists $\eta > 0$ such that

$$\liminf_{n\to\infty} p(\Phi^n(x)) \geq \eta \quad \text{for all} \quad x \in X_0.$$

By Definition A.2.5, it is easy to see that for every $x \in X_0$, either $p(x) > 0$ or $p(\Phi(x)) > 0$. Note that $\omega(x) = \omega(\Phi(x))$. Thus, $W^s(M_i) \cap p^{-1}(0, \infty) = \varnothing$ implies $\omega(x) \not\subset M_i$, $\forall x \in X_0$. By Lemma A.2.4 and Theorem A.2.3, we have the following result.

Theorem A.2.4. Let p be a generalized distance function for a continuous map $\Phi : X \to X$. Assume that $(P1)$ and $(P2)$ hold. Then, Φ is said to be uniformly persistent with respect to $(X_0, \partial X_0, p)$.

A.3 Dynamical systems defined by a system of ODEs

The model presented in 2 and the first model presented in 3 are temporal and governed by systems of ODEs representing the evolution in time of a compartmented mosquito population. Thus, the state of the system at time t is a real vector $x(t)$ representing the population densities in the respective compartments at time t. Hence, we consider a dynamical system defined via a system of ODEs on a subset of $\mathbb{R}^n$ as discussed below.

Let $\mathcal{D} \subset \mathbb{R}^n$, we consider the autonomous system of ODEs

$$\begin{cases} \dfrac{dx}{dt} &= f(x), \\ x(0) &= x_0 \in \mathcal{D}, \end{cases} \tag{A.2}$$

where $f : \mathcal{D} \longrightarrow \mathbb{R}^n$.

We recall here some of the fundamental theory following mostly [66].

Theorem A.3.1 ([66], Theorem 1, pg.162.)**.** Let $\mathcal{D} \subset \mathbb{R}^n$ be an open, $f : \mathcal{D} \longrightarrow \mathbb{R}^n$ a C^1 map and $x_0 \in \mathbb{R}^n$. Then there is some $a > 0$ and a unique solution $x : [-a, a] \longrightarrow \mathcal{D}$ of the differential equation (A.2).

Theorem A.3.2 ([66], Theorem, pg.171.)**.** Let $\mathcal{D} \subset \mathbb{R}^n$ be an open, $f : \mathcal{D} \longrightarrow \mathbb{R}^n$ a C^1 map. Let $x(t)$ be a solution on a maximal open interval $J = (\alpha, \beta)$, $\beta < \infty$. Then, given any compact set $K \subset \mathcal{D}$, there is some $t \in (\alpha, \beta)$ such that $x(t) \notin K$.

In other words, Theorem A.3.2 says that if $x(t)$ cannot be extended to a larger interval than (α, β), then it leaves any compact set. As a consequence, as t tends to β, $x(t)$ either tends to the boundary of $\mathcal{D}$ or $|x(t)|$ tends to ∞.

If for every $x_0 \in \mathcal{D}$, the system (A.2) has a unique solution $x(t)$ on $[0, \infty)$, then (A.2) defines a dynamical system $\mathcal{D}$ in terms of Definition A.1.1. In this case, the operator φ_t is given by $\varphi_t(x_0) = x(t), \quad t \geq 0$. Then, f defines a vector field satisfying : $f(x) = \left.\frac{d\varphi_t(x)}{dt}\right|_{t=0}$.

The continuity of φ_t on x_0 is shown in Theorem 2, pg. in [66]. The global existence required above is obtained typically by using the concept of invariant set.

Definition A.3.1 (Invariant set)**.** A subset K of $\mathcal{D}$ is called (positively) invariant set of (A.2) if for every $x_0 \in K$, any solution of (A.2) of the form $x : [0, \beta] \longrightarrow \mathcal{D}$ is such that $x(t) \in K$, $\forall t \in [0, \beta]$.

Proposition A.3.1 (Global existence, [66], Proposition, pg.172)**.** Let K be a compact invariant subset of the open set $\mathcal{D} \subset \mathbb{R}^n$ and let $f : \mathcal{D} \longrightarrow \mathbb{R}^n$ a C^1 map. Then for every $y_0 \in K$, there exists a unique solution $y : [0, \beta] \longrightarrow \mathcal{D}$, $y(0) = y_0$, and $y(t) \in K$, $\forall t \geq 0$.

A.3.1 Asymptotic properties

The asymptotic properties describe the behaviour of a dynamical system when time tends to infinity. We denote by O_x^+, $x \in \mathcal{D}$, the forward orbits or trajectories of the dynamical system on $\mathcal{D}$ described by the semiflow φ, i.e. the set of states that followed from an initial given state x,

$$O_x^+ \equiv \{\varphi_t(x) \quad : \quad t \geq 0\}.$$

A point $x \in \mathcal{D}$ such that $O_x^+ = \{x\}$ is called an equilibrium. We denote by E the set of all equilibria of the system. If there is a $T > 0$ such that $\varphi_{t+T}(x) = \varphi_t(x)$, $\forall t \geq 0$, then $O_x^+ \equiv \{\varphi_t(x) \quad : \quad 0 \leq t \leq T\}$ and $\varphi_t(x)$ is called a T-periodic solution.

We define the ω-limit set of $x \in \mathcal{D}$ by

$$\omega(x) = \bigcap_{t \geq 0} \overline{\bigcup_{s \geq t} \varphi_s(x)}.$$

For a dynamical system defined via (A.2), a point x^* is an equilibrium if and only if $f(x^*) = 0$.

Definition A.3.2. An equilibrium x^* of a semiflow φ is stable if for every neighborhood N of x^*, there is a neighborhood $M \subset N$ such that if $x \in M$, then $\varphi_t(x) \in N$, $\forall t \geq 0$.

Definition A.3.3. An equilibrium x^* of a semiflow φ is asymptotically stable if it is stable and there is neighborhood N of x^*, such that every point in N approaches x^* as $t \to \infty$.

In other words, an equilibrium is stable the orbits that start "near" an equilibrium stay "nearby". More strongly, an equilibrium is asymptotically stable if in addition the orbits that start "near" an equilibrium converge to the equilibrium.

To obtain stability properties of an equilibrium, we use the Jacobian matrix $Df(x^*)$ of the vector field f at x^*. Indeed, by the well-known theorem of Hartman and Grobman, the solutions of (A.2) in a neighborhood of an equilibrium x^* behave topologically equivalently to the solutions of the linear system

$$\frac{dy}{dt} = Df(x^*)y, \tag{A.3}$$

around 0. Techniques for solving linear systems can be applied to solve (A.3). In particular, properties of the equilibrium x^* are obtain by investigating the sign of the real parts of the eigenvalues of the matrix $Df(x^*)$.

Definition A.3.4. A equilibrium x^* of a C^1 vector field f is hyperbolic if none of the eigenvalues of $Df(x^*)$ have zero real parts.

Assume that x^* is a hyperbolic equilibrium, we have the following properties :

Proposition A.3.2.

1. If all the eigenvalues of $Df(x^*)$ have negative real parts then x^* stable.
2. If some of the eigenvalues of $Df(x^*)$ have positive real parts then x^* is unstable.

Definition A.3.5. Let x^* be an asymptotically stable equilibrium. The basin of attraction of x^* is the union of all the solution curves of (A.2) that tend towards x^* as $t \to \infty$.

A common method to study the global stability of dynamical systems is to show the existence of a Lyapunov function :

Definition A.3.6. Let x^* be an equilibrium of the dynamical system defined via (A.2) on $\mathcal{D}$. If there is a neighborhood U of x^* and a function $L \in C^1(U, \mathbb{R})$

(i) $L(x^*) = 0$,

(ii) $L(x) > 0$, for $x \neq x^*$,

(iii) $\nabla L(x) \cdot f(x) \leq 0$, $x \in U$,

then L is called a Lyapunov function. Further, if $\nabla L(x) \cdot f(x) < 0$, $x \in U \setminus \{x^*\}$, then L is called a strict Lyapunov function for x^*.

The expression in (*iii*) is often called the Lyapunov derivative since for every solution $x(t)$ of (A.2) we have

$$\frac{dL(x(t))}{dt} = \nabla L(x(t)) \cdot \frac{dx}{dt} = \nabla L(x(t)) \cdot f(x(t)).$$

Theorem A.3.3. Let x^* be an equilibrium of a dynamical system defined via (A.2).

(i) If there exists a Lyapunov function in a neighborhood U of x^*, then x^* is stable.

(ii) If there exists a strict Lyapunov function in a neighborhood U of x^*, then x^* is asymptotically stable with basin of attraction containing U.

There are some alternative tools to prove stability and attractiveness of equilibria without using Lyapunov-LaSalle techniques. Monotone dynamical systems approach can be used to prove stability of equilibria and provide a method for characterizing the basins of attraction.

A.3.2 Monotone dynamical systems

A monotone dynamical system is just a dynamical system on an ordered metric space which has the property that ordered initial states lead to ordered subsequent states [124]. A particularity of monotone dynamical systems is that they behave in a very "orderly" way.

A semiflow φ is said to be monotone if it satisfies

$$\varphi_t(x) \leq \varphi_t(y), \quad \text{whenever} \quad x \leq y \quad \text{and} \quad t \geq 0. \tag{A.4}$$

Further, φ is said to be Strongly Order Preserving (SOP) if it is monotone and if $x < y$, there exist open subsets $U, V \subset \mathcal{D}$ with $x \in U$, $y \in V$ and $t_0 > 0$ such that

$$\varphi_{t_0}(\widetilde{x}) \leq \varphi_{t_0}(\widetilde{y}), \quad \forall \widetilde{x} \in U, \ \ \forall \widetilde{y} \in V.$$

In particular, the monotonicity of φ implies that $\varphi_t U \leq \varphi_t V$, $\forall t \geq t_0$.

We introduce the notion of quasi-convergence which gives an essential property of monotone dynamical systems. A point $x \in \mathcal{D}$ is quasi-convergent if $\omega(x) \subset E$. We denote by Q the set of all quasi-convergent points. A point $x \in \mathcal{D}$ is convergent if $\omega(x)$ consists of a single point of E. We denote by C the set of all convergent points. In other words,

$$x \in Q \Leftrightarrow \omega(x) \subset E \quad \text{and} \quad x \in C \Leftrightarrow \omega(x) = x^* \in E.$$

If E consists of disjoint equilibria, then $Q = C$.

Theorem A.3.4 (Convergence criterion, [124], Theorem 2.1, pg. 3)**.** Let $\varphi_T(x) \geq x$ for some $T \geq 0$. Then $\omega(x)$ is a T-periodic orbit. If $\varphi_t(x) \geq x$ for t belonging to a non-empty open subset of $\mathbb{R}^+\backslash\{0\}$, then $\varphi_t(x) \to p \in E$ as $t \to \infty$. In particular, if φ is SOP and $\varphi_T(x) > x$ for some $T > 0$, then $\varphi_t(x) \to p \in E$ as $t \to \infty$.

As a consequence of Theorem A.3.4, a monotone dynamical system cannot have an attracting periodic orbit since a periodic orbit O is attractive if there is an open set U containing O such that $\omega(x) = O$, $\forall x \in U$.

If $x \in \mathcal{D}$, we say that x can be approximated from below (resp. above) in $\mathcal{D}$ if there is a sequence $\{x_n\}$ in $\mathcal{D}$ such that $x_n < x_{n+1} < x$ (resp. $x_n > x_{n+1} > x$) for $n \geq 1$ and $x_n \to x$ as $n \to \infty$.

Theorem A.3.5 ([124], Theorem 4.3, pg. 9)**.** Suppose that each point of $\mathcal{D}$ can be approximated either from above or from below in $\mathcal{D}$. If φ is SOP, then

$$\mathcal{D} = \text{Int}\mathcal{Q} \cup \overline{\text{Int}\mathcal{C}}.$$

In particular, Int$\mathcal{Q}$ is dense in $\mathcal{D}$.

Theorem A.3.5 shows that the property of quasi-convergence is generic for SOP dynamical systems in the sense that the set $\mathcal{Q}$ of all quasi-convergent points contains an open and dense subset of $\mathcal{D}$. The power of this property is further demonstrated in the particular case of E being a singleton as stated in the next theorem.

Theorem A.3.6 (Global stability, [124], Theorem 3.1, pg. 18)**.** Suppose that $\mathcal{D}$ contains exactly one equilibrium x^* and that every point of $\mathcal{D}\backslash\{x^*\}$ can be approximated from above and from below in $\mathcal{D}$. Then, $\omega(x) = x^*$, $\forall x \in \mathcal{D}$.

Let (A.2) define a dynamical system on $\mathcal{D} \subset \mathbb{R}^n$. We consider the usual partial order on $\mathbb{R}^n$, that is, for $x, y \in \mathbb{R}^n$, we have $x \leq y$ if $x - y \in \mathbb{R}^n_+$, or equivalently $x \leq y \Leftrightarrow x_i \leq y_i$, $\forall i = 1, 2, \ldots, n$. In addition, we use the following inequalities

$$\begin{aligned} x < y &\Leftrightarrow x \leq y, \quad x \neq y. \\ x \ll y &\Leftrightarrow x_i < y_i, \quad i = 1, \ldots, n. \end{aligned}$$

It is common that the systems describing population dynamics are coupled via feedbacks between the compartments. For instance, for a system of the type (A.2), for $i = 1, 2, \ldots, n$,

- if f_i is monotone increasing with respect to x_j for $i \neq j$, then x_j is said to have a positive feedback on x_i ;
- if f_i is monotone decreasing with respect to x_j for $i \neq j$, then x_j is said to have a negative feedback on x_i.

Definition A.3.7. System (A.2) is said to be cooperative if for every $i, j \in \{1, \ldots, n\}$ such that $i \neq j$, x_j has a positive feedback on x_i.

Theorem A.3.7. If f is differentiable on $\mathcal{D}$, then the system (A.2) is cooperative if and only if $\dfrac{\partial f_i(x)}{\partial x_j} \geq 0$, $i \neq j$, $x \in \mathcal{D}$.

In the other words, if f is differentiable on $\mathcal{D}$, the system is cooperative if the jacobian $\frac{df(t,x)}{dx}$ is a Metzler matrix for every $t \in [0, \infty)$ and $x \in \mathcal{D}$. Let us recall that a matrix is called Metzler if its non-diagonal entries are nonnegative. This condition on f is sometimes called quasimonotonicity with respect to x. The next theorem characterizes monotone solutions of cooperative systems.

Theorem A.3.8 ([124], Proposition 3.2.1, pg. 34)**.** Let system (A.2) be cooperative. If $a \in \mathcal{D}$ is such that $f(a) \geq \mathbf{0}$ (resp. $f(a) \leq \mathbf{0}$), then the solution $x(a,t)$ is monotone increasing (resp. decreasing) function of $t \in [0, T_a)$.

Theorem A.3.9 ([136], Theorem II, pg.12)**.** Let (A.2) be a cooperative system and let $x(x_0,t)$ be a solution of (A.2) on $[0,T)$. If $y(t)$ is a differentiable function on $[0,T)$ satisfying $\frac{dy}{dt} \leq f(y)$, $y(0) \leq x_0$, then $y(t) \leq x(x_0,t)$, $t \in [0,T)$.

Theorem A.3.10 ([124], Theorem 3.1.1, pg. 32)**.** Let (A.2) be a cooperative system and $a, b \in \mathcal{D}$. If $a \leq b$ and $x(a,t)$ and $x(b,t)$ are defined for $t > 0$, then $x(a,t) \leq x(b,t)$.

Definition A.3.8. A system of the form (A.2) is called irreducible if its Jacobian $\frac{df}{dx}$ is an irreducible matrix for every $x \in \mathcal{D}$.

Theorem A.3.11 (Kamke's theorem, [136])**.** Let the system (A.2) be cooperative. Then for every $a, b \in \mathcal{D}$,

$$a \leq b \Rightarrow x(a,t) \leq x(b,t), \quad t \in [0, \min\{T_a, T_b\}).$$

Theorem A.3.11 equivalently means that the evolution semi-group operator $\varphi_t : \mathcal{D}_t \to \mathcal{D}$ defined by $\varphi_t(a) = x(a,t)$ is monotone increasing on its domain $\mathcal{D}_t = \{a \in \mathcal{D} \quad T_a > t\}$ for every $t > 0$. For cooperative irreducible systems, the Kamke's theorem admits a stronger form as stated below.

Theorem A.3.12 ([124], Theorem 4.1.1, pg. 56)**.** If the system (A.2) is cooperative and irreducible, then for every $a, b \in \mathcal{D}$

$$a < b \Rightarrow x(a,t) \ll x(b,t), \quad t \in [0, \min\{T_a, T_b\}).$$

The combined application of the monotonicity of the evolution operator φ_t given in Theorems A.3.11 and A.3.12, and the monotonicity of the solutions given in Theorem A.3.8 is an efficient tool for studying asymptotic stability of equilibria of monotone dynamical systems. As usual, we call an equilibrium asymptotically stable if it is both stable and attractive. An asymptotically stable equilibrium is called globally asymptotically stable if the basin of attraction is the whole domain $\mathcal{D}$. Basins of attraction are often represented as n-dimensional intervals : given $a, b \in \mathbb{R}^n$ with $a \leq b$,

$$[a,b] = \{x \in \mathbb{R}^n \quad : \quad a \leq x \leq b\}.$$

The following results establish the global asymptotic stability of the equilibria using Theorems A.3.11, A.3.12 and A.3.8, which is a consequence of Theorem A.3.6.

Theorem A.3.13. Let $a, b \in \mathcal{D}$ be such that $a < b$, $[a,b] \subseteq \mathcal{D}$ and $f(b) \leq \mathbf{0} \leq f(a)$. Then system (A.2) defines a (positive) dynamical system on $[a,b]$. Moreover, if $[a,b]$ contains a unique equilibrium p, then p is globally asymptotically stable on $[a,b]$.

A.4 Dynamical systems defined by a system of PDEs

In the model of chapter 3, we consider the spatio-temporal variations of abundance of mosquitoes governed by reaction-advection-diffusion equations (RAD). The density of mosquitoes is denoted $u(t,x)$ and defined on a time-space $\Omega_T = [0,T] \times \Omega$, where $T \in \mathbb{R}^+$ and Ω is a domain in $\mathbb{R}$ with a piecewise smooth boundary $\Gamma = \partial\Omega$. The RAD equation can be written in the general form :

$$\frac{\partial u}{\partial t} + Lu = F(x, u(t,x)), \quad \text{in} \quad \Omega_T, \quad u(0,x) = u_0(x), \tag{A.5}$$

with

$$Lu = -\sum_{i,j=1}^{n} \frac{\partial}{\partial x_j}\left(D_{ij}\frac{\partial u}{\partial x_i}\right) + \sum_{i=1}^{n} v_i \frac{\partial u}{\partial x_i}.$$

Further, to complete the formulation of the problem, we provide information on the dynamics at the boundary Γ of the domain. We can distinguish two main types of boundary conditions :

- Homogeneous Dirichlet : If we consider a domain out of which individuals cannot survive, then we have $u(t,x) = 0$, $x \in \Gamma$, $\forall t \in [0,T]$.
- Homogeneous Neumann : If we consider an isolated domain with no movement of individuals in and out of the domain, then we have $\frac{\partial}{\partial \nu}u(t,x) = 0$, $x \in \Gamma$, $\forall t \in [0,T]$, where ν denotes the outward normal vector to Γ.
- Robin : $\alpha(x)u(t,x) + \delta\frac{\partial}{\partial \nu}u(t,x) = 0$, $x \in \Gamma$, $\forall t \in [0,T]$. The Robin boundary condition is a combination of Dirichlet and Neumann, where the flux at the boundary depends on the density of u at the boundary.

In this thesis, we consider homogeneous Neumann and Robin conditions. Given problem (A.5), a solution is expected to lie in the space of real-valued functions of class C^1 with respect to t and C^2 with respect to x, and it is referred to as a classical solution.

A.4.1 The maximum principle and the comparison principle

Maximum principle plays a central role in the theory of parabolic partial differential equations. It provide a useful tool to study properties of elliptic and parabolic equations [47, 124]. This principle states that the maximum of a solution is achieved on the boundary of the domain where it is defined. Assume that the operator L has the non-divergent form:

$$Lu = -\sum_{i,j=1}^{n} D_{ij}\frac{\partial^2 u}{\partial x_i x_j} + \sum_{i=1}^{n} v_i \frac{\partial u}{\partial x_i},$$

where the coefficients D_{ij} and v_i are continuous. We also assume that $D_{ij} = D_{ji}$. Denote $\Omega_T = [0,T] \times \Omega$ and $\overline{\Omega}_T$ its closure.

Theorem A.4.1 ((Strong maximum principle)[47], Theorem 11, section 7.1). Assume that $u \in C^2(\Omega_T) \cap C(\overline{\Omega}_T)$.

(i) If

$$u_t + Lu \leq 0 \quad \text{in} \quad \overline{\Omega}_T,$$

and u attains its maximum over $\overline{\Omega}_T$ at a point $(t_0, x_0) \in \Omega_T$, then u is constant on Ω_{t_0}.

(ii) If

$$u_t + Lu \geq 0 \quad \text{in} \quad \overline{\Omega}_T,$$

and u attains its minimum over $\overline{\Omega}_T$ at a point $(t_0, x_0) \in \Omega_T$, then u is constant on Ω_{t_0}.

Now, suppose that (A.5) has a classical solution. Let Λ be a nonempty, closed, convex subset of $\mathbb{R}^n$. Let $v^+(t,x)$ and $v^-(t,x)$ be continuous on $[0,T)\times\overline{\Omega}$, continuously differentiable on $(0,T)\times\overline{\Omega}$ and twice continuously differentiable in $x \in \Omega$ for $t > 0$. Furthermore, assume that

$$v^-(t,x) \leq v^+(t,x) \quad \text{and} \quad v^-(t,x), v^+(t,x) \in \Lambda, \quad [0,T)\times\overline{\Omega}.$$

Let $F^{\pm} : \overline{\Omega}\times\Lambda \to \mathbb{R}^n$ be two functions satisfying

$$\frac{\partial F_i^{\pm}}{\partial u_j}(x,u) \geq 0, \quad (x,u) \in \overline{\Omega}\times\Lambda, \quad i \neq j.$$

When this holds, we say that $F_i^{\pm}$ is cooperative. In the literature of partial differential equations it is more commun to refer to this condition as the *quasimonotone* condition. Finally, assume that $v^{\pm}$ satisfy the differential inequalities

$$\begin{aligned} \frac{\partial v^+}{\partial t} &\geq Lv^+ + F^+(x,v^+), \quad t>0, \quad x\in\Omega \\ \alpha v^+ + \delta\frac{\partial v^+}{\partial \nu} &\geq 0, \quad t>0, \quad x\in\partial\Omega \end{aligned} \tag{A.6}$$

and

$$\begin{aligned} \frac{\partial v^-}{\partial t} &\leq Lv^- + F^+(x,v^-), \quad t>0, \quad x\in\Omega \\ \alpha v^- + \delta\frac{\partial v^-}{\partial \nu} &\leq 0, \quad t>0, \quad x\in\partial\Omega \end{aligned} \tag{A.7}$$

The function v^+ is called a *super – solution* and v^- is called a *sub – solution* in the literature of partial differential equations. The next result is a fundamental comparison technique.

Theorem A.4.2 ([124], Theorem 7.3.4). Suppose that $v^{\pm}$ satisfy (A.6)-(A.7) and $F^{\pm}$ are cooperative. Suppose further that

$$F^-(x,u) \leq F(x,u) \leq F^+(x,u), \quad (x,u) \in \overline{\Omega}\times\Lambda$$

and

$$v^-(x,0) \leq u_0(x) \leq v^+(x,0), \quad x \in \overline{\Omega}.$$

Then the unique solution of (A.5) exists on $[0,\sigma)$ where $\sigma > T$ and

$$v^-(t,x) \leq u(t,x) \leq v^+(t,x), \quad (t,x) \in [0,T)\times\overline{\Omega}.$$

♣ Bibliography ♣

[1] A. Abdelrazec, A. B. Gumel, Mathematical assessment of the role of temperature and rainfall on mosquito population dynamics, J. Math. Biol. 74 (6) (2017) 1351–1395.

[2] R. Anguelov, Y. Dumont, J. Lubuma, Mathematical modeling of sterile insect technology for control of anopheles mosquito, Comp. Math. Appl. 64 (3) (2012) 374–389.

[3] Anopheles Mosquitoes, Centers for Disease Control and Prevention, http://www.cdc.gov/malaria/about/biology/mosquitoes/, accessed: May, 2016.

[4] J. Arino, A. Ducrot, and P. Zongo, A metapopulation model for malaria with transmission-blocking partial immunity in hosts, J. Math. Biol. 64 (3) (2012) 423–448.

[5] P. Auger, E. Kouokam, G. Sallet, M. Tchuente, B. Tsanou, The ross-macdonald model in a patchy environment, Math. Biosci. 216 (2008) 123–131.

[6] S. Bachelard, Quelques aspects historiques des notions de modèle et de justfication des modèles, In P. Delattre and M. Thellier, editors, Elaboration et justfication des modeles, volume 1, pages 9–20. Maloine SA, Paris, 1979.

[7] H.J. Barclay, P. Van Den Driessche, A sterile release model for control of a pest with two life stages under predation, The Rocky Mountain J. Math. 20 (4) (1990) 847–855.

[8] T. Berge, S. Bowong, J. Lubuma, M. L. Mann Manyombe, Modeling Ebola Virus Disease transmission with reservoir in a complex virus life ecology, Math. Biosci. Eng 15 (1) (2018) 21–56.

[9] N. Becker, D. Petric, M. Zgomba, C. Boase, C. Dahl, M. Madon, A. Kaiser, Mosquitoes and Their Control. Springer 2010, Second edition.

[10] H. C. Berg, Random Walks in Biology, Princeton University Press, 1993.

[11] M. Boguna, R. Pastor-Satorras, Epidemic spreading in correlated complex networks, Phys. Rev. E 66(2002) 047104.

[12] A. Brannstrom, D. J. T. Sumper, The role of competition and clustering in population dynamics, Proc. R. Soc. B 275 (2005) 2065–2072.

[13] N.F. Britton, Essential Mathematical Biology, Springer, 2003.

[14] L. Cai, S. Ai, J. Li, Dynamics of mosquitoes populations with different strategies for releasing sterile mosquitoes, SIAM J. Appl. Math. 74 (6) (2014) 1786–1809.

[15] P. Cailly, A. Tran, T. Balenghien, G. L'Ambert, C. Toty, P. Ezanno, A climate-driven abundance model to assess mosquito control strategies, Ecol. Model. 227 (2012) 7–17.

[16] J. Cano et al., Spatial variability in the density, distribution and vectorial capacity of anopheline species in a high transmission village, Malaria Journal, 5 (2006) (21).

[17] E.R. Carson, C. Cobelli, Modelling Methodology for Physiology and Medicine, San Diego CA Academic Press, 2001.

[18] R. Carter, K.N. Mendis, D. Roberts, Spatial targeting of interventions against malaria, Bull W.H.O 78 (2000) 1404–1411.

[19] M. Chapwanya, J. M. Lubuma, R.E. Mickens, Nonstandard finite difference schemes for Michaelis-Menten type reaction-diffusion equations, Num. Meth. Part. D. E. 29 (1) 337–360.

[20] N. Chitnis, T. Smith, R. Steketee, A mathematical model for the dynamics of malaria in mosquitoes feeding on a heterogeneous host population, J. Biol. Dyn. 2 (3) (2008) 259–285.

[21] N. Chitnis, J.M. Cushin, J.M. Hyman, Bifurcation analysis of a mathematical model for malaria transmission, SIAM J. Appl. Math. 67 (1) (2006) 24–45.

[22] N. Chitnis, J.M. Hyman, J.M. Cushin, Determining important parameters in the spread through the sensitivity analysis of a mathematical model, Bull. Math. Biol. 70 (2008) 1272–1296.

[23] S. Chow, C. Li, D. Wang, Normal Forms and Bifurcation of Planar Vector Fields, Cambridge University Press, 1994.

[24] A. N. Clement, The Biology of Mosquitoes : Sensory Reception and Behaviour, Vol.2, CABI Publishing Inc, New York, 1999.

[25] C. Cobelli, E.R. Carson, Introductio to modeling in physiology and medecine, Academic Press, 2008.

[26] V. Colizza, A. Vespignani, Invasion threshold in heterogeneous metapopulation networks, Phys. Rev. Lett. 99 (2007) 148701.

[27] V. Colizza, A. Vespignani, Epidemic modeling in metapopulation systems with heterogeneous coupling pattern: Theory and simulations, J. Theor. Biol. 251 (2008) 450–457.

[28] K. Cooke, P. Van den Driessche, X. Zou, Interaction of maturation delay and nonlinear birth in population and epidemic models, J. Math. Biol. 39 (4) (1999) 332–352.

[29] J. Crank, The Mathematics of Diffusion, Oxford university press, 1979.

[30] B. Cummins, R. Cortez, I. Foppa, J. Walbeck, J. Hyman, A spatial model of mosquito host-seeking behavior, PLoS Comput. Biol. 8 (5) (2012) e1002500.

[31] R. Courant, D. Hilbert (1962), Methods of Mathematical Physics, vol. 2, vol. 2, Partial Differential Equations, Interscience Publishers Inc. New York, John Wiley & Sons.

[32] R. Dautray, J.-L. Lions (2000), Mathematical Analysis and Numerical Methods for Science and Technology, Vol. 2, Functional and Variational Method, Springer.

[33] R. Dautray, J.-L. Lions (2000), Mathematical Analysis and Numerical Methods for Science and Technology, Vol. 4, Integral Equations and Numerical Methods, Springer.

[34] R. Dautray, J.-L. Lions (2000), Mathematical Analysis and Numerical Methods for Science and Technology, Vol. 5, Evolution Problems I, Springer.

[35] P. Daykin, F. Kellogg, R. Wright, Host-finding and repulsion of Aedes aegypti, Can. Entomol. 97 (1965) 239–263.

[36] K. Deimling, Nonlinear Functional Analysis, Springer-Verlag, Berlin, 1988.

[37] H. Delatte, G. Gimonneau, A. Triboire, D. Fontenille, Influence of temperature on immature development, survival, longevity, fecundity, and gonotrophic cycles of Aedes albopictus, vector of chikungunya and dengue in the Indian Ocean, J. Med. Entomol. 46 (2009) 33–41.

[38] J. M. O. Depinay, C. M. Mbogo, G. Killeen, B. Knols, J. Beier, A simulation model of African Anopheles ecology and population dynamics for the analysis of malaria transmission, Malaria J. 3 (1) (2004) 29.

[39] A. Deutsch, S. Dormann, Cellular automaton modeling of biological pattern formation: characterization, applications, and analysis, Birkhauser Boston, c/o Springer Science & Business Media, 2005.

[40] P. van den Driessche, J. Watmough, Reproduction numbers and sub-threshold endemic equilibria for the compartmental models of disease transmission, Math. Biosci. 180 (2002) 29–48.

[41] C. Dufourd, Y. Dumont, Modeling and simulations of mosquito dispersal. The case of Aedes albopictus, BioMath 1 (2012) 1209262.

[42] C. Dufourd, Yves Dumont, Impact of environmental factors on mosquito dispersal in the prospect of sterile insect technique control, Comp. Math. Appl. 66 (2013) 1695–1715.

[43] C. C. Dufourd, Spatio-temporal mathematical models of insect trapping: analysis, parameter estimation and applications to control, PhD thesis at the University of Pretoria.

[44] L. Edelstein-Keshet, Mathematical Models in Biology, volume 46. Siam, 1988.

[45] A.R.W. Elbers, C.J.M. Koenraadt, R. Meiswinkel, Mosquitoes and Culicoides biting midges: vector range and the influence of climate change, Rev. Sci. Tech. Off. Int. Epiz. 34 (1) (2015) 123–137.

[46] L. Esteva, H.M. Yang, Mathematical model to assess the control of Aedes aegypti mosquitos by the sterile insect technique, Math. Biosci. 198 (2005) 132–147.

[47] L. C. Evans, Partial Differential Equations, volume 19 of Graduate Studies in Mathematics, Providence, Rhode Island, 1998.

[48] P. Ezanno, M. Aubry-Kientza, S. Arnoux, P. Cailly, G. L'Ambert, C. Toty, T. Balenghien, A. Tran, A generic weather-driven model to predict mosquito population dynamics applied to species of Anopheles, Culex and Aedes genera of southern France, PREVET (2015).

[49] P. Fife, M. Tang, Comparison principles for reaction-diffusion systems: irregular comparison functions and applications to questions of stability and speed of propagation of disturbances, J. Diff. Equ., 40 (1981), 168–185.

[50] T. G. George, Positive Definite Matrices and Sylvester's Criterion, Am. Math. Mon. 98 (1991) 44–46.

[51] P. W. Gething et al., A new world malaria map: Plasmodium falciparum endemicity in 2010, Malaria Journal, (2011a) 10:378.

[52] H. M. Giles, D. A. Warrel, Bruce-Chwatt's Essential Malariology, 3rd edition, Heinemann Medical Books, Portsmouth, NH. 1993.

[53] M. Gillies et al., The role of carbon dioxide in host-finding by mosquitoes (diptera: Culicidae): a review, B. Entomol. Res. 70 (1980) 525–532.

[54] M. T. Gillies, Studies on the dispersion and survival of Anopheles Gambiae Giles in East Africa, by means of marking and release experiments, Bulletin of Entomological Research 52 (1961) 99–127.

[55] M. T. Gillies, T. J. Wilkes, The effect of high fences on the dispersal of some West African mosquitoes (Diptera: Culicidae), Bulletin of Entomological Research 68 (1978) 401–408.

[56] M. T. Gillies, T. J. Wilkes, Field experiments with a wind tunnel on the flight speed of some West African mosquitoes (Diptera: Culicidae), Bulletin of Entomological Research 71 (1981) 65–70.

[57] Abba B. Gumel, Suzanne Lenhart (2010), Modeling Paradigms and Analysis of Disease Transmission Models, Series in Discrete Mathematics and Theoretical Computer Sciences, Volume 75.

[58] J. K. Hale, Asymptotics Behavior of Dissipative Systems, Mathematical surveys and monographs, American Mathematics Society, Providence, Rhode Island, 1988.

[59] I. Hanski, Metapopulation dynamics, Nature 396(6706) (1998) 41–49, 1179.

[60] I. Hanski, Metapopulation Ecology, Oxford University Press, 1999.

[61] M. P. Hassell, H. N. Comins, and R. M. May, Spatial structure and chaos in insect population dynamics, Nature 353(6341) (1991) 255–258.

[62] S. I. Hay et al., A World Malaria map: Plasmodium falciparum endemicity in 2007, PLoS Med, 6(3) (2009).

[63] S. I. Hay et al., The global distribution and population at risk of malaria: past, present, and future, The Lancet Infectious Diseases 4(6) (2004) 327–336.

[64] D. Hershkowitz, Recent directions in matrix stability, Linear Algebra Appl. 171 (1992) 161–186.

[65] H.W. Hethcote, H.R. Thieme, Stability of the endemic equilibrium in epidemic models with subpopulations, Math. Biosci. 75 (1985) 205–227.

[66] M. W. Hirsch, S. Smale, Differential Equations, Dynamical Systems, and Linear Algebra, Volume 60, Academic press, 1974.

[67] P.I. Howell, B.G.J. Knols, Male mating biology, Malar. J. 8 (2) (2009) S8. http://dx.doi.org/10.1186/1475-2875-8-S2-S8.

[68] I. L. Freire, M. Torrisi, Symmetry methods in mathematical modeling of Aedes aegypti dispersal dynamics, Nonlinear Analysis: Real World Applications 14 (2013) 1300–1307.

[69] H. Inaba, Mathematical analysis of an age-structured SIR epidemic model with vertical transmission, Discrete Contin. Dyn. Sys. Ser. B 6 (2006) 69–96.

[70] W. Jiang, X. Lin, X. Zou, On a reaction-diffusion model for sterile insect release method on a bounded domain, International Journal of Biomathematics 7 (2014) 1450030.

[71] G.F. Killeen, B.G.J. Knols, W. Gu, Taking malaria transmission out of the bottle: implications of mosquito dispersal for vector control interventions, Lancet. Infect. Dis. 3 (2003) 297–302. [PubMed: 12726980]

[72] B.G.J. Knols, J. Meijerink, Odors influence mosquito behavior, Science and Medicine 4 (5) (1997) 56–63.

[73] Kweka, Eliningaya J. et al., Urbanization, Climate Change and Malaria Transmission in Sub-Saharan Africa, Climate Change Impacts on Urban Pests 10 (2016) 141.

[74] S. A. Levin, Dispersion and population interactions, American Naturalist 108 (960) (1974) 207–228.

[75] M. Y. Li, J. S. Muldowney, A geometric approach to global-stability problems, SIAM J. Appl. Math. 27 (1996) 155–164.

[76] L. Li, L. Bian and G. Yan, A study of the distribution and abundance of the adult malaria vector in western Kenya highlands, International Journal of Health Geographic, (2008) 7.

[77] S. Liu, E. Beretta, A stage-structured predator-prey model of Beddington-DeAngelis type, SIAM J. Appl. Math. 66 (2006) 1101–1129.

[78] A. Lloyd, R.M. May, Spatial heterogeneity in epidemic models, J. Theor. Biol. 179 (1996) 1–11.

[79] J.D. Logan (1994), Introduction to nonlinear partial differentiel equations, John Wiley & Sons.

[80] Y. Lou, J. Wu, Global dynamics of a tick ixodes scapularis model, Canad. Appl. Math. Quart. 19 (2011) 65–75.

[81] Y. Lou, X.-Q. Zhao, A climate-based malaria transmission model with structured vector population, SIAM J. Appl. Math. 70 (2010) 2023–2044.

[82] Y. Lou, X.-Q. Zhao, A reaction-diffusion malaria model with incubation period in the vector population, J. Math. Biol. 62 (2011) 543–568.

[83] A. Lutambi, M.A. Penny, T. Smith, N. Chitnis, Mathematical modelling of mosquito dispersal in a heterogeneous environment, Math. Biosci. 213 (2013) 198–216.

[84] P. Magal, X.-Q. Zhao, Global attractors and steady states for uniformly persistent dynamical systems, SIAM J. Math. Anal. 37 (2005) 251–275.

[85] K. Magori, M. Legros, M.E. Puente et al., Skeeter Buster: a stochastic, spatially-explicit modeling tool for studying Aedes aegypti population replacement and population suppression strategies, PLoS Negl. Trop. Dis. 3 (2009) e508.

[86] S. Manguin, Anopheles mosquitoes : new insights into malaria vectors, BoD-Books on Demand, 2013.

[87] M. L. Mann Manyombe, J. Mbang, J. Lubuma, B. Tsanou, Global dynamics of a vaccination model for infectious diseases with asymptomatic carriers, Math. Biosci. Eng, 13 (2016), 813–840.

[88] M.L. Mann Manyombe, B. Tsanou, J. Mbang, S. Bowong, A metapopulation model for the population dynamics of Anopheles mosquito, Appl. Math. Comp. 307 (2017) 71–91.

[89] M.L. Mann Manyombe, J. Mbang, B. Tsanou, S. Bowong, J. Lubuma, Mathematical analysis of a spatio-temporal model for the population ecology of anopheles mosquito, Math. Meth. Appl. Sci. (2020), 1–32. https://doi.org/10.1002/mma.6136

[90] S. Marino, I.B. Hogue, C.J. Ray and D.E. Kirschner, A methodology for performing global uncertainty and sensitivity analysis in systems biology, J. Theor. Biol. 254 (2008) 178–196.

[91] R. Martin and H. L. Smith, Abstract functional differential equations and reaction-diffusion systems, Trans. Amer. Math. Soc., 321 (1990), 1–44.

[92] M. A. McKibben, Discovering Evolution Equations with Applications: Volume 1-Deterministic Equations, Chapman & Hall/CRC Taylor & Francis Group, 2011.

[93] R.E. Mickens (2000), Applications of Nonstandard Finite Difference Schemes, Singapore, World Scientific.

[94] R.E. Mickens (2005), Advances In The Applications Of Nonstandard Finite Difference Schemes, Singapore, World Scientific.

[95] J. T. Midega et al, Estimating dispersal and survival of Anopheles gambia and Anopheles funestus along the Kenyan coast by using mark-release-recapture methods, J Med Entomol 6 (44) (2007), 923–929.

[96] R. E. Mickens, Nonstandard finite difference schemes for reaction-diffusion equations, Numer. Methods Partial Differ. Equ. 15 (2009) 201–214.

[97] N. Minakawa, P. Seda, G. Yan, Influence of host and larval habitat distribution on the abundance of African malaria vectors in western Kenya, Am. J. Trop. Med. Hyg. 67 (1) (2002) 32–38.

[98] S. J. Moore, S. T. Darling, M. Sihuincha, N. Padilla, G. J. Devine, A low-cost repellent for malaria vectors in the americas: results of two field trials in guatemala and peru, Malaria Journal, 6 (2007).

[99] E. A. Mordecai et al., Optimal temperature for malaria transmission is dramatically lower than previously predicted, Ecology Letters, 16 (2013) 22–30.

[100] C. Mwandawiro, M. Boots, N. Tuno, W. Suwonkerd, Y. Tsuda, M. Takagi, Heterogeneity in the host preference of japanese encephalitis vectors in chiang mai, northern thailand, Trans. R. Soc. Tro.p Med. Hyg. 94 (3) (2000) 238–242.

[101] Mosquito Life Cycle, American Mosquito Control Association, http://www.mosquito.org/life-cycle, accessed: May, 2016.

[102] J.D. Murray, Mathematical Biology II: Spatial Models and Biomedical Applications, Third Edition, Springer, 2003.

[103] M. E. J. Newman, S. H. Strogatz, D. J. Watt, Random graphs with arbitrary degree distributions and their applications, Phys. Rev. E 64 (2001) 026118.

[104] G. A. Ngwa, On the population dynamics of the malaria vector, Bull. Math. Biol. 68 (2006) 2161–2189.

[105] G. A. Ngwa, A. M Niger, A. B. Gumel, Mathematical assessment of the role of non-linear birth and maturation delay in the population dynamics of the malaria vector, Appl. Math. Comp. 217 (2010) 3286–3313.

[106] S. Nourridine, M. I. Teboh-Ewungkem, G.A. Ngwa, A mathematical model of the population dynamics of disease-transmitting vectors with spatial consideration, J. Biol. Dyn. 5 (2011) 335–365.

[107] A. Okubo, Diffusion and Ecological Problems: Mathematical Models, volume 10. Springer-Verlag Berlin, 1980.

[108] K. Okuneye, A. Abdelrazec, A.B. Gumel, Mathematical analysis of a weather-driven model for the population ecology of mosquitoes, Math. Biosci. Eng. 15 (2018) 57–93.

[109] T.P. Oléron Evans, S.R. Bishop, A spatial model with pulsed releases to compare strategies for the sterile insect technique applied to the mosquito Aedes aegypti, Math. Biosci. 254 (2014) 6–27.

[110] O.O. Oluwagbemi, C.M. Fornadel, E.F Adebiyi, D.E. Norris, J.L. Rasgon, ANOSPEX: a stochastic, spatially explicit model for studying Anopheles metapopulation dynamics, PLOS ONE 8 (7), e68040, http://dx.doi.org/10.1371/journal.pone.0068040.

[111] M. Otero, N. Schweigmann, H.G. Solari, A stochastic spatial dynamical model for Aedes aegypti, Bull. Math. Biol. 70 (2008) 1297–1325.

[112] H. G. Othmer, S. R. Dunbar, and W. Alt, Models of dispersal in biological systems, J. Math. Biol. 26 (1988) 263–298.

[113] P. C. Park, A new proof of Hermite's stability criterion and a generalization of Orlando's formula, Int. J. Control 26 (2012) 197–206.

[114] R. Pastor-Satorras, V. Vespignani, Epidemic spreading in scale-free networks, Phys. Rev. Lett. 86 (2001) 3200–3204.

[115] H. Pates, C. Curtis, Mosquito behaviour and vector control, Annual Review of Entomology 50 (2005) 53–70.

[116] A. M. Reynolds, M. A. Frye, Free-Flight Odor Tracking in Drosophila Is Consistent with an Optimal Intermittent Scale-Free Search, PLoS One 2 (4) (2007) e354. doi:10.1371/journal.pone.0000354.

[117] R. Ross, The relationship of malaria and the mosquito, Lancet 2 (1900) 48-50.

[118] M. Rowland et al., DEET mosquito repellent provides personal protection against malaria: a household randomized trial in an afghan refugee camp in pakistan, Tropical Medicine and International Health 9 (2004) 335–342.

[119] J. Saldana, Modelling the spread of infectious diseases in complex metapopulations, Math. Mod. Nat. Pheno. 5 (6) (2010) 22–37.

[120] M.W. Service, Mosquito (Diptera: Culicidae) dispersal: the long and short of it, J. Med. Entomol. 34 (1997) 579–588. [PubMed: 9439109]

[121] M. E. Sinka et al., A global map of dominant malaria vectors, Parasites and Vectors, 5 (2012) 69.

[122] D.L. Smith, J. Dushoff and F. E. McKenzie, The risk of a mosquito borne infection in a heterogeneous environment, PLoS Biology (2004) 2.

[123] H. L. Smith, X.-Q. Zhao, Robust persistence for semidynamical systems, Nonlinear Anal. 47 (2001) 6169–6179.

[124] H. L. Smith, Monotone Dynamical Systems : an Introduction to the Theory of Competitive and Cooperative Systems (mathematical surveys and monographs), Am. Math. Soc. 41 (1995) 1–174.

[125] J. Smoller, Shock waves and reaction-diffusion equations, A Series of Comprehensive Studies in Mathematics, Vol. 258, Springer-Verlag, New York, 581 pages, 1983.

[126] L. T. Takahashi, N. A. Maidana, W. C. Ferreira Jr., P. Pulino, H. M. Yang, Mathematical models for the Aedes aegypti dispersal dynamics: travelling waves by wing and wind, Bull. Math. Bull. 67 (2005) 509–528.

[127] W. Takken, B.G.J. Knols, Odor-mediated behavior of afrotropical malaria mosquitoes, Annual Review of Entomology 44 (1999) 131–157.

[128] H. R. Thieme, Convergence results and Poincare-Bendixon trichotomy for asymptotically autonomous differential equations, J. Math. Biol. 30 (1992) 755–763.

[129] H. R. Thieme, Spectral bound and reproduction number for infinite-dimensional population structure and time heterogeneity, SIAM J. Appl. Math. 70 (2009) 188–211.

[130] H. R. Thieme, X-Q. Zhao, A non-local delayed and diffusive predator-prey model, Nonlinear Analysis : Real World Applications 2 (2001) 145–160.

[131] R.C.A. Thomé, H.M. Yang, L. Esteva, Optimal control of Aedes aegypti mosquitoes by the sterile insect technique and insecticide, Math. Biosci. 223 (2010) 12–23.

[132] C. R. Tian, S. G. Ruan, A free boundary problem for Aedes aegypti mosquito invasion, Appl. Math. Model., 46 (2017) 203–217.

[133] Y.T. Toure et al., Mark release recapture experiments with Anopheles gambiae s.l. in Binambani village, Mali to determine population size and structure, Medical and Veterinary Entomology 12 (1997) 74–83.

[134] A. Pazy, Semigroups of Linear Operators and Applications to Partial Differential Equations, Springer-Verlag, Berlin, 1983.

[135] M. Vidyasagar, Decomposition techniques for large-scale systems with nonadditive interactions: Stability and stabilization, IEEE Trans. Autom. Control. 25 (1980) 773-779.

[136] W. Walter, Differential and Integral Inequalities, Springer-Verlag, Berlin-Heidelberg-New York, 1970.

[137] Y. Wang, J. Cao, Global dynamics of a networks epidemic model for waterborne diseases spread, Appl. Math. Comp. 237 (2014) 474–488.

[138] Y. Wang, J. Cao, A. Alofi, A. AL-Mazrooei, A. Elaiw, Revisiting node-based SIR models in complex networks with degree correlations, Physica A 437 (2015) 75–88.

[139] Y. Wang, J. Cao, G. Sun, J. Li, Effect of time delay on pattern dynamics in a spatial epidemic model, Physica A 412 (2014) 137–148.

[140] J. Cao, Y. Wang, A. Alofi, A. AL-Mazrooei, A. Elaiw, Global stability of an epidemic model with carrier state in heterogeneous networks, IMA Journal of Applied Mathematics 80 (2015) 1025–1048.

[141] X. Wang, D. Posny, J. Wang, A reaction-convection-diffusion model for cholera spatial dynamics, Discrete Contin. Dyn. Syst. Ser. B 21 (2016) 2785–2809.

[142] X. Wang, J. Wang, Analysis of cholera epidemics with bacterial growth and spatial movement, J. Biol. Dyn. 9 (2015) 233–261.

[143] W. Wang, X.-Q. Zhao, A nonlocal and time-delayed reaction-diffusion model of dengue transmission, SIAM J. Appl. Math. 71 (2011) 147–168.

[144] W. Wang, X.-Q. Zhao, Basic reproduction numbers for reaction-diffusion epidemic models, SIAM J. Appl. Dyn. Syst. 11 (2012) 1652–1673.

[145] X. Wang, Y. Chen,S. Liu, Dynamics of an age-structured host-vector model for malaria transmission, Math. Meth. Appl. Sci. 41 (2018) 1966–1987.https://doi.org/10.1002/mma.4723

[146] S. Wanji, F.F. Mafo, N. Tendongfor, M.C. Tanga, F. Tchuente, C.F. Bilong Bilong, T. Njine, Spatial distribution, environmental and physicochemical characterization of anopheles breeding sites in the mount cameroon region, J. Vector Borne Dis. 46 (2009) 75–80.

[147] G.B. White, Malaria vector ecology and genetics, British Medical Bulletin 38 (1982) 207–212.

[148] The World Health Report, Online: http://www.who.int/whr/2012/en/, 2002.

[149] WHO, A global brief on vector-borne diseases, http://apps.who.int/iris/bitstream/10665/111008/1/WHO_DCO_WHD_2014.1_eng.pdf, accessed: June 2017.

[150] World Health Organization, WHO global health days, http://www.who.int/campaigns/world-health-day/2014/vector-borne-diseases/en/, accessed: June, 2016.

[151] WHO, World Malaria Report, Technical report, World Health Organization, Geneva (2011).

[152] Z. Wang, X.-Q. Zhao, Global dynamics of a time-delayed dengue transmission model, Canad. Appl. Math. Quart. 20 (2012) 89–113.

[153] W. Wang, X. Zhao, Threshold dynamics for compartmental epidemic models in periodic environments, J. Dyn. Differ. Equ. 20 (2008) 699–717.

[154] L. Yakob, G. Yan, A network population model of the dynamics and control of African malaria vectors, Trans. R. Soc. Med. Hyg. 104 (10) (2010), 669–675.

[155] W.M.S. Yamashita, L.T. Takahashi, G. Chapiro, Traveling wave solutions for the dispersive models describing population dynamics of Aedes aegypti, Math. Comput. Simulation (2017).

[156] K. Yamazaki, X. Wang, Global stability and uniform persistence of the reaction-convection-diffusion cholera epidemic model, Math. Biosci. Eng. 14 (2017) 559–579.

[157] K. Yamazaki, X. Wang, Global well-posedness and asymptotic behavior of solutions to a reaction-convection-diffusion cholera epidemic model, Discrete Contin. Dyn. Syst. Ser. B 21 (2016) 1297–1316.

[158] W. M. S. Yamashita, L. T. Takahashi, G. Chapiro, Travelling wave solutions for the dispersive models describing population dynamics of Aedes Aegypti, Math. Comput. Simulation 146 (2018) 90–99.

[159] X.-Q. Zhao, Z. Jing, Global asymptotic behavior in some cooperative systems of functional-differential equations, Canad. Appl. Math. Quart. 4 (1996) 421–444.

[160] X.-Q. Zhao, Dynamical Systems in Population Biology, Springer International Publishing AG, Second edition, 2017.

[161] M. Zhang, J. Ge, Z. Lin, The invasive dynamics of Aedes aegypti mosquito in a heterogenous environment, arXiv preprint arxiv:1706.08652 (2017).

[162] D. Zhu, J. Ren, H. Zhu, Spatial-temporal basic reproduction number and dynamics for a dengue disease diffusion model, Math. Meth. Appl. Sci. 41 (14) (2018) 5388–5403.https://doi.org/10.1002/mma.5085

[163] Z. Zhen, J. Wei, L. Tian, J. Zhou, W. Chen, Wave propagation in a diffusive SIR epidemic model with spatiotemporal delay, Math. Meth. Appl. Sci. 41 (16) (2018) 7074–7098.

Applied Mathematics and Computation 307 (2017) 71–91

Contents lists available at ScienceDirect

Applied Mathematics and Computation

journal homepage: www.elsevier.com/locate/amc

A metapopulation model for the population dynamics of anopheles mosquito

M.L. Mann Manyombe [a,d,e], B. Tsanou [b,d,e,*], J. Mbang [a,d,e], S. Bowong [c,d,e]

[a] Department of Mathematics, Faculty of Science, University of Yaounde I, P.O. Box 812, Yaounde, Cameroon
[b] Department of Mathematics and Computer Science, University of Dschang, P.O. Box 67, Dschang, Cameroon
[c] Department of Mathematics and Computer Science, University of Douala, P.O. Box 24157, Douala, Cameroon
[d] IRD UMI 209 UMMISCO, University of Yaounde I, P.O. Box 337, Yaounde, Cameroon
[e] LIRIMA-GRIMCAPE Team Project, University of Yaounde I, P.O. Box 812, Yaounde, Cameroon

ARTICLE INFO

Keywords:
Anopheles mosquito
Dispersal
Monotone system
Stability analysis
Metapopulation
Simulation

ABSTRACT

A more robust assessment of malaria control will come from a better understanding of the distribution and connectivity of breeding and blood feeding sites. Spatial heterogeneity of mosquito resources, such as hosts and breeding sites, affects mosquito dispersal behavior. This paper analyzes and simulates the spreading of anopheles mosquito on a complex metapopulation, that is, networks of populations connected by migratory flows whose configurations are described in terms of connectivity distribution of nodes (patches) and the conditional probabilities of connections between nodes. We examine the impacts of vector dispersal on the persistence and extinction of a mosquito population in both homogeneous and heterogeneous landscapes. For uncorrelated networks in a homogeneous landscape, we derive an explicit formula of the basic offspring number $\mathcal{R}_0^{(m)}$. Using the theory of monotone operators, we obtain sufficient conditions for the global asymptotic stability of equilibria. Precisely, the value 1 of the basic offspring number is a forward bifurcation for the dynamics of anopheles mosquito, with the trivial (mosquito-free) equilibrium point being globally asymptotically stable (GAS) when $\mathcal{R}_0^{(m)} \leq 1$, and one stable nontrivial (mosquito-persistent) equilibrium point being born with well determined basins of attraction when $\mathcal{R}_0^{(m)} > 1$. Theoretical results are numerically supported and the impact of the migration of mosquitoes are discussed through global sensitivity analysis and numerical simulations.

1. Introduction

For many centuries, vector-borne diseases among all infectious diseases of human beings, have constituted a major cause of human mortality and morbidity. Even with the recent advances in the biomedical sciences, vector-borne diseases still seriously threaten world health. For example, according to the latest WHO estimates, released in December 2015, there were 214 million cases of malaria in 2015 and 438,000 deaths [1]. It is well known that the malaria parasite is transmitted from human-to-human through the anopheles mosquito bites, and that the transmission cycle is essentially driven by the human biting habit of the mosquito [2]. Now, the female anopheles mosquito bites a human being for the sole purpose of harvesting blood that she needs for the development of her eggs. The malaria parasite has exploited the mosquito's life

* Corresponding author at: Department of Mathematics and Computer Science, University of Dschang, P.O. Box 67, Dschang, Cameroon.
E-mail addresses: bergetsanou@yahoo.fr, berge.tsanou@univ-dschang.org (B. Tsanou).

http://dx.doi.org/10.1016/j.amc.2017.02.039
0096-3003/

style by adapting its life cycle so that part of it is in the human being and the other part in the mosquito. By so doing, the mosquito can then propagate the parasite from human to human. Transmission of most indirectly transmitted diseases of human being follows the same pattern. The vector (in most cases an insect) interacts with a human being, and depending on the disease status of both organisms, will either infect or be infected. Thus, understanding the population dynamics of mosquitoes, and relationship between mosquitoes and the environment is fundamental to the study of the epidemiology of mosquito-borne diseases. Mosquito abundance is a key determining factor that affects the persistence or resurgence of mosquito-borne diseases in a given region [3]. Hence, it is crucial to study the dynamics of mosquitoes, and devise effective and realistic methods for controlling mosquito population in communities.

The spatial distribution of anopheles vectors has shown great potential to affect malaria transmission intensity [3]. Therefore, a better understanding of the distribution, productivity and connectivity of anopheles breeding sites in order to determine their influence on anopheles distribution could be very useful in malaria control. Several theoretical studies of malaria vector dynamics have emphasized the importance of considering individual larval habitats, but few have addressed the effects of interactions between larval habitat connectivity [3,4].

Mathematical models play an important role in understanding and providing solutions to natural phenomena which are difficult to measure in the field, and some models have incorporated dispersal or heterogeneity when modeling mosquito population [5–7]. Spatial models usually used the diffusion approach, which considers space as a continuous variable. Although partial differential equations (PDEs) are a good and classical way of modeling such dispersal [6,8], their analysis is usually limited and do not incorporate the various factors that affect migrations. However, discrete approaches offer a better and simpler way of modeling heterogeneity [5,9]. Thus, in areas where resources can be located in patches, mosquito dispersal is more suitably modeled by using a metapopulation approach, in which the population is subdivided into discrete patches. Then, in each patch, the population is subdivided into compartments corresponding to different status. This leads to a multi-patch, multi-compartment system.

Talking about the metapopulation setting, a recent approach based on the formalism used in statistical mechanics of complex networks is presented in [10–13]. Under this approach, the structure of the spatial network of patches is encapsulated by means of the connectivity (degree) distribution $p(k)$ defined as the probability that a randomly chosen patch has connectivity k. Note that the degree or connectivity of a patch (node) is the number of links connected to that node (i.e., the number its neighbors). Recent works have shown that it is possible to investigate the dynamics of epidemic spread using statistical mechanics on configuration model networks [14–18]. Most of above-mentioned investigations [13,15,16,18] mainly considered epidemic models on networks with no degree correlation (i.e., uncorrelated networks). In such networks, a patch which is only constrained by degree distribution (and hence by the number of neighbors it has), can point to any patch from a pool of the network. However, few recent works [14,17] have taken into account the degree correlation in complex networks and have conducted comparison studies on the prediction of disease evolution on correlated networks.

Many other works have focused on a metapopulation approach to model the mosquito population [4,5]. In their work in [4], the authors presented a stochastic network model not governed by a dynamical system and did not consider all main stages of the mosquito life cycle to analyze the significance of the productivity of breeding sites. The work in [5] considered a set of discrete hexagonal patches to investigated the effects of mosquito dispersal on its dynamics.

In this work, we intend to fill some of the gaps mentioned above in order to better take into account the heterogeneity in the connectivity of the nodes of network. To fulfill our goal, we make use of an approach based on statistical mechanics which could allow us identifying other breeding site characteristics which could best explain the distribution and abundance of mosquitoes. The methodology and objectives of this paper are to design a complex network extension of the seminal model in [19], analyze and simulate a mathematical model for the spatio-temporal dynamics of anopheles mosquito using the alternative approach based on a statistical mechanics. This extension is inspired by the works [4,5,11–13] and some references therein. We consider the spread of anopheles mosquitoes on complex metapopulations, i.e., networks of populations connected by migratory flows whose configurations are described in terms of the conditional probabilities of connections between nodes. Note that nodes of the network represent potential breeding and feeding sites of mosquitoes, around which are human hosts habitations.

From the modeling perspective, the model proposed in this manuscript is a substantial extension of the basic model in [19] by incorporating the dispersal of mosquitoes. It also extends and enriches the work in [4,5] by considering: (i) all the stages of the mosquito life cycle and (ii) heterogeneity in the connectivity of patches. From the theoretical and numerical perspectives, we examine the significance of larval habitat connectivity and mosquito dispersal in a homogeneous and a heterogeneous landscapes on the persistence of mosquitoes populations. More precisely, we construct corresponding metapopulation models and perform their qualitative and quantitative analyzes. Specifically, for the mathematical tractability, uncorrelated networks in a homogeneous landscape are considered and the following investigations are highlighted:

- The bifurcation/threshold parameter (basic offspring number) is explicitly computed.
- The sensitivity analysis of the threshold parameter, the model variables with respect to model parameters is given.
- A simple and digestive proof based on the Hethcote–Thieme fixed point theorem [20], of a unique nontrivial equilibrium point is provided.
- Contrary to the few existing works where, Lyapunov–LaSalle techniques are usually used, the monotone operator theory [21] is the main ingredient here for the establishment of global asymptotic stability of both trivial and nontrivial equilibrium points.

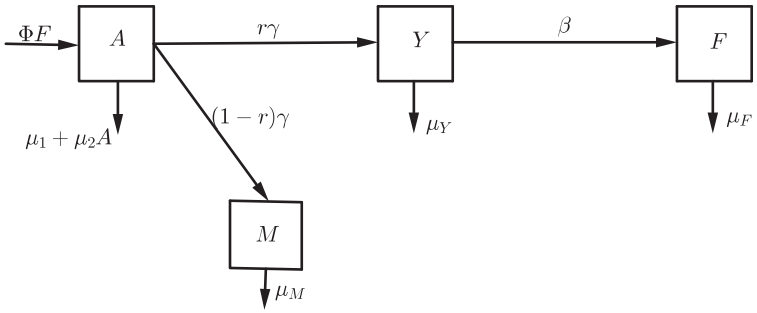

Fig. 1. Wild mosquito flow chart.

Moreover for both homogeneous and heterogeneous landscapes, the effects of dispersal/migration and patch heterogeneity on the mosquito population are numerically investigated. Finally, the comparison of metapopulation models in homogeneous and heterogeneous landscapes are presented through numerical simulations. The rest of the paper is organized as follows. After the presentation of the basic model without mosquito dispersal in Section 2, we formulate metapopulation models for both homogeneous and heterogeneous landscapes in Section 3. Their qualitative and quantitative analyses are further presented. Theoretical results and the role of dispersal, patch connectivities and migration are investigated through numerical simulations in Section 4. The summary of the main results of our work and its possible extensions conclude the paper in Section 5.

2. The basic model in a single patch: mosquito dynamics without dispersal

We consider the classical Anguelov–Dumont–Lubuma model [19]:

$$\begin{cases} \dot{A} = \Phi F - (\gamma + \mu_1 + \mu_2 A)A, \\ \dot{Y} = r\gamma A - (\beta + \mu_Y)Y, \\ \dot{M} = (1-r)\gamma A - \mu_M M, \\ \dot{F} = \beta Y - \mu_F F. \end{cases} \tag{2.1}$$

This model was developed according to the following biological and entomological facts recalled hereafter. The life cycle of mosquitos consists of two main stages: aquatic (egg, larva, pupa) and adult. After emergence from pupa, a female mosquito needs to mate and get a blood meal before it starts laying eggs. Depending on the condition, this takes about a week. Then, every 4–5 days she will take a blood meal and lay 100–150 eggs at different places (10–15 per place). Mathematically, the population of mosquitoes is then divided into the following compartments: population in aquatic stage A; young female not yet laying eggs Y; fertilized and eggs laying females F and males M. This description was depicted in [19] by the flowchart in Fig. 1.

Note that the first equation of system (2.1) can be combined as logistic population with harvesting. A female needs to mate successfully only once. The eggs are laid in the so-called gonotrophic cycle, which consists of taking blood meal, maturation of the eggs and oviposition. Before a female begins to lay eggs, two essential events need to take place, mating and taking a blood meal, occurring in varying order.

A female mosquito is considered to be in the Y-compartment since its emergence from pupa until her gonotrophic cycle has began, that is the time needed to mate and take the first blood meal, which takes typically 3–4 days. The death rate during that period reflects essentially only death from predators and adverse climatic conditions. Therefore, it is generally lower than the death rate for the F-compartment. Typically, the male mosquitoes are (depending on the temperature) about half or 40% of the total population.

In the model, the fraction of the emerging female mosquitoes is denoted by r, with $(1-r)$ being the fraction of emerging male mosquitoes. A male mosquito can mate practically through all its life. Since a female needs one successful mating, there is an overabundance of males. Therefore, in general, it is reasonable to assume that the waiting time for mating does not depend on the number of males (M) in the sense that, if M is increased further this rate remains the same. For the model, this means that the transfer rate β from compartment Y to compartment F is independent of M. Mathematically, this means that the third equation of system (2.1) can be decoupled from the system. Sometimes β is referred to as "mating rate", which, as explained above, can be abetted misleading and does not defined well the boundary between compartments Y and F. The model under derivation clearly fixed boundary at the beginning of the first gonotrophic cycle of female, which is immediately after the mating and first blood meal. Then, the rate (per day) of laying eggs in the breeding sites is ϕF, where ϕ is the average amount of eggs laid per fertilized female per day. In the model, the size of the population is restricted by a density dependent death rate similar to [22,23]. However, the density dependent death rate is used only for the aquatic stage. The reason is that in a typical environment the size of the mosquito population is also restricted mainly by the available breeding sites. In [24], the size of the population is also restricted only in the aquatic stages but in a different way

Table 1
Numerical values for the parameters of system (2.1) [19].

Parameter	Description	Value
r	Fraction of the emerging female mosquitoes (per day)	0.5
γnontrivial	Maturation rate from larvae to adult (per day)	0.1
β	Transfer rate from the compartment Y to F (per day)	0.25
$1/\mu_M$	Average lifespan of male mosquitoes (in days)	7
$1/\mu_F$	Average lifespan of female mosquitoes (in days)	10
$1/\mu_Y$	Average lifespan of adult female mosquitoes (in days)	20
Φ	Number of eggs at each deposit per capita (per day)	Variable
μ_1	Mortality rate of the aquatic stage (per day)	0.25
μ_2	Density mortality rate of the aquatic stage (per day)	10^{-5}

by an explicit carrying capacity beyond which no egg is laid. In equation (2.1), the parameters μ_1 and μ_2 denote the density independent and the density dependent death rates of the aquatic stage, respectively. In all equations of model (2.1), μ with respective index refers to the death rate for the specific compartment (which is density independent).

The parameter values of model (2.1) used for simulations are given in Table 1 and the analytical results for this model can be found in [19]. However, for the easier readability of our work, we recall without proof the main results.

System (2.1) has two equilibria: the trivial equilibrium $Q_0 = (0, 0, 0, 0)$ and the nontrivial equilibrium $Q^* = (A^*, Y^*, F^*, M^*)^T$ where A^*, Y^*, F^* and M^* are defined as follows:

$$A^* = \frac{(\gamma+\mu_1)(\mathcal{R}_0-1)}{\mu_2}, \qquad Y^* = \frac{r\gamma(\gamma+\mu_1)(\mathcal{R}_0-1)}{\mu_2(\beta+\mu_Y)},$$
$$F^* = \frac{\beta r\gamma(\gamma+\mu_1)(\mathcal{R}_0-1)}{\mu_F\mu_2(\beta+\mu_Y)} \quad \text{and} \quad M^* = \frac{(1-r)\gamma(\gamma+\mu_1)(\mathcal{R}_0-1)}{\mu_2\mu_M}, \tag{2.2}$$

where $\mathcal{R}_0$ is given by

$$\mathcal{R}_0 = \frac{r\gamma\beta\Phi}{(\gamma+\mu_1)(\beta+\mu_Y)\mu_F}. \tag{2.3}$$

The nontrivial equilibrium Q^* has a biological meaning if and only if $\mathcal{R}_0 \geq 1$. The threshold quantity $\mathcal{R}_0$ is the basic offspring number for the population of anopheles mosquitoes in a single patch model [19]. It is the average number of the newly anopheles mosquitoes generated by a single fertilized and eggs laying female anopheles mosquito during her life when she is introduced into a population of male anopheles mosquitoes in the absence of any given intervention strategies.

The following result summarizes the asymptotic behavior of model (2.1) as shown in [19].

Theorem 2.1. *System (2.1) is a dissipative dynamical system in* $\Omega = \mathbb{R}^4_+ = \{(S, Y, F, M) \in \mathbb{R}^4 \ / \ S, Y, F, M \geq 0\}$. *Moreover,*

(i) *If* $\mathcal{R}_0 \leq 1$, *then the trivial (mosquito-free) equilibrium* Q_0 *is globally asymptotically stable on* Ω.
(ii) *If* $\mathcal{R}_0 > 1$, *then the system has two equilibria* Q_0 *and* Q^* *on* Ω *where* Q^**(the mosquito-persistent equilibrium) is stable with basin of attraction* $\Omega \setminus \{(A, Y, M, F) \in \mathbb{R}^4_+, \ A = Y = F = 0\}$ *and* Q_0 *is unstable with the nonnegative M-axis being a stable manifold.*

3. Metapopulation models in complex networks

3.1. A generic reaction–diffusion model in a complex network

Herein, we extend model (2.1) to incorporate the diffusion/migration process. Mosquitoes disperse while searching for hosts or breeding sites [4]. We consider the dynamical evolution of the population of anopheles mosquitoes in heterogeneous metapopulation. The model consists of n patches. We recall that these patches represent breeding–feeding sites around which are potential human habitats and between which mosquitoes move creating links between these nodes. A given fraction of adult mosquitoes searching for hosts and a fraction of adult mosquitoes searching for breeding sites leave their current patches of residence, while the remaining fraction is motionless. We assume that the architecture of the network of patches (nodes) where local populations live is mathematically encoded by means of the connectivity (degree) distribution $p(k)$. Typically, $p(k)$ is defined as the probability that a randomly chosen path has degree k. We recall that the degree or connectivity of a patch is the number of links connected to that patch. At any given time, in each patch, an individual mosquito is in one of the following states: population in aquatic stage ($\rho_{A,k}$), young female not yet laying eggs ($\rho_{Y,k}$), fertilized and eggs laying females ($\rho_{F,k}$), male mosquitoes ($\rho_{M,k}$). The total variable population size in patches of degree k at time t is given by $\rho_k(t) = \rho_{A,k}(t) + \rho_{Y,k}(t) + \rho_{F,k}(t) + \rho_{M,k}(t)$. Note again that, we focus in this part on the migration of mosquitoes from patch to patch (that is the case of connected patches). A reasonable assumption is that, mosquitoes in aquatic phase cannot move out of their residence patch, while those in adult phase can migrate.

In Fig. 2, we give an example of a n-patches network: each patch here is breeding–feeding site. Without loss of generality, we suppose that in each patch, the population dynamics of anopheles mosquitoes is governed by the basic system (2.1).

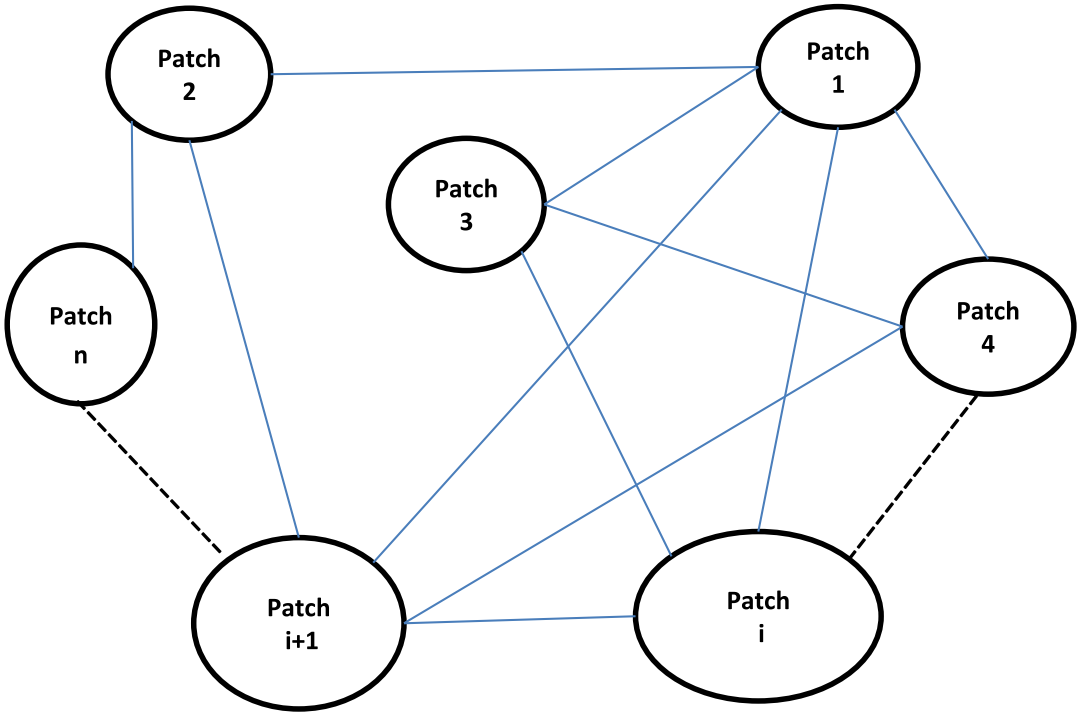

Fig. 2. A general n-patches network for the population dynamics of anopheles mosquito between n feeding-breeding sites.

Mosquitoes move from a patch with degree k to another with degree k' with a diffusion rate $D_{kk'}$ that depends on the degrees of the origin and destination patches. The probability P_k of leaving a patch with degree k is then given by

$$P_k = k\sum_{k'} P(k'|k)D_{kk'}, \tag{3.1}$$

where $P(k'|k)$ is the conditional probability that any given edge departing from a node of degree k is pointing to a node of degree k' [12].

Under this generic type of diffusion, the equations governing the spatio-temporal evolution of anopheles mosquitoes are giving by the system below:

$$\begin{cases} \dot{\rho}_{A,k} = \Phi\rho_{F,k} - (\gamma + \mu_1 + \mu_2\rho_{A,k})\rho_{A,k}, \\ \dot{\rho}_{Y,k} = r\gamma\rho_{A,k} - (\beta + \mu_Y)\rho_{Y,k} - P_k\rho_{Y,k} + k\sum_{k'} P(k'|k)D_{k'k}\rho_{Y,k'}, \\ \dot{\rho}_{M,k} = (1-r)\gamma\rho_{A,k} - \mu_M\rho_{M,k} - P_k\rho_{M,k} + k\sum_{k'} P(k'|k)D_{k'k}\rho_{M,k'}, \\ \dot{\rho}_{F,k} = \beta\rho_{Y,k} - \mu_F\rho_{F,k} - P_k\rho_{F,k} + k\sum_{k'} P(k'|k)D_{k'k}\rho_{F,k'}. \end{cases} \tag{3.2}$$

As in classical reaction–diffusion processes, system (3.2) expresses the time variation of the subpopulations of mosquitoes in aquatic phase, young female not yet laying eggs, fertilized and eggs laying females and males mosquitoes as the sum of two independent contributions: reaction and diffusion. In particular, the diffusion term includes the outflow of mosquitoes (diffusing particles) from patches of degree k and the inflow of migratory mosquitoes from the nearest patches of degree k'. In general, with n different patches of corresponding degrees $k_1, k_2, \ldots, k_n$ in the network, Eq. (3.2) is a $4 \times n$ system of differential equations. The solutions of system (3.2) remain nonnegative in $\mathbb{R}^{4n}_+$ because the out movement always stops when the corresponding patch is emptied. This latter assertion is mathematically established in the following result.

Theorem 3.1. *If system (3.2) with initial condition in $\mathbb{R}^{4n}_+$ has a solution, then the latter solution remains in $\mathbb{R}^{4n}_+$ (i.e. nonnegative) for all times.*

Proof. It suffices to show that system (3.2) can written in the following form:

$$\dot{X} = \mathcal{M}(X)X, \tag{3.3}$$

where $\mathcal{M}(X)$ is a $4n \times 4n$ cooperative (Metzler) matrix, and X a $4n$ column matrix to be determined below. To this end, system (3.2) rewrites:

$$\begin{cases} \dot{\rho}_{A,k_i} = \Phi\rho_{F,k_i} - (\gamma + \mu_1 + \mu_2\rho_{A,k_i})\rho_{A,k_i}, \\ \dot{\rho}_{Y,k_i} = r\gamma\rho_{A,k_i} - (\beta + \mu_Y)\rho_{Y,k_i} - P_{k_i}\rho_{Y,k_i} + k_i\sum_{j=1}^{n} P(k_j|k_i)D_{k_jk_i}\rho_{Y,k_j}, \\ \dot{\rho}_{M,k_i} = (1-r)\gamma\rho_{A,k_i} - \mu_M\rho_{M,k_i} - P_{k_i}\rho_{M,k_i} + k_i\sum_{j=1}^{n} P(k_j|k_i)D_{k_jk_i}\rho_{M,k_j} \qquad i = \{1,2,\ldots,n\}, \\ \dot{\rho}_{F,k_i} = \beta\rho_{Y,k_i} - \mu_F\rho_{F,k_i} - P_{k_i}\rho_{F,k_i} + k_i\sum_{j=1}^{n} P(k_j|k_i)D_{k_jk_i}\rho_{F,k_j}. \end{cases} \tag{3.4}$$

Now, let

$$X_A = (\rho_{A,k_1}, \rho_{A,k_2}, \ldots, \rho_{A,k_n})^T, \quad X_Y = (\rho_{Y,k_1}, \rho_{Y,k_2}, \ldots, \rho_{Y,k_n})^T,$$
$$X_M = (\rho_{M,k_1}, \rho_{M,k_2}, \ldots, \rho_{M,k_n})^T, \quad X_F = (\rho_{F,k_1}, \rho_{F,k_2}, \ldots, \rho_{F,k_n})^T,$$

$$\mathcal{Q}_1 = \mathrm{diag}(P_{k_1}, \cdots, P_{k_n}), \quad \mathcal{Q}_2 = \left(k_i P\left(k_j|k_i\right) D_{k_j k_i}\right)_{(i,j)}, \quad M_A = -(\gamma + \mu_1) I_n - \mu_2 \mathrm{diag}(X_A),$$
$$M_Y = -(\beta + \mu_Y + \mathcal{Q}_1) I_n + \mathcal{Q}_2, \quad M_M = -(\mu_M + \mathcal{Q}_1) I_n + \mathcal{Q}_2 \quad M_F = -(\mu_F + \mathcal{Q}_1) I_n + \mathcal{Q}_2,$$

and

$$\mathcal{M}(X) = \begin{pmatrix} M_A & O_n & O_n & \Phi I_n \\ r\gamma I_n & M_Y & O_n & O_n \\ (1-r)\gamma I_n & O_n & M_M & O_n \\ O_n & \beta I_n & O_n & M_F \end{pmatrix},$$

where I_n and O_n denote the $n \times n$ identity and null matrices, respectively. Since the entries of $\mathcal{Q}_1$ and $\mathcal{Q}_2$ are nonnegative, it is straightforward that M_A, M_Y, M_M, M_F are Metzler matrices, so is $\mathcal{M}(X)$. Finally, let

$$X = (X_A,\ X_Y,\ X_M,\ X_F)^T,$$

then model (3.4) becomes

$$\dot{X} = \mathcal{M}(X)X.$$

This achieves the proof. □

In the following subsections we study special cases of system (3.2) depending on the type of diffusion processes by considering diffusion rates that are inherent to the traffic characteristics of each node. Typically there are two distinguishable landscapes with different features which must retain our attention.

3.2. The metapopulation model in a homogeneous landscape

A landscape is homogeneous when all its patches have similar characteristics. Thus, in such landscapes, it is reasonable to assume that the mosquitoes have the same dispersal/diffusion rate between patches. The mosquitoes searching for breeding sites to lay their eggs are attracted by the availability of breeding sites [25]. Therefore they move randomly in any breeding sites to lay their eggs. Mosquitoes can detect host odor, but it is unclear whether they have the learning capacity they would need to enable them to return to particular hosts or breeding sites [5,26]. In the case where all patches have similar characteristics (i.e. homogeneous landscape), the mosquitoes disperse equally between the patches and the dispersal parameter is the same for all patches. In this case, the diffusion rate along any given link of a node with degree k is simply equal to

$$D_{kk'} = \frac{D_i}{k}, \quad i = Y, M, F. \tag{3.5}$$

For the sake of brevity, we consider strictly positive diffusion rates D_Y, D_F, $D_M > 0$. Thus, assuming that distance has no bearing on the probability of mosquito flying between breeding sites and, using the fact that $\sum_k P(k|k') = 1$, the dynamics of free-flying mosquitoes in a patch of degree k is

$$\begin{cases} \dot{\rho}_{A,k} = \Phi\rho_{F,k} - (\gamma + \mu_1 + \mu_2\rho_{A,k})\rho_{A,k}, \\ \dot{\rho}_{Y,k} = r\gamma\rho_{A,k} - (\beta + \mu_Y)\rho_{Y,k} - D_Y\rho_{Y,k} + kD_Y\sum_{k'} P(k'|k)\frac{\rho_{Y,k'}}{k'}, \\ \dot{\rho}_{M,k} = (1-r)\gamma\rho_{A,k} - \mu_M\rho_{M,k} - D_M\rho_{M,k} + kD_M\sum_{k'} P(k'|k)\frac{\rho_{M,k'}}{k'}, \\ \dot{\rho}_{F,k} = \beta\rho_{Y,k} - \mu_F\rho_{F,k} - D_F\rho_{F,k} + kD_F\sum_{k'} P(k'|k)\frac{\rho_{F,k'}}{k'}, \end{cases} \tag{3.6}$$

Note that, since the number of links emanating from nodes of degree k to nodes of degree k' must be equal to the number of links emanating from nodes of degree k' to nodes of degree k in non-directed graphs, we have the following relationship between $p(k)$ and $P(k'|k)$ [14]:

$$kP(k'|k)p(k) = k'P(k|k')p(k'). \tag{3.7}$$

For networks with a connectivity pattern defined by a set of conditional probabilities $P(k'|k)$, we define the elements of the connectivity matrix C as

$$C_{kk'} = \frac{k}{k'}P(k'|k). \tag{3.8}$$

Note that these elements are the average number of mosquitoes that patches of degree k receive from neighboring patches of degree k' assuming that one mosquito leaves each of these patches by choosing at random one of the k' connections [13]. On the other hand, for those degrees k that are not present in the network, one must have $P(k'|k) = 0$, $\forall k'$. Hereafter in

this paper, when talking about degrees, we implicitly mean those degrees that are present in the network. Furthermore, the case where all patches have the same connectivity is excluded from our consideration because, under the present approach, the model equations reduce to those of a single patch model.

In order to obtain further analytical results about the metapopulation dynamics of anopheles mosquitoes, we need to be precise about the form of $P(k'|k)$. As in most network models, the easiest and usual assumption is to restrict ourselves to uncorrelated networks.

3.2.1. Uncorrelated networks

In these networks, the degrees of the nodes at the end of any given link are independent. In other words, there is no degree-degree correlation between the connected nodes. Therefore, we have

$$P(k'|k) = k'p(k')/\langle k\rangle, \tag{3.9}$$

which corresponds to the degree distribution of nodes (patches) that arrive at by following a randomly chosen link [10]. Using Eqs. (3.7)–(3.9), $\sum_k P(k|k') = 1$ and change the order of summations in system (3.4), one obtains the following equations for the time evolution of anopheles mosquitoes in metapopulations described by uncorrelated networks:

$$\begin{cases} \dot{\rho}_{A,k} = \Phi\rho_{F,k} - (\gamma + \mu_1 + \mu_2\rho_{A,k})\rho_{A,k}, \\ \dot{\rho}_{Y,k} = r\gamma\rho_{A,k} - (\beta + \mu_Y)\rho_{Y,k} - D_Y\left(\rho_{Y,k} - \frac{k}{\langle k\rangle}\rho_Y\right), \\ \dot{\rho}_{M,k} = (1-r)\gamma\rho_{A,k} - \mu_M\rho_{M,k} - D_M\left(\rho_{M,k} - \frac{k}{\langle k\rangle}\rho_M\right), \\ \dot{\rho}_{F,k} = \beta\rho_{Y,k} - \mu_F\rho_{F,k} - D_F\left(\rho_{F,k} - \frac{k}{\langle k\rangle}\rho_F\right), \end{cases} \tag{3.10}$$

where

$$\langle k\rangle = \sum_k kp(k) \quad \text{and} \quad \rho_j(t) = \sum_k p(k)\rho_{j,k}, \quad j = A, Y, M, F.$$

$\langle k\rangle$ is defined as the average network degree. ρ_A, ρ_Y, ρ_F and ρ_M, represent the average number of population in aquatic stage, young females and eggs laying females, and population of males mosquitoes in each patch at time t, respectively. In this case, the diffusion term is simply given by the difference between the outflow of young females not yet laying eggs ($D_Y\rho_{Y,k}$), fertilized and eggs laying females ($D_F\rho_{F,k}$) and male mosquitoes ($D_M\rho_{M,k}$) in patches of connectivity k and the total inflow of young females not yet laying eggs ($D_Y\rho_Y/\langle k\rangle$), fertilized and eggs laying females ($D_F\rho_F/\langle k\rangle$) and male mosquitoes ($D_M\rho_M/\langle k\rangle$) in patches of connectivity k, respectively; across all their k connections, which is k times the average flow of mosquitoes across a connection in the network. Note that this average flow across a connection does not depend on the degree k of the considered patch because we have assumed that the architecture of the metapopulation is described by an uncorrelated network. In these network configurations, the elements of the connectivity matrix C are simply

$$C_{kk'} = \frac{kp(k')}{\langle k\rangle}. \tag{3.11}$$

Clearly, C is a rank-one matrix and the vector v, whose components $v_k = k$, is its eigenvector corresponding to its unique non-zero eigenvalue 1. Thus, if there are (as assumed above) n different patches in the network, then the eigenvalues of the said connectivity matrix are $\lambda = 0$ (with algebraic multiplicity $n-1$) and $\lambda = 1$ (which is a simple eigenvalue). This latter remark will be used to prove the stability of equilibria of the model. For the way forward, we first "vectorialize" system (3.10), using the following set of vectors as formerly defined:

$$X_A = (\rho_{A,k_1}, \rho_{A,k_2}, \ldots, \rho_{A,k_n})^T, \quad X_Y = (\rho_{Y,k_1}, \rho_{Y,k_2}, \ldots, \rho_{Y,k_n})^T,$$
$$X_M = (\rho_{M,k_1}, \rho_{M,k_2}, \ldots, \rho_{M,k_n})^T, \quad X_F = (\rho_{F,k_1}, \rho_{F,k_2}, \ldots, \rho_{F,k_n})^T.$$

Remind that, if $X \in \mathbb{R}^n$ is a vector, $\mathrm{diag}(X)$ denotes the $n \times n$ diagonal matrix whose entries are given by the respective components of X. With these notations, system (3.10) becomes

$$\begin{cases} \dot{X}_A = f_1(X) = \Phi X_F - [\gamma + \mu_1 + \mu_2\mathrm{diag}(X_A)]X_A, \\ \dot{X}_Y = f_2(X) = r\gamma X_A - [\beta + \mu_Y + D_Y]X_Y + D_YCX_Y, \\ \dot{X}_M = f_3(X) = (1-r)\gamma X_A - [\mu_M + D_M]X_M + D_MCX_M, \\ \dot{X}_F = f_4(X) = \beta X_Y - [\mu_F + D_F]X_F + D_FCX_F, \end{cases} \tag{3.12}$$

where C is the connectivity matrix defined in Eq. (3.11).

Notice that, in the case where the parameters Φ, γ, β, μ_1, μ_2, μ_Y, μ_M and μ_F are not the same for all patches, they are replaced in system (3.12) by nonnegative diagonal blocs matrices and this does not change the fundamental structure of the system.

(a) Basic offspring number

System (3.12) has a trivial (mosquito-free) equilibrium $\mathcal{P}_0 = (\mathbf{0}, \mathbf{0}, \mathbf{0}, \mathbf{0})$ with $\mathbf{0}$ standing for the zero vector of dimension n when there is no fertilized and eggs laying females in each patch. We calculate the basic offspring number, $\mathcal{R}_0^{(m)}$ (where the subscript "m" stands for "metapopulation" and simply differentiate it with the single patch basic offspring number $\mathcal{R}_0$), using the next generation approach developed in [27]. Let

$$\mathcal{F} = \begin{pmatrix} \Phi X_F \\ \mathbf{0} \\ \mathbf{0} \end{pmatrix} \quad \text{and} \quad \mathcal{V} = \begin{pmatrix} \gamma X_A + (\mu_1 + \mu_2 \text{diag}(X_A))X_A \\ -r\gamma X_A + (\mu_Y + \beta)X_Y + D_Y X_Y - D_Y C X_Y \\ -\beta X_Y + \mu_F X_F + D_F X_F - D_F C X_F \end{pmatrix}.$$

The Jacobian matrices of $\mathcal{F}$ and $\mathcal{V}$ at the trivial equilibrium $\mathcal{P}_0$ are

$$F = \begin{bmatrix} F_{11} & F_{12} \\ F_{21} & F_{22} \end{bmatrix} \quad \text{and} \quad V = \begin{bmatrix} (\gamma + \mu_1)I_n & \mathbf{0} & \mathbf{0} \\ -r\gamma I_n & (\beta + \mu_Y + D_Y - D_Y C)I_n & \mathbf{0} \\ \mathbf{0} & -\beta I_n & (\mu_F + D_F - D_F C)I_n \end{bmatrix},$$

where

$$F_{11} = \mathbf{0}, \quad F_{12} = \begin{bmatrix} \mathbf{0}, & \Phi \end{bmatrix}, \quad F_{21} = \begin{bmatrix} \mathbf{0} \\ \mathbf{0} \end{bmatrix} \quad \text{and} \quad F_{22} = \begin{bmatrix} \mathbf{0} & \mathbf{0} \\ \mathbf{0} & \mathbf{0} \end{bmatrix}.$$

To compute V^{-1}, denote

$$V = \begin{bmatrix} V_1 & V_2 \\ V_3 & V_4 \end{bmatrix}, \quad \text{where} \quad V_1 = (\gamma + \mu_1)I_n, \quad V_2 = \begin{bmatrix} \mathbf{0} & \mathbf{0} \end{bmatrix}, \quad V_3 = \begin{bmatrix} -r\gamma I_n \\ \mathbf{0} \end{bmatrix}$$

and

$$V_4 = \begin{bmatrix} (\beta + \mu_Y + D_Y - D_Y C)I_n & \mathbf{0} \\ -\beta I_n & (\mu_F + D_F)I_n - D_F C \end{bmatrix}.$$

We emphasize that, since V is a M-matrix and $-V$ is stable, $V^{-1} \geq 0$. Let the inverse matrix of V be written in the following form:

$$V^{-1} = \begin{bmatrix} W_{11} & W_{12} \\ W_{21} & W_{22} \end{bmatrix},$$

where W_{11} and W_{22} are square matrices of dimension $(2n \times 2n)$ and $(n \times n)$, respectively. With this in mind, one has

$$FV^{-1} = \begin{bmatrix} \mathcal{A} & \mathcal{B} \\ \mathbf{0} & \mathbf{0} \end{bmatrix},$$

where $\mathcal{A} = F_{12}W_{21}$ and $\mathcal{B} = F_{12}W_{22}$. Then following [27], the basic offspring number $\mathcal{R}_0^{(m)}$ is defined as the spectral radius of the next generation matrix, FV^{-1}. Precisely,

$$\mathcal{R}_0^{(m)} = \rho(FV^{-1}) = \rho(F_{12}W_{21}). \tag{3.13}$$

To obtain an explicit expression of the basic offspring number, we only need to compute W_{21}. The following lemma demonstrated in Appendix A, is instrumental:

Lemma 3.2. *Let N be a square block matrix of the following form:*

$$N = \begin{bmatrix} N_1 & N_2 \\ N_3 & N_4 \end{bmatrix},$$

where N_1 and N_4 are square matrices.

If N_1 and $D = N_4 - N_3N_1^{-1}N_2$ are invertible, then the inverse matrix of N is given by

$$N^{-1} = \begin{bmatrix} N_1^{-1} + N_1^{-1}N_2D^{-1}N_3N_1^{-1} & -N_1^{-1}N_2D^{-1} \\ -D^{-1}N_3N_1^{-1} & D^{-1} \end{bmatrix}.$$

Notice that V defined above has the same form as N defined in Lemma 3.2 (with: $N_1 = V_1$, $N_2 = V_2$, $N_3 = V_3$ and $N_4 = V_4$). Moreover, it is easy to check that V satisfies all the assumptions in Lemma 3.2. Thus, applying Lemma 3.2, V^{-1} is given by

$$V^{-1} = \begin{bmatrix} V_1^{-1} & \mathbf{0} \\ -V_4^{-1}V_3V_1^{-1} & V_4^{-1} \end{bmatrix},$$

from which one can extract $W_{21} = -V_4^{-1}V_3V_1^{-1}$. Thus, computing W_{21} amounts to compute V_4^{-1} since V_3 is given and V_1^{-1} is obvious. Notice also that V_4 has the same form as N in Lemma 3.2 (with $N_1 = (\beta + \mu_Y + D_Y - D_YC)I_n$, $N_2 = 0$, $N_3 = -\beta I_n$ and $N_4 = (\mu_F + D_F)I_n - D_F C$). Hence, another application of Lemma 3.2 yields

$$V_4^{-1} = \begin{bmatrix} N_1^{-1} & \mathbf{0} \\ -N_4^{-1}N_3N_1^{-1} & N_4^{-1} \end{bmatrix}.$$

From the above expressions, it appears that to obtain an explicit expressions of V_4^{-1}, we need to compute the inverse matrices of N_1^{-1} and N_4^{-1}. These shall be done using another instrumental lemma, stated below and proved in Appendix B.

Lemma 3.3. *Let $G = U + KWZ$ be an $n \times n$ invertible matrix. Assume the matrices U, W and $W^{-1} + ZU^{-1}K$ are invertible. Then the inverse matrix of G is given by*

$$G^{-1} = U^{-1} - U^{-1}K[W^{-1} + ZU^{-1}K]^{-1}ZU^{-1}. \tag{3.14}$$

Now, we can explicitly calculate N_1^{-1} and N_4^{-1}. We shall use recursively Lemma 3.3 and the fact that $C^m = C, \forall m \in \mathbb{N}^*$. Note that $N_4 = (\mu_F + D_F)I_n - D_FC$ has the form of the matrix G with

$$U = (\mu_F + D_F)I_n, \qquad K = (k_1, \dots, k_n)^T, \qquad W = I_n \qquad \text{and}$$
$$Z = \frac{-D_F}{\langle k \rangle}(P(k_1), \dots, P(k_n)).$$

With this in mind and using Lemma 3.3, it is straightforward that

$$\begin{aligned} N_4^{-1} &= \frac{I_n}{(\mu_F + D_F)} - \frac{I_n}{(\mu_F + D_F)} \begin{pmatrix} k_1 \\ \vdots \\ k_n \end{pmatrix} \left[I_n - \frac{D_F}{\mu_F + D_F} \right]^{-1} \\ &\times \frac{-D_F}{\langle k \rangle (\mu_F + D_F)}(P(k_1), \dots, P(k_2)), \\ &= \frac{I_n}{(\mu_F + D_F)} + \frac{I_n}{(\mu_F + D_F)} \frac{D_FC}{\mu_F} = \frac{1}{(\mu_F + D_F)} \left[I_n + \frac{D_F}{\mu_F} C \right]. \end{aligned}$$

Now, let us compute $N_1 = (\beta + \mu_Y + D_Y - D_YC)I_n$. One can also observe that N_1 has the form of G in Lemma 3.3, with

$$U = (\beta + \mu_Y + D_Y)I_n, \qquad K = (k_1, \dots, k_n)^T, \qquad W = I_n \qquad \text{and}$$
$$Z = \frac{-D_Y}{\langle k \rangle}(P(k_1), \dots, P(k_n)).$$

Thus, another application of Lemma 3.3 yields

$$N_1^{-1} = \frac{1}{(\beta + \mu_Y + D_Y)} \left[I_n + \frac{D_Y}{\beta + \mu_Y} C \right].$$

Using the expressions of N_1^{-1} and N_4^{-1}, one has

$$N_4^{-1}N_3N_1^{-1} = \frac{-\beta}{(\mu_F + D_F)(\beta + \mu_Y + D_Y)} \left(I_n + \frac{D_YC}{\beta + \mu_Y} + \frac{D_FC}{\mu_F} + \frac{D_FD_YC}{\mu_F(\beta + \mu_Y)} \right).$$

Thus,

$$F_{12}W_{21} = \frac{r\beta\gamma\Phi}{(\gamma + \mu_1)(\mu_F + D_F)(\beta + \mu_Y + D_Y)} \left[I_n + \frac{D_YC}{\beta + \mu_Y} + \frac{D_F}{\mu_F} C + \frac{D_FD_Y}{\mu_F(\beta + \mu_Y)} C \right].$$

The basic offspring number is therefore

$$\begin{aligned} \mathcal{R}_0^{(m)} &= \rho(F_{12}W_{21}), \\ &= \rho[\Gamma(a_0I_n + (b_0 + c_0 + d_0)C)], \end{aligned} \tag{3.15}$$

where

$$a_0 = 1, \quad b_0 = \frac{D_Y}{\beta + \mu_Y}, \quad c_0 = \frac{D_F}{\mu_F}, \quad d_0 = \frac{D_FD_Y}{\mu_F(\beta + \mu_Y)} \quad \text{and} \quad \Gamma = \frac{r\beta\gamma\Phi}{(\gamma + \mu_1)(\mu_F + D_F)(\beta + \mu_Y + D_Y)}.$$

Since the rank of C is one and $\lambda = 1$ is its unique non-zero and positive eigenvalue, the largest eigenvalue of the matrix $\Gamma[a_0I_n + (b_0 + c_0 + d_0)C)$ is $\Gamma(a_0 + b_0 + c_0 + d_0) > 0$. Thus, $\mathcal{R}_0^{(m)}$ for system (3.10) is

$$\mathcal{R}_0^{(m)} = \frac{r\beta\gamma\Phi}{(\gamma + \mu_1)(\mu_F + D_F)(\beta + \mu_Y + D_Y)} \left[1 + \frac{D_Y}{\beta + \mu_Y} + \frac{D_F}{\mu_F} + \frac{D_FD_Y}{\mu_F(\beta + \mu_Y)} \right]. \tag{3.16}$$

Table 2
Parameter value ranges of model (3.12) used as input for the LHS method.

Parameter	Range	Parameter	Range	Parameter	Range
r	[0.49, 0.51]	μ_2	$[10^{-6}, 10^{-4}]$	μ_F	[0.05, 0.2]
γ	[0.05, 0.2]	β	[0.05, 0.35]	D_Y	$[10^{-2}, 1]$
Φ	[0.5, 50]	μ_Y	[0.01, 0.2]	D_M	$[10^{-2}, 1]$
μ_1	[0.1, 0.5]	μ_M	[0.05, 0.2]	D_F	$[10^{-2}, 1]$

Table 3
PRCCs between $\mathcal{R}_0^{(m)}$, ρ_A, ρ_Y, ρ_F and each parameter.

Parameter	$\mathcal{R}_0^{(m)}$	ρ_A	ρ_Y	ρ_F
r	0.0831	0.0003	0.0325	0.0593
γ	0.6617**	0.3648	0.2364	0.4401
Φ	0.9281***	0.4003	0.5414*	0.5079*
μ_1	−0.7047**	−0.0565	−0.0123	−0.0520
μ_2	–	−0.3327	−0.4112	−0.3789
β	0.5329*	0.2586	0.2033	0.1317
μ_Y	−0.5770*	−0.2008	−0.1530	−0.1389
μ_M	–	0.0874	−0.0066	−0.1577
μ_F	−0.7959**	−0.3169	−0.2749	−0.1873
D_Y	0.0136	0.9103***	0.8641***	0.8411***
D_M	–	−0.0237	0.0283	0.0231
D_F	0.0402	−0.9058***	−0.8712***	−0.8547***

The (⋆)'s indicate the most influential parameters. Precisely, (⋆) indicates a parameter whose sensitivity level (in absolute value) is between 0.5 and 0.65. The (⋆⋆) indicates a parameter whose sensitivity level (in absolute value) is between 0.66 and 0.8. The (⋆⋆⋆) indicates a parameter whose sensitivity level (in absolute value) is above 0.84.

Remark 3.4. The relevance of the above techniques (Lemmas 3.2 and 3.3) used to compute $\mathcal{R}_0^{(m)}$ lies in that it enables us to obtain an explicit formula of the basic offspring number for a complex metapopulation model. More importantly, it gives an easy interpretable expression of the basic offspring number. In metapopulation settings, this kind of result is quite rare (or does not exist at all). It is worth pointing out that, this achievement have been probably made possible due the "statistical" modeling approach used in this work.

(b) Sensitivity analysis

We carried out sensitivity analysis to determine the model robustness to parameter values [28,29]. This amounts to single out the most influential parameters on $\mathcal{R}_0^{(m)}$ and mosquito subpopulation dynamics. A Latin Hypercube Sampling (LHS) scheme [29] samples 1000 values for each input parameter using a uniform distribution over the range of biologically realistic values, listed in Table 3 with descriptions and references given in Tables 1 and 2. Using system (3.12), 1000 model simulations are performed by randomly pairing sampled values for all LHS parameters. Outcome measures are calculated for each run : the basic offspring number ($\mathcal{R}_0^{(m)}$), the average number of population in aquatic stage (ρ_A), young females (ρ_Y) and fertilized females (ρ_F) for a network of five patches. Partial Rank Correlation Coefficients (PRCC) and corresponding p-Values are computed. An output is assumed sensitive to an input if the corresponding PRCC is less than -0.50 or greater than $+0.50$, and the corresponding p-Value is less than 5%.

Table 3 suggests that parameter Φ has the highest influence on the offspring number $\mathcal{R}_0^{(m)}$, following in decreasing order by the parameters μ_F, μ_1, γ, μ_Y and β. One can also observe that, for the values of ρ_A, ρ_Y and ρ_F, the parameters with more influence are D_Y, D_F and Φ. This suggests that the migration of female mosquitoes between the patches may play a dominant role on the persistence of the mosquito's population.

(c) Global stability of the trivial (mosquito-free) equilibrium point.

Using Theorem 2 in [27], the following result is straightforward.

Lemma 3.5. *The trivial (mosquito-free) equilibrium point $\mathcal{P}_0$ of system (3.12) is locally asymptotically stable whenever $\mathcal{R}_0^{(m)} < 1$, and unstable if $\mathcal{R}_0^{(m)} > 1$.*

Biologically speaking, Lemma 3.5 implies that mosquitoes can be eliminated in all breeding sites (when $\mathcal{R}_0^{(m)} < 1$) if the initial sizes of the population of anopheles mosquitoes are in the basin of attraction of the trivial equilibrium point $\mathcal{P}_0$.

System (3.12) can be written in the form $\dot{X} = f(X)$, where $X = (X_A, X_Y, X_M, X_F)^T$ and $f(X) = (f_1(X), f_2(X), f_3(X), f_4(X))^T$. It is straightforward that system (3.12) is cooperative on $\Omega = \mathbb{R}_+^{4n}$ because the Jacobian matrix of (3.12) is a Metzler matrix. Furthermore, f is continuous on Ω and the vector field defined by f is directed inwards on the border $\partial\Omega$ of Ω. Thus, Theorems 2, 5 and 6 in [19] can be applied to extend the local result in Lemma 3.5 to a global one on Ω as follows:

Theorem 3.6. *System (3.12) defines a dissipative dynamical system on $\Omega = \mathbb{R}_+^{4n}$. Moreover, if $\mathcal{R}_0^{(m)} \leq 1$ then the trivial (mosquito-free) equilibrium point $\mathcal{P}_0$ is globally asymptotically stable on Ω.*

Proof. It hinges basically on the monotone properties of model (3.12). The inequalities

$$\frac{4\mathcal{R}_0^{(m)}k_ip(k_i)+4\Gamma\sum_{j=1,j\neq i}^{n}k_jp(k_j)}{\langle k\rangle}<\frac{\gamma+\mu_1+\mu_2\rho_{A,k_i}}{\gamma+\mu_1},\quad i=1,2,\ldots,n, \tag{3.17}$$

hold for all sufficiently large X_A. Let $m=(m_1,m_2,\ldots,m_n)>0$ and let X_{A_m} be so large that in addition to (3.17) the following inequalities also hold:

$$X_{A_m}\geq m, \tag{3.18}$$

$$X_{F_m}:=\frac{(\gamma+\mu_1+\mu_2\mathrm{diag}(X_{A_m}))X_{A_m}}{2\Phi}\geq m, \tag{3.19}$$

$$X_{Y_m}:=\frac{(\mu_F I_n+D_F I_n-D_F C)X_{F_m}}{2\beta}\geq m, \tag{3.20}$$

$$X_{M_m}:=\frac{2(1-r)\gamma}{\mu_M+D_M}\left[I_n+\frac{D_M}{\mu_M}C\right]X_{A_m}\geq m. \tag{3.21}$$

Let $b_m=(X_{A_m},X_{Y_m},X_{F_m},X_{M_m})^T$. Then, one has

$$f_1(b_m)=-\Phi X_{F_m}<0;\quad f_3(b_m)=-(1-r)\gamma X_{A_m}<0;\quad f_4(b_m)=-\beta X_{Y_m}<0;$$

$$\begin{aligned}f_2(b_m)&=r\gamma\left[I_n-\frac{(N_1^{-1})^{-1}(N_4^{-1})^{-1}[\gamma+\mu_1+\mu_2\mathrm{diag}(X_{A_m})]}{4\beta\Phi r\gamma}\right]X_{A_m},\\&=r\gamma\left[I_n-\frac{(a_0I_n+(b_0+c_0+d_0)C)^{-1}}{4\Gamma}\frac{[\gamma+\mu_1+\mu_2\mathrm{diag}(X_{A_m})]}{\gamma+\mu_1}\right]X_{A_m},\\&<0\quad\text{if}\quad 4\Gamma(a_0I_n+(b_0+c_0+d_0)C)<\frac{\gamma+\mu_1+\mu_2\mathrm{diag}(X_{A_m})}{\gamma+\mu_1},\end{aligned}$$

i.e.

$$f_2(b_m)<0\quad\text{if}\quad\frac{4\mathcal{R}_0^{(m)}k_ip(k_i)+4\Gamma\sum_{j=1,j\neq i}^{n}k_jp(k_j)}{\langle k\rangle}<\frac{\gamma+\mu_1+\mu_2\rho_{A,k_i}}{\gamma+\mu_1},\quad i=1,2,\ldots,n.$$

So, $f(b_m)=(f_1(b_m),f_2(b_m),f_3(b_m),f_4(b_m))^T<0$. Applying Theorem 6 in [19] with $a=0$ and $b=b_m$, we obtain that (3.12) defines a dynamical system on $[0,b_m]$. However, b_m can be selected larger than any $X\in\mathbb{R}_+^{4n}$. Thus, (3.12) defines a dynamical system on $\Omega=\mathbb{R}_+^{4n}$. The only equilibrium point in Ω is the trivial equilibrium $\mathcal{P}_0$. It follows from Theorem 6 in [19] that $\mathcal{P}_0$ is globally asymptotically stable on $[0,b_m]$ for any $m>0$, and therefore is globally asymptotically stable on $\Omega=\mathbb{R}_+^{4n}$. □

(d) Nontrivial (mosquito-persistent) equilibrium point and its stability

In this paragraph, we begin by showing that system (3.12) has a unique nontrivial equilibrium point when $\mathcal{R}_0^{(m)}>1$. To achieve our goal, we reformulate the problem in terms of fixed point problem and use Theorem 2.1 in [20] for the existence and uniqueness of a positive fixed point of a multi-variable function. To be self contained, Theorem 2.1 in [20] is recalled hereafter.

Theorem 3.7 ([20], Theorem 2.1)**.** *Let $F(x)$ be a continuous, monotone non-decreasing, strictly sublinear, bounded function which maps the non-negative orthant $\mathbb{R}_+^n$ into itself. Let $F(0)=0$ and $F'(0)$ exists and be irreducible. Then $F(x)$ does not have a nontrivial fixed point on the boundary of $\mathbb{R}_+^n$. Moreover, $F(x)$ has a positive fixed point iff $\rho(F'(0))>1$. If there is a positive fixed point, then it is unique.*

An equilibrium point $\mathcal{P}^*=(X_A^*,X_Y^*,X_M^*,X_F^*)$ for system (3.12) satisfies the following system of equations:

$$\begin{cases}\Phi X_F^*-\left[\gamma+\mu_1+\mu_2\mathrm{diag}(X_A^*)\right]X_A^*=0,\\ r\gamma X_A^*-[(\beta+\mu_Y)+D_Y]X_Y^*+D_YCX_Y^*=0,\\(1-r)\gamma X_A^*-[\mu_M+D_M]X_M^*+D_MCX_M^*=0,\\ \beta X_Y^*-[\mu_F+D_F]X_F^*+D_FCX_F^*=0.\end{cases} \tag{3.22}$$

Solving (3.22) yields

$$X_F^* = \frac{[\gamma+\mu_1+\mu_2\text{diag}(X_A^*)]X_A^*}{\Phi},$$
$$X_Y^* = \frac{(\mu_F I_n + D_F I_n - D_F C)[\gamma+\mu_1+\mu_2\text{diag}(X_A^*)]X_A^*}{\beta\Phi},$$
$$X_M^* = \frac{(1-r)\gamma}{\mu_M+D_M}\left[I_n+\frac{D_M}{\mu_M}C\right]X_A^*. \tag{3.23}$$

Replacing (3.23) in the second equation of system (3.22), one obtain

$$r\gamma\left[I_n - \frac{N_1N_4[\gamma+\mu_1+\mu_2\text{diag}(X_A^*)]}{\beta\Phi r\gamma}\right]X_A^* = 0.$$

Hence, the existence of the nontrivial equilibrium point is reformulated as the following fixed point problem: Find a unique positive X_A^*, such that $X_A^* = F(X_A^*)$, where

$$F(X_A^*) = r\beta\gamma\Phi[\gamma+\mu_1+\mu_2\text{diag}(X_A^*)]^{-1}N_4^{-1}N_1^{-1}X_A^*.$$

Notice that F is a continuous, bounded function that maps $\mathbb{R}_+^n$ into itself and it is infinitely differentiable.

Let us prove that F is strictly sublinear in $\mathbb{R}_+^n$ i.e. $F(\nu X_A^*) > \nu F(X_A^*)$, for any $X_A^* \in \mathbb{R}_+^n$ with $X_A^* > 0$, and $\nu \in (0, 1)$. Direct, but lengthy calculations give

$$\nu F(X_A^*)[F(\nu X_A^*)]^{-1} = \text{diag}\left(\frac{\gamma+\mu_1+\nu\mu_2\rho_{A,k_1}}{\gamma+\mu_1+\mu_2\rho_{A,k_1}}, \ldots, \frac{\gamma+\mu_1+\nu\mu_2\rho_{A,k_n}}{\gamma+\mu_1+\mu_2\rho_{A,k_n}}\right).$$

Since $\nu \in (0, 1)$, we have

$$\frac{\gamma+\mu_1+\nu\mu_2\rho_{A,k_i}}{\gamma+\mu_1+\mu_2\rho_{A,k_i}} < 1, \qquad i = 1, 2, \ldots, n.$$

Thus, $\nu F(X_A^*)[F(\nu X_A^*)]^{-1} < I_n$ i.e. $\nu F(X_A^*) < F(\nu X_A^*)$. Hence, F is strictly sublinear.

One can easily check that the off-diagonal elements $a_{i,j}(i \neq j)$ of the matrix $F'(X_A^*)$ are

$$a_{ij} = \frac{\Gamma(b_0+c_0+d_0)k_i p(k_j)}{\langle k\rangle(\gamma+\mu_1+\mu_2\rho_{A,k_i})} > 0, \quad \forall i \neq j \in \{1, 2, \ldots, n\}.$$

Thus, F is a monotone non-decreasing function. We have also that $F(0) = 0$ and $F'(0) = \Gamma(a_0 I_n + (b_0 + c_0 C + d_0)C)$. Therefore $\rho(F'(0)) = \mathcal{R}_0^{(m)} > 1$ iff $\mathcal{R}_0^{(m)} > 1$. Thanks to the graph theory and the irreducibility of the matrix C, $F'(0)$ is irreducible because its associated graph is strongly connected. Thus, we have established the following theorem:

Theorem 3.8. *If $\mathcal{R}_0^{(m)} \leq 1$, the only equilibrium point of the system is the trivial equilibrium $\mathcal{P}_0$. If $\mathcal{R}_0^{(m)} > 1$ there also exists a unique nontrivial (mosquito-persistent) equilibrium point $\mathcal{P}^*$ in* int(Ω).

By Lemma 3.5, the trivial equilibrium point $\mathcal{P}_0$ is unstable whenever $\mathcal{R}_0^{(m)} > 1$. We terminate this section by proving the following result which establishes the global stability of the nontrivial equilibrium.

Theorem 3.9. *If $\mathcal{R}_0^{(m)} > 1$, the nontrivial (mosquito-persistent) equilibrium $\mathcal{P}^*$ of the system (3.12) is GAS on Ω.*

Proof. Since $\mathcal{R}_0^{(m)} > 1$, the inequalities

$$\frac{\gamma+\mu_1+\mu_2\rho_{A,k_i}}{\gamma+\mu_1} < \frac{\mathcal{R}_0^{(m)}k_i p(k_i) + \Gamma\sum_{j=1,j\neq i}^n k_j p(k_j)}{\sqrt{\mathcal{R}_0^{(m)}}\,\langle k\rangle}, \quad i = 1, 2, \ldots, n, \tag{3.24}$$

hold for all sufficiently small values X_A. Let $\varepsilon = (\varepsilon_1, \varepsilon_2, \ldots, \varepsilon_n) > 0$ and let X_{A_ε} be so small that in addition to (3.24) the following inequalities also hold:

$$X_{A_\varepsilon} \leq \varepsilon, \tag{3.25}$$

$$X_{F_\varepsilon} := \frac{\sqrt[4]{\mathcal{R}_0^{(m)}}\,(\gamma+\mu_1+\mu_2\text{diag}(X_{A_\varepsilon}))X_{A_\varepsilon}}{\Phi} \leq \varepsilon, \tag{3.26}$$

$$X_{Y_\varepsilon} := \frac{\sqrt[4]{\mathcal{R}_0^{(m)}}\,(\mu_F I_n + D_F I_n - D_F C)X_{F_\varepsilon}}{\beta} \leq \varepsilon, \tag{3.27}$$

$$X_{M_\varepsilon} := \frac{(1-r)\gamma}{\sqrt[4]{\mathcal{R}_0^{(m)}}\,(\mu_M + D_M)}\left[I_n + \frac{D_M}{\mu_M}C\right]X_{A_\varepsilon} \le \varepsilon. \tag{3.28}$$

Let $a_\varepsilon = (X_{A_\varepsilon}, X_{Y_\varepsilon}, X_{F_\varepsilon}, X_{M_\varepsilon})^T$. Then, one has

$$f_1(a_\varepsilon) = \left(1 - \frac{1}{\sqrt[4]{\mathcal{R}_0^{(m)}}}\right)\Phi X_{F_\varepsilon} > 0; \quad f_3(a_\varepsilon) = \frac{\left(\sqrt{\mathcal{R}_0^{(m)}} - 1\right)(1-r)\gamma}{\sqrt{\mathcal{R}_0^{(m)}}}X_{A_\varepsilon} > 0;$$

$$f_4(a_\varepsilon) = \left(1 - \frac{1}{\sqrt[4]{\mathcal{R}_0^{(m)}}}\right)\beta X_{Y_\varepsilon} > 0;$$

$$\begin{aligned} f_2(a_\varepsilon) &= r\gamma\left[I_n - \frac{\sqrt{\mathcal{R}_0^{(m)}}(N_1^{-1})^{-1}(N_4^{-1})^{-1}[\gamma + \mu_1 + \mu_2\mathrm{diag}(X_{A_m})]}{\beta\Phi r\gamma}\right]X_{A_m}, \\ &= r\gamma\left[I_n - \frac{\sqrt{\mathcal{R}_0^{(m)}}(a_0 I_n + b_0 I_n C + c_0 I_n C + d_0 I_n C)^{-1}}{\Gamma}\,\frac{[\gamma + \mu_1 + \mu_2\mathrm{diag}(X_{A_m})]}{\gamma + \mu_1}\right]X_{A_m} \\ &> 0 \quad \text{if} \quad \frac{\Gamma(a_0 I_n + b_0 I_n C + c_0 I_n C + d_0 I_n C)}{\sqrt{\mathcal{R}_0^{(m)}}} > \frac{\gamma + \mu_1 + \mu_2\mathrm{diag}(X_{A_m})}{\gamma + \mu_1}, \end{aligned}$$

i.e.

$$f_2(a_\varepsilon) > 0 \quad \text{if} \quad \frac{\gamma + \mu_1 + \mu_2\rho_{A,k_i}}{\gamma + \mu_1} < \frac{\mathcal{R}_0^{(m)}k_i p(k_i) + \Gamma\sum_{j=1, j\neq i}^{n} k_j p(k_j)}{\sqrt{\mathcal{R}_0^{(m)}}\,\langle k\rangle}, \quad i = 1, 2, \ldots, n.$$

Thus, $f(a_\varepsilon) = (f_1(a_\varepsilon), f_2(a_\varepsilon), f_3(a_\varepsilon), f_4(a_\varepsilon))^T > 0$. Applying once again Theorem 6 in [19] (with $a = a_\varepsilon$ and $b = b_m$), we obtain that the nontrivial equilibrium point $\mathcal{P}^*$ is globally asymptotically stable on $[a_\varepsilon, b_m]$. Since a_ε can be selected to be smaller than any $X > 0$ and b_m can be selected to be larger than any $X > 0$, we obtain that $\mathcal{P}^*$ is asymptotically stable on $\Omega = \mathbb{R}_+^{4n}$ with basin of attraction being at least the interior of Ω. □

3.3. The metapopulation model in a heterogeneous landscape

Differences in the distribution of resources create heterogeneity on the network, since patches may have different degrees of attractiveness to mosquitoes. According to [5] we describe how heterogeneity and differences in patch attractiveness to mosquitoes during movement is incorporated. Here, each patch represent a potential breeding–feeding site. The number of hosts is allowed to differ between patches across the local network, introducing heterogeneity. Heterogeneity of breeding sites is incorporated here by taking different values for parameter μ_2 in each patch. In this case, the carrying capacities of breeding sites would be different.

Let H be the total population of hosts in the network and H_k the population of hosts in patches of degree k. The proportion of hosts in patches of degree k is

$$\overline{H}_k = \frac{H_k}{H}, \quad \text{with} \quad \sum_k \overline{H}_k = 1. \tag{3.29}$$

Mosquitoes are attracted to odors released by hosts, this leads to mosquitoes being less likely to leave the patch if their current patch is a home to many hosts and more likely to move out of the patch if there are few hosts [26,30]. As in [5], we mimic this phenomenon by using a decreasing exponential function to model the movement rate. We assume that heterogeneity of hosts also influence the males dispersal because females go to the hosts for blood-meal and males go to meet females [31]. Note that immature females are not subjected to the attraction of hosts, they diffuse randomly in any direction. We also incorporate the spatial proximity of patches by using a decreasing linear function, since mosquitoes have a limited mobility. Hence, we can define the diffusion rate along any given link of a patch of degree k to a patch of degree k' as

$$D_{kk'} = \frac{D_Y\psi(d_{kk'})}{k} \quad \text{and} \quad D_{kk'} = \frac{D_i\psi(d_{kk'})}{k}e^{-\lambda(\overline{H}_k - \overline{H}_{k'})}, \quad i = M, F, \tag{3.30}$$

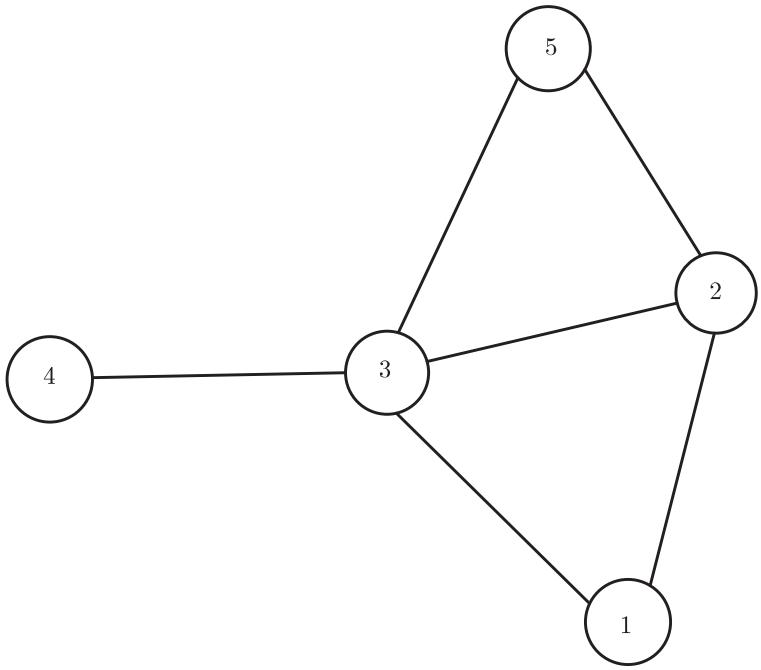

Fig. 3. An example of a network with five patches.

where λ is a constant parameter for the decay function, $d_{kk'} = \sqrt{(x_k - x_{k'})^2 + (y_k - y_{k'})^2}$ is the Cartesian distance between a node of degree k and a node of degree k'; ψ the distance function defined as

$$\psi(d_{kk'}) = \begin{cases} \dfrac{d_{max} - d_{kk'}}{d_{max}} & \text{if} \quad d_{kk'} < d_{max}, \\ 0 & \text{else}, \end{cases} \tag{3.31}$$

with d_{max} the maximal mobility distance.

Thus, the equations governing the spatio-temporal evolution of anopheles mosquitoes in this case for a n-patches in an uncorrelated network are giving by the system below:

$$\begin{cases} \dot{\rho}_{A,k} = \Phi_k \rho_{F,k} - (\gamma_k + \mu_{1k} + \mu_{2k}\rho_{A,k})\rho_{A,k}, \\ \dot{\rho}_{Y,k} = r\gamma_k \rho_{A,k} - (\beta_k + \mu_{Y_k})\rho_{Y,k} - \dfrac{D_Y}{\langle k \rangle}\left(\sum_{k'} k' p(k')\psi(d_{kk'})\right)\rho_{Y,k} + \dfrac{kD_Y}{\langle k \rangle}\sum_{k'} p(k')\psi(d_{kk'})\rho_{Y,k'}, \\ \dot{\rho}_{M,k} = (1-r)\gamma_k \rho_{A,k} - \mu_{M_k}\rho_{M,k} - \dfrac{D_M}{\langle k \rangle}\left(\sum_{k'} e^{-\lambda(\overline{H}_k - \overline{H}_{k'})} k' p(k')\psi(d_{kk'})\right)\rho_{M,k} \\ \quad + \dfrac{kD_M}{\langle k \rangle}\sum_{k'} e^{-\lambda(\overline{H}_{k'} - \overline{H}_k)} p(k')\psi(d_{kk'})\rho_{M,k'}, \\ \dot{\rho}_{F,k} = \beta_k \rho_{Y,k} - \mu_{F_k}\rho_{F,k} - \dfrac{D_F}{\langle k \rangle}\left(\sum_{k'} e^{-\lambda(\overline{H}_k - \overline{H}_{k'})} k' p(k')\psi(d_{kk'})\right)\rho_{F,k} \\ \quad + \dfrac{kD_F}{\langle k \rangle}\sum_{k'} e^{-\lambda(\overline{H}_{k'} - \overline{H}_k)} p(k')\psi(d_{kk'})\rho_{F,k'}, \end{cases} \tag{3.32}$$

From Theorem 3.1 above, one can easily see that (3.32) is a dynamical system in $\mathbb{R}_+^{4n}$. A patch of degree k is at a mosquito-free equilibrium point if $\rho_{A,k} = \rho_{Y,k} = \rho_{M,k} = \rho_{F,k} = 0$. However, given the complexity of the equations, we do not perform further theoretical analysis for model (3.32). We shall rather focus on numerical analysis in the next section.

4. Numerical simulations

To illustrate the various theoretical results of the previous sections, we consider a metapopulation network with five patches and the following connectivities: $k_1 = 2$; $k_2 = 3$; $k_3 = 4$; $k_4 = 1$ and $k_5 = 2$ (see Fig. 3). Since we do not know what trajectories mosquitoes adopt in reality, we use strategies such as Levy-flight (which are comprised of random sequences of movement-segments with lengths l drawn from a probability distribution function having a power-law tail $p(l) \sim l^{-\mu}$ where $1 < \mu \leq 3$) to optimize foraging efficiency [32]. Thus, we consider an architecture network given by the distribution $p(k) \sim k^{-3}$ [12,13].

Models (3.12) and (3.32) are both simulated by using data from recent works. These data are summarized in Table 1. As far as mosquito dispersal is concerned, some studies have shown that daily flights range from 200 to 400 m, where the maximum distance recorded is 661 m [33]. We run all simulations with the following initial conditions: the total number

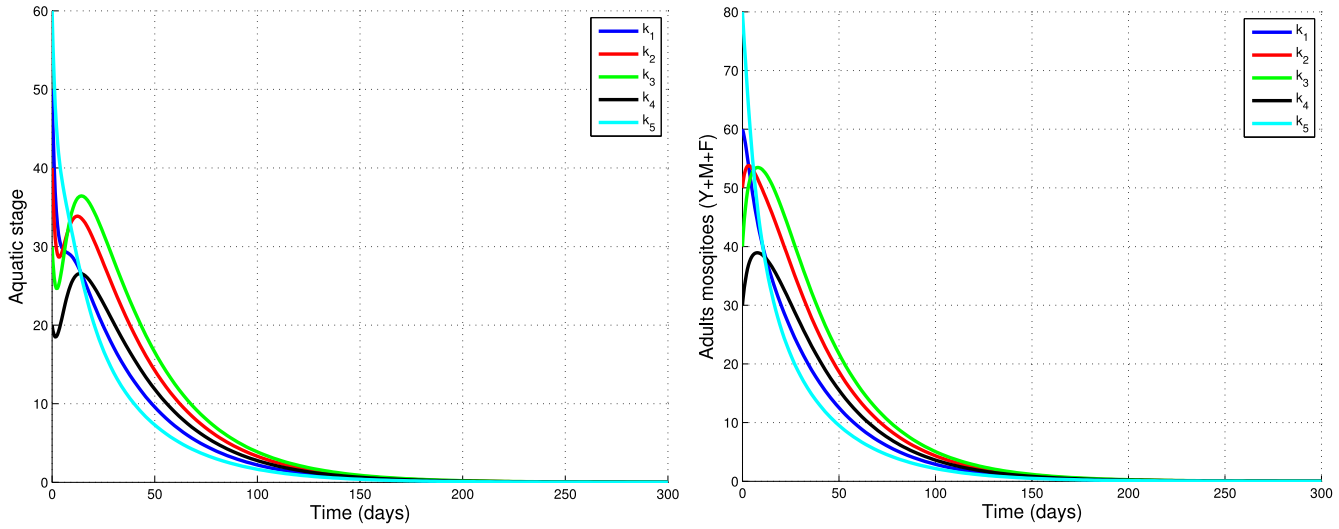

Fig. 4. Simulation results showing the GAS of the trivial equilibrium $\mathcal{P}_0$ for the basic model when $\Phi = 0.5$, $D_Y = D_M = D_F = 0.1$ and $\mathcal{R}_0^{(m)} \leq 1$. All other parameters are as in Table 1.

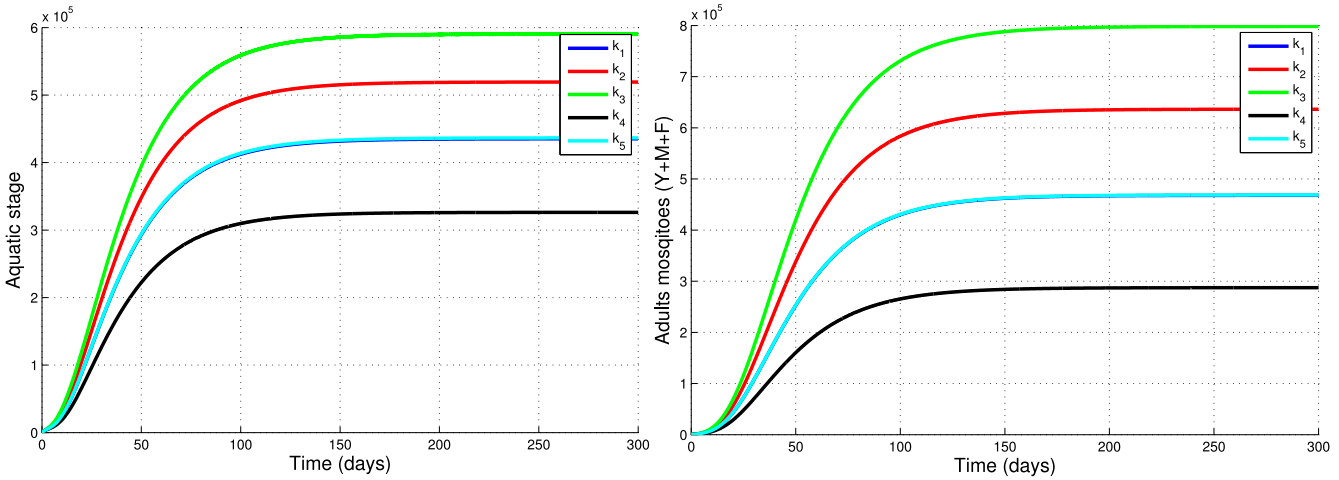

Fig. 5. Simulation results showing the GAS of the nontrivial equilibrium $\mathcal{P}^*$ when $\Phi = 10$, $D_Y = D_M = D_F = 0.1$ and $\mathcal{R}_0^{(m)} > 1$. All other parameters are as in Table 1.

mosquitoes in aquatic stages is 1500, 1000 young mosquitoes are females not yet laying eggs, 1000 are males, while 1250 are fertilized and eggs laying females. They are evenly distributed across the network.

4.1. General dynamics

In this subsection, we numerically illustrate the asymptomatic behavior of model (3.12). For that, we consider a network of metapopulation with five patches. The dynamics of all compartments are very similar to each other. Hence, only the graphs of mosquitoes at the aquatic stage and total flying mosquito population (that is, $Y + M + F$) are presented here. Fig. 4 presents the trajectories of model (3.12) for all patches when $\Phi = 0.5$, $D_Y = D_M = D_F = 0.1$ and the basic offspring number $\mathcal{R}_0^{(m)}$ is less than one ($\mathcal{R}_0^{(m)} = 0.6531$). From this figure, we can see that the mosquito populations die out in all patches. Thus, the trajectories converge to the trivial equilibrium as shown in Theorem 3.6.

Fig. 5 plots the trajectories of system (3.12) when $\Phi = 10$, $D_Y = D_M = D_F = 0.1$ and the basic offspring number $\mathcal{R}_0^{(m)}$ is greater than one ($\mathcal{R}_0^{(m)} = 13.0612$). This illustrates the fact that the mosquitoes are always present in all patches and the trajectories converge to the nontrivial equilibrium as established in Theorem 3.9.

4.2. Impact of dispersal on population dynamics

To evaluate the impact of dispersal on population dynamics, we carry out in Fig. 6 numerical simulations (when $\Phi = 10$) on system (3.12) both without and with dispersal. This figure shows that persistence of mosquito population is more important in the presence of dispersal than in the case without dispersal, especially in high-degree patches.

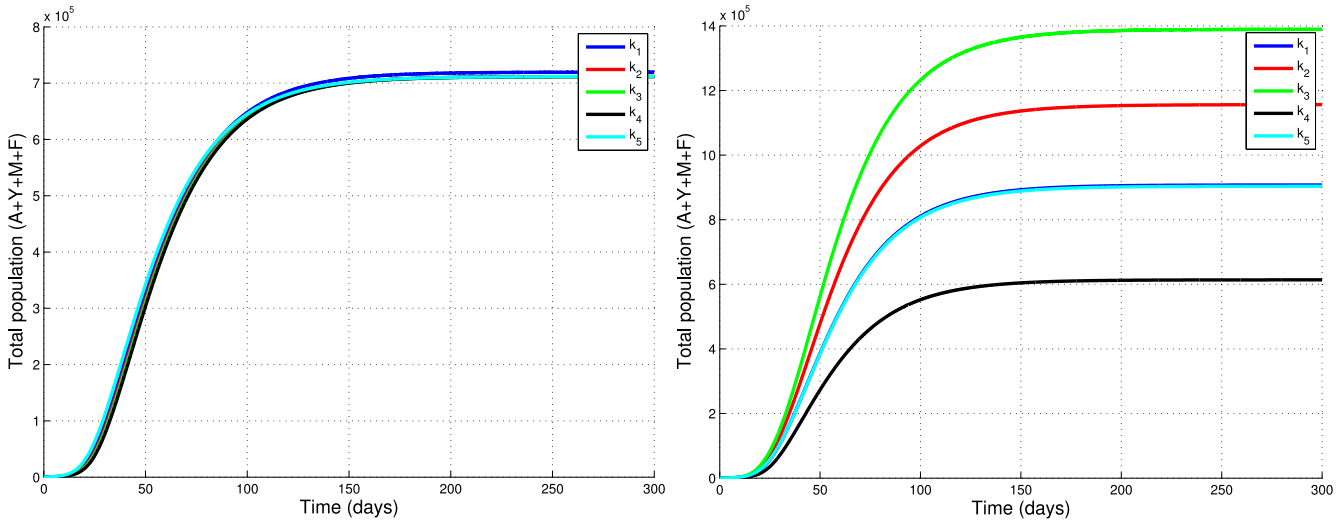

Fig. 6. Trajectories plots of model (3.12) without dispersal (left) and with dispersal (right) when $\Phi = 10$: the total mosquito population increases as the diffusion coefficients increase.

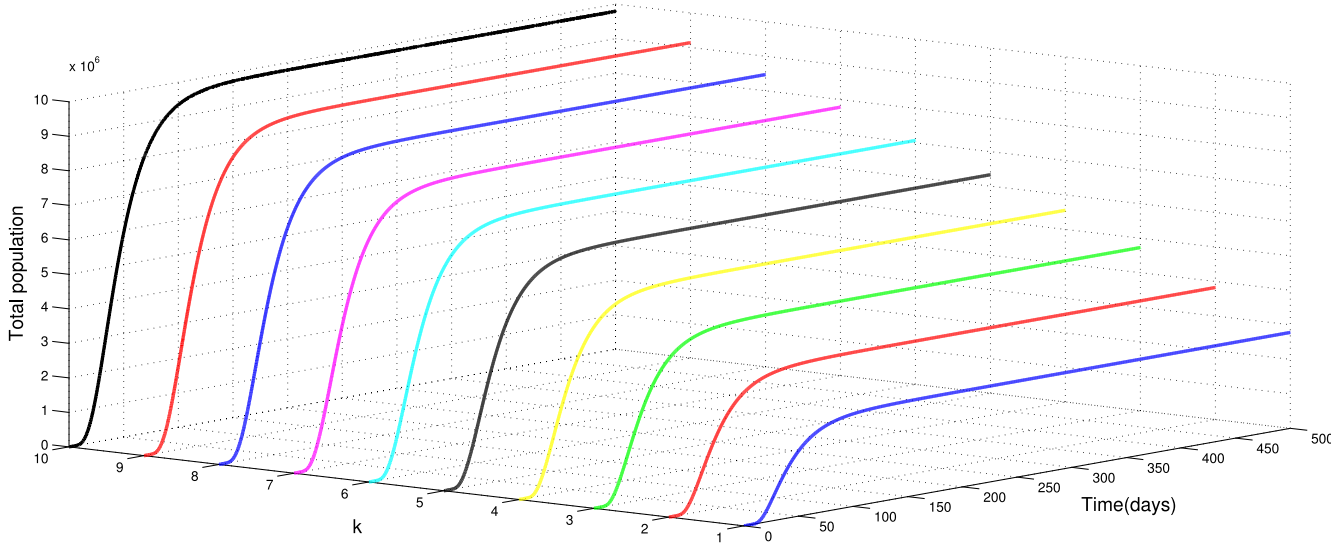

Fig. 7. Mosquito population in patches of degree $k = 1, 2, \ldots, 10$, when $\Phi = 10$ and $D_M = D_Y = D_F = 0.1$: the total mosquito population increases as the patch connectivity increases.

4.3. Impact of the heterogeneous connectivity of patches on population dynamics

To investigate the significance of heterogeneous connectivity of patches on vector population dynamics, system (3.12) is simulated in Fig. 7 with variable degree of patches. Fig. 7 illustrates the fact that, with the same diffusion coefficients ($D_M = D_Y = D_F$), the total mosquito population increases as the connectivity of the patch increases. This suggests that the heterogeneous connectivity of patches play an important role on vector population dynamics. This heterogeneity may come from the daily productivity and destruction of some breeding sites, since small pools of water are continually destroyed and reformed [4].

4.4. Impact of migration and heterogeneity on mosquito spread

In this section, numerical simulations are carried out to investigate the role of dispersal/diffusion and heterogeneity on mosquito spread. Models (3.12) and (3.32) are both simulated with different values of Φ in each patch. In order to observe more effects of the migration on the dynamics of models (3.12) and (3.32), we consider the hypothetical scenario where the mosquito-persistent equilibrium is GAS in the patch of minimal degree (patch 4) and unstable in the other patches (patch 1, 2, 3, 5). Model (3.32) is simulated with $\overline{H}_{k_1} = 0.6$, $\overline{H}_{k_2} = 0.07$, $\overline{H}_{k_3} = 0.06$, $\overline{H}_{k_4} = 0.03$, $\overline{H}_{k_5} = 0.24$, $d_{\max} = 661$ m and $\lambda = 0.5$. Let $\mathcal{R}_0^{(i)}$, $i = 1, 2, 3, 4, 5$, denotes the basic offspring number for the local population of anopheles mosquito in patch i as defined in (2.3). Choose $\Phi_1 = \Phi_2 = \Phi_3 = \Phi_5 = 0.5$, $\Phi_4 = 10$ so that $\mathcal{R}_0^{(1)} = \mathcal{R}_0^{(2)} = \mathcal{R}_0^{(3)} = \mathcal{R}_0^{(5)} = 0.5714 < 1$

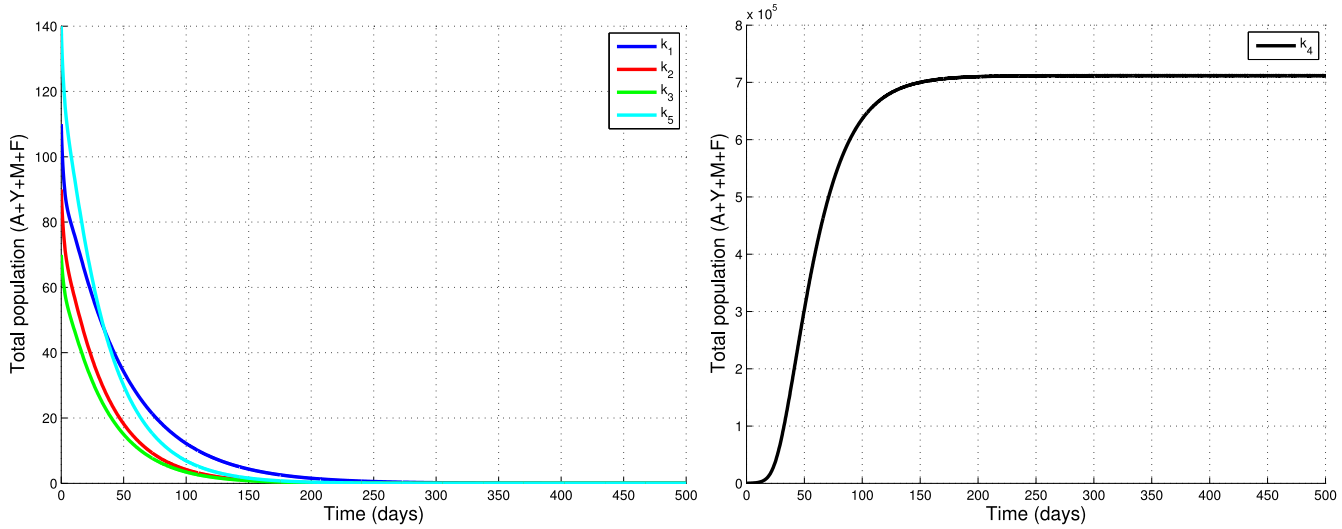

Fig. 8. Simulation results of systems (3.12) and (3.32) showing the mosquito population in mosquito-free patches (left) and mosquito-persistent patch (right) in absence of migration. $\mathcal{R}_0^{(i)} < 1$, $i = 1, 2, 3, 5$ and $\mathcal{R}_0^{(4)} > 1$. All other parameters are as in Table 1.

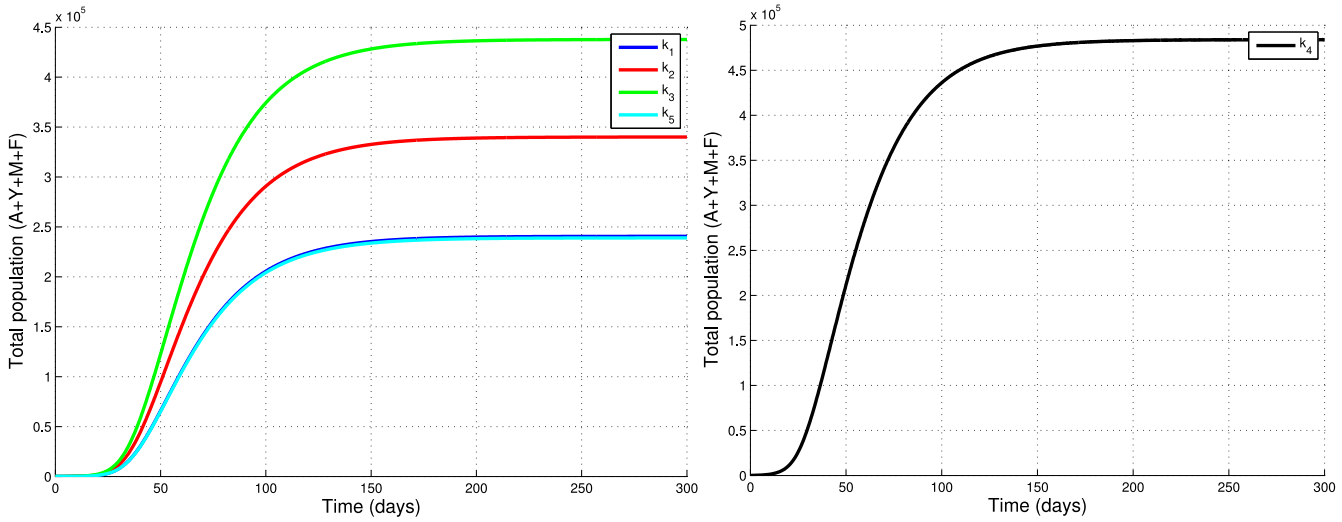

Fig. 9. Simulation result showing the mosquito spread from mosquito-persistent patch (right) to mosquito-free patches (left) in a homogeneous landscape (Eq. (3.12)) with $D_M = D_Y = D_F = 0.1$ and all other parameters are as in Table 1. $\mathcal{R}_0^{(i)} < 1$, $i = 1, 2, 3, 5$ and $\mathcal{R}_0^{(4)} > 1$.

and $\mathcal{R}_0^{(4)} = 11.4286 > 1$. It is observed from Fig. 8 that, in the absence of migration/diffusion (i.e. $D_M = D_Y = D_F = 0$), the mosquito-persistent equilibrium point is unstable in patches 1, 2, 3, 5 and stable in the fourth patch, as expected.

Figs. 9–12 present the mosquito spread from an mosquito-persistent patch (patch 4) to mosquito-free patches (patches 1, 2, 3, 5) under different scenario when $D_M = D_Y = D_F = 0.1$.

Observing these latter figures, one can see that in the presence of dispersal, mosquitoes moving out of an mosquito-persistent patch (patch 4) migrate into the mosquito-free patches (patches 1, 2, 3, 5). This illustrates the fact that mosquito dispersal could lead to a larger presence of mosquitoes in all patches and, shows the important effects of dispersal and connectivity of patches on population spread. However, this diffusion varies according to the type of landscape.

4.4.1. Dispersal in a homogeneous landscape

Fig. 9 presents the trajectories of the mosquito spread from mosquito-persistent patch (right) to mosquito-free patches (left) in a homogeneous landscape (Eq. (3.12)). We observe in this case that mosquitoes coming from mosquito-persistent patch (patch 4) migrate more to the high-degree patches (see patches 3 and 2) and equitably to the patches with equal degree (see patches 1 and 5).

4.4.2. Dispersal in a heterogeneous landscape

Fig. 10 gives numerical solutions of model (3.32), depicting the mosquito spread from mosquito-persistent patch (right) to non mosquito-persistent patches (left) in a heterogeneous landscape (heterogeneity of hosts and homogeneity of breeding

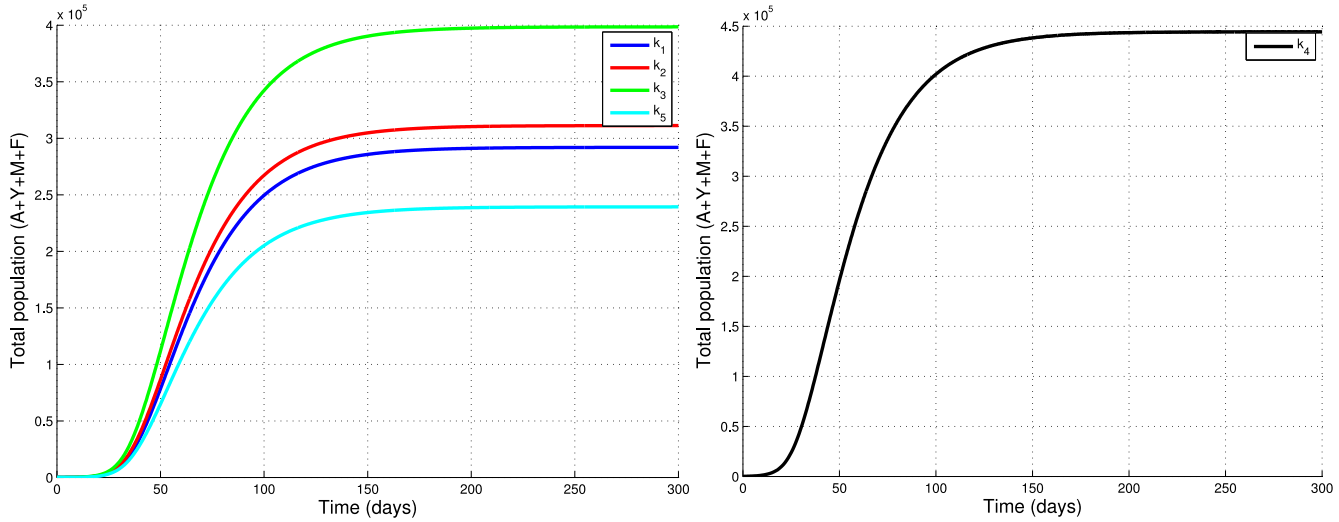

Fig. 10. Simulation results showing the mosquito spread from mosquito-persistent patch (right) to mosquito-free patches (left) in a heterogeneous landscape (heterogeneity of hosts and homogeneity of breeding sites) with $\psi(d_{kk'}) = 1$, $\forall k, k'$, $D_M = D_Y = D_F = 0.1$ and all other parameters are as in Table 1. $\mathcal{R}_0^{(i)} < 1$, $i = 1, 2, 3, 5$ and $\mathcal{R}_0^{(4)} > 1$.

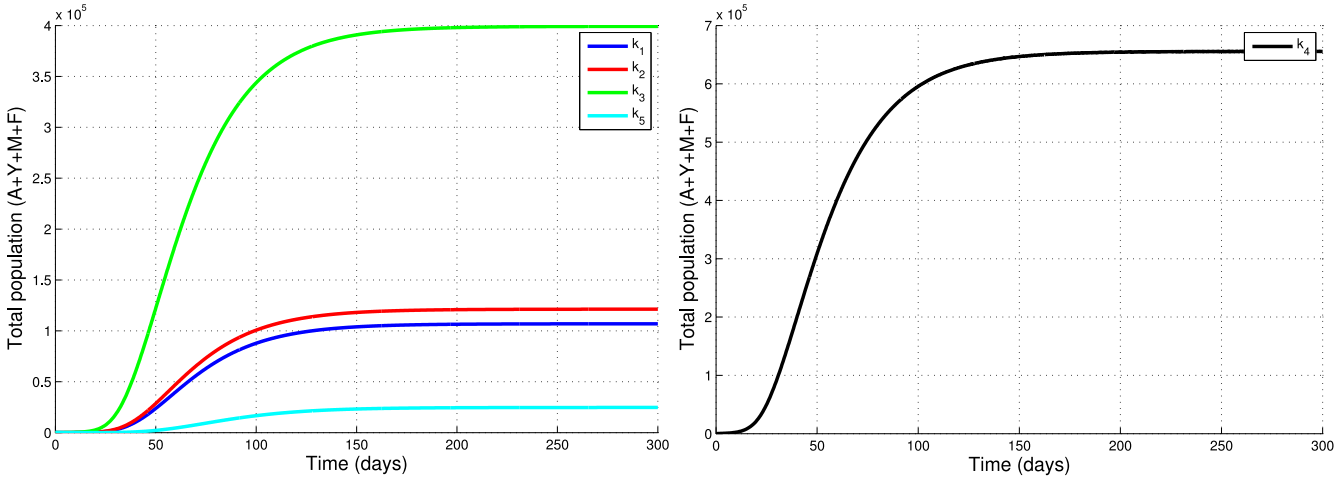

Fig. 11. Simulation results showing the mosquito spread from mosquito-persistent patch (right) to non mosquito-persistent patches (left) in a heterogeneous landscape (heterogeneity of hosts and homogeneity of breeding sites) with $\psi(d_{kk'})$ as in (3.31), $D_M = D_Y = D_F = 0.1$ and all other parameters are as in Table 1. $\mathcal{R}_0^{(i)} < 1$, $i = 1, 2, 3, 5$ and $\mathcal{R}_0^{(4)} > 1$.

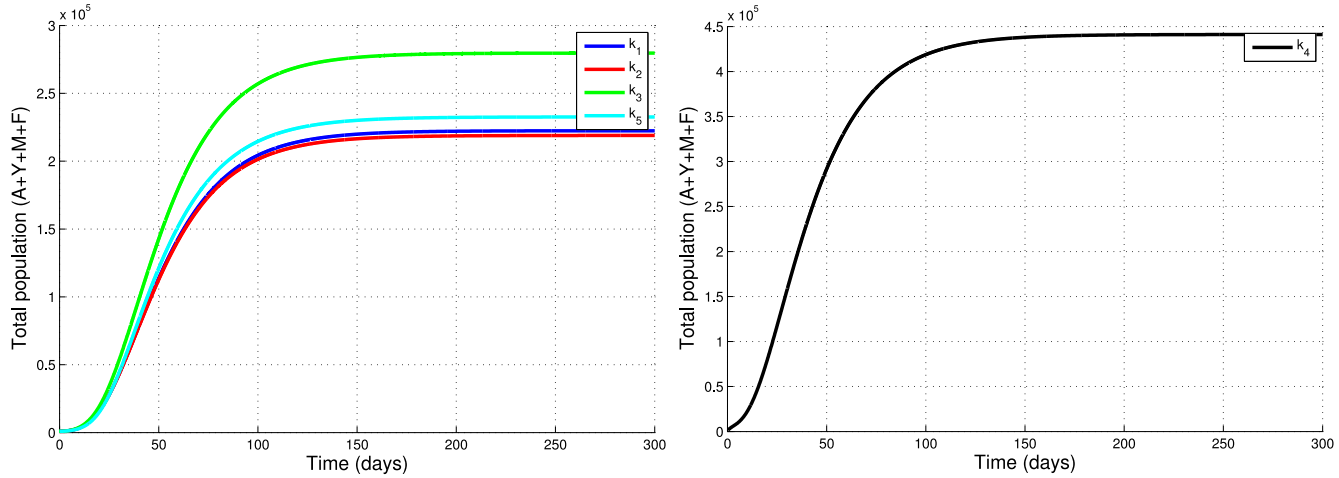

Fig. 12. Simulation result showing the mosquito spread from mosquito-persistent patch (right) to non mosquito-persistent patches (left) in a heterogeneous landscape (heterogeneous hosts and breeding sites) with $\psi(d_{kk'}) = 1$, $\forall k, k'$, $\mu_{21} = 10^{-4}$, $\mu_{22} = 10^{-3}$, $\mu_{23} = 10^{-2}$, $\mu_{24} = 10^{-5}$, $\mu_{25} = 10^{-5}$ and $D_M = D_Y = D_F = 0.1$ $D_M = D_Y = D_F = 0.1$. $\mathcal{R}_0^{(i)} < 1$, $i = 1, 2, 3, 5$ and $\mathcal{R}_0^{(4)} > 1$.

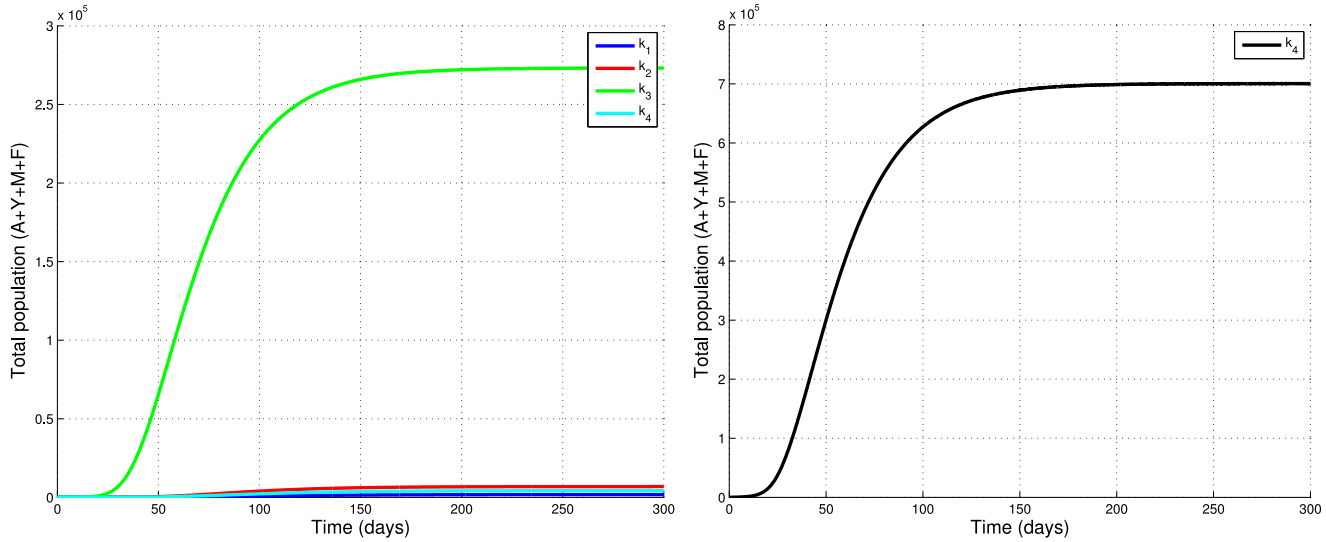

Fig. 13. Simulation result showing the mosquito spread from mosquito-persistent patch (right) to non mosquito-persistent patches (left) (heterogeneity of hosts and homogeneity of breeding sites) with $\psi(d_{kk'})$ as in (3.31), when distances between patches 1, 2, 3, 5 are large.

sites), when distance has no effect on mosquito flights (i.e. $\psi(d_{kk'}) = 1,\ \forall k, k'$). Even though a great number of mosquitoes moves into the patches of high degree, the dispersal becomes more important in the patches with more hosts.

Fig. 11 simulates the solutions of model (3.32) and displays the mosquito spread from mosquito-persistent patch (right) to non mosquito-persistent patches (left) in a heterogeneous landscape (heterogeneity of hosts and homogeneity of breeding sites), when distance affects mosquito dispersal (i.e. $\psi(d_{kk'})$ as in (3.31), with $d_{k_3k_4} = 300$ m, $d_{k_5k_1} = 370$ m, $d_{k_3k_1} = 361$ m, $d_{k_3k_2} = 361$ m, $d_{k_3k_5} = 400$ m, $d_{k_2k_5} = 380$ m). As in the latter Fig. 10, similar result is observed, with the difference in that the mosquito dispersal from mosquito-persistent patch (patch 4) to mosquito-free patches (patches 1, 2, 3 and 5) is less important in this case.

Fig. 12 presents the simulation results of model (3.32), showing the mosquito spread from mosquito-persistent patch (right) to mosquito-free patches (left) in a heterogeneous landscape (heterogeneity of hosts and breeding sites), with $\mu_{21} = 10^{-4}$, $\mu_{22} = 10^{-3}$, $\mu_{23} = 10^{-2}$, $\mu_{24} = 10^{-5}$, $\mu_{25} = 10^{-5}$ and $\psi(d_{kk'}) = 1,\ \forall k, k'$. From this figure, it is noticeable that heterogeneity of hosts and breeding sites greatly influences the mosquito dispersal and their spatial distribution. This suggests that the heterogeneous connectivity of patches and heterogeneous distribution of hosts and breeding sites may play an important role on the spatial distribution of mosquitoes.

Fig. 13 simulates model (3.32) and shows that the mosquito spread from mosquito-persistent patch (right) to mosquito-free patches (left) in a heterogeneous landscape (heterogeneity of hosts and homogeneity of breeding sites), with $\psi(d_{kk'})$ as in (3.31) when patches are highly distanced from each other and close to the maximal distance d_{max} between nodes ($d_{k_3k_4} = 500$ m, $d_{k_5k_1} = 510$ m, $d_{k_3k_1} = 589$ m, $d_{k_3k_2} = 539$ m, $d_{k_3k_5} = 400$ m, $d_{k_2k_5} = 539$ m). From this figure, one observe that mosquito migration rate to distant patches is very low. This is coherent with the known preference of the mosquito dispersal: indeed, according to [34] the dispersal of adult mosquitoes can be classified into long-range and short-range dispersals. Long-range dispersal is often unintentional and aided by wind or human transport while short-range dispersal is often intentional. Furthermore, Fig. 13 shows that the availability and abundance of sites have a strong influence on the distance that individual adult female mosquitoes need to fly in order to lay their eggs, since spatial distance between patches is large when breeding sites are eliminated from neighborhoods of hosts or are not available in most patches. Similar findings were obtained in [23]. Thus, more efforts to reduce breeding sites in close proximity to houses (mechanical control) is needed and can be very efficient as a vector control strategy.

Our simulations results in homogeneous landscape (Eq. (3.12)) and heterogeneous landscape (Eq. (3.32)) reveal that the heterogeneous connectivity of patches plays an important role on the spatial distribution of mosquito population. Simulations in a homogeneous landscape indicate that there is a linear relationship between connectivity of patches and mosquitoes distribution (see Figs. 6 and 9). However, when there are heterogeneities in the network (hosts, distances), this linear relationship is perturbed and induces a strong influence on spatial distribution and population dynamics of mosquitoes (see Figs. 10–13).

5. Conclusion and perspectives

In this paper, we have developed a reaction–diffusion type model to describe the spatial evolution of anopheles mosquito in heterogeneous complex metapopulations and assess the influences of larvae habitats (breeding–feeding sites) connectivity and vector on the spatial distribution and populations dynamics of mosquitoes. We have focused on the migration of

mosquitoes from one patch to another in both homogeneous and heterogeneous landscapes. The spatial configuration was given by the degree $p(k)$ and the conditional probabilities $P(k'|k)$.

For uncorrelated networks in a homogeneous landscape, we have derived an explicit formula for the basic offspring number, $\mathcal{R}_0^{(m)}$, which has been proven to be a sharp threshold parameter for our model. The most influential parameter on the expression for $\mathcal{R}_0^{(m)}$ is the number of eggs at each deposit Φ. Using the theory of monotone operators, we have established the global stability of equilibrium points. Precisely, we have shown that the mosquito-free equilibrium is GAS whenever $\mathcal{R}_0^{(m)} \leq 1$ and unstable otherwise. In the case where $\mathcal{R}_0^{(m)} > 1$, we have shown that there exists a unique mosquito-persistent equilibrium, which is GAS.

For uncorrelated networks in a heterogeneous landscape, we have only carried out numerical studies. Comparing our simulation results in Figs. 6–12, we have concluded that numerous factors considered in our models play important roles in spatial distribution of mosquitoes and could lead to a larger amount of mosquitoes. Further, our sensitivity analysis results have revealed that an efficient strategy to reduce the amount of mosquitoes in all patches could be to control the production of eggs (by mechanical control for example) and minimize the migration of female mosquitoes.

To summarize our contributions in few words, the methodology and results we have obtained are as follows:

- From the modeling perspective, we have extended to a complex network of patches the single patch models in [4,19] by incorporating the dispersal of mosquitoes and patch connectivity.
- From the theoretical and numerical perspectives, we have examined the impacts of larval habitat connectivity and mosquito dispersal in a homogeneous and a heterogeneous landscapes on the persistence of mosquitoes populations.
- From the qualitative and quantitative aspects for uncorrelated networks have obtained the following analytical results:
    1. The bifurcation/threshold parameter (basic offspring number) has been explicitly computed.
    2. The sensitivity analysis of the threshold parameter has been performed.
    3. A simple and digestive proof based on Hethcote–Thieme fixed point theorem [20], of a unique mosquito-persistent equilibrium has been provided.
    4. Contrary to the few existing works where, Lyapunov–LaSalle techniques are usually used, the monotone operator approach [21] has been the main ingredient here, for the establishment of the global asymptotic stability of both mosquito-free and mosquito-persistent equilibria.

An immediate possible extension of this work we are already working on is to consider correlated networks with precise configuration/distribution of patches (i.e., some assortative or assortative networks) and investigate if the techniques used here could be applied to obtain similar theoretical/analytical results. Moreover, since we take into account the male dispersal, another extension of this work could be to consider the Sterile Insect Technique (SIT) in our model by releasing sterilized male mosquitoes near of high-degree patches. We hope our model could be used to develop other possible and efficient vector control strategies, which can optimize the allocation of scarce resources.

Fundings

This research did not receive any specific grant from funding agencies in the public, commercial, or not-for-profit sectors.

Acknowledgments

The authors will like to thank the three anonymous reviewers and the Associate Editor for highly relevant remarks and suggestions that have substantially improved the work.

Appendix A. Proof of Lemma 3.2

Note that the matrix N can be written as

$$N = \begin{bmatrix} N_1 & N_2 \\ N_3 & N_4 \end{bmatrix} = \begin{bmatrix} N_1 & \mathbf{0} \\ N_3 & I \end{bmatrix} \begin{bmatrix} I & N_1^{-1}N_2 \\ \mathbf{0} & D \end{bmatrix}.$$

Then, one can deduce that

$$\begin{aligned} N^{-1} &= \begin{bmatrix} I & N_1^{-1}N_2 \\ \mathbf{0} & D \end{bmatrix}^{-1} \begin{bmatrix} N_1 & \mathbf{0} \\ N_3 & I \end{bmatrix}^{-1} = \begin{bmatrix} I & -N_1^{-1}N_2 D^{-1} \\ \mathbf{0} & D^{-1} \end{bmatrix} \begin{bmatrix} N_1^{-1} & \mathbf{0} \\ -N_3N_1^{-1} & I \end{bmatrix}, \\ &= \begin{bmatrix} N_1^{-1} + N_1^{-1}N_2D^{-1}N_3N_1^{-1} & -N_1^{-1}N_2D^{-1} \\ -D^{-1}N_3N_1^{-1} & D^{-1} \end{bmatrix}. \end{aligned}$$

This ends the proof. □

Appendix B. Proof of Lemma 3.3

It suffices to verified that $GG^{-1} = I_n$. Indeed, one has

$$\begin{aligned}
GG^{-1} &= UU^{-1} - K\left[W^{-1} + ZU^{-1}X\right]^{-1}ZU^{-1} + KWZU^{-1} \\
&\quad - KWZU^{-1}K\left[W^{-1} + ZU^{-1}K\right]^{-1}ZU^{-1}, \\
&= I_n - K\left[\left[W^{-1} + ZU^{-1}K\right]^{-1} + W - WZU^{-1}K\left[W^{-1} + ZU^{-1}K\right]^{-1}\right]ZU^{-1}, \\
&= I_n - KW\left[W^{-1}\left[W^{-1} + ZU^{-1}K\right]^{-1} - I_n + ZU^{-1}K\left[W^{-1} + ZU^{-1}K\right]^{-1}\right]ZU^{-1}, \\
&= I_n - KW\left[\left[W^{-1} + ZU^{-1}K\right]\left[W^{-1} + ZU^{-1}K\right]^{-1} - I_n\right]ZU^{-1}, \\
&= I_n - KW(I_n - I_n)ZU^{-1}, \\
&= I_n.
\end{aligned}$$

This concludes the proof. □

References

[1] World Health Organization, Malaria-Media Centre, http://www.who.int/mediacentre/factsheets/fs094/en/, 2016 (accessed 06.12.16).
[2] H.M. Giles, D.A. Warrel, Bruce-Chwatt's essential malariology, 3rd ed., Heinemann Medical Books, Portsmouth, NH, 1993.
[3] S. Wanji, F.F. Mafo, N. Tendongfor, M.C. Tanga, F. Tchuente, C.F. Bilong Bilong, T. Njine, Spatial distribution, environmental and physicochemical characterization of anopheles breeding sites in the mount cameroon region, J. Vector Borne Dis. 46 (2009) 75–80.
[4] L. Yakob, G. Yan, A network population model of the dynamics and control of African malaria vectors, Trans. R. Soc. Med. Hyg. 104 (10) (2010) 669–675.
[5] A. Lutambi, M.A. Penny, T. Smith, N. Chitnis, Mathematical modelling of mosquito dispersal in a heterogeneous environment, Math. Biosci. 213 (2013) 198–216.
[6] C. Dufourd, Y. Dumont, Impact of environmental factors on mosquito dispersal in the prospect of sterile insect technique control, Comput. Math. Appl. 66 (2013) 1695–1715.
[7] A. Lloyd, R.M. May, Spatial heterogeneity in epidemic models, J. Theor. Biol. 179 (1996) 1–11.
[8] Y. Wang, J. Cao, G. Sun, J. Li, Effect of time delay on pattern dynamics in a spatial epidemic model, Physica A 412 (2014) 137–148.
[9] P. Auger, E. Kouokam, G. Sallet, M. Tchuente, B. Tsanou, The Ross–Macdonald model in a patchy environment, Math. Biosci. 216 (2008) 123–131.
[10] M.E.J. Newman, S.H. Strogatz, D.J. Watt, Random graphs with arbitrary degree distributions and their applications, Phys. Rev. E 64 (2001) 026118.
[11] V. Colizza, A. Vespignani, Invasion threshold in heterogeneous metapopulation networks, Phys. Rev. Lett. 99 (2007) 148701.
[12] V. Colizza, A. Vespignani, Epidemic modeling in metapopulation systems with heterogeneous coupling pattern: theory and simulations, J. Theor. Biol. 251 (2008) 450–457.
[13] J. Saldana, Modelling the spread of infectious diseases in complex metapopulations, Math. Model. Nat. Phenom. 5 (6) (2010) 22–37.
[14] M. Boguna, R. Pastor-Satorras, Epidemic spreading in correlated complex networks, Phys. Rev. E 66 (2002) 047104.
[15] R. Pastor-Satorras, V. Vespignani, Epidemic spreading in scale-free networks, Phys. Rev. Lett. 86 (2001) 3200–3204.
[16] Y. Wang, J. Cao, Global dynamics of a networks epidemic model for waterborne diseases spread, Appl. Math. Comput. 237 (2014) 474–488.
[17] Y. Wang, J. Cao, A. Alofi, A. AL-Mazrooei, A. Elaiw, Revisiting node-based sir models in complex networks with degree correlations, Physica A 437 (2015) 75–88.
[18] J. Cao, Y. Wang, A. Alofi, A. AL-Mazrooei, A. Elaiw, Global stability of an epidemic model with carrier state in heterogeneous networks, IMA J. Appl. Math. 80 (2015) 1025–1048.
[19] R. Anguelov, Y. Dumont, J. Lubuma, Mathematical modeling of sterile insect technology for control of anopheles mosquito, Comput. Math. Appl. 64 (2012) 374–389.
[20] H.W. Hethcote, H.R. Thieme, Stability of the endemic equilibrium in epidemic models with subpopulations, Math. Biosci. 75 (1985) 205–227.
[21] H.J. Smith, Monotone dynamical systems: an introduction to the theory of competitive and cooperative systems (mathematical surveys and monographs), Am. Math. Soc. 41 (1995) 1–174.
[22] N. Chitnis, J.M. Cushin, J.M. Hyman, Bifurcation analysis of a mathematical model for Malaria transmission, SIAM J. Appl. Math. 67 (2006) 24–45.
[23] N. Chitnis, J.M. Hyman, J.M. Cushin, Determining important parameters in the spread through the sensitivity analysis of a mathematical model, Bull. Math. Biol. 70 (2008) 1272–1296.
[24] L. Esteva, H.M. Yang, Mathematical model to assess the control of Aedes aegypti mosquitos by the sterile insect technique, Math. Biosci. 198 (2005) 132–147.
[25] N. Minakawa, P. Seda, G. Yan, Influence of host and larval habitat distribution on the abundance of african malaria vectors in Western Kenya, Am. J. Trop. Med. Hyg. 67 (1) (2002) 32–38.
[26] B.G.J. Knols, J. Meijerink, Odors influence mosquito behavior, Sci. Med. 4 (5) (1997) 56–63.
[27] P. van den Driessche, J. Watmough, Reproduction numbers and sub-threshold endemic equilibria for the compartmental models of disease transmission, Math. Biosci. 180 (2002) 29–48.
[28] M.L. Mann Manyombe, J. Mbang, J. Lubuma, B. Tsanou, Global dynamics of a vaccination model for infectious diseases with asymptomatic carriers, Math. Biosci. Eng. 13 (2016) 813–840.
[29] S. Marino, I.B. Hogue, C.J. Ray, D.E. Kirschner, A methodology for performing global uncertainty and sensitivity analysis in systems biology, J. Theor. Biol. 254 (2008) 178–196.
[30] C. Mwandawiro, M. Boots, N. Tuno, W. Suwonkerd, Y. Tsuda, M. Takagi, Heterogeneity in the host preference of japanese encephalitis vectors in Chiang Mai, Northern Thailand, Trans. R. Soc. Trop. Med. Hyg. 94 (3) (2000) 238–242.
[31] A.N. Clement, The Biology of Mosquitoes: Sensory Reception and Behaviour, 2, CABI Publishing Inc., New York, 1999.
[32] A.M. Reynolds, M.A. Frye, Free-flight odor tracking in drosophila is consistent with an optimal intermittent scale-free search, PLoS One 2 (4) (2007) e354, doi:10.1371/journal.pone.0000354.
[33] J.T. Midega, C.M. Mbogo, H. Mwambi, M.D. Wilson, G. Ojwang, J.M. Mwangangi, J.G. Nzovu, J.I. Githure, G. Yan, J.C. Beier, Estimating dispersal and survival of Anopheles gambia and Anopheles funestus along the Kenyan coast by using mark-release-recapture methods, J. Med. Entomol. 6 (44) (2007) 923–929.
[34] A.R.W. Elbers, C.J.M. Koenraadt, R. Meiswinkel, Mosquitoes and culicoides biting midges: vector range and the influence of climate change, Rev. Sci. Tech. Off. Int. Epizoot. 34 (1) (2015) 123–137.

Received: 25 December 2018

DOI: 10.1002/mma.6136

RESEARCH ARTICLE

WILEY

Mathematical analysis of a spatio-temporal model for the population ecology of anopheles mosquito

Martin Luther Mann Manyombe[1,6] | Joseph Mbang[1,4,5] | Berge Tsanou[2,4,5] | Samuel Bowong[3,4,5] | Jean Lubuma[2]

[1]Department of Mathematics, Faculty of Science, University of Yaounde I, P.O. Box 812 Yaounde, Cameroon

[2]Department of Mathematics and Applied Mathematics, University of Pretoria, 0002 Pretoria, South Africa

[3]Department of Mathematics and Computer Science, University of Douala, P.O. Box 24157, Cameroon

[4]IRD UMI 209 UMMISCO, University of Yaounde I, P.O. Box 337, Cameroon

[5]LIRIMA-EPITAG Team Project, University of Yaounde I, P.O. Box 812 Yaounde, Cameroon

[6]African Center of Excellence in Information and Communication Technologies, University of Yaounde I, Cameroon

Correspondence
Berge Tsanou, Department of Mathematics and Computer Science, University of Dschang, P.O. Box 67 Dschang, Cameroon.
Email: bergetsanou@yahoo.fsr; berge.tsanou@univ-dschang.org

Communicated by: J. Banasiak

Funding information
University of Pretoria, Grant/Award Number: Senior Postdoctoral Programme Grant (2017-2020)

We propose a novel model for the population dynamics of mosquitoes by considering the dispersal states of female mosquitoes of oviposition's cycle and spatial variations. From the modeling perspective, a general functional form of eggs oviposition rate is used including the Malthusian, the Verhlust-Pearl logistic, the Hassell, and the Maynard-Smith-Slatkin functions. From the theoretical and numerical perspectives, the study is done in two steps using the more realistic birth Maynard-Smith-Slatkin function. First, we consider an ordinary differential equations model and show that the mosquito-free equilibrium (MFE) is globally asymptotically stable, whenever the basic offspring number $\mathcal{R}_0^{ode}$ is less than unity. Using a fluctuation argument, we prove that the unique mosquito-persistent equilibrium (MPE) is globally attractive, whenever $\mathcal{R}_0^{ode}$ exceeds the unity. Moreover, the temporal model undergoes a Hopf bifurcation in the absence of density-dependent mortality in the aquatic stage of mosquitoes. Second, the temporal model is extended into an advection-reaction-diffusion model in order to account for the movement of mosquitoes and their spatial source of heterogeneity. We establish the uniform persistence and the existence of at least one positive steady state whenever the spatial basic offspring number $\mathcal{R}_0^{pde}$ is greater than unity. Finally, for the case study of malaria vector agent (*Anopheles* mosquito), we construct a nonstandard finite difference scheme that is dynamically consistent with the features of the continuous model to illustrate our results, including the spatial heterogeneity of mosquito resources.

KEYWORDS

Anopheles mosquito, Basic offspring number, Fluctuation method, Global Stability, Nonstandard method, Spatial heterogeneity

MSC CLASSIFICATION

92B30; 34C23; 92C45

1 | INTRODUCTION

Among all infectious diseases of humans, vector-borne diseases (VBDs) constitute a major cause of human mortality and morbidity. They account for 17% of the estimated global burden of all infectious diseases.[1,2] Mosquitoes are the best known vectors of such diseases. They are responsible for many diseases throughout the world, such as malaria, yellow fever, chikungunya, west Nile virus, dengue fever, Zika virus, and other arboviruses.[3,4] These diseases are transmitted

from human to human through effective mosquito bite. The transmission cycle is essentially driven by the human bite habit of the mosquito.[5] Typically, the vector interacts with a human being. Then depending on the disease status of both organisms, they will either infect or be infected. Due to the significant burden caused by mosquitoes on human health, specifically as reflected through the persistence and/or resurgence of vector-borne diseases, mosquitoes have become a target of medical, veterinary, and conservation research since the nineteenth century.[6] In order to devise effective control and realistic control methods, it is crucial and essential to study the mosquitoes population dynamics, their interaction with their biotope, and subsequently the epidemiology of mosquito-borne diseases.[7,8] Like many other insect species, mosquitoes can move and disperse in any direction for various reasons such as searching for resource availability. At local scales (ie from 100 m to 1 km), mosquito behavior and ecology play an important role in determining the distribution of transmission.[9] The spatial distribution of *anopheles* has shown great potential to affect malaria transmission intensity.[8,10] The success and optimal impact of methods for controlling mosquito population (eg sterile insect technique [SIT], genetically modified mosquitoes [GMM] or mechanical control) are based on a good knowledge of the biology and the behavior of mosquitoes, as well as on an accurate modeling of their dispersal. Thus, to achieve a high level of effectiveness in reducing the mosquito population, control interventions should consider mosquito location and its ability to move. In view of the challenge and high costs to conduct field experiments, mathematical modeling adds value to validate and improve vector control strategies. Mathematical models have proven to be useful in gaining insights into the interactive dynamics[11] and control of mosquito populations,[5,6,12-16] as well as into the influence of mosquito mobility and dispersal.[7,9,17-23] Partial differential equations (PDEs) constitute a classical setting to model real-life situations such as dispersal.[10,24,25] For linear PDEs, the theory and the corresponding constructive treatment by numerical methods are well developed (see for instance the famous books[26-32]). However, the complexity of biological processes and particularly the strong nonlinearity in the transmission dynamics of diseases in time and space lead to mathematical challenging nonlinear PDEs, which include advection-reaction-diffusion equations and cross-diffusion equations.[33,34] It is therefore not surprising that the authors could identify only very few PDEs models on mosquito population dynamics that have investigated the well-posedness and the asymptotic behavior of the solutions.[18-23] A metapopulation setting has been used in[7,9] for *anopheles* mosquito population dynamics as an intermediate approach between temporal and spatio-temporal modeling. To explore the temporal and spatial dispersal of the mosquitoes, the authors in[20-23] proposed advection-reaction-diffusion models where the mosquito population is divided into two stages: aquatic and adult female stages. These studies gave sufficient conditions for mosquitoes to persist and spread or to vanish. However, the oviposition/gonotrophic cycle has been recognized as an important feature that may determine population levels, distribution, and biting behavior of mosquitoes. Thus, it is necessary to take into account all stages in the gonotrophic cycle (questing, resting, and breeding females) for the adult female mosquitoes in order to get insights into the behavior and dynamics of mosquitoes. The ultimate purpose of this paper is to extend the works,[20-23] as well as the temporal models in[6,12,13] into an advection-reaction-diffusion system in which spatial heterogeneity is taken into consideration explicitly. Heterogeneity in the behaviour of *anopheles* mosquitoes is present in all malaria endemic regions. Some species of mosquito prefer human blood (anthropophilic), while others prefer animal blood (zoophilic). Another species, depending on the geographical region, have both anthropophilic and zoophilic tendencies.[35] However, different factors can influence the behaviour of the *anopheles* mosquitoes. For example, host availability plays an important factor in the final host choice of the vector. Thus, *anopheles* mosquitoes can adapt their host choice in case of a lower availability of human hosts.[35] So, given that the dynamics of indirectly transmitted infectious diseases of humans is driven, in the most part, by the human biting rate of the vector, it is necessary to understand the dynamics of populations for those disease vectors themselves by carefully analyzing the dynamics of the human-vector interaction and how this interaction drives the population dynamics of the vector. Hence, similar to the models in,[5,6,16] we derive a more general mathematical model for the population dynamics of *anopheles* mosquitoes that feed on human blood but breed outside the human body at a distinct spatial location, far away from the human habitats. We develop models that incorporate both intrinsic dynamics and spatial variation of mosquitoes, taking into consideration the dynamics of the human-vector interaction. We will start with a temporal model that allows a general description of the mosquito's growth. This initial model captures the mosquito oviposition cycle as well as its main behavior (which could be useful when one considers chemical or biological control tools, such as SIT or GMM). Moreover, unlike the works in,[7,13,18] where a constant generating rate was used for the population in the aquatic stage, we consider a more general function for egg oviposition rate. Next, we will extend the obtained temporal model to a PDE system by adding both advection and diffusion terms that reflect mosquito's mobility. We study the global well-posedness and the asymptotic behavior of the solutions of this PDE model. Finally, we assess the impact of mosquito dispersal, heterogeneous distribution of mosquito resources (hosts), and other parameters on the spatial distribution, dynamics, and persistence of mosquito populations.

As mentioned earlier, the nonlinearity of the ordinary differential equation (ODE) model and its extended PDE counterpart results in challenging mathematical equations. This necessitates, on the one hand, the use of a variety of techniques, methods, and approaches including Lyapunov-Lasalle techniques, monotone dynamical systems approach, semigroup applications, fluctuation method, and spectral theory approach. On the other hand, reliable numerical methods being of paramount importance for the type of complex models investigated in this work, we have constructed nonstandard finite difference schemes, which to our knowledge have never been studied for malaria models in the framework of partial differential equations. The paper is organized as follows. In Section 2, we present a compartmental temporal model, which is analyzed quantitatively (eg existence/uniqueness of positive solutions, existence of equilibria points, etc.) and qualitatively (eg global stability of equilibria and existence of Hopf bifurcation). In Section 3, we extend the temporal model to an advection-reaction-diffusion system of equations, the global well-posedness, the asymptotic behavior, and the threshold-type dynamics of which are investigated. In Subsection 3.4, a case study is handled, namely malaria which is the world's most devastating parasitic infectious disease caused by *anopheles* mosquitoes as vector agents. We develop a nonstandard finite difference (NFSD) scheme, which is dynamically consistent with the continuous model as illustrated by numerical simulations in which parameters relevant to the population biology of adult female *anopheles* mosquitoes are used. Concluding remarks that show how our findings fit in the literature and a brief discussion are provided in Section 4.

2 | TEMPORAL MODEL

2.1 | Model formulation

It is well known that there are two main stages in the development of mosquitoes represented by the aquatic and the adult stages. The aquatic stage, reduced to one compartment (A), gathers eggs, larvae, and pupae.[13,18] The adult stage is divided into five compartments including four for females and one for males as follows: immature females (Y), feeding/questing females (Q), resting females (U), breeding females (W) (or more precisely "egg laying females"), and males (M). We assume that there is no sex differences for mosquitoes in the aquatic stage. Moreover, after emergence, mosquitoes are distributed between the immature female and the male compartments. We denote by r the sex ratio of emerging females. According to,[36] r can be set to $\frac{1}{2}$ in the case when the number of emerging females and males is balanced. We further assume that a female mates only once with a male during her lifespan. After mating, immature females start their gonotrophic cycle by entering the feeding female compartment.[37] The gonotrophic cycle starts with a blood meal and ends with the first laid egg.[37] Then, after blood meals, females progress to the resting compartment, allowing egg maturation. Afterward, they pass into the breeding compartment, seeking for a breeding site to deposit eggs. Once eggs are deposited, these females start a new gonotrophic cycle. The eggs laid by the breeding females supply the aquatic stage. Note that unlike female mosquitoes where four subcompartments are considered due to their involvement in the gonotrophic cycle, we only consider one compartment for the males.

At time t, and following,[16,38] we assume that the population in the aquatic stage is generated from breeding females by a decreasing, continuously differentiable and positive function that is a general form of the eggs oviposition. The population in the aquatic stage is decreased by maturation to adult mosquitoes (at the rate Γ), density-independent mortality (at the rate μ_1), and density-dependent mortality (at the rate μ_2). After emergence, immature females (Y) need successful mating. The number of matings that occur per unit of time is β (mating rate). Actually, β can be regarded as the product of the likelihood of a mating producing eggs, the (fixed) proportion of the population that is female, the likelihood that an appropriate place can be found so that, when the eggs are laid, they will certainly hatch. Also, when the number of males is large, we expect that immature females will have no difficulty finding a mate.[13,18] Thus, after mating with males, immature females exit breeding sites and arrive at the human habitats where they become feeding/questing females Q at rate β. At the human habitat, questing females interact with humans by mass action contact, during which they can either survive to reproduce or get killed.[5,16] Questing females that feed successfully become resting females at rate $\alpha\varphi H$, where φ is the biting rate of questing females, α ($\alpha \in [0, 1]$) is the probability of successfully taking a blood meal, and H is a parameter representing the density of human habitats. Questing females die at rate μ_Q. Once settled, resting females become breeding females at rate a and die at rate μ_U. The compartment of breeding females is affected by a mortality rate μ_W. After laying eggs, breeding females (W) from the breeding site can make visits to humans at human habitat sites in search for a blood meal at rate $b > 0$, which also represents the rate at which breeding females leave the site to restart their gonotrophic cycle. We assume here that the decision to visit a particular human is influenced solely by the presence of a human at the human habitat site. Therefore, from the breeding site, breeding females are actually attracted to humans and enter in the questing class at rate $\frac{bH}{H+K}$, where $\frac{H}{H+K}$ represents the proportion of humans that are visited by breeding

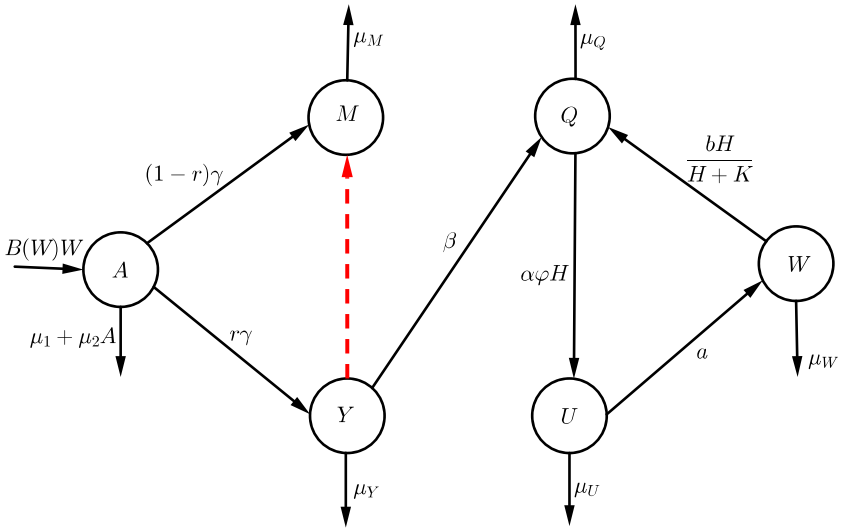

FIGURE 1 *Anopheles* mosquito simplified life cycle. The dashed arrow indicates the mating between male and immature female mosquitoes

vectors.[6,16,39] K is a positive constant representing a constant alternative food source for the site. Thus, $b\frac{H}{H+K}W$ is the density of breeding females, which after laying eggs are attracted by human hosts. The above-mentioned biological and entomological descriptions lead to the following deterministic and autonomous system of nonlinear differential equations whose flow diagram, state variables, and parameters are given in Figure 1 and in Table 1, respectively:

$$\begin{cases} \dot{A} &= B(W)W - [\Gamma + \mu_1 + \mu_2 A]A, \\ \dot{Y} &= r\Gamma A - [\mu_Y + \beta]Y, \\ \dot{M} &= (1-r)\Gamma A - \mu_M M, \\ \dot{Q} &= \beta Y + \frac{bH}{H+K}W - [\alpha\varphi H + \mu_Q]Q, \\ \dot{U} &= \alpha\varphi HQ - [a + \mu_U]U, \\ \dot{W} &= aU - \left[\frac{bH}{H+K} + \mu_W\right]W. \end{cases} \tag{1}$$

In this study, $B(W)$ is the general form of the eggs oviposition function. It is assumed that function $B(W)$ is strictly nonnegative, continuously differentiable, and satisfies the following conditions:

$$\begin{aligned} &\bullet\ B(0) = N_{egg}, \\ &\bullet\ B'(W) \leq 0,\ \forall W \geq 0, \\ &\bullet\ B(W)W \text{ is monotone or bounded by } N_{egg}L, \end{aligned} \tag{2}$$

where, N_{egg} is the average number of eggs laid per fertilized female per day, and $L > 0$ is the environmental carrying capacity of fertilized females. Let $\mathcal{R}_0^{ode}$ denotes the basic offspring number of model (1) and $F_{\mathcal{R}_0^{ode}}$ the function given by

$$F_{\mathcal{R}_0^{ode}}(s) = \nu_1 \mathcal{R}_0^{ode} B\left(\frac{\nu_1 \mathcal{R}_0^{ode}}{N_{egg}} s\right) - N_{egg}(\nu_1 + \mu_2 s),\ \forall \quad s \geq 0, \tag{3}$$

where ν_1 is defined below in (5). We further assume that the general egg oviposition function B is such that

$$F_{\mathcal{R}_0^{ode}}(0) F_{\mathcal{R}_0^{ode}}(+\infty) < 0,\ \text{when } \mathcal{R}_0^{ode} > 1. \tag{4}$$

In Table 2, we have gathered typical examples of function $B(W)$, which are used in the literature.

TABLE 1 Examples of oviposition function $B(W)$ used in the literature which satisfy (2)-(4)

Names	$\boldsymbol{B(W)}$	$\boldsymbol{B}(0)$	$F_{\mathcal{R}_0^{ode}}(0)$	$F_{\mathcal{R}_0^{ode}}(+\infty)$	**Sources**
Malthus (B_M)	N_{egg}	N_{egg}	$\nu_1 N_{egg}\left(\mathcal{R}_0^{ode}-1\right)$	$-\infty$	13,38
Verhulst-Pearl logistic (B_L)	$N_{egg}\left(1-\frac{W}{L}\right), \quad W<L$	N_{egg}	$\nu_1 N_{egg}\left(\mathcal{R}_0^{ode}-1\right)$	$-\infty$	12,16,38,40
Maynard-Smith-Slatkin (B_S)	$\frac{N_{egg}}{1+\left(\frac{W}{L}\right)^n}, \quad n>0$	N_{egg}	$\nu_1 N_{egg}\left(\mathcal{R}_0^{ode}-1\right)$	$-\infty$	12,16,38,40
Hassell (B_H)	$\frac{N_{egg}}{\left(1+\frac{W}{L}\right)^n}, \quad n>0$	N_{egg}	$\nu_1 N_{egg}\left(\mathcal{R}_0^{ode}-1\right)$	$-\infty$	40

TABLE 2 Description of state variables and parameters of model (1)

Variables	**Description**
A	Population in the aquatic stage (eggs, larvae, pupae).
Y	Population of immature females not yet laying eggs.
M	Population of males.
Q	Population of feeding females.
U	Population of resting females.
W	Population of breeding females.

Parameters	**Description**
r	Fraction of the emerging female mosquitoes.
Γ	Rate of emerging mosquitoes from the aquatic stage.
N_{egg}	Number of eggs at each deposit per capita.
L	Environmental carrying capacity of female adult mosquitoes.
β	Transfer rate (mating rate) from the compartment Y to Q
μ_2	Density-dependent mortality rate in the aquatic stage.
μ_1	Mortality rate in the aquatic stage.
μ_M	Mortality rate of male mosquitoes.
μ_Y	Mortality rate of immature females.
μ_Q	Mortality rate of questing females.
μ_U	Mortality rate of resting females.
μ_W	Mortality rate of breeding females.
φ	Biting rate of feeding females.
α	Probability of successfully taking a blood meal.
H	Constant population density of humans at human resource sites.
K	Constant alternative of blood meal for vectors.
b	Rate at which breeding females leave the site to restart their gonotrophic cycle.
a	Rate at which resting females become breeding females.

We point out that the model (1) extends some of the existing models in many respects. Unlike,[7,12,13] it incorporates the gonotrophic cycle of adult female mosquito population. It further extends the model in[6,7,12,13] by incorporating the more general egg oviposition function (a new birth rate function for modeling mosquito oviposition is proposed). Moreover, due to gonotrophic cycle, more particularly to the equation of questing females (Q), our model is different from stage-structured models in.[11,41]

Remark 1. From the ecological point of view, it is well known that the Maynard-Smith-Slatkin oviposition function is more suitable to model the mosquito oviposition rate, compared with the Malthus and Verhulst-Pearl logistic functions.[12,16] Therefore, the latter function will be our focus throughout the theoretical and numerical investigations in this work, with one of the main target of solving the opened problem in[6,12] regarding the global asymptotic stability of the MPE. However, our results can readily apply to the Hassell oviposition function,[40] whereas for Malthus and Verhulst-Pearl functions, we refer the reader to.[5,12,13,16]

2.2 | Basic properties

In this section, the basic properties of model (1) are explored. Model (1) takes the matrix form $\dot{X} = \mathcal{A}(X)X$, where $X(t) = (A(t), Y(t), M(t), Q(t), U(t), W(t))^T$,

$$\mathcal{A}(X) = \begin{pmatrix} -[\nu_1 + \mu_2 A] & 0 & 0 & 0 & 0 & B(W) \\ r\Gamma & -\nu_2 & 0 & 0 & 0 & 0 \\ (1-r)\Gamma & 0 & -\mu_M & 0 & 0 & 0 \\ 0 & \beta & 0 & -\nu_3 & 0 & b_1 \\ 0 & 0 & 0 & \alpha\varphi_1 & -\nu_4 & 0 \\ 0 & 0 & 0 & 0 & a & -\nu_5 \end{pmatrix},$$

and

$$\nu_1 = \Gamma + \mu_1,\ \nu_2 = \mu_Y + \beta,\ \varphi_1 = \varphi H,\ \nu_3 = \alpha\varphi_1 + \mu_Q,\ b_1 = \frac{bH}{H+K},\ \nu_4 = a + \mu_U,\ \nu_5 = \mu_W + b_1. \tag{5}$$

Since all the parameters are positive, the right-hand side of system (1)-(2) is locally Lipschitz continuous; there exists a local solution. To show that solutions that start in $\mathbb{R}^6_+$ stay in $\mathbb{R}^6_+$ in forward time as long as they exist, we use Theorem 3.2 in[11] since for all $X \in \mathbb{R}^6_+$, $B(X)X \leq N_{egg}\|X\|$. Then, for each $X(0) = X_0 \in \mathbb{R}^6_+$, there exists a unique solution $X : \mathbb{R}^6_+ \to \mathbb{R}^6_+$ with $X(0) = X_0$. Thus, the analysis of the model can be carried out in the following invariant region

$$\Gamma = \left\{(A, Y, M, Q, U, W) \in \mathbb{R}^6 \quad : \quad A(t), Y(t), M(t), Q(t), U(t), W(t) \geq 0\right\}.$$

The invariance of Γ implies that all solutions of (1) with nonnegative initial data remain nonnegative for all $t \geq 0$. To be more precise, one has the following result.

Theorem 1. *Denote $\mu_v = \min\left\{\mu_1, \mu_Y, \mu_M, \mu_Q, \mu_U, \mu_W\right\}$. Then the model (1) is a dynamical system in the region*

$$\Gamma_L = \left\{(A, Y, M, Q, U, W) \in \Gamma : \quad V(t) \leq \frac{N_{egg}L}{\mu_v}\right\}.$$

Proof. Define the total mosquito population

$$V(t) = A(t) + Y(t) + M(t) + Q(t) + U(t) + W(t).$$

Add all the terms on the right-hand side of (1). Then, it follows that

$$\dot{V}(t) \leq B(W)W - \mu_v V(t). \tag{6}$$

Using assumption (2), one has $B(W)W \leq N_{egg}L$, which yields

$$\dot{V}(t) \leq N_{egg}L - \mu_v V(t).$$

Thus,

$$\lim_{t\to\infty} \sup(A(t) + Y(t) + M(t) + Q(t) + U(t) + W(t)) \leq \frac{N_{egg}L}{\mu_v}.$$

We conclude that every solution of (1) is bounded, and consequently, the initial value problem associated with system (1) has a unique solution defined for all $t > 0$. □

Theorem 1 implies that system (1) is mathematically and ecologically well-posed.

2.3 | The MFE and basic offspring number $\mathcal{R}_0^{ode}$

Model (1) has a trivial equilibrium or mosquito-free equilibrium (MFE) $\mathcal{T}_0 = (0, 0, 0, 0, 0, 0)$, which is obtained by setting the right-hand side of (1) to zero. Thanks to the next generation approach,[42] the associated basic offspring number $\mathcal{R}_0^{ode}$ of (1) is given by

$$\mathcal{R}_0^{ode} = \frac{N_{egg}r\Gamma\beta\alpha\varphi_1 a}{\nu_1\nu_2 m_1}, \tag{7}$$

where for notational convenience, we have set

$$m_1 = a\alpha\varphi_1\mu_W + \nu_5\left[\alpha\varphi_1\mu_U + \mu_Q\nu_4\right]; \quad m_2 = \nu_1\nu_2 m_1\left(1 - \frac{1}{\mathcal{R}_0^{ode}}\right). \tag{8}$$

Remark 2. The threshold quantity $\mathcal{R}_0^{ode}$ measures the average expected number of new adult female offsprings produced by a single female mosquito during its lifespan. It can be ecologically interpreted as the product of the fraction of mosquitoes in aquatic stage that survived to become immature female mosquitoes $\left(\frac{N_{egg}r\Gamma}{\nu_1}\right)$, the fraction of immature females that survived and start their gonotrophic cycle by entering the questing female compartment $\left(\frac{\beta}{\nu_2}\right)$, and the fraction of fertilized adult females that survived and completed their gonotrophic cycle $\left(\frac{\alpha\varphi_1 a}{m_1}\right)$.

Following Theorem 2 in,[42] one has:

Lemma 1. *The trivial equilibrium or MFE $\mathcal{T}_0$ of system (1) is locally asymptotically stable (LAS), whenever $\mathcal{R}_0^{ode} < 1$, and unstable otherwise.*

Ecologically speaking, Lemma 1 implies that mosquitoes can be eliminated if the initial sizes of the population of *anopheles* mosquitoes are in the basin of attraction of the MFE $\mathcal{T}_0$. Thus, the mosquito population can be effectively controlled if $\mathcal{R}_0^{ode} < 1$. To ensure that the effective control of the mosquito population is independent of the initial size of the mosquito population, a global asymptotic stability result must be established for the trivial equilibrium.

Theorem 2. *The MFE $\mathcal{T}_0$ of system (1) is globally asymptotically stable (GAS) in Γ, whenever $\mathcal{R}_0^{ode} \leq 1$.*

Proof. Thanks to the boundedness of solutions, we use the reduction theorem by Vidyasagar.[43] Denote $y(t) = (A(t), Y(t), Q(t), U(t), W(t))^T$ and $z(t) = M(t)$. Then system (1) takes the form

$$\begin{cases} \frac{dy}{dt} = f(y), \\ \frac{dz}{dt} = g(y,z). \end{cases} \tag{9}$$

Let us first show that the equilibrium $0_5 = (0,0,0,0,0)$ is GAS for the subsystem $\frac{dy}{dt} = f(y)$. Consider the Lyapunov function

$$V_0(y) = \frac{1}{\nu_1}\left[r\Gamma A + \nu_1 Y\right] + \frac{\nu_2}{\beta\alpha\varphi_1}\left[\alpha\varphi_1 Q + \nu_3 U\right] + \frac{\nu_2\nu_3\nu_4}{a\beta\alpha\varphi_1}W.$$

It is obvious that $V_0(0) = 0$, and $V_0(y) > 0$, for all $y > 0$. Moreover,

$$\begin{aligned} \dot{V}_0(y) &= \tfrac{1}{\nu_1}\left[r\Gamma\dot{A} + \nu_1\dot{Y}\right] + \tfrac{\nu_2}{\beta\alpha\varphi_1}\left[\alpha\varphi_1\dot{Q} + \nu_3\dot{U}\right] + \tfrac{\nu_2\nu_3\nu_4}{a\beta\alpha\varphi_1}\dot{W}, \\ &= \tfrac{1}{\nu_1}\left[r\Gamma B(W)W - \nu_1\nu_2 Y - r\Gamma\mu_2 A^2\right] + \tfrac{\nu_2}{\beta\alpha\varphi_1}\left[\alpha\varphi_1\beta Y + b_1\alpha\varphi_1 W - \nu_3\nu_4 U\right] + \tfrac{\nu_2\nu_3\nu_4}{a\beta\alpha\varphi_1}\left[aU - \nu_5 W\right], \\ &= \left[\frac{r\Gamma}{\nu_1}B(W)W + \frac{\nu_2 b_1}{\beta} - \frac{\nu_2\nu_3\nu_4\nu_5}{a\beta\alpha\varphi_1}\right]W - \frac{r\Gamma\mu_2}{\nu_1}A^2, \\ &= -\frac{r\Gamma N_{egg}}{\nu_1\mathcal{R}_0^{ode}}\left[1 - \frac{\mathcal{R}_0^{ode}}{N_{egg}}B(W)\right]W - \frac{r\Gamma\mu_2}{\nu_1}A^2. \end{aligned}$$

Since, $\max_W B(W) \leq N_{egg}$ and $\mathcal{R}_0^{ode} \leq 1$, we have $\frac{\mathcal{R}_0^{ode}}{N_{egg}}B(W) < 1$. Hence, $\dot{V}(y) \leq 0$. On the other hand, let $\mathcal{H}$ be the largest invariant set such that $\mathcal{H} \subset \{(A,Y,Q,U,W) \in \mathbb{R}_+^5 / \dot{V}_0(y) = 0\}$. Then $\mathcal{H} = \{\mathbf{0_5}\}$. Thus, by the LaSalle Invariance Principle, we deduce that 0_5 is GAS in $\mathbb{R}_+^5$ for system $\frac{dy}{dt} = f(y)$. Finally, using the fact 0 is GAS in $\mathbb{R}_+$ for system $\frac{dz}{dt} = g(\mathbf{0_5}, z)$, we conclude that $\mathcal{T}_0$ is GAS in Γ. This completes the proof. □

2.4 | The non-trivial equilibrium or MPE

2.4.1 | Existence and uniqueness

The existence and stability of an MPE of the system (1) are addressed. Let such a MPE be denoted by $\mathcal{T}^* = (A^*, Y^*, M^*, Q^*, U^*, W^*)^T$. Then $A^*, Y^*, M^*, Q^*, U^*, W^*$ are

$$\begin{cases} Y^* = \frac{r\Gamma}{\nu_2}A^*, \quad M^* = \frac{(1-r)\Gamma}{\mu_M}A^*, \quad Q^* = \frac{\nu_1\nu_4\nu_5\mathcal{R}_0^{ode}}{aN_{egg}\alpha\varphi_1}A^*, \\ U^* = \frac{\nu_1\nu_5\mathcal{R}_0^{ode}}{aN_{egg}}A^*, \quad W^* = \frac{\nu_1\mathcal{R}_0^{ode}}{N_{egg}}A^*, \end{cases} \tag{10}$$

where A^* is a positive solution of the equation $F_{\mathcal{R}_0^{ode}}(A^*) = 0$, where the function $F_{\mathcal{R}_0^{ode}}$ is given in Equation (3). Notice that $F_{\mathcal{R}_0^{ode}}(0) = \nu_1 N_{egg}(\mathcal{R}_0^{ode} - 1) > 0$ whenever $\mathcal{R}_0^{ode} > 1$, $F_{\mathcal{R}_0^{ode}}(+\infty) = -\infty$, and $F_{\mathcal{R}_0^{ode}}$ is continuous and strictly decreasing on interval $]0; +\infty[$. Thus, by the intermediate value theorem, $F_{\mathcal{R}_0^{ode}}$ vanishes exactly once in $]0; +\infty[$. This proves the existence and uniqueness of a positive A^* when $\mathcal{R}_0^{ode} > 1$. Replacing the value of A^* in (10) yields the existence and uniqueness of $\mathcal{T}^*$. This result is summarized as follows.

Theorem 3. *Model (1) has a unique MPE $\mathcal{T}^*$ whenever $\mathcal{R}_0^{ode} > 1$. Moreover, for the special case B_S and in the absence of density dependent mortality (ie $\mu_2 = 0$), the unique solution of $F_{\mathcal{R}_0^{ode}}(A^*) = 0$ is explicitly given by*

$$A^* = \frac{N_{egg}L}{\nu_1\mathcal{R}_0^{ode}}\left(\mathcal{R}_0^{ode} - 1\right)^{\frac{1}{n}}. \tag{11}$$

Remark 3. Similar to,[44] it can be easily proved that (a) the GAS of $\mathcal{T}_0$ given in Theorem 2, (b) the instability of $\mathcal{T}_0$ shown in Lemma 1, (c) the existence of a unique MPE $\mathcal{T}^*$ established by Theorem 3 whenever $\mathcal{R}_0^{ode} > 1$, and (d) the fact that $\mathcal{T}_0 \in \partial\Gamma$ imply the persistence of system (1).

2.4.2 | Local stability and existence of Hopf bifurcation for the special case where $\mu_2 = 0$

Theorem 4. *Consider model (1) subject to the Maynard-Smith-Slatkin oviposition function (B_S) with $\mu_2 = 0$. Then, there exists two thresholds n_0^* and n_0^{**} such that*

1. The MPE $\mathcal{T}^*$ is LAS in $\Gamma \setminus \{\mathcal{T}_0\}$ whenever $\mathcal{R}_0^{ode} > 1$ and $1 < n < \min\{n_0^*, n_0^{**}\}$.
2. The system (1) undergoes a Hopf bifurcation whenever n crosses the critical value n_0^{**}.

The proof of Theorem 4 is provided in Appendix B, where the values of n_0^* and n_0^{**} are specified. Theorem 4 is numerically illustrated by Figure 2. The LAS of $\mathcal{T}^*$ is depicted in Figure 2A and shows that, without competition in the aquatic stage (ie $\mu_2 = 0$), the mosquito population will persist as long as $\mathcal{R}_0^{ode} > 1$ and $1 < n < \min\{n_0^*, n_0^{**}\}$. On the other hand, the Hopf bifurcation shown by Figure 2B proves that sustained oscillations are possible when $\mu_2 = 0$. Moreover, Figure 2B suggests that, if competition is negligible in the aquatic stage (ie $\mu_2 = 0$), the solutions of model (1) converge to a periodic solution, whenever $n > n_0^{**}$. This is in agreement with the studies in.[6,12,16]

2.4.3 | Global stability

We explore the global asymptotic property of the MPE $\mathcal{T}^*$ of model (1) with density dependent mortality in the aquatic stage (ie $\mu_2 > 0$).

Theorem 5. *Consider the system (1) subject to the Maynard-Smith-Slatkin oviposition function (B_S) with n = 1. Then, the MPE $\mathcal{T}^*$ is GAS in $\Gamma \setminus \{\mathcal{T}_0\}$ whenever $\mathcal{R}_0^{ode} > 1$.*

The proof of Theorem 5 can be cheaply done, thanks to the monotone (cooperative) properties of system (1). It can also be proven by Lyapunov-LaSalle techniques, with the construction of a suitable Lyapunov function of Goh-Volterra type. The latter proof is provided in Appendix C. Unfortunately, for the case n > 1, none of these latter theories can easily apply. This is because, due to high nonlinearity, the system (1) is neither cooperative nor amenable for Lyapunov-LaSalle techniques. Alternatively, to prove the global attractivity of $\mathcal{T}^*$ when n > 1, we shall adopt a generic approach (which can also apply for n = 1) based on a fluctuation argument.[41,45-47] We shall construct two monotone convergent sequences

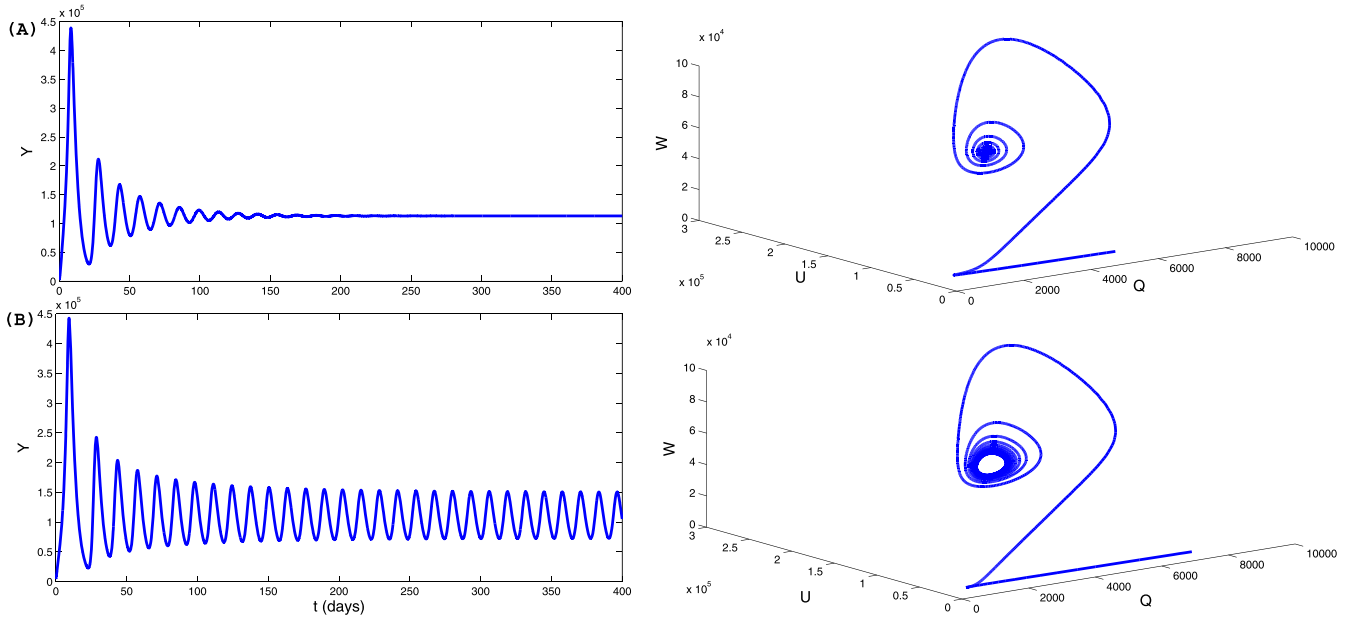

FIGURE 2 **(A)** Locally asymptotically stable (LAS) of $\mathcal{T}^*$ for model (1) with $\mu_2 = 0$, n = 10, and $N_{egg} = 25$ (so that $\mathcal{R}_0^{ode} = 13.9399 > 1$ and $n_0^{**} = 12.4606$). **(B)** Hopf bifurcation in model (1) around of the mosquito-persistent equilibrium (MPE) $\mathcal{T}^*$ with $\mu_2 = 0$, n = 13, and $N_{egg} = 25$ (so that $\mathcal{R}_0^{ode} = 13.9399 > 1$ and $n_0^{**} = 12.4606$). All other parameters are as in Table 4 [Colour figure can be viewed at wileyonlinelibrary.com]

such that one is the upper bound and the other is the lower bound of the constant solution $\mathcal{T}^*$. Moreover, the constructed sequences must share the same limit. Before the implementation of the above-mentioned approach, let us give some useful preliminaries. For two vectors $a, b \in \mathbb{R}^5$, we write: $a \geq b$ if $a_i \geq b_i$; $a > b$ if $a \geq b$ and $a \neq b$ and $a \gg b$ if $a_i > b_i$. Let $y = (A, Y, Q, U, W)^T = (y_1, y_2, y_3, y_4, y_5)^T \in \mathbb{R}^5_+$, $g \geq 0$ be any nonnegative quantity and

$$F(y,g) = \begin{pmatrix} gW - (\nu_1 + \mu_2 A)A \\ r\Gamma A - \nu_2 Y \\ \beta Y + b_1 W - \nu_3 Q \\ \alpha\varphi_1 Q - \nu_4 U \\ aU - \nu_5 W \end{pmatrix}.$$

Consider the system

$$\frac{dy}{dt} = F(y,g). \tag{12}$$

One can easily verify that the function F satisfies the following conditions:

1. F is cooperative on $\mathbb{R}^5_+$ and $DF(y,g)$ is irreducible for every $y \in \mathbb{R}^5_+$;
2. $F(0,g) = 0$ and $F_i(y,g) \geq 0$ for all $y \in \mathbb{R}^5_+$ with $y_i = 0$, $i = 1, 2, \ldots, 5$;
3. F is strictly sublinear on $\mathbb{R}^5_+$.

Thus, thanks to[48] (Corollary 3.2), the following result holds.

Lemma 2. *Consider the system (12). Denote* $s(DF(0,g)) = s(F'_y(0,g)) = \max\{Re\lambda : det(\lambda I_5 - DF(0,g)) = 0\}$, *the stability modulus of the matrix* $DF(0,g)$. *Then,*

1. *If* $s(DF(0,g)) \leq 0$, *then* $y = 0$ *is GAS in* $\mathbb{R}^5_+$.
2. *If* $s(DF(0,g)) > 0$, *then* $\frac{dy}{dt} = F(y,g)$ *admits a unique positive equilibrium* $y^*(g)$ *which is GAS in* $\mathbb{R}^5_+ \setminus \{0\}$.

To stress the dependence of $\mathcal{T}^*$ on the oviposition function $B(W)$, we denote $\mathcal{T}^* = \mathcal{T}^*(B(W^*))$.

Remark 4. In the case when $s(DF(0,g)) > 0$, the positive equilibrium $y^*(g)$ is an increasing function of g, that is $g_1 > g_2$ implies $y^*(g_1) \gg y^*(g_2)$. Indeed, by the comparison principle, we prove that $y^*(g_1) \geq y^*(g_2)$ and use condition (1) above to conclude (since F is strongly monotone[49]) that $y^*(g_1) \gg y^*(g_2)$. Furthermore, by setting $g = B(0) = N_{egg}$,

Theorem 5 with $B(W)$ replaced by $B(0) = N_{egg}$ and item (2) of Lemma 2 imply that, for $\mathcal{R}_0^{ode} > 1$ (or equivalently, $s(DF(0, B(0))) > 0$), there is a MPE $y^*(B(0)) = \mathcal{T}^*(B(0))$ which is GAS for the system $\frac{dy}{dt} = F(y, B(0))$.

Denote

$$x^{(1)} = \mathcal{T}^*(B(0)) = y^*(B(0)) = \left(x_1^{(1)}, x_2^{(1)}, x_3^{(1)}, x_4^{(1)}, x_5^{(1)}\right)^T.$$

Using Equation (10), the fifth coordinate of $x^{(1)}$ is

$$x_5^{(1)} = W^*(B(0)) = \frac{\mathcal{R}_0^{ode}}{N_{egg}} \frac{\nu_1^2}{\mu_2} \left(\mathcal{R}_0^{ode} - 1\right).$$

Clearly, $x^{(1)}$ is the MPE of system (1) when $B(W)$ is replaced by $B(0) = N_{egg}$.

The following result proves the global attractivity of $\mathcal{T}^*$ when $n > 1$ and $\mathcal{R}_0^{ode} > 1$.

Theorem 6. *Suppose $\mathcal{R}_0^{ode} > 1$ and $s(DF(0, B(x_5^{(1)}))) > 0$, then the MPE $\mathcal{T}^*$ of system (1) for $B(W)$ with n>1 is globally attractive.*

Proof. We prove this theorem by implementing the fluctuation method in two steps as mentioned earlier in the Introduction section.

Step 1 : Construction of two monotone sequences $\{z^{(m)}\}_{m=1}^{\infty}$ and $\{x^{(m)}\}_{m=1}^{\infty}$. If $y \in \mathbb{R}_+^5$ be any solution of system (1). Since $\frac{dA}{dt} \leq B(0)W - (\nu_1 + \mu_2 A)A$, then system (1) is bounded from above by the cooperative system $\frac{d\tilde{y}}{dt} = F(\tilde{y}, B(0))$, where $\tilde{y} = y = (A, Y, Q, U, W)^T$. It follows from the global stability of $\mathcal{T}^*(B(0))$ and the comparison principle that, for any $\epsilon = (\epsilon_1, \epsilon_2, \epsilon_3, \epsilon_4, \epsilon_5)^T \gg 0$, there exists a $t_1 > 0$ such that $y(t) \leq \mathcal{T}^*(B(0)) + \epsilon = x^{(1)} + \epsilon$, $\forall t > t_1$. Since $s(DF(0, B(x_5^{(1)}))) > 0$, we can choose ϵ small enough such that $s(DF(0, B(x_5^{(1)} + \epsilon_5))) > 0$. It follows from Lemma 2 that there exists a unique positive equilibrium $y^*(B(x_5^{(1)} + \epsilon_5)) = \mathcal{T}^*(B(x_5^{(1)} + \epsilon_5))$ for $\frac{d\bar{y}}{dt} = F(\bar{y}, B(x_5^{(1)} + \epsilon_5))$, with $\bar{y} = y = (A, Y, Q, U, W)^T$, which is globally asymptotically stable in $\mathbb{R}_+^5 \setminus \{0\}$. Denote $z^{(1)} = \mathcal{T}^*(B(x_5^{(1)} + \epsilon_5))$, and $z_5^{(1)} = W^*(B(x_5^{(1)} + \epsilon_5))$ the fifth coordinate of $z^{(1)}$. Since $W(t) \leq x_5^{(1)} + \epsilon_5$, $\forall t > t_1$, we have $B(W(t)) \geq B(x_5^{(1)} + \epsilon_5)$ for $t > t_1$. Hence, $\frac{dA}{dt} \geq B(x_5^{(1)} + \epsilon_5)W - (\nu_1 + \mu_2 A)A$, $\forall t > t_1$. Therefore, the system (1) is bounded from below by cooperative system $\frac{d\bar{y}}{dt} = F(\bar{y}, B(x_5^{(1)} + \epsilon_5))$, $\forall t > t_1$. Thus, the global stability of $z^{(1)} = \mathcal{T}^*(B(x_5^{(1)} + \epsilon_5))$ and the comparison principle imply that for any $\epsilon > 0$, with $z^{(1)} - \epsilon \gg 0$, there exists $t_2 > t_1$ such that $y(t) \geq z^{(1)} - \epsilon$, $\forall t > t_2$. Using Remark 4, we have $z^{(1)} \ll x^{(1)}$. Iterating this process, we construct two vectors $x^{(2)} = \mathcal{T}^*(B(z_5^{(1)} - \epsilon_5))$ and $z^{(2)} = \mathcal{T}^*(B(x_5^{(2)} + \epsilon_5))$ with $x_5^{(2)} = W^*(B(z_5^{(1)} - \epsilon_5))$ and subsequently find $t_3 > t_2$ such that $y(t) \leq x^{(2)} + \epsilon$, $\forall t > t_3$ and $t_4 > t_3$ such that $y(t) \geq z^{(2)} - \epsilon$, $\forall t > t_4$. Hence, $z^{(2)} - \epsilon \leq y(t) \leq x^{(2)} + \epsilon$, $\forall t > t_4$. Furthermore, the relationship $z^{(1)} \ll z^{(2)} \ll x^{(2)} \ll x^{(1)}$ is verified. Indeed, since $B(z_5^{(1)} - \epsilon_5) < B(0)$, we have $x^{(2)} = \mathcal{T}^*(B(z_5^{(1)} - \epsilon_5)) \ll \mathcal{T}^*(B(0)) = x^{(1)}$. Similarly, since $B(x_5^{(2)} + \epsilon_5) > B(x_5^{(1)} + \epsilon_5)$, we have $z^{(2)} = \mathcal{T}^*(B(x_5^{(2)} + \epsilon_5)) \gg \mathcal{T}^*(B(x_5^{(1)} + \epsilon_5)) = z^{(1)}$. Since $B(z_5^{(1)} - \epsilon_5) > B(x_5^{(1)} + \epsilon_5)$, we have $x^{(2)} = \mathcal{T}^*(B(z_5^{(1)} - \epsilon_5)) \gg \mathcal{T}^*(B(x_5^{(1)} + \epsilon_5)) = z^{(1)}$. Hence, $B(x_5^{(2)} + \epsilon_5) < B(z_5^{(1)} - \epsilon_5)$, and consequently, $z^{(2)} = \mathcal{T}^*(B(x_5^{(2)} + \epsilon_5)) \ll \mathcal{T}^*(B(z_5^{(1)} - \epsilon_5)) = x^{(2)}$. Therefore, $z^{(1)} \ll z^{(2)} \ll x^{(2)} \ll x^{(1)}$. Repeating the above arguments, we get two monotone sequences of vectors $\{z^{(m)}\}_{m=1}^{\infty}$ and $\{x^{(m)}\}_{m=1}^{\infty}$ such that $0 \ll z^{(1)} \ll z^{(2)} \ll \ldots \ll z^{(m)} \ll x^{(m)} \ll \ldots \ll x^{(2)} \ll x^{(1)}$, with $F(z^{(m)}, B(x_5^{(m)} + \epsilon_5)) = 0$ and $F(x^{(m)}, B(z_5^{(m)} - \epsilon_5)) = 0$, $\forall m \geq 2$. Moreover, there exists $t_{2m} > 0$ such that

$$z^{(m)} - \epsilon \leq y(t) \leq x^{(m)} + \epsilon, \forall t > t_{2m}.$$

Hence, there exist two positive vectors X^* and Z^* with $X \geq Z$ such that $\lim_{m\to\infty} z^{(m)} = Z^*$ and $\lim_{m\to\infty} x^{(m)} = X^*$. Furthermore, $Z^* \leq \mathcal{T}^* \leq X^*$.

Step 2 : Passage to the limit. For any $y_0 \neq 0$, the omega limit set $w(y_0) \in [Z^*, X^*]$ because the ordered interval $[Z^*, X^*]$ is positively invariant. If $Z^* = X^*$, then we have proved that $Z^* = X^* = \mathcal{T}^*$ and $\mathcal{T}^*$ is globally attractive. If $Z^* \neq X^*$, that is $Z^* < X^*$, then it is easy to see that $Z^* \ll X^*$. Moreover, by the persistence in Remark 3, there exists $\eta > 0$ such that $w(y_0) \in [Z^*, X^*]$ with $Z_5^* + \eta \leq w_5(y_0) \leq X_5^* - \eta$, where $w_5(y_0)$ is the fifth coordinate of $w(y_0)$. By repeating the previous process, we can construct two vectors $Z^{*(1)}$ and $X^{*(1)}$ such that for any nonzero point y_0, $Z^* \ll Z^{*(1)} \ll \mathcal{T}^* \ll X^{*(1)} \ll X^*$ and $w(y_0) \in [Z^{*(1)}, X^{*(1)}]$. If $Z^{*(1)} = X^{*(1)}$, then $Z^{*(1)} = X^{*(1)} = \mathcal{T}^*$, and $\mathcal{T}^*$ is globally attractive. If not, $Z^{*(1)} < X^{*(1)}$, then $Z^{*(1)} \ll X^{*(1)}$. Repeating the procedure, we can construct two sequences $Z^{*(m)}$ and $X^{*(m)}$ such that $Z^{*(1)} \ll Z^{*(2)} \ll \ldots \ll Z^{*(m-1)} \ll Z^{*(m)} \leq \mathcal{T}^* \leq X^{*(m)} \ll X^{*(m-1)} \ll X^{*(m-2)} \ll \ldots \ll X^{*(2)} \ll X^{*(1)}$ and

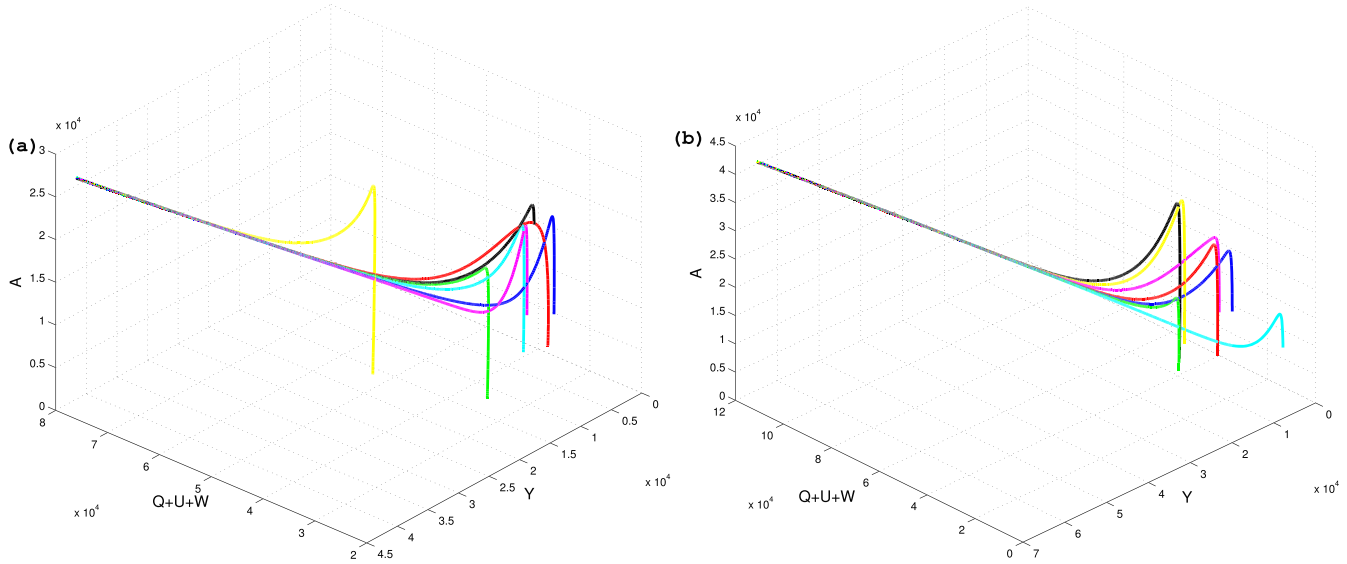

FIGURE 3 Globally asymptotically stable (GAS) of the mosquito-persistent equilibrium (MPE) $\mathcal{T}^*$ for model (1). $\mu_2 = 0.0004$, $N_{egg} = 25$ and all other parameters are as in Table 4 (so that $\mathcal{R}_0^{ode} = 13.9399 > 1$): (A) n = 1. (B) n = 13 [Colour figure can be viewed at wileyonlinelibrary.com]

$\lim_{m\to\infty} Z^{*(m)} = \lim_{m\to\infty} X^{*(m)} = \mathcal{T}^*$, which implies that the omega limit set of every nonzero point y is $\mathcal{T}^*$, and thus, $\mathcal{T}^*$ is globally attractive. □

Ecologically speaking, Theorems 5 and 6 imply that mosquitoes will persist in the community whenever the associated conditions for the global stability/attractivity of $\mathcal{T}^*$ hold. These theorems are numerically supported by simulating the model (1) using n = 1 for Figure 3A and n = 13 for Figure 3B. Figure 3B show that, in the presence of density dependent mortality in the aquatic stage (ie $\mu_2 \neq 0$), the solutions of model (1) converge to $\mathcal{T}^*$ even if the conditions of Theorem 4 are satisfied. This suggests that the phenomenon of Hopf bifurcation can be ruled out in the system by addicting a positive density dependent mortality rate $\mu_2 > 0$ in the aquatic stage of the mosquitoes.

In Table 3 below, we summarize the long run behavior of the solutions of the ODE model (1) subject to either of the four egg oviposition functions given in Table 2. The expressions of $\mathcal{R}, ^{\mathcal{L}}$ and n_{1^*} are specified in Appendix B.

2.5 | Sensitivity analysis

We carried out sensitivity analysis to determine the model robustness to parameter values. This is a tool to identify the most influential parameters in determining mosquito dynamics. A latin hypercupe Sampling (LHS) scheme[50] samples 1000 values for each input parameter using a distribution over the range of ecologically realistic values is given in Figures 4

$B(W)$	n and μ_2	$\mathcal{R}_0^{ode}$	$\mathcal{T}_0$	$\mathcal{T}^*$	Stable limit cycle	Source
B_M	$\mu_2 \geq 0$	$\mathcal{R}_0^{ode} \leq 1$	GAS	No	No	7,13
	$\mu_2 > 0$	$\mathcal{R}_0^{ode} > 1$	Unstable	GAS	No	7,13
B_L	$\mu_2 \geq 0$	$\mathcal{R}_0^{ode} \leq 1$	GAS	No	No	6
	$\mu_2 = 0$	$1 < \mathcal{R}_0^{ode} \leq \mathcal{R}_0^{\mathcal{L}}$	Unstable	LAS	No	6
	$\mu_2 = 0$	$\mathcal{R}_0^{ode} > \mathcal{R}_0^{\mathcal{L}}$	Unstable	Unstable	Yes	6
	$\mu_2 > 0$	$\mathcal{R}_0^{ode} > 1$	Unstable	GAS	No	†
B_S	$n > 0, \mu_2 \geq 0$	$\mathcal{R}_0^{ode} \leq 1$	GAS	No	No	†
	$1 < n < n_0^{**}, \mu_2 = 0$	$\mathcal{R}_0^{ode} > 1$	Unstable	LAS	No	†
	$n > n_0^{**}, \mu_2 = 0$	$\mathcal{R}_0^{ode} > 1$	Unstable	Unstable	Yes	†
	$n > 0, \mu_2 > 0$	$\mathcal{R}_0^{ode} > 1$	Unstable	GAS	No	†
B_H	$n > 0, \mu_2 \geq 0$	$\mathcal{R}_0^{ode} \leq 1$	GAS	No	No	†
	$1 < n < n_{1^*}, \mu_2 = 0$	$\mathcal{R}_0^{ode} > 1$	Unstable	LAS	No	†
	$n > n_{1^*}, \mu_2 = 0$	$\mathcal{R}_0^{ode} > 1$	Unstable	Unstable	Yes	†
	$n > 0, \mu_2 > 0$	$\mathcal{R}_0^{ode} > 1$	Unstable	GAS	No	†

Abbreviations: GAS, globally asymptotically stable; LAS, locally asymptotically stable.

TABLE 3 Stability properties of the model (1). † denotes a result established exclusively in this paper

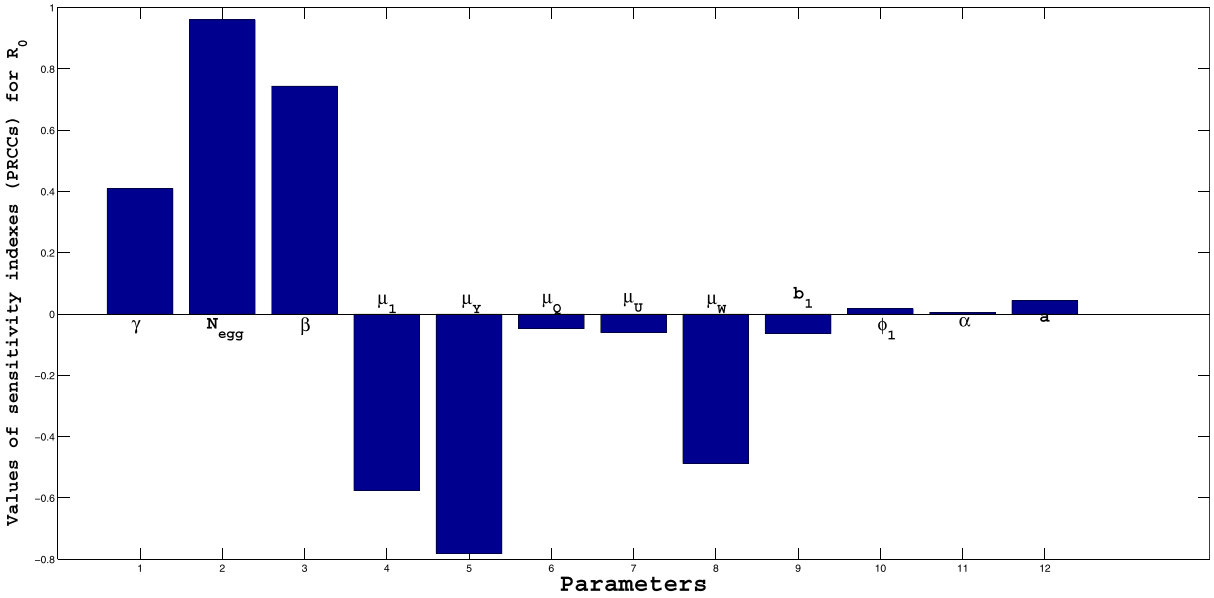

FIGURE 4 Sensitivity analysis between $\mathcal{R}_0^{ode}$ and each parameter [Colour figure can be viewed at wileyonlinelibrary.com]

and 5 with descriptions and references given in Table 4. Using the system of differential equations that describe (1) for oviposition function B_S with n = 1, 5000 model simulations are performed by randomly pairing sampled values for all LHS parameters. Partial Rank Correlation Coefficients (PRCC) and corresponding *P*-values between $\mathcal{R}_0^{ode}$ and each parameter are computed. An output is assumed sensitive to an input if the corresponding PRCC is less than −0.50 or greater than +0.50, and the corresponding *P*-value is less than 5%.

From Figures 4 and 5, we can identify five parameters that strongly influence the population dynamics and dispersal of the mosquito, namely the natural mortality rate of immature females (μ_Y), the natural mortality rate of the aquatic stage (μ_1), the natural mortality rate of breeding females (μ_W), the transfer rate (β) (also referred to as mating rate), the maturation rate (Γ), and the deposit rate of eggs by females (N_{egg}). Thus, from this sensitivity analysis, the following suggestions are made:

1. The mechanical control (such as removal of stagnant waters) could be an effective control measure against the growing of mosquitoes because the value of N_{egg} and the population size of mosquitoes are minimized;
2. The use of larvicides and removal of mosquito breeding sites seem to be important control measures against the mosquitoes because they increase in the value of μ_1 and reduce the value of Γ;

TABLE 4 Values and ranges of the parameters of the model (1)

Parameters	Baseline Value	Range	Source
r	0.5		
Γ	0.8/day	0.5 – 0.89	[51]
N_{egg}	50/day	10 – 100	[6,51]
L	40000	$50 - 3 \times 10^6$	[6]
β	0.2/day	0.05 – 0.35	
μ_2	0.04/ml	0.02 – 0.06	[6]
μ_1	0.51/day	0.28 – 0.76	[51]
μ_M	0.14/day	0.02 – 0.2	[7,13]
μ_Y	0.05/day	0.01 – 0.2	[7,13]
μ_Q	0.18/day	0.125 – 0.233	[52]
μ_U	0.0043/day	0.0034 – 0.01	[52]
μ_W	0.41/day	0.41 – 0.56	[52]
φ_1	16	12 – 20	[5]
α	0.86	0.75 – 0.95	[5]
b_1	0.8/day	0.46 – 0.92	[5,16]
a	0.43	0.30 – 0.56	[52]

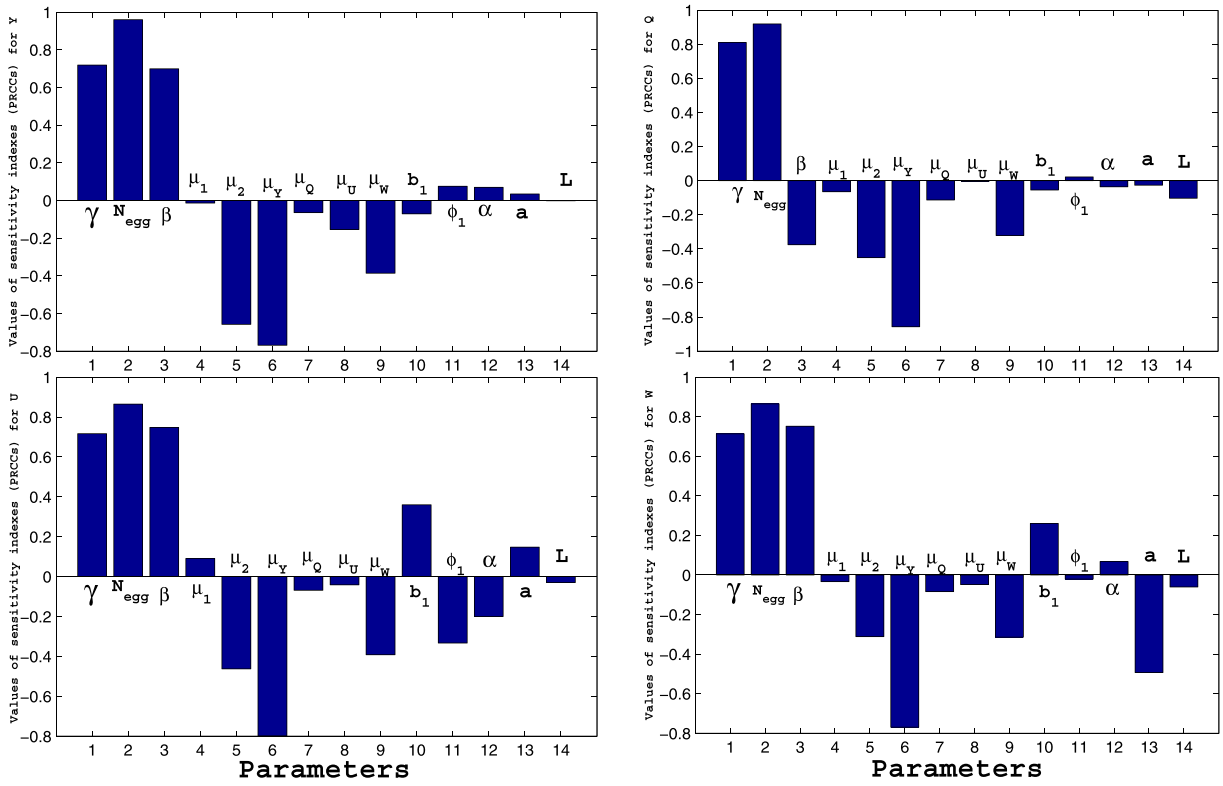

FIGURE 5 Sensitivity analysis between Y, Q, U, W, and each parameter [Colour figure can be viewed at wileyonlinelibrary.com]

3. The use of insecticides is potentially another good control tool against mosquito population because it helps increasing the values of μ_Y and μ_W;
4. The use of sterile insect technique (SIT) and genetically modified mosquitoes (GMM) may play an important role in minimizing the size of mosquito population by reducing the transfer rate (β) and maturation rate (Γ).

3 | SPATIO-TEMPORAL MODEL

3.1 | Modeling framework

In order to assess the influence of mobility on the spread of mosquitoes, we extend model (1) by taking into account the spatial component. In this new setting, we give additional assumptions based on the mosquito ability to move, knowing that the mosquitoes in the aquatic stage often live in closed habitats such as unattended water containers. Therefore, it is reasonable to assume that resting females mosquitoes, as well as mosquitoes in the aquatic stage, do not move. The remaining classes of adult mosquitoes disperse while searching for hosts for blood meals or breeding sites for reproduction.[53] The movements of adult mosquitoes can be classified into long-range and short-range dispersals. Long-range dispersal is often unintentional and aided by wind or human transport, while short-range dispersal is often intentional and can be divided into non-oriented flights or oriented flights towards sites.[54] Mosquitoes follow odors and carbon dioxide carried by the wind, which give their main direction of migration.[55] Therefore, we add advection or drift terms to account for the fact that, when mosquitoes are stimulated by attractants (eg wind, hosts, and breeding sites), they move preferably in certain directions.[17,18] We use ε_M, ε_Q, and ε_W to denote the constant velocity fluxes (migration coefficients) of males, questing females, and breeding females, respectively. When mosquitoes are not submitted to stimuli, it is possible to assume that they move randomly in any direction.[18,56] For simplicity, to describe the random movement of mosquitoes, we use diffusion to model it according to Fick's law. We denote D_Y, D_M, D_Q, and D_W the diffusion coefficients for immature females, males, questing females, and breeding females, respectively. To make it simple, we concentrate on one dimensional spatial habitat $\Omega = (0, l), l > 0$ and assume that the mosquitoes are confined in that line segment all the time. The number of hosts is allowed to differ across Ω, introducing heterogeneity. Thus, the population density of humans $H(x)$ is location-dependent, implying that the parameters $\varphi_1(x)$, $b_1(x)$, $\nu_3(x)$ and $\nu_5(x)$ are location-dependent as

well. According to the above description, we propose the following spatio-temporal model

$$\begin{cases} \frac{\partial A}{\partial t} = B(W(t,x))W(t,x) - [\nu_1 + \mu_2 A(t,x)]A(t,x), \\ \frac{\partial Y}{\partial t} = D_Y \frac{\partial^2 Y}{\partial x^2} + r\Gamma A(t,x) - \nu_2 Y(t,x), \\ \frac{\partial Q}{\partial t} = D_Q \frac{\partial^2 Q}{\partial x^2} - \varepsilon_Q \frac{\partial Q}{\partial x} + \beta Y(t,x) + b_1(x)W(t,x) - \nu_3(x)Q(t,x), \\ \frac{\partial U}{\partial t} = \alpha\varphi_1(x)Q(t,x) - \nu_4 U(t,x), \\ \frac{\partial W}{\partial t} = D_W \frac{\partial^2 W}{\partial x^2} - \varepsilon_W \frac{\partial W}{\partial x} + aU(t,x) - \nu_5(x)W(t,x), \end{cases} \tag{13}$$

Here, $A(t,x)$, $Y(t,x)$, $Q(t,x)$, $U(t,x)$, and $W(t,x)$ measure the density of mosquitoes at location x and time t. Note that the equation for the density of male mosquitoes $M(t,x)$ is

$$\frac{\partial M}{\partial t} = D_M \frac{\partial^2 M}{\partial x^2} - \varepsilon_M \frac{\partial M}{\partial x} + (1-r)\Gamma A(t,x) - \mu_M M(t,x). \tag{14}$$

We discard Equation (14) from system (13) because the unknown $M(t,x)$ can be determined if $A(t)$ is known. Indeed, once $A(t)$ is found, (14) is a scalar advection-diffusion-reaction equation. Thereafter, it is well known that, along the characteristics $x \to x - t\varepsilon_M$, is transformed into a scalar reaction-diffusion equation that can be solved in a classical manner.[57] System (13) is appended with the initial conditions

$$\begin{cases} A(0,x) = \phi_1(x), & Y(0,x) = \phi_2(x), & Q(0,x) = \phi_3(x), \\ U(0,x) = \phi_4(x), & W(0,x) = \phi_5(x), & x \in \Omega, \end{cases} \tag{15}$$

the Neumann boundary conditions

$$\frac{\partial Y}{\partial x}(t,0) = \frac{\partial Y}{\partial x}(t,l) = 0, \tag{16}$$

and the Robin boundary conditions

$$D_Z \frac{\partial Z}{\partial x}(t,0) - \varepsilon_Z Z(t,0) = \frac{\partial Z}{\partial x}(t,l) = 0, \quad Z = Q, W, \tag{17}$$

where each ϕ_i $(i = 1,2,3,4,5)$ is assumed to be nonnegative and continuous in the space variable x.

3.2 | Existence of positive solutions

The aim here is to give the preliminary results for the well-posedness of system (13)-(17). These results include the existence of the unique maximal bounded semiflow associated with (13)-(17). Let $u(t,x) = (A(t,x), Y(t,x), Q(t,x), U(t,x), W(t,x)) = (u_1(t,x), u_2(t,x), u_3(t,x), u_4(t,x), u_5(t,x))$ denote a solution for (13) corresponding to the initial condition $\phi = (\phi_1, \phi_2, \phi_3, \phi_4, \phi_5)$. Let $X := C(\overline{\Omega}, \mathbb{R}^5) = \prod_{i=1}^5 X_i$, $X_i := C(\overline{\Omega}, \mathbb{R})$, $i = 1, ..., 5$ be the Banach space of $\mathbb{R}^5$-valued functions continuous in $x \in \overline{\Omega}$ equipped with the usual sup norm $\|u\|_X = \sum_{i=1}^5 \|u_i\|_{X_i}$, $X^+ := C(\overline{\Omega}, \mathbb{R}^5_+) = \prod_{i=1}^5 X_i^+$, where $X_i^+ := C(\overline{\Omega}, \mathbb{R}_+)$ the positive cone of X_i. Denote by $\mathbb{I}$ the identity operator on X_i. Let $T_i(t) : X_i \to X_i, t \geq 0, i = 1, \ldots, 5$ be the semigroups associated with the operators $-\nu_1\mathbb{I}$, $D_Y\partial_{xx}^2 - \nu_2\mathbb{I}$, $D_Q\partial_{xx}^2 - \varepsilon_Q\partial_x - \nu_3(\cdot)\mathbb{I}$, $-\nu_4\mathbb{I}$ and $D_W\partial_{xx}^2 - \varepsilon_W\partial_x - \nu_5(\cdot)\mathbb{I}$, respectively, subject to the Neumann boundary condition. Let $\mathcal{S}_i : D(\mathcal{S}_i) \to X_i$ be the infinitesimal generator of the analytic semigroup of bounded linear operator T_i. Then,

$$T(t) = (T_1(t), T_2(t), T_3(t), T_4(t), T_5(t)) : X \to X \tag{18}$$

is a semigroup generated by the operator $\mathcal{S} := (\mathcal{S}_1, \mathcal{S}_2, \mathcal{S}_3, \mathcal{S}_4, \mathcal{S}_5)$ defined on $D(\mathcal{S}) := \prod_{i=1}^5 D(\mathcal{S}_i)$. It follows from[49] that $T(t)$ is compact. Moreover, thanks to Corollary 7.2.3 in,[49] $T(t)$ is strongly positive. Define $F = (F_1, F_2, F_3, F_4, F_5) : \overline{\Omega} \times \mathbb{R}^5_+ \to$

$\mathbb{R}^5$ by

$$F(x,u(t,x)) := \begin{pmatrix} B(u_5)u_5 - \mu_2 u_1^2 \\ r\Gamma u_1 \\ \beta u_2 + b_1(x)u_5 \\ \alpha\varphi_1(x)u_3 \\ au_4 \end{pmatrix}, \ \forall x \in \overline{\Omega}. \tag{19}$$

Then, system (13)-(17) takes the abstract functional differential form

$$\begin{cases} \frac{du}{dt} &= \mathcal{S}u + F(u), \quad t > 0 \\ u(0,x) &= u_0(x) = \phi(x) \in X. \end{cases} \tag{20}$$

It is well known[29] that system (20) is equivalent to the integral equation

$$u(t) := T(t)\phi + \int_0^t T(t-s)F(u(s,x))ds, \tag{21}$$

whose solution is called mild solution (see pg. 105[58]). Thanks to[49] (see Theorem 7.3.1, Corollary 7.3.2, and pg. 121), the following result insures the local well-posedness of (13)-(17).

Theorem 7. *For all $\phi \in X^+$, the system (13)-(17) admits a unique mild solution on the interval of existence $[0,\sigma)$, where $\sigma = \sigma(\phi)$. The solution (A,Y,Q,U,W) remains nonnegative for all $t \in [0,\sigma)$. Moreover, if $\sigma < \infty$, then $\|(A,Y,Q,U,W)\|_X \to \infty$ as $t \to \sigma$ from below.*

Proof. By (15)-(17), we have $\phi \in X^+$. Since the functions $B(W)$ are positive, it is clear that (19) satisfies the assumptions in Corollary 7.3.2 in,[49] which complete the proof. □

The following result establishes the global well-posedness result for (13)-(17).

Theorem 8. *For any $\phi \in X^+$, system (13)-(17) admits a unique solution $u(t,x,\phi)$ defined on $[0,\infty)\times\overline{\Omega}$, and the solution semiflow $\Phi_t : X^+ \to X^+$ has a global compact attractor.*

Proof. For any $\phi \in X^+$, we denote by $u(t,x,\phi)$ the unique solution of system (13)-(17) satisfying $u(0,x) = u_0(x) = \phi(x)$ with the maximal interval of existence $[0,\sigma)$ for some $\sigma > 0$. By Theorem 7, we have $u(t,x,\phi) \geq 0$. Having in mind that $B(W)W$ is bounded above by $N_{egg}L$, it comes that

$$\partial_t A(t,x) \leq N_{egg}L - \nu_1 A, \quad \forall t \geq 0, \quad x \in \overline{\Omega}.$$

This implies that there exists $t_1 = t_1(\phi) > 0$ such that $A(t,x) \leq \frac{N_{egg}L}{\nu_1}$, $\forall t \geq t_1, x \in \overline{\Omega}$.

Next, from Equation (13), one has

$$\partial_t Y(t,x) \leq D_Y \partial_{xx}^2 Y + r\Gamma M_0 - \nu_2 Y, \quad \forall t \geq t_1.$$

The comparison principle (see[59] or[34], Theorem 10.1) and Proposition 1 in[60], with $\overline{D} = D_Y$, $\overline{\varepsilon} = 0$, $g(x) = r\Gamma M_0$, $\lambda = \nu_2$, imply that there exists $t_2 = t_2(\phi) > t_1 > 0$ large enough so that

$$Y(t,x) \leq \frac{r\Gamma M_0}{\nu_2} := M_1, \quad \forall t \geq t_2, \quad x \in \overline{\Omega}.$$

Let $V := Q + U + W$, then from (13), we have

$$\partial_t V(t,x) \leq D_0 \partial_{xx}^2 V - \varepsilon_0 \partial_x V + \beta M_1 - \mu_0 V, \quad \forall t > t_2,$$

where $D_0 = \max\{D_Q, D_W\}$, $\varepsilon_0 = \min\{\varepsilon_Q, \varepsilon_W\}$ and $\mu_0 = \min\{\mu_Q, \mu_U, \mu_W\}$. Another application of the comparison principle and Proposition 1 in[60], with $\overline{\varepsilon} = \varepsilon_0 > 0$, $\overline{D} = D_0$, $g(x) = \beta M_1$, $\lambda = \mu_0$, yields $t_3 = t_3(\phi) > t_2 > 0$ large enough so that

$$Q(t,x) + U(t,x) + W(t,x) \leq \frac{\beta M_1}{\mu_0} := M_2, \quad \forall t \geq t_3, \quad x \in \overline{\Omega}.$$

Hence, the solutions of (13)-(17) are ultimately bounded with respect to the maximum norm. Therefore, the latter results, combined with the local existence in Theorem 7, yield the global existence of the solution $u(t,x,\phi)$ in $[0,\infty)$.

It follows that the solution semiflow Φ_t is point dissipative. Noticing that F is locally Lipschitz in $C([0,l],X^+)$ and that $T(t)$ is analytic, compact and strongly continuous (see pg. 1, 4 in[58]), one concludes that Φ_t is compact for any $t>0$. Thus, thanks to Theorem 3.4.8 in[61], Φ_t has a global compact attractor. □

3.3 | Threshold dynamics of model (13)

In order to define the basic offspring ratio $\mathcal{R}_0^{pde}$ for system (13)-(17), we first observe that system (13) has a spatially homogeneous trivial equilibrium $\mathcal{T}_0=(0,0,0,0,0)$. Note that, while a huge number of works deals with the threshold dynamics for ODE models, very few such studies are devoted to PDE models. This is probably due to the fact that the concept of basic reproduction number has just recently been extended to PDE models such as reaction-diffusion and reaction-convection-diffusion epidemic models with mixed boundary conditions.[62-65] The definition of $\mathcal{R}_0^{pde}$ in this work follows the approach developed in.[62] That is, $\mathcal{R}_0^{pde}=r(\mathcal{L})$ is the spectral radius of the operator $\mathcal{L}:=-\mathcal{G}\mathcal{S}^{-1}$, where

$$\mathcal{S}=\operatorname{diag}(-\nu_1, D_Y\partial_{xx}^2-\nu_2, D_Q\partial_{xx}^2-\varepsilon_Q\partial_x-\nu_3(.), -\nu_4, D_W\partial_{xx}^2-\varepsilon_W\partial_x-\nu_5(.)),$$

being the infinitesimal generator of the semigroup $T(t)$ defined in Equation (18) and $\mathcal{G}$ defined by

$$\mathcal{G}(x)=\begin{pmatrix} 0 & 0 & 0 & 0 & N_{egg}\\ r\Gamma & 0 & 0 & 0 & 0\\ 0 & \beta & 0 & 0 & b_1(x)\\ 0 & 0 & \alpha\varphi_1(x) & 0 & 0\\ 0 & 0 & 0 & a & 0\end{pmatrix},$$

such that, for all $\psi\in X$, and $x\in\Omega$,

$$\mathcal{L}(\psi)(x)=(-\mathcal{G}\mathcal{S}^{-1}\psi)(x)=\mathcal{G}(x)(-\mathcal{S}^{-1}\psi)(x)=\mathcal{G}(x)\int_0^\infty T(t)(\psi(x))dt.$$

As above defined, the basic offspring number, $\mathcal{R}_0^{pde}$ also depends on spatial parameters, which could permit the assessment of spatial control strategies. However, its analytical determination is very difficult in general. Therefore, $\mathcal{R}_0^{pde}$ can be numerically evaluated by using, for example, the method described in.[64]

In what follows, we show that $\mathcal{R}_0^{pde}$ is a threshold that determines dynamics of model (13). The result below establishes the global attractivity of $\mathcal{T}_0$.

Theorem 9. *Consider the model (13)-(17). Then, the spatially homogeneous trivial equilibrium $\mathcal{T}_0$ is globally attractive whenever $\mathcal{R}_0^{pde}<1$.*

Proof. Linearizing system (13)-(17) around $\mathcal{T}_0$, we obtain the linear cooperative system

$$\begin{cases}\frac{\partial A}{\partial t}=N_{egg}W(t,x)-\nu_1A(t,x),\\ \frac{\partial Y}{\partial t}=D_Y\frac{\partial^2Y}{\partial x^2}+r\Gamma A(t,x)-\nu_2Y(t,x),\\ \frac{\partial Q}{\partial t}=D_Q\frac{\partial^2Q}{\partial x^2}-\varepsilon_Q\frac{\partial Q}{\partial x}+\beta Y(t,x)+b_1(x)W(t,x)-\nu_3(x)Q(t,x),\\ \frac{\partial U}{\partial t}=\alpha\varphi_1(x)Q(t,x)-\nu_4U(t,x),\\ \frac{\partial W}{\partial t}=D_W\frac{\partial^2W}{\partial x^2}-\varepsilon_W\frac{\partial W}{\partial x}+aU(t,x)-\nu_5(x)W(t,x),\\ \partial_xY(t,0)=\partial_xY(t,l)=0,\\ D_Z\partial_xZ(t,0)-\varepsilon_ZZ(t,0)=\partial_xZ(t,l)=0,\quad Z=Q,W.\end{cases}\tag{22}$$

Substituting $(A,Y,Q,U,W)=(e^{\lambda t}\psi_1(x),e^{\lambda t}\psi_2(x),e^{\lambda t}\psi_3(x),e^{\lambda t}\psi_4(x),e^{\lambda t}\psi_5(x))$ in (22), with $\lambda\in\mathbb{C}$, yields the eigenvalue problem

$$\begin{cases}\lambda\psi_1=N_{egg}\psi_5-\nu_1\psi_1,\\ \lambda\psi_2=D_Y\partial_{xx}^2\psi_2+r\Gamma\psi_1-\nu_2\psi_2,\\ \lambda\psi_3=D_Q\partial_{xx}^2\psi_3-\varepsilon_Q\partial_x\psi_3+\beta\psi_2+b_1(x)\psi_5-\nu_3(x)\psi_3,\\ \lambda\psi_4=\alpha\varphi_1(x)\psi_3-\nu_4\psi_4,\\ \lambda\psi_5=D_W\partial_{xx}^2\psi_5-\varepsilon_W\partial_x\psi_5+a\psi_4-\nu_5(x)\psi_5,\\ \partial_x\psi_2(t,0)=\partial_x\psi_2(t,l)=0,\\ D_Z\partial_x\psi_i(t,0)-\varepsilon_Z\psi_i(t,0)=\partial_x\psi_i(t,l)=0,\quad i=3,5,\quad Z=Q,W.\end{cases}\tag{23}$$

The right-hand side of first five equations of eigenvalue problem (23) takes the form

$$\Theta\psi := (\mathcal{S}+\mathcal{G})\psi, \text{ where, } \psi = (\psi_1, \psi_2, ..., \psi_5)^T. \tag{24}$$

Note that $\mathcal{G}$ is a positive and cooperative. Thanks to the graph theory, $\mathcal{G}$ is also irreducible. Moreover, $\mathcal{S}$ and $\mathcal{G}$ are both generators of positive C_0-semigroups. Hence, by Theorem 3.12 in,[62] $\mathcal{S}$ and $\mathcal{G}$ are both resolvent-positive (see Definition 3.1 in[66]). Following the arguments in[49] or,[66] one can prove that the spectral bound $s(\mathcal{S})$ of $\mathcal{S}$ is negative. In fact, let us consider the system

$$\begin{cases} \partial_t Z = D_Z\partial^2_{xx}Z - \varepsilon_Z\partial_x Z, \\ D_Z\partial_x Z(t,0) - \varepsilon_Z Z(t,0) = \partial_x Z(t,l) = 0, \quad Z = Q, W. \end{cases} \tag{25}$$

The substitution of $P = e^{\lambda t}\zeta(x)$ in (25) gives

$$\begin{cases} \lambda\zeta(x) = D\partial^2_{xx}\zeta - \varepsilon\partial_x\zeta. \\ D_Z\partial_x\zeta(t,0) - \varepsilon_Z\zeta(t,0) = \partial_x\zeta(t,L_1) = 0, \quad Z = Q, W. \end{cases} \tag{26}$$

The asymptotic behavior of solutions to (25) is determined by that of the eigenvalue problem (26). Theorem 7.6.1 in[49] implies that the eigenvalue problem (26) has a real principal eigenvalue λ_0 and a corresponding eigenvector $\zeta_0(x) > 0$ for all $x \in \Omega$. We claim that $\lambda_0 < 0$. Indeed, if $\mathcal{Q}_1(\zeta) := D_Z\partial^2_{xx}\zeta - \varepsilon_Z\partial_x\zeta$ denotes the differential operator on the right hand side of (26), then integration by parts yields

$$\begin{aligned} \lambda_0\int_\Omega|\zeta_0(x)|^2dx &= \int_\Omega(\mathcal{Q}_1(\zeta_0))(x)\zeta_0(x)dx \\ &= \int_0^l[D_Z\partial^2_{xx}\zeta_0 - \varepsilon_Z\partial_x\zeta_0]\zeta_0(x)dx, \\ &= -\tfrac{\varepsilon_Z}{2}[\zeta_0^2(0)+\zeta_0^2(l)] - D_Z\int_0^l|\partial_x\zeta_0(x)|^2dx < 0. \end{aligned}$$

Since $\zeta_0(x) > 0$ for all $x \in \overline{\Omega}$, we have $\lambda_0 < 0$. One can prove that an eigenvalue of $\mathcal{Q}_1$ is also an eigenvalue of $\partial_t Z = D_Z\partial^2_{xx}Z - \varepsilon_Z\partial_x Z - \nu_i(x)Z$, with $i = 3, 5$. Indeed, the operator $\mathcal{Q}_{1,i} = D_Z\partial^2_{xx} - \varepsilon_Z\partial_x - \nu_i(x)$ is a sum of $\mathcal{Q}_1$ and the linear operator M_i defined by $M_i(Z)(x) = -\nu_i(x)Z$, with $\nu_i(x) > 0$. Thus, using Theorem 7.6.1 in,[49] there exists a real principal eigenvalue λ^* and an associated eigenfunction $\zeta^* > 0$ such that

$$\lambda^*\zeta^* = D_Z\partial^2_{xx}\zeta^* - \varepsilon_Z\partial_x\zeta^* - \nu_i(x)\zeta^* \quad \text{or} \quad (\lambda^* + \nu_i(x))\zeta^* = D_Z\partial^2_{xx}\zeta^* - \varepsilon_Z\partial_x\zeta^*. \tag{27}$$

Since the eigenvalue problem (26) has eigenvalues λ_n, $n \geq 0$, then the eigenvalues of (27) are $\lambda_n - \nu_i(x)$, $n \geq 0$. Hence, $\lambda^* = \lambda_0 - \nu_i(x) < 0$ because $\lambda_0 < 0$, $\nu_i(x) > 0$. Therefore, $s(\mathcal{S}) < 0$. It follows from Theorem 3.5 in[62] that the spectral bound, $s(\Theta)$ of $\Theta = \mathcal{S} + \mathcal{G}$, has the same sign as $r(-\mathcal{G}\mathcal{S}^{-1}) - 1 = \mathcal{R}_0^{pde} - 1$. That is, $\mathcal{R}_0^{pde} - 1$ and the principal eigenvalue of Θ, $\lambda = \lambda(\mathcal{T}_0)$, have same sign. Since $\mathcal{R}_0^{pde} < 1$, we have $\lambda(\mathcal{T}_0) < 0$ and $\lim_{\epsilon\to 0}\lambda(\mathcal{T}_0 + \epsilon) = \lambda(\mathcal{T}_0) < 0$. Thus, there is an $\epsilon_0 > 0$ such that $\lambda_{\epsilon_0} = \lambda(\mathcal{T}_0 + \epsilon_0) < 0$. Fixing $\epsilon_0 > 0$, and using the fact that A is nonnegative, gives the existence of t_0 such that for all $t \geq t_0$, $x \in \overline{\Omega}$, $A(t,x) \geq \epsilon_0$. Thus, from (2), we have $\partial_t A \leq N_{egg}W - (\nu_1 + \mu_2\epsilon_0)A$, $\forall t \geq t_0, x \in \overline{\Omega}$. Finally, we consider the linear system.

$$\begin{cases} \frac{\partial v_1}{\partial t} = N_{egg}v_5 - (\nu_1 + \mu_2\epsilon_0)v_1, \\ \frac{\partial v_2}{\partial t} = D_Y\frac{\partial^2 v_2}{\partial x^2} + r\Gamma v_1 - \nu_2 v_2, \\ \frac{\partial v_3}{\partial t} = D_Q\frac{\partial^2 v_3}{\partial x^2} - \varepsilon_Q\frac{\partial v_3}{\partial x} + \beta v_2 + \overline{b}_1 v_5 - \tilde{\nu}_3 v_3, \\ \frac{\partial v_4}{\partial t} = \alpha\overline{\varphi}_1 v_3 - \nu_4 v_4, \\ \frac{\partial v_5}{\partial t} = D_W\frac{\partial^2 v_5}{\partial x^2} - \varepsilon_W\frac{\partial v_5}{\partial x} + a v_4 - \tilde{\nu}_5 v_5, \end{cases} \tag{28}$$

where $\overline{b}_1 = \max_{x\in\overline{\Omega}} b_1(x)$, $\overline{\varphi}_1 = \max_{x\in\overline{\Omega}}\varphi_1(x)$, $\tilde{\nu}_3 = \min_{x\in\overline{\Omega}}\nu_3(x)$ and $\tilde{\nu}_5 = \min_{x\in\overline{\Omega}}\nu_5(x)$. Notice that system (28) controls system (13) from above. Moreover, similar arguments as in Theorem 2.2 in[67] yield the following result.

Lemma 3. *The problem (28) has a principal eigenvalue $\overline{\lambda}_{\epsilon_0}$ with a positive eigenfunction ψ_0, and $\overline{\lambda}_{\epsilon_0}$ has the same sign as λ_0.*

Since $\lambda_0 < 0$, we have $\overline{\lambda}_{\epsilon_0} < 0$, and system (28) admits a positive solution

$$v(t,x) = e^{\overline{\lambda}_{\epsilon_0}(t-t_0)}\psi_0(x), \quad t \geq t_0.$$

For any $\phi \in X^+$, there exists some $\eta > 0$ sufficiently large such that

$$u(t,\cdot,\phi) \leq \eta v(t,\cdot), \quad t \geq t_0.$$

Since the reaction term F^+ of system (28) is cooperative, we conclude by the comparison principle (see Theorem 7.3.4 in[49]) that

$$(A(t,x,\phi), Y(t,x,\phi), Q(t,x,\phi), U(t,x,\phi), W(t,x,\phi))^T \leq \eta e^{\overline{\lambda}_{\epsilon_0}(t-t_0)}\psi_0(x), \ \forall t \geq t_0.$$

Hence, $\lim_{t\to\infty} (A(t,x,\phi), Y(t,x,\phi), Q(t,x,\phi), U(t,x,\phi), W(t,x,\phi))^T = 0$ uniformly for $x \in \overline{\Omega}$. This achieves the proof of Theorem 9. □

The ecologically implication of Theorem 9 is that the mosquito population can be effectively controlled (or eliminated) in a given bounded region as long as the associated spatial offspring number $\mathcal{R}_0^{pde}$ can be brought (and kept) to a value less than or equal to unity. In order to prove the uniform persistence of the mosquito population, we need to show that $\mathcal{T}_0$ is a weak repeller. That is,

Lemma 4. *If $\mathcal{R}_0^{pde} > 1$, then there exists $\delta > 0$ such that for any $\phi \in X^+$ with $\phi_i(0) \not\equiv 0$, $i = 1,2,3,4,5$, the solution $u(t,\cdot,\phi)$ of system (13)-(17) satisfies*

$$\limsup_{t\to\infty} \|u(t,\cdot,\phi) - \mathcal{T}_0\|_X \geq \delta. \tag{29}$$

Proof. Since $\mathcal{R}_0^{pde} > 1$, by the proof of Theorem 9, the principal eigenvalue $\lambda(\mathcal{T}_0)$ of $\Theta = \mathcal{S} + \mathcal{G}$ is positive. Assume, by contradiction that there exists some $\phi \in X^+$ with $\phi_i(0) \not\equiv 0$, $i = 1,2,3,4,5$ such that for every $\delta > 0$, $\limsup_{t\to\infty} \|u(t,\cdot,\phi) - \mathcal{T}_0\|_X < \delta$. Then, there exists $t_1 = t_1(\phi) > 0$ sufficiently large such that $A(t,x) \leq \delta$ and $W(t,x) \leq \delta$, $\forall t \geq t_1, x \in \overline{\Omega}$. Since $B'(W) \leq 0$ for all $W \geq 0$, it follows that $B(W) \geq B(\delta)$. Hence, we have

$$\partial_t A(t,x) \geq B(\delta)W(t,x) - (\nu_1 + \mu_2\delta)A(t,x), \forall t \geq t_1, x \in \overline{\Omega}.$$

Consider the following linear system.

$$\begin{cases} \frac{\partial w_1}{\partial t} = B(\delta)w_5 - (\nu_1 + \mu_2\delta)w_1, \\ \frac{\partial w_2}{\partial t} = D_Y\frac{\partial^2 w_2}{\partial x^2} + r\Gamma w_1 - \nu_2 w_2, \\ \frac{\partial w_3}{\partial t} = D_Q\frac{\partial^2 w_3}{\partial x^2} - \varepsilon_Q\frac{\partial w_3}{\partial x} + \beta w_2 + \tilde{b}_1 w_5 - \overline{\nu}_3 w_3, \\ \frac{\partial w_4}{\partial t} = \alpha\tilde{\varphi}_1 w_3 - \nu_4 w_4, \\ \frac{\partial w_5}{\partial t} = D_W\frac{\partial^2 w_5}{\partial x^2} - \varepsilon_W\frac{\partial w_5}{\partial x} + a w_4 - \overline{\nu}_5 w_5, \end{cases} \tag{30}$$

where $\tilde{b}_1 = \min_{x\in\overline{\Omega}} b_1(x)$, $\tilde{\varphi}_1 = \min_{x\in\overline{\Omega}} \varphi_1(x)$, $\overline{\nu}_3 = \max_{x\in\overline{\Omega}} \nu_3(x)$, and $\overline{\nu}_5 = \max_{x\in\overline{\Omega}} \nu_5(x)$. It is straightforward that (30) controls system (13) from below. Another application of Lemma 3 yields a principal eigenvalue $\overline{\lambda}_\delta$ of (30) associated with a strongly positive eigenvector $w_0(x)$. Moreover, $\overline{\lambda}_\delta$ and $\lambda(\mathcal{T}_0)$ have the same sign. Thus, system (30) has a positive solution $w(t,x) = e^{\overline{\lambda}_\delta(t-t_1)}w_0(x)$, $t \geq t_1$, $x \in \overline{\Omega}$. For any $\phi \in X^+$ with $\phi_i(0) \not\equiv 0$, $i = 1,2,3,4,5$, it follows from the parabolic maximum principle that

$$A(t,x) > 0, \ Y(t,x) > 0, \ Q(t,x) > 0, \ U(t,x) > 0, \ W(t,x) > 0, \ \forall t > 0, \ x \in \overline{\Omega}. \tag{31}$$

Therefore, we can choose a sufficiently small number $\eta_0 > 0$ such that

$$(A(t_1,x,\phi), Y(t_1,x,\phi), Q(t_1,x,\phi), U(t_1,x,\phi), W(t_1,x,\phi)) \geq \eta_0 w_0(x).$$

Since the reaction term F^- of system (30) is cooperative, another application of the comparison principle[49] leads us to

$$(A(t,x,\phi), Y(t,x,\phi), Q(t,x,\phi), U(t,x,\phi), W(t,x,\phi)) \geq \eta_0 e^{\overline{\lambda}_\delta (t-t_1)} w_0(x), \ \forall t \geq t_1, \ x \in \overline{\Omega}.$$

Therefore, since $\overline{\lambda}_\delta > 0$, one has $\eta_0 e^{\overline{\lambda}_\delta (t-t_1)} w_0(x) \to \infty$ as $t \to \infty$. This implies $(A, Y, Q, U, W)(t,x,\phi)$ is unbounded, which is a contradiction, and the proof of Lemma 4 is achieved. □

We are now in a position to state and prove the uniform persistence result, which indicates that $\mathcal{R}_0^{pde}$ is a threshold for mosquito persistence.

Theorem 10. *If $\mathcal{R}_0^{pde} > 1$, then there exists $\delta_1 > 0$ such that any nonnegative solution $u(t,x,\phi)$ of (13)-(17) with $\phi_i(0) \not\equiv 0$ satisfies*

$$\liminf_{t\to\infty} u_i(t,x,\phi) \geq \delta_1, \quad \forall i = 1,2,3,4,5, \tag{32}$$

uniformly for all $x \in \overline{\Omega}$.

Proof. For $\mathcal{R}_0^{pde} > 1$, we use the persistence theory developed in.[68] To that end, set

$$\mathbb{D}_0 := \{\phi = (\phi_1, \phi_2, \phi_3, \phi_4, \phi_5) \in X^+ : \phi_i(0) \not\equiv 0\}.$$

Clearly, we have

$$\partial\mathbb{D}_0 := X^+ \setminus \mathbb{D}_0 = \{\phi \in X^+ : \phi_1(0) \equiv 0 \text{ or } \phi_2(0) \equiv 0 \text{ or } \phi_3(0) \equiv 0 \text{ or } \phi_4(0) \equiv 0 \text{ or } \phi_5(0) \equiv 0\},$$

and $\Phi_t(\mathbb{D}_0) \subset \mathbb{D}_0$, $\forall t \geq 0$. If $\phi \in \mathbb{D}_0$, then, from (31), one has $u(t,x,\phi) \gg 0$, $\forall x \in \overline{\Omega}$, $t > 0$. Define

$$K_\partial := \{\phi \in \partial\mathbb{D}_0 \ : \ \Phi_t(\phi) \in \partial\mathbb{D}_0, \ \forall t \geq 0\},$$

and let $\Omega(\phi)$ be the Ω-limit set of the positive orbit $\Gamma^+(\phi) := \{\Phi_t(\phi)\}_{t\geq 0}$. We claim that

$$\bigcup_{\phi\in K_\partial} \Omega(\phi) = \{\mathcal{T}_0\}.$$

Indeed, for any given $\phi \in K_\partial$, we have $\Phi_t(\phi) \in \partial\mathbb{D}_0$, $\forall t \geq 0$. Thus, for every $t \geq 0$, either $A(t,\phi) \equiv 0$ or $Y(t,\phi) \equiv 0$ or $Q(t,\phi) \equiv 0$ or $U(t,\phi) \equiv 0$ or $W(t,\phi) \equiv 0$. In the case where $A(t,\phi) \equiv 0$, we see from the first equation of (13) that $\lim_{t\to\infty} W(t,x) = 0$ uniformly for $x \in \Omega$. From the second, third, and fourth equations in (13), and thanks to the theory of asymptotically autonomous semiflows,[69] we have $\lim_{t\to\infty} Y(t,x) = 0$, $\lim_{t\to\infty} Q(t,x) = 0$, and $\lim_{t\to\infty} U(t,x) = 0$ uniformly for $x \in \overline{\Omega}$. If $Y(t,\phi) \equiv 0$, $\forall t \geq 0$, the second equation in (13) yields $\lim_{t\to\infty} A(t,x) = 0$ uniformly for $x \in \overline{\Omega}$. Similar arguments show that $\lim_{t\to\infty} W(t,x) = 0$, $\lim_{t\to\infty} Q(t,x) = 0$, and $\lim_{t\to\infty} U(t,x) = 0$ uniformly for $x \in \overline{\Omega}$. Similar arguments and conclusions hold for the cases where $Q(t,\phi) \equiv 0$, $U(t,\phi) \equiv 0$, and $W(t,\phi) \equiv 0$. Therefore, in either case, the Ω-limit set of $\Gamma^+(\phi)$ for $\phi \in K_\partial$ is $\{\mathcal{T}_0\}$. Hence the claim. Now, we define the function $p : X^+ \to \mathbb{R}_+$ by

$$p(\phi) = \min\left\{\min_{x\in\overline{\Omega}} \phi_i(x), \ i = 1,2,3,4,5\right\}.$$

It is straightforward that $p^{-1}((0,\infty)) \subset \mathbb{D}_0$. Suppose $p(\phi) = 0$ and $\phi \in \mathbb{D}_0$, then we have $\phi_i(\cdot) \not\equiv 0$, $i = 1,2,3,4,5$. By (31), one has $\min\left\{\min_{x\in\overline{\Omega}} u(t,x,\phi)\right\} > 0$, $\forall t > 0$, which implies that $p(\Phi_t(\phi)) > 0$, $\forall t > 0$. Thus, p is a generalized distance function for the semiflow $\Phi_t : X^+ \to X^+$ (see[68]). Note that, by the above claim, any positive orbit of $\Phi(t)$ in K_∂ converges to $\mathcal{T}_0$. In view of Lemma 4, we conclude that $\{\mathcal{T}_0\}$ is an isolated invariant set in X^+ and that $W^s(\mathcal{T}_0) \cap \mathbb{D}_0 = \emptyset$, where $W^s(\mathcal{T}_0)$ is the stable manifold of $\mathcal{T}_0$. Therefore, making use of Theorem 8, we conclude that there exists $\delta_1 > 0$ such that $\min\{p(\psi) : \psi \in \Omega(\phi)\} > \delta_1$ for any $\phi \in \mathbb{D}_0$. This implies that $\liminf_{t\to\infty} u_i(t,x,\phi) \geq \delta_1$, $\forall \phi \in \mathbb{D}_0$. □

3.4 | Numerical simulations: case study of *anopheles* mosquitoes, the malaria vector agent agent

This section deals with numerical simulations for system (13). Our main objective here is to investigate through numerical simulations, the impacts of dispersal and heterogeneity on the dynamics, and persistence of mosquitoes, as well as illustrating some of our theoretical results. To make it simple, we concentrate on one dimensional domain Ω. Model (13) is simulated by using data from recent works, who are summarized in Table 4. We choose $D_Y = D_Q = D_W = D_M = 0.04m^2/s$ and $\varepsilon_Q = \varepsilon_W = 0.1m/s$.[18] To describe the spatial heterogeneity, we assume that the hosts are unevenly distributed. In order to capture the fact that, the more people leave villages and farms to cities, the faster the distribution of human density changes, and the more the urbanization have impact on mosquito distribution,[46,70] we choose the location-dependent parameters as follows:

$$\varphi_1(x) = 16(1 + p\cos(2x)),\ \ b_1(x) = 0.8(1 + p\cos(2x)),$$

where, $p \in [0, 1]$ is the magnitude of host's heterogeneity. Note that when $P = 0$, humans distribute evenly in space (homogeneity in human's distribution). With this set of parameters, the spatial average of $\varphi_1(x)$ and $b_1(x)$ remain 16 and 0.8, respectively. Since analytical determination of $\mathcal{R}_0^{pde}$ is very difficult, we apply the numerical method described in[63,64] to compute the basic offspring number $\mathcal{R}_0^{pde}$ of model (13).

3.4.1 | A nonstandard numerical scheme for the system (13)-(17)

In this subsection, we consider the full discretization of model (13)-(17). This is achieved by the nonstandard finite difference (NSFD) approach, which has shown great potential in providing reliable numerical schemes that replicate the dynamics of continuous models in Mathematical Biology.[71-73] The construction in the papers[74,75] is appropriate for the case under consideration.

Let $dt > 0$ and $dx > 0$ be the time and space step-size, respectively. We denote by u_j^n, an approximation of $u(t, x)$ at the grid point $t_n = ndt$ and $x_j = jdx$, for n = 1,2, … , $j = 1, 2, \ldots, N_e$. The challenge in the approximation of the model Equations 13-(14) arises from the fact that it consists of three types of equations. These are (a) ordinary system of differential equations (ie $(13)_1$, $(13)_4$) ; (b) reaction-diffusion equation (ie $(13)_2$) ; and (c) advection-reaction-diffusion equations (ie $(13)_3$, $(13)_5$ and (14)). The ODE Equations $(13)_1$ and $(13)_4$ are approximated by

$$\begin{cases} \frac{A_j^{n+1} - A_j^n}{\rho(dt)} = B(W_j^n)W_j^n - [\nu_1 + \mu_2 A_j^n]A_j^{n+1}, \\ \frac{U_j^{n+1} - U_j^n}{\rho(dt)} = \alpha\varphi_1(x_j)Q_{j-1}^n - \nu_4 U_j^{n+1}, \end{cases} \tag{33}$$

where the complex denominator function ρ is given by

$$\rho(dt) = \frac{1 - e^{-p_0 dt}}{p_0}, \quad \text{with} \quad p_0 = \max\{\nu_1, \nu_2, \nu_3, \nu_4, \nu_5, \mu_M\}.$$

The reaction-diffusion Equation $(13)_2$ is approximated by

$$\frac{Y_j^{n+1} - Y_j^n}{\rho(dt)} = D_Y \frac{Y_{j+1}^{n+1} - 2Y_j^{n+1} + Y_{j-1}^{n+1}}{dx^2} + r\Gamma A_j^{n+1} - \nu_2 Y_j^{n+1}. \tag{34}$$

For the advection-reaction-diffusion equations, we assume for simplicity that the advection coefficients are the same that is $\varepsilon_0 = \varepsilon_Q = \varepsilon_W = \varepsilon_M$. We impose the functional relation $dx = \varepsilon_0 dt$ between the step sizes. Then the advection-reaction-diffusion Equations $(13)_3$, $(13)_5$, and (14) are approximated by

$$\begin{cases} \frac{Q_j^{n+1} - Q_{j-1}^n}{\rho(dt)} = D_Q \frac{Q_{j+1}^{n+1} - 2Q_j^{n+1} + Q_{j-1}^{n+1}}{dx^2} + \beta Y_j^{n+1} + b_1(x_j)W_{j-1}^n - \nu_3(x_j)Q_{j-1}^n, \\ \frac{W_j^{n+1} - W_{j-1}^n}{\rho(dt)} = D_W \frac{W_{j+1}^{n+1} - 2W_j^{n+1} + W_{j-1}^{n+1}}{dx^2} + aU_j^{n+1} - \nu_5(x_j)W_{j-1}^n, \\ \frac{M_j^{n+1} - M_{j-1}^n}{\rho(dt)} = D_M \frac{M_{j+1}^{n+1} - 2M_j^{n+1} + M_{j-1}^{n+1}}{dx^2} + (1 - r)\Gamma A_j^{n+1} - \mu_M M_j^{n+1}. \end{cases} \tag{35}$$

It should be noted that the left-hand side of (35) is a discretization of the continuous advection term. Indeed,

$$\frac{\partial Z}{\partial t}+\varepsilon_0\frac{\partial Z}{\partial x}\approx\frac{Z_j^{n+1}-Z_j^n}{\rho(dt)}+\varepsilon_0\frac{Z_j^n-Z_{j-1}^n}{\varepsilon_0\rho\left(\frac{dx}{\varepsilon_0}\right)},\quad\text{where}\quad Z=Q,W,M.$$

The discrete method (33)-(35) is indeed an NFSD scheme because it is constructed according to Mickens' rule [71,72,75] formalized as follows:

Rule 1: The standard denominator $h=dt$ of the discrete derivatives is replaced by the complex denominator function $\rho(dt)=(1-e^{-p_0dt})/p_0$, which satisfies the asymptotic relation $\varphi(dt)=h+\mathcal{O}(h^2)$.

Rule 2: The nonlinear term μ_2A^2 is approximated in a nonlocal way. We have $A_j(t_n)A_j(t_n)\approx A_j^nA_j^{n+1}$ instead of $A_j(t_n)A_j(t_n)\approx A_j^nA_j^n$.

Grouping (33)-(35), we obtain the following NSFD scheme, which by construction preserves the conservation laws associated with the continuous model:

$$\begin{cases}\frac{A_j^{n+1}-A_j^n}{\rho(dt)}=B(W_j^n)W_j^n-[\nu_1+\mu_2A_j^n]A_j^{n+1},\\ \frac{Y_j^{n+1}-Y_j^n}{\rho(dt)}=D_Y\frac{Y_{j+1}^{n+1}-2Y_j^{n+1}+Y_{j-1}^{n+1}}{dx^2}+r\Gamma A_j^{n+1}-\nu_2Y_j^{n+1},\\ \frac{Q_j^{n+1}-Q_{j-1}^n}{\rho(dt)}=D_Q\frac{Q_{j+1}^{n+1}-2Q_j^{n+1}+Q_{j-1}^{n+1}}{dx^2}+\beta Y_j^{n+1}+b_1(x_j)W_{j-1}^n-\nu_3(x_j)Q_{j-1}^n,\\ \frac{U_j^{n+1}-U_j^n}{\rho(dt)}=\alpha\varphi_1(x_j)Q_{j-1}^n-\nu_4U_j^{n+1},\\ \frac{W_j^{n+1}-W_{j-1}^n}{\rho(dt)}=D_W\frac{W_{j+1}^{n+1}-2W_j^{n+1}+W_{j-1}^{n+1}}{dx^2}+aU_j^{n+1}-\nu_5(x_j)W_{j-1}^n,\\ \frac{M_j^{n+1}-M_{j-1}^n}{\rho(dt)}=D_M\frac{M_{j+1}^{n+1}-2M_j^{n+1}+M_{j-1}^{n+1}}{dx^2}+(1-r)\Gamma A_j^{n+1}-\mu_MM_j^{n+1}.\end{cases}\tag{36}$$

However, for computational purposes, it is preferable to work with the NSFD scheme (36) in the Gauss-Seidel-type and sequential order (33), (34), and (35), which leads to an explicit scheme as explained below. It is clear from (33) that

$$A_j^{n+1}=\frac{A_j^n+\rho(dt)B(W_j^n)W_j^n}{1+\rho(dt)[\nu_1+\mu_2A_j^n]}\quad\text{and}\quad U_j^{n+1}=\frac{U_j^n+\rho(dt)\alpha\varphi_1(x_j)Q_{j-1}^n}{1+\rho(dt)\nu_4}.$$

Equation (34) is equivalent to

$$-D_Y\frac{\rho(dt)}{dx^2}Y_{j+1}^{n+1}+\left(1+\rho(dt)\nu_2+2D_Y\frac{\rho(dt)}{dx^2}\right)Y_j^{n+1}-D_Y\frac{\rho(dt)}{dx^2}Y_{j-1}^{n+1}=Y_j^n+\rho(dt)r\Gamma A_j^{n+1}.\tag{37}$$

This takes the equivalent vector form

$$\mathcal{M}_1\underline{\mathbf{Y}}^{n+1}=\underline{\mathbf{N}}^{1,n}\geq 0,$$

where the matrix $\mathcal{M}_1$, in which boundary values are incorporated, is an M-matrix because it is strictly diagonally dominant and has positive diagonal entries. Thus,

$$\underline{\mathbf{Y}}^{n+1}=\mathcal{M}_1^{-1}\underline{\mathbf{N}}^{1,n}.$$

The first equation in (35) is equivalent to

$$-D_Q\frac{\rho(dt)}{dx^2}Q_{j+1}^{n+1}+\left(1+2D_Q\frac{\rho(dt)}{dx^2}\right)Q_j^{n+1}-D_Q\frac{\rho(dt)}{dx^2}Q_{j-1}^{n+1}=Q_{j-1}^n+\rho(dt)\beta Y_j^{n+1}+\rho(dt)b_1(x_j)W_{j-1}^n-\rho(dt)\nu_3(x_j)Q_{j-1}^n.$$

This takes the equivalent vector form

$$\mathcal{M}_2\underline{\mathbf{Q}}^{n+1}=\underline{\mathbf{N}}^{2,n},$$

where as in the previous case $\mathcal{M}_2$ is an M-matrix. Note that the vector $\underline{\mathbf{N}}^{2,n}$ is nonnegative because $1-\rho(dt)\nu_3(x_j) \geq 0$ by the choice of $\rho(dt)$. Thus,

$$\underline{\mathbf{Q}}^{n+1} = \mathcal{M}_2^{-1}\underline{\mathbf{N}}^{2,n}.$$

In a similar manner, one obtains that the second and last equations in (35) have the equivalent vector form

$$\mathcal{M}_3\underline{\mathbf{W}}^{n+1} = \underline{\mathbf{N}}^{3,n} \geq 0, \quad \mathcal{M}_4\underline{\mathbf{M}}^{n+1} = \underline{\mathbf{N}}^{4,n} \geq 0,$$

so that

$$\underline{\mathbf{W}}^{n+1} = \mathcal{M}_3^{-1}\underline{\mathbf{N}}^{3,n} \quad \text{and} \quad \underline{\mathbf{M}}^{n+1} = \mathcal{M}_4^{-1}\underline{\mathbf{N}}^{4,n}.$$

At this stage, a comment is in order to explain how the boundary values are actually incorporated in the matrices M_k ($k = 1, 2, 3, 4$). To illustrate the process for the matrix $\mathcal{M}_1$, put $j = 0$ and $j = N_e$ in Equation (37). From the known data $\frac{\partial Y}{\partial x}(t_{n+1}, 0)$ and $\frac{\partial Y}{\partial x}(t_{n+1}, l)$, we can use the approximations

$$\frac{\partial Y}{\partial x}(t_{n+1}, 0) \simeq \frac{Y_1^{n+1} - Y_{-1}^{n+1}}{2dx} \quad \text{and} \quad \frac{\partial Y}{\partial x}(t_{n+1}, l) \simeq \frac{Y_{N_e+1}^{n+1} - Y_{N_e}^{n+1}}{dx}.$$

We can then take

$$Y_{-1}^{n+1} = Y_1^{n+1} - 2dx\frac{\partial Y}{\partial x}(t_{n+1}, 0) \quad \text{and} \quad Y_{N_e+1}^{n+1} = Y_{N_e}^{n+1} + dx\frac{\partial Y}{\partial x}(t_{n+1}, l).$$

We then replace Y_{-1}^{n+1} an $Y_{N_e+1}^{n+1}$ with these expressions in the scheme (37).

3.4.2 | General dynamics

The long run behavior of system (13) is simulated using $\Omega = [0, 10]$. Figures 6 and 8 show the numerical plots of the female mosquito compartments $Y(t,x)$, $Q(t,x)$, $U(t,x)$ and $W(t,x)$, with the initial conditions $A(0,x) = 500 - \cos(2x)$, $Y(0,x) = 75 - \sin(2x)$, $Q(0,x) = 50 - \cos(2x)$, $U(0,x) = 50 - \cos(2x)$, and $W(0,x) = 75 - \cos(2x)$. For the aforementioned set of parameters, we compute $\mathcal{R}_0^{pde} = 11.8292 > 1$, and Figure 6 illustrates the distribution of mature females as time and space vary when the distribution of hosts is uniform and $\mathcal{R}_0^{pde} > 1$. Its shows as established in Theorem 10 that mosquito population persists over time when $\mathcal{R}_0^{pde} > 1$.

Figure 6 depicts the solutions of model (13) when $P = 0$ (ie with homogeneity in host's distribution), while Figures 7, 8, 9, and 10 show the solutions of model (13) in a landscape with heterogeneity in hosts distribution ($P > 0$). Although mosquito population persists over time, its distribution in the domain is not the same. Figure 6 shows that spatial distribution of mosquitoes is homogeneous in the domain when the hosts density is too, while Figure 7 shows a drastic change in the spatial distribution of mosquitoes in gonotrophic cycle when the hosts density is heterogeneous.

3.4.3 | Impact of spatial heterogeneity on mosquito spread

To investigate the spatial heterogeneity effect on the mosquito dynamics, we take the variation of human distribution.

Figures 8, 9, and 10 show the influence of the spatial heterogeneity of hosts on the dynamics of female mosquitoes. From these figures, one observes that spatial distribution of females in gonotrophic cycle is strongly influenced by the hosts density. Moreover, when P increases from 0 to 1, an increase on the heterogeneity is observed in spatial distribution of female mosquitoes. Note that the larger the value of P, the higher the heterogeneity of spatial density of hosts. It follows that the population distribution is strongly dependent on the distribution of hosts. Thus, we can conclude that urbanization strongly influences the mosquito dynamics and therefore increases or decreases malaria risk depending on the range of the remaining model parameters.

Altogether, the above plotted figures show that landscape really play an important role in the dispersal of mosquitoes. From a practical point of view, it may be useful to know how mosquitoes are distributed on a domain, in order to determine where they are likely to gather, before conducting vector control. Our simulations show that, when we consider a homogeneous distribution of hosts, the distribution of mature females is homogeneous on the domain (see Figure 6). But, when we consider a heterogeneous distribution of hosts, we observe a drastic change in the distribution (see Figures 8-10). This indicates that there exists a linear relationship between hosts density and mosquitoes distribution when there is homogeneity (ie $P = 0$). However, when there is heterogeneity (ie $P > 0$), this relationship is perturbed and induces a strong influence on spatial distribution.

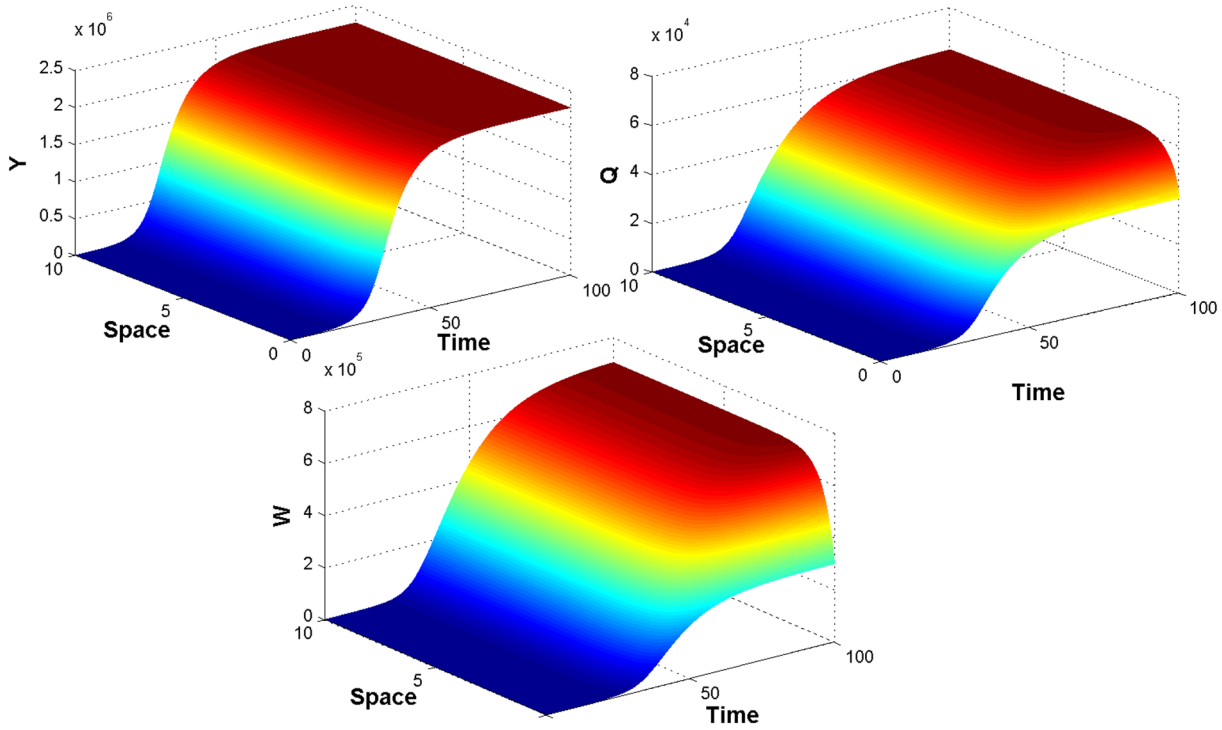

FIGURE 6 Distribution of mature females in a domain with homogeneous distribution of humans ($P = 0$). n = 1 and all other parameters as in Table 4. $\mathcal{R}_0^{pde} = 11.8292 > 1$ [Colour figure can be viewed at wileyonlinelibrary.com]

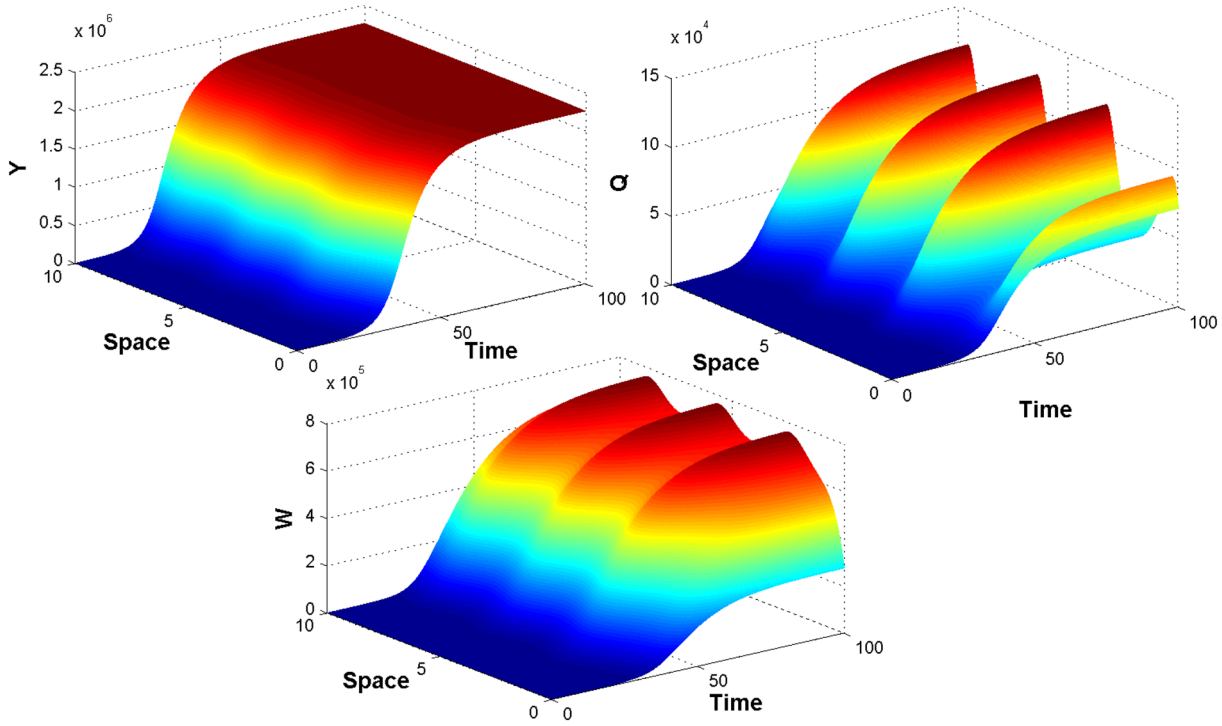

FIGURE 7 Distribution of mature females in a domain with heterogeneous distribution of humans ($P = .5$). n = 1 and all other parameters as in Table 4 [Colour figure can be viewed at wileyonlinelibrary.com]

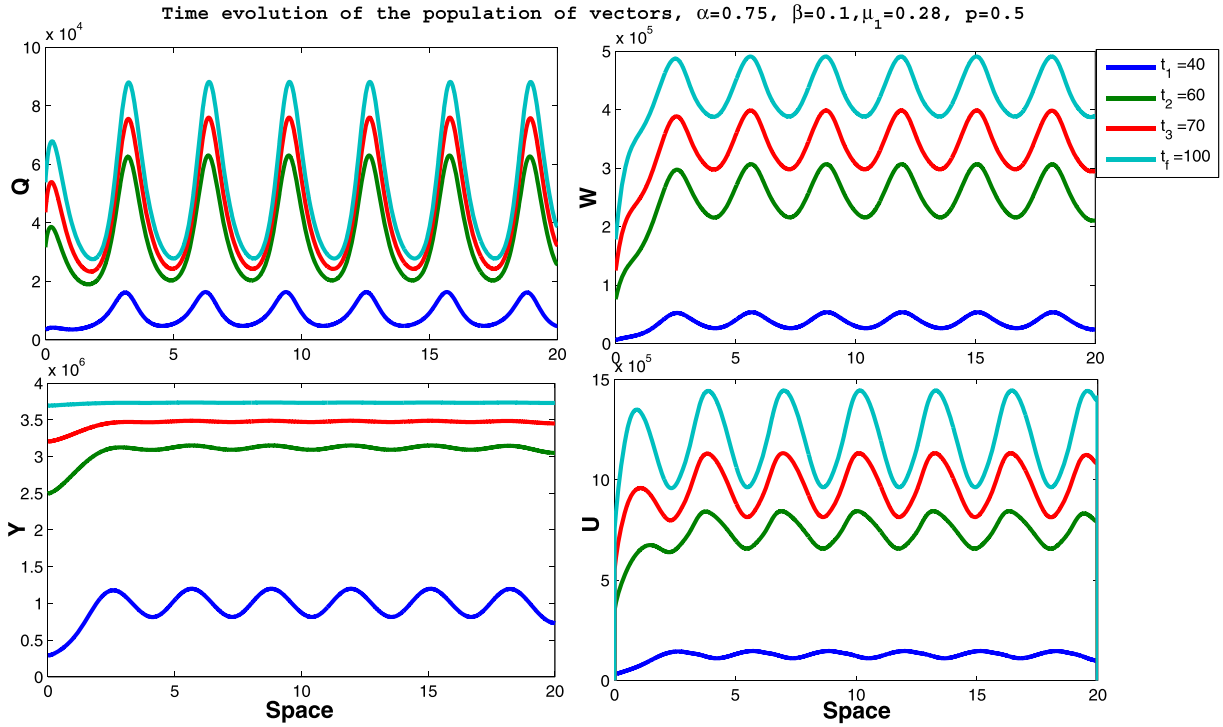

FIGURE 8 Distribution of mature females in a domain with heterogeneous distribution of humans ($P = .5$). n = 1 and all other parameters as in Table 4

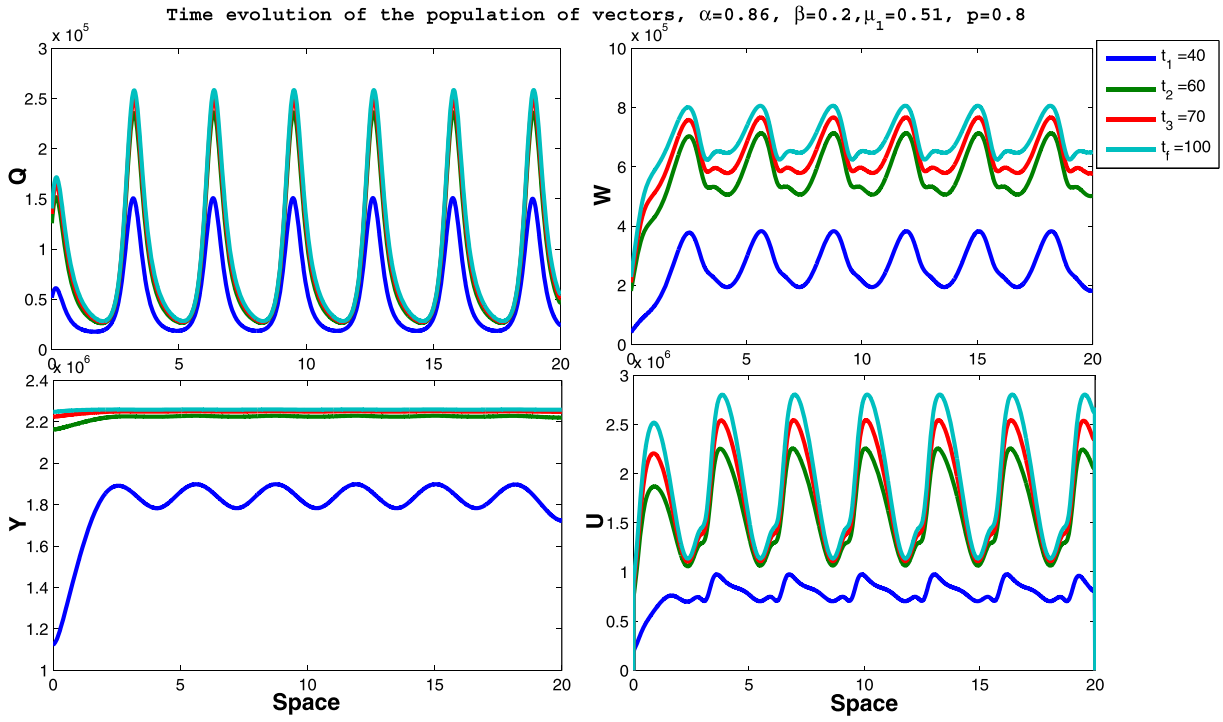

FIGURE 9 Distribution of mature females in a domain with heterogeneous distribution of humans ($P = .8$). n = 1 and all other parameters as in Table 4

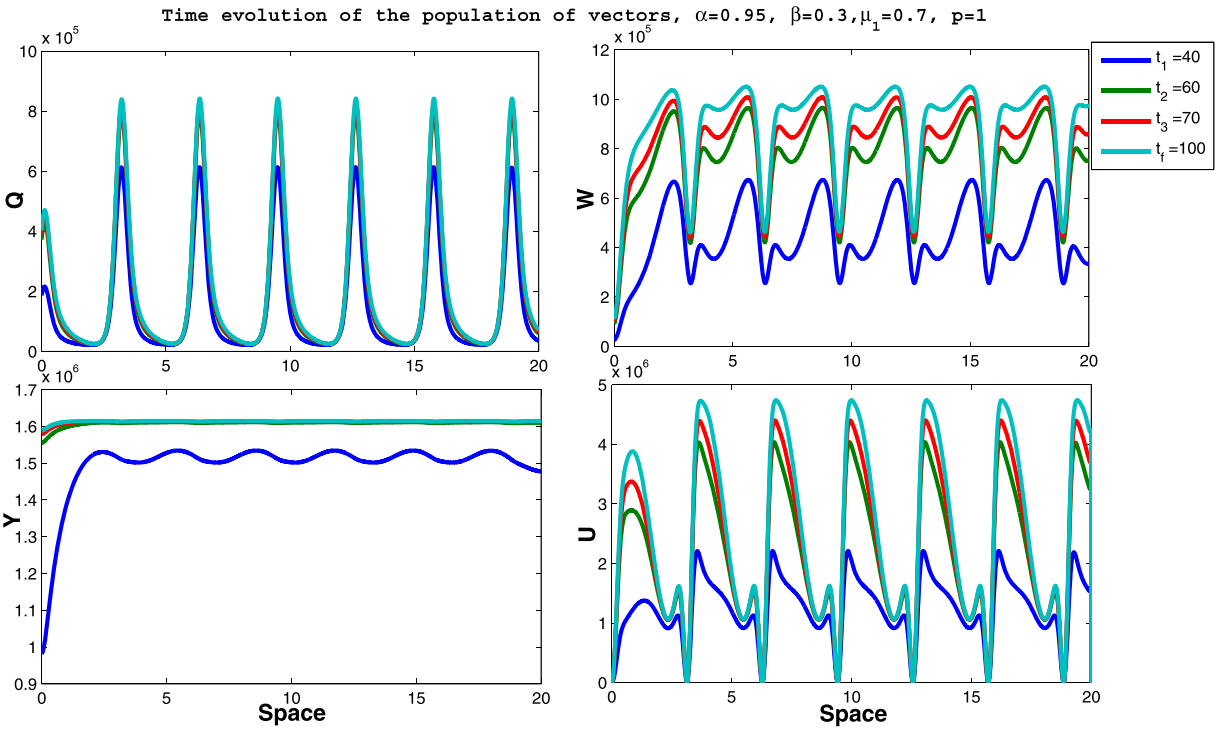

FIGURE 10 Distribution of mature females in a domain with heterogeneous distribution of humans ($P = 1$). n = 1 and all other parameters as in Table 4

4 | CONCLUSION AND DISCUSSION

In this paper, we have assessed the impact of dispersal and the spatial heterogeneity on the distribution of mosquito population. To achieve our goal, we have described the spatial evolution of *anopheles* mosquito by developing a temporal model subject to a general form of the oviposition function and extended it to a spatio-temporal one. Our models have been rigorously analyzed using, among others, the more realistic Maynard-Smith-Slatkin oviposition function. However, our results remain valid even if the latter oviposition function is replaced by any function drawn from Table 2, including the Hassell function that was considered for the first time in this work. Our models have been investigated in many aspects. From the modeling point of view, we have extended some recent ODE models[6,7,12,13] by (a) incorporating the gonotrophic cycle (Q, U, and W) of adult female mosquitoes and considering a general egg oviposition function; (b) taking into account the mating behavior and human-vector interaction; (c) including a spatial component in order to taking into account movement of vectors and spatial heterogeneity of mosquito resources. Moreover, our PDE model has extended some recent dispersal models[20-23] by incorporating the gonotrophic cycle of adult female mosquitoes, by considering a general egg oviposition function, and by including the spatial heterogeneity of mosquito resources. From the theoretical perspective, due to the high nonlinearity of the ODE model and its extended PDE counterpart, we made use of a variety techniques and approaches, including and not limited to Lyapunov-Lasalle techniques, monotone dynamical systems approach, semigroup application, and spectral theory approach. The main results read as follows:

- For the temporal model (1), we have derived the basic offspring number $\mathcal{R}_0^{ode}$, and through a sensitivity analysis, we have realized that the natural mortality rate of immature females μ_Y, the mating rate β, and the deposit rate of eggs by females N_{egg} are the top three more influential parameters on the dynamics of mosquito population. The trivial equilibrium of the temporal model is GAS whenever $\mathcal{R}_0^{ode}$ is less than unity. In the case where $\mathcal{R}_0^{ode}$ exceeds unity, there exists a unique non-trivial equilibrium, which is GAS for n = 1 and globally attractive for $n > 1$. When there is no density-dependent mortality in the aquatic stage (ie $\mu_2 = 0$), the model exhibits the Hopf bifurcation phenomenon. These results hold for the Verhlust-Pearl logistic and Hassell oviposition functions. For the remaining four oviposition functions in Table 2, we have summarized the long run behavior of the solutions of their corresponding ODE model (1) in in Table 3.

- For the spatio-temporal model (13), we have given the formula for the basic offspring ratio $\mathcal{R}_0^{pde}$ for the PDE model. On the one hand, we have shown that spatio-temporal model has a spatially homogeneous trivial equilibrium, which is globally attractive whenever $\mathcal{R}_0^{pde}$ is less than unity. On the other hand, the persistence theory has been used to show that the mosquito population persists whenever the $\mathcal{R}_0^{pde}$ exceeds unity.

From the computational aspect, we have used ODE45 in Matlab and perform numerical simulations of the ODE model to illustrate our theoretical results. Precisely, the Hopf bifurcation occurrence and GAS of the MPE have been illustrated; sensitivity analysis for $\mathcal{R}_0^{ode}$ and sensitivity indices have been calculated. In the presence of density-dependent mortality in the aquatic stage (ie $\mu_2 > 0$), we have extended the global stability results for the ODE models in[6,12] by establishing the global attractivity of the MPE whenever the basic offspring number is above unity. Though, it is still challenging to theoretically prove the local asymptotic stability of the non-trivial equilibrium of the model (1) in the presence of density-dependent mortality in the aquatic stage; alternatively, numerical simulations were used to conjecture it (Figure 3). Together with the latter conjecture, our global attractivity result conjectures the global asymptotical stability of the MPE of the model (1) in presence of the density-dependent mortality in the aquatic stage whenever $\mathcal{R}_0^{ode}$ exceeds unity.

Unlike the temporel model (1), where a standard numerical scheme (ie Runge-Kutta of Order 4) has been used, for spatio-temporal PDE model, we have constructed a dynamical consistent (with respect to the positivity and boundeness) nonstandard difference scheme, using the Maynard-Smith-Slatkin oviposition function and the parameters associated with the *anopheles* species, to show that the spatial heterogeneity of mosquito resources (humans) strongly influences the spatial distribution of adult female mosquitoes (Figures 6-10). Since there is no efficient vaccine for malaria, any sustainable strategy for the fight of malaria must also concentrate effort on the control of mosquito populations, especially in endemic regions. We have presented here a framework for studying the dynamics of the mosquito populations by interpreting its life cycle. On the one hand, we have used several approaches to prove global stability of equilibria and for some nonlinear birth functions; we have characterized the asymptotic behavior of our model. Our results on stability study show that, in absence of density-dependent mortality ($\mu_2 = 0$), Hopf bifurcation phenomenon can occur at the MPE, while in the presence of density-dependent mortality ($\mu_2 > 0$), the MPE is always asymptotically stable. On the other hand, a special emphasis of this paper is the role played by the spatial component and variation of human distribution on mosquitoes distribution. Our study indicates that there is a relationship between hosts density and mosquitoes distribution, and this relationship has far-reaching the effects on spatial distribution of mosquitoes. Through numerical simulations, our work suggests that spatial variation of human distribution strongly influences the spatial distribution of adult female mosquitoes. As shown in Figures 8-10, when the index describing urbanization process (P) varies from 0 to 1, the distribution of females in the gonotrophic cycle is strongly disturbed. This shows that urbanization may increase or decrease malaria risk in regions where this disease is endemic. With regard to control measure, a probably efficient strategy for the containment of *anopheles* mosquito could be the mitigation of human-mosquito contact. It is well known that so far that a sustainable and efficient method of reducing this human-mosquito contact remains the use of mosquito bed nets, and it should be noted that the consideration of such measure alongside with the spatial effects (as in this paper) on mosquito population dynamics will bring further interesting and chalenging modeling and mathematical questions. As far as future investigations are concerned, we are planning to perform a sensitivity analysis and tackle the existence of traveling fronts for the spatial model. On the one hand, it is well known that seasonality and climatic changes, such as temperature and rainfall, affect the life cycle of mosquitoes. Thus, a possible extension of this manuscript, on which we are already working, is to incorporate these latter features in our models in order to assess the impact of temperature and rainfall on the abundance of mosquitoes. On the other hand, the comparison with real experiments in order to validate, modified, or adapt the models is another challenge we intend to face in the near future. To better reflect the details of spatial variation, an equally challenging problem will be to consider the situation where the diffusion and convection coefficients, as well as other parameters depend on a two dimensional spatial variable.

ACKNOWLEDGEMENTS

The first author (MLMM) is grateful to the Research and Graduate Studies in Mathematics and its Applications (RGSMA) Botswana for their support during the preparation of this manuscript. The second author (TB) acknowledges the financial support of the University of Pretoria Senior Postdoctoral Programme Grant (2017-2019). The authors are also grateful to the two anonymous referees and to Prof Wolfgang Sprößig, Editor in Chief of this journal, who, through their suggestions and patience, made it possible for the paper to be substantially revised and improved.

CONFLICT OF INTEREST

This work does not have any conflicts of interest.

REFERENCES

1. WHO, A global brief on vector-borne diseases, http://apps.who.int/iris/bitstream/10665/111008/1/WHO_DCO_WHD_2014.1_eng.pdf, accessed: June 2017.
2. World Health Organization, WHO global health days, http://www.who.int/campaigns/world-health-day/2014/vector-borne-diseases/en/, accessed: June, 2016.
3. Anopheles Mosquitoes, Centers for Disease Control and Prevention, http://www.cdc.gov/malaria/about/biology/mosquitoes/, accessed: May, 2016.
4. Mosquito Life Cycle, American Mosquito Control Association, http://www.mosquito.org/life-cycle, accessed: May, 2016.
5. Ngwa GA. On the population dynamics of the malaria vector. *Bull Math Biol*. 2006;68:2161-2189.
6. Okuneye K, Abdelrazec A, Gumel AB. Mathematical analysis of a weather-driven model for the population ecology of mosquitoes. *Math Biosci Eng*. 2018;15:57-93.
7. Mann Manyombe ML, Tsanou B, Mbang J, Bowong S. A metapopulation model for the population dynamics of Anopheles mosquito. *Appl Math Comp*. 2017;307:71-91.
8. Wanji S, Mafo FF, Tendongfor N, et al. Spatial distribution, environmental and physicochemical characterization of anopheles breeding sites in the mount cameroon region. *J Vector Borne Dis*. 2009;46:75-80.
9. Lutambi A, Penny MA, Smith T, Chitnis N. Mathematical modelling of mosquito dispersal in a heterogeneous environment. *Math Biosci*. 2013;213:198-216.
10. Zhu D, Ren J, Zhu H. Spatial-temporal basic reproduction number and dynamics for a dengue disease diffusion model. *Math Meth Appl Sci*. 2018;41(14):5388-5403. https://doi.org/10.1002/mma.5085
11. Fan G, Lou Y, Thieme HR, Wu J. Stability and persistence in ODE models for populations with many stages. *Math Biosci Eng*. 2015;12:661-686.
12. Abdelrazec A, Gumel AB. Mathematical assessment of the role of temperature and rainfall on mosquito population dynamics. *J Math Biol*. 2017;74(6):1351-1395.
13. Anguelov R, Dumont Y, Lubuma J. Mathematical modeling of sterile insect technology for control of anopheles mosquito. *Comp Math Appl*. 2012;64(3):374-389.
14. Cai L, Ai S, Li J. Dynamics of mosquitoes populations with different strategies for releasing sterile mosquitoes. *SIAM J Appl Math*. 2014;74(6):1786-1809.
15. Esteva L, Yang HM. Mathematical model to assess the control of Aedes aegypti mosquitos by the sterile insect technique. *Math Biosci*. 2005;198:132-147.
16. Ngwa GA, Niger AM, Gumel AB. Mathematical assessment of the role of non-linear birth and maturation delay in the population dynamics of the malaria vector, Appl. Math. Comp. 217 (2010) 3286–3313.
17. Cummins B, Cortez R, Foppa IM, Walbeck J, Hyman JM. A spatial model of mosquito host-seeking behavior. *PLoS Comput Biol*. 2012;8(5):e1002500.
18. Dufourd C,Dumont Y. Impact of environmental factors on mosquito dispersal in the prospect of sterile insect technique control. *Comp Math Appl*. 2013;66:1695-1715.
19. Dufourd C, Dumont Y. Modeling and simulations of mosquito dispersal. The case of Aedes albopictus, BioMath 1 (2012) 1209262.
20. Freire IL, Torrisi M. Symmetry methods in mathematical modeling of Aedes aegypti dispersal dynamics. *Nonlinear Analysis: Real World Applications*. 2013;14:1300-1307.
21. Takahashi LT, Maidana NA, Ferreira WC Jr, Pulino P, Yang HM. Mathematical models for the Aedes aegypti dispersal dynamics: travelling waves by wing and wind. *Bull Math Bull*. 2005;67:509-528.
22. Tian CR, Ruan SG. A free boundary problem for Aedes aegypti mosquito invasion. *Appl Math Model*. 2017;46:203-217.
23. Yamashita WMS, Takahashi LT, Chapiro G. Travelling wave solutions for the dispersive models describing population dynamics of Aedes Aegypti. *Math Comput Simul*. 2018;146:90-99.
24. Wang X, Chen Y, Liu S. Dynamics of an age-structured host-vector model for malaria transmission. *Math Meth Appl Sci*. 2018;41:1966-1987. https://doi.org/10.1002/mma.4723
25. Zhen Z, Wei J, Tian L, Zhou J, Chen W. Wave propagation in a diffusive SIR epidemic model with spatiotemporal delay. *Math Meth Appl Sci*. 2018;41(16):7074-7098.
26. Courant R, Hilbert D. *Methods of Mathematical Physics*. 2, vol. 2, Partial Differential Equations, Interscience Publishers Inc New York: John Wiley & Sons; 1962.
27. Dautray R, Lions J-L. *Mathematical Analysis and Numerical Methods for Science and Technology*. 1 Physical Origins and Classical Methods: Springer; 2000.
28. Dautray R, Lions J-L. *Mathematical Analysis and Numerical Methods for Science and Technology*. 2 Functional and Variational Method: Springer; 2000.
29. Dautray R, Lions J-L. *Mathematical Analysis and Numerical Methods for Science and Technology*. 3 Spectral Theory and Applications: Springer; 2000.

30. Dautray R, Lions J-L. *Mathematical Analysis and Numerical Methods for Science and Technology*. 4 Integral Equations and Numerical Methods: Springer; 2000.
31. Dautray R, Lions J-L. *Mathematical Analysis and Numerical Methods for Science and Technology*. 5 Evolution Problems I: Springer; 2000.
32. Dautray R, Lions J-L. *Mathematical Analysis and Numerical Methods for Science and Technology*. 6 Evolution Problems II: Springer; 2000.
33. Murray JD. *Mathematical Biology II: Spatial Models and Biomedical Applications*. Third Edition: Springer; 2003.
34. Smoller J. *Shock waves and reaction-diffusion equations, A Series of Comprehensive Studies in Mathematics*. 258 New York: Springer-Verlag; 1983 581 pages.
35. Manguin S. *Anopheles mosquitoes: new insights into malaria vectors*. BoD-Books on Demand; 2013.
36. Delatte H, Gimonneau G, Triboire A, Fontenille D. Influence of temperature on immature development, survival, longevity, fecundity, and gonotrophic cycles of Aedes albopictus, vector of chikungunya and dengue in the Indian Ocean. *J. Med. Entomol.* 2009;46:33-41.
37. Barclay HJ, Van Den Driessche P. A sterile release model for control of a pest with two life stages under predation. *The Rocky Mountain J. Math.* 1990;20(4):847-855.
38. Cooke K, Van den Driessche P, Zou X. Interaction of maturation delay and nonlinear birth in population and epidemic models. *J. Math. Biol.* 1999;39(4):332-352.
39. Giles HM, Warrel DA. *Bruce-Chwatt's Essential Malariology*. 3rd ed. Portsmouth, NH: Heinemann Medical Books; 1993.
40. Brannstrom A, Sumper DJT. The role of competition and clustering in population dynamics. *Proc. R. Soc. B*. 2005;275:2065-2072.
41. Lou Y, Wu J. Global dynamics of a tick ixodes scapularis model. *Canad. Appl. Math. Quart.* 2011;19:65-75.
42. van den Driessche P, Watmough J. Reproduction numbers and sub-threshold endemic equilibria for the compartmental models of disease transmission. *Math. Biosci.* 2002;180:29-48.
43. Vidyasagar M. Decomposition techniques for large-scale systems with nonadditive interactions: stability and stabilization. *IEEE Trans. Autom. Control.* 1980;25:773-779.
44. Li MY, Muldowney JS. A geometric approach to global-stability problems. *SIAM J. Appl. Math.* 1996;27:155-164.
45. Liu S, Beretta E. A stage-structured predator-prey model of Beddington-DeAngelis type. *SIAM J. Appl. Math.* 2006;66:1101-1129.
46. Lou Y, Zhao X-Q. A reaction-diffusion malaria model with incubation period in the vector population. *J. Math. Biol.* 2011;62:543-568.
47. Wang Z, Zhao X-Q. Global dynamics of a time-delayed dengue transmission model. *Canad. Appl. Math. Quart.* 2012;20:89-113.
48. Zhao X-Q, Jing Z. Global asymptotic behavior in some cooperative systems of functional-differential equations. *Canad. Appl. Math. Quart.* 1996;4:421-444.
49. Smith HL. Monotone Dynamical Systems: An Introduction to the Theory of Competitive and Cooperative Systems. In: *Math. Surveys Monogr*. 41. Providence, Rhode Island: American Mathematical Society; 1995.
50. Marino S, Hogue IB, Ray CJ, Kirschner DE. A methodology for performing global uncertainty and sensitivity analysis in systems biology. *J Theor Biol*. 2008;254:178-196.
51. Depinay JMO, Mbogo CM, Killeen G, et al. A simulation model of African Anopheles ecology and population dynamics for the analysis of malaria transmission. *Malaria J*. 2004;3(1):29.
52. Chitnis N, Smith T, Steketee R. A mathematical model for the dynamics of malaria in mosquitoes feeding on a heterogeneous host population. *J Biol Dyn*. 2008;2(3):259-285.
53. Yakob L, Yan G. A network population model of the dynamics and control of African malaria vectors. *Trans R Soc Med Hyg*. 2010;104(10):669-675.
54. Elbers ARW, Koenraadt CJM, Meiswinkel R. Mosquitoes and Culicoides biting midges: vector range and the influence of climate change. *Rev Sci Tech Off Int Epiz*. 2015;34(1):123-137.
55. Gillies MT. The role of carbon dioxide in host-finding by mosquitoes (diptera: Culicidae): a review. *B Entomol Res*. 1980;70:525-532.
56. Daykin P, Kellogg F, Wright R. Host-finding and repulsion of Aedes aegypti. *Can Entomol*. 1965;97:239-263.
57. Logan JD. *Introduction to nonlinear partial differentiel equations*. John Wiley & Sons; 1994.
58. Pazy A. *Semigroups of Linear Operators and Applications to Partial Differential Equations*. Berlin: Springer-Verlag; 1983.
59. Fife P, Tang M. Comparison principles for reaction-diffusion systems: irregular comparison functions and applications to questions of stability and speed of propagation of disturbances. *J Diff Equ*. 1981;40:168-185.
60. Yamazaki K, Wang X. Global stability and uniform persistence of the reaction-convection-diffusion cholera epidemic model. *Math Biosci Eng*. 2017;14:559-579.
61. Hale JK. *Asymptotics Behavior of Dissipative Systems, Mathematical surveys and monographs*. Providence, Rhode Island: American Mathematics Society; 1988.
62. Thieme HR. Spectral bound and reproduction number for infinite-dimensional population structure and time heterogeneity. *SIAM J Appl Math*. 2009;70:188-211.
63. Wang X, Posny D, Wang J. A reaction-convection-diffusion model for cholera spatial dynamics. *Discrete Contin Dyn Syst Ser B*. 2016;21:2785-2809.
64. Wang X, Wang J. Analysis of cholera epidemics with bacterial growth and spatial movement. *J Biol Dyn*. 2015;9:233-261.
65. Wang W, Zhao X-Q. Basic reproduction numbers for reaction-diffusion epidemic models. *SIAM J Appl Dyn Syst*. 2012;11:1652-1673.
66. Yamazaki K, Wang X. Global well-posedness and asymptotic behavior of solutions to a reaction-convection-diffusion cholera epidemic model. *Discrete Contin Dyn Syst Ser B*. 2016;21:1297-1316.
67. Thieme HR, Zhao X-Q. A non-local delayed and diffusive predator-prey model. *Nonlinear Analysis: Real World Applications*. 2001;2:145-160.

68. Smith HL, Zhao X-Q. Robust persistence for semidynamical systems. *Nonlinear Anal.* 2001;47:6169-6179.
69. Thieme HR. Convergence results and Poincare-Bendixon trichotomy for asymptotically autonomous differential equations. *J. Math. Biol.* 1992;30:755-763.
70. Kweka EJ, Mazigo HD, Himeidan YE, Morona D, Munga S. Urbanization, climate change and malaria transmission in sub-Saharan Africa. *Climate Change Impacts on Urban Pests*. 2016;10:141.
71. Mickens RE. *Applications of Nonstandard Finite Difference Schemes*. Singapore: World Scientific; 2000.
72. Mickens RE. *Advances In The Applications Of Nonstandard Finite Difference Schemes*. Singapore: World Scientific; 2005.
73. Gumel AB, Lenhart S. Modeling Paradigms and Analysis of Disease Transmission Models (DIMACS: Series in Discrete Mathematics and Theoretical Computer Science). *American Mathematical Society*. 2010;10.
74. Chapwanya M, Lubuma JM, Mickens RE. Nonstandard finite difference schemes for Michaelis-Menten type reaction-diffusion equations. *Num. Meth. Part. D. E.* 29(1):337-360.
75. Mickens RE. Nonstandard finite difference schemes for reaction-diffusion equations. *Numer. Methods Partial Differ. Equ.* 2009;15:201-214.
76. Hershkowitz D. Recent directions in matrix stability. *Linear Algebra Appl.* 1992;171:161-186.
77. George TG. Positive definite matrices and Sylvester's criterion. *Am. Math. Mon.* 1991;98:44-46.
78. Park PC. A new proof of Hermite's stability criterion and a generalization of Orlando's formula. *Int. J. Control*. 2012;26:197-206.
79. Chow S, Li C, Wang D. *Normal Forms and Bifurcation of Planar Vector Fields*. Cambridge University Press; 1994.

How to cite this article: Mann Manyombe ML, Mbang J, Tsanou B, Bowong S, Lubuma J. Mathematical analysis of a spatio-temporal model for the population ecology of anopheles mosquito. *Math Meth Appl Sci*. 2020;1–32. https://doi.org/10.1002/mma.6136

APPENDIX A: PROOF OF THEOREM 4

Proof. This will be done in two steps. In the first step, we prove the local asymptotic stability. The second step is devoted to the proof of the existence of Hopf bifurcation.

Step 1: The LAS of $\mathcal{T}^*$ is explored using the properties of Bézout matrices. To that end, let us recall the following instrumental results. We consider the model (1) in the absence of density-dependent mortality in aquatic stage (ie $\mu_2 = 0$). Evaluating the Jacobian matrix at $\mathcal{T}^*$ gives

$$\mathcal{J}(\mathcal{T}^*) = \begin{pmatrix} -\nu_1 & 0 & 0 & 0 & 0 & B(W^*) + W^* \frac{dB(W^*)}{dW} \\ r\Gamma & -\nu_2 & 0 & 0 & 0 & 0 \\ (1-r)\Gamma & 0 & -\mu_M & 0 & 0 & 0 \\ 0 & \beta & 0 & -\nu_3 & 0 & b_1 \\ 0 & 0 & 0 & \alpha\varphi_1 & -\nu_4 & 0 \\ 0 & 0 & 0 & 0 & a & -\nu_5 \end{pmatrix}.$$

The eigenvalues of $\mathcal{J}(\mathcal{T}^*)$ are the roots of the polynomial

$$P(\lambda) = (\lambda + \mu_M)\left[\lambda^5 + b_4\lambda^4 + b_3\lambda^3 + b_2\lambda^2 + b_1\lambda + b_0\right], \tag{A1}$$

where

$$\begin{cases} b_4 = \nu_5 + \nu_4 + \nu_3 + \nu_2 + \nu_1, \\ b_3 = \nu_5(\nu_4 + \nu_3 + \nu_2 + \nu_1) + \nu_4(\nu_3 + \nu_2 + \nu_1) + \nu_3(\nu_2 + \nu_1) + \nu_2\nu_1, \\ b_2 = m_1 + \nu_5\nu_4(\nu_1 + \nu_2) + \nu_5\nu_3(\nu_1 + \nu_2) + \nu_5\nu_2\nu_1 + \nu_4\nu_3(\nu_1 + \nu_2) \\ \qquad +\nu_4\nu_2\nu_1 + \nu_3\nu_2\nu_1, \\ b_1 = m_1(\nu_1 + \nu_2) + \nu_5\nu_4\nu_2\nu_1 + \nu_5\nu_3\nu_2\nu_1 + \nu_4\nu_3\nu_2\nu_1, \\ b_0 = \nu_1\nu_2 m_1 - a\alpha\varphi_1 r\beta\Gamma\left[B(W^*) + W^*\frac{dB(W^*)}{dW}\right]. \end{cases} \tag{A2}$$

In order to show that the polynomial $P(\lambda)$ is negative stable, we apply Theorem 2.8 in[76] and define

$$h(u) = b_0 + b_2u + b_4u^2 \text{ and } g(u) = b_1 + b_3u + u^2.$$

It follows from Definition 2.7 in[76] that the corresponding Bézout matrix $B_{h,g}(P)$ of $P(\lambda)$ given by (A1) is

$$B_{h,g}(P) = \begin{pmatrix} b_{0,0} & b_{0,1} \\ b_{0,1} & b_{1,1} \end{pmatrix},$$

where $b_{0,0} = b_2b_1 - b_3b_0$, $b_{0,1} = b_4b_1 - b_0$ and $b_{1,1} = b_4b_3 - b_2$. Since $B_{h,g}(P)$ is symmetric, it suffices by Sylvester's Criterion[77] to show that the k^{th} leading principal minor Δ_k of $B_{h,g}(P)$ is positive. Since $\mathcal{R}_0^{ode} > 1$, we have $b_0 = n\nu_1\nu_2m_1\left(1 - \frac{1}{\mathcal{R}_0^{ode}}\right) = nm_2 > 0$. The first leading principal minor of $B_{h,g}(P)$, $\Delta_1 = b_{0,0} = b_2b_1 - b_3b_0$ is positive whenever

$$n < n_0^*, \quad \text{where} \quad n_0^* = \frac{b_2b_1}{b_3m_2}.$$

The second leading principal minor of $B_{h,g}(P)$,

$$\Delta_2 = b_{1,1}b_{0,0} - b_{0,1}^2 = b_{1,1}b_2b_1 - (b_4b_1)^2 + m_2(2b_1b_4 - b_{1,1}b_3)n - m_2^2n^2,$$

is positive whenever

$$n < n_0^{**}, \quad \text{where} \quad n_0^{**} = \frac{b_{1,1}\sqrt{b_3^2 - 4b_1} + 2b_1b_4 - b_{1,1}b_3}{2m_2} > 0.$$

We conclude by choosing the integer n such that $1 < n < \min\{n_0^*, n_0^{**}\}$.

Step 2: Consider the model (1) with $\mathcal{R}_0^{ode} > 1$. A Hopf bifurcation can occur when the Jacobian matrix $\mathcal{J}(\mathcal{T}^*)$ of (1), evaluated at $\mathcal{T}^*$, has a pair of purely imaginary eigenvalues. Note that when the rank of the Bézout matrix $B_{h,g}(P)$ is reduced by exactly one, then the characteristic polynomial P has a pair of purely imaginary eigenvalues.[78] Thus, to prove the existence of Hopf bifurcation, it suffices to verify the transversality condition.[79] Let $n = n_0{}^{**}$ be a bifurcation parameter. Let us fix all other parameters of model (1). Then, by the Step 1, $\Delta_1 > 0$. Hence, $\Delta_2(n) = 0$ if and only if $n = n_0{}^{**}$. Moreover,

$$\left.\frac{d\Delta_2(n)}{dn}\right|_{n=n_0^{**}} = -m_2b_{1,1}\sqrt{b_3^2 - 4b_1} < 0.$$

□

One should note that the stability analysis of the temporal model (1) subject to the newly considered Hassell oviposition function B_H and the stability results with respect of the existing works are summarized in Table 3. Note that $\mathcal{R}_0^{\mathcal{L}}$, n_1^*, n_1^{**} $b_0, b_1, ..., b_4$ and $b_{1,1}$ are computed similarly to the above proof such that

1. For $B(W)$ given by B_L, $b_0 = \nu_1\nu_2m_1(\mathcal{R}_0^{ode} - 1) > 0$ and $\mathcal{R}_0^{\mathcal{L}} = 1 + \frac{b_{1,1}\sqrt{b_3^2-4b_1}+2b_1b_4-b_{1,1}b_3}{2\nu_1\nu_2m_1}$.
2. For $B(W)$ given by B_H, $b_0 = n\nu_1\nu_2m_1\left(1 - \frac{1}{(\mathcal{R}_0^{ode})^{\frac{1}{n}}}\right) > 0$. Thus, $n_{1*} = \min\{n_1^*, n_1^{**}\}$ where n_1^* and n_1^{**} are the positive roots of the equations $\Delta_1(n) = 0$ and $\Delta_2(n) = 0$, respectively.

APPENDIX B: PROOF OF THEOREM 5

Proof. Suppose $\mathcal{R}_0^{ode} > 1$ in system (1). Let us first show that the equilibrium $\mathcal{T}^* = (A^*, Y^*, Q^*, U^*, W^*)^T$ is globally asymptotically stable for system $\frac{dx}{dt} = f(x)$. To this end, consider the nonlinear Lyapunov function of Goh-Volterra type

$$V_1(x) = a_1(A - A^* \ln A) + a_2(Y - Y^* \ln Y) + a_3(Q - Q^* \ln Q) + a_4(U - U^* \ln U) + a_5(W - W^* \ln W),$$

where

$$a_1 = \frac{r\Gamma\beta a\alpha\varphi_1 N_{egg}}{\nu_1\nu_2\nu_3\nu_4 B(W^*)\mathcal{R}_0^{ode}}, \quad a_2 = \frac{\beta a\alpha\varphi_1}{\nu_2\nu_3\nu_4}, \quad a_3 = \frac{a\alpha\varphi_1}{\nu_3\nu_4}, \quad a_4 = \frac{a}{\nu_4}, \quad \text{and} \quad a_5 = 1.$$

At the steady state $\mathcal{T}^*$, the following relations hold

$$\begin{aligned} &B(W^*)W^* = (\nu_1 + \mu_2 A^*)A^* = \nu_1\mathcal{R}_0\tfrac{B(W^*)}{N_{egg}}A^*, \quad \nu_3 Q^* = \beta Y^* + b_1 W^*, \\ &r\Gamma A^* = \nu_2 Y^*, \alpha\varphi_1 Q^* = \nu_4 U^* \quad \text{and} \quad aU^* = \nu_5 W^*. \end{aligned} \tag{B1}$$

The time derivative of $V_1(x)$ is

$$\begin{aligned} \dot{V}_1(x) &= a_1\left(1 - \frac{A^*}{A}\right)\dot{A} + a_2\left(1 - \frac{Y^*}{Y}\right)\dot{Y} + a_3\left(1 - \frac{Q^*}{Q}\right)\dot{Q} + a_4\left(1 - \frac{U^*}{U}\right)\dot{U} + a_5\left(1 - \frac{W^*}{W}\right)\dot{W}, \\ &= a_1\left[B(W)W - (\nu_1 + \mu_2 A)A - \frac{B(W)WA^*}{A} + (\nu_1 + \mu_2 A)A^*\right] + a_2\left[r\Gamma A - \nu_2 Y\right. \\ &\left. - \frac{r\Gamma A Y^*}{Y} + \nu_2 Y^*\right] + a_3\left[\beta Y + b_1 W - \nu_3 Q - \frac{\beta Y Q^*}{Q} - b_1\frac{WQ^*}{Q} + \nu_3 Q^*\right] \\ &+ a_4\left[\alpha\varphi_1 Q - \nu_4 U - \frac{\alpha\varphi_1 QU^*}{U} + \nu_4 U^*\right] + a_5\left[aU - \nu_5 W - \frac{aUW^*}{W} + \nu_5 W^*\right]. \end{aligned}$$

Using (B1), Equation (B2) becomes

$$\begin{aligned} \dot{V}_1(x) = a_1\mu_2 A^* A\left(2 - \frac{A}{A^*} - \frac{A^*}{A}\right) + a_1 B(W^*)W^* + a_2\nu_2 Y^* + a_3\nu_3 Q^* + a_4\nu_4 U^* + a_5\nu_5 W^* \\ - a_1\frac{B(W)WA^*}{A} - a_2\frac{r\Gamma A Y^*}{Y} - a_3\frac{\beta Y Q^*}{Q} - a_3 b_1\frac{WQ^*}{Q} - a_4\frac{\alpha\varphi_1 QU^*}{U} - a_5\frac{aUW^*}{W}, \end{aligned} \tag{B2}$$

and the relations

$$\begin{aligned} &a_1 B(W^*)W^* = a_2\nu_2 Y^* = a_3\beta Y^* = a_2 r\Gamma A^* \; ; \; a_5\nu_5 W^* = a_2 r\Gamma A^* + a_3 b_1 W^* \\ &a_3\nu_3 Q^* = a_4\nu_4 U^* = a_4\alpha\varphi_1 Q^* = a_5 aU^* = a_2 r\Gamma A^* + a_3 b_1 W^* \end{aligned} \tag{B3}$$

are satisfied. Substituting the expressions in Equation (B3) yields

$$\begin{aligned} \dot{V}_1(x) &= a_1\mu_2 A^* A\left(2 - \frac{A}{A^*} - \frac{A^*}{A}\right) + 6a_2 r\Gamma A^* + 3a_3 b_1 W^* - a_2 r\Gamma A^*\left(\frac{B(W)WA^*}{B(W^*)W^*A}\right. \\ &\left. + \frac{AY^*}{A^*Y} + \frac{YQ^*}{Y^*Q} + \frac{QU^*}{Q^*U} + \frac{UW^*}{U^*W} + \frac{B(W^*)}{B(W)}\right) - a_3 b_1 W^*\left(\frac{WQ^*}{W^*Q} + \frac{QU^*}{Q^*U} + \frac{UW^*}{U^*W}\right) \\ &+ a_2 r\Gamma A^*\left(\frac{B(W^*)}{B(W)} - 1\right) + \left(\frac{\nu_3\nu_4\nu_5 - b_1\alpha\varphi_1 a}{\nu_3\nu_4}\right)\left(\frac{B(W)}{B(W^*)} - 1\right)W \\ &= a_1\mu_2 A^* A\left(2 - \frac{A}{A^*} - \frac{A^*}{A}\right) + a_2 r\Gamma A^*\left(6 - \frac{B(W)WA^*}{B(W^*)W^*A} - \frac{AY^*}{A^*Y} - \frac{YQ^*}{Y^*Q}\right. \\ &\left. - \frac{QU^*}{Q^*U} - \frac{UW^*}{U^*W} - \frac{B(W^*)}{B(W)}\right) + a_3 b_1 W^*\left(3 - \frac{WQ^*}{W^*Q} - \frac{QU^*}{Q^*U} - \frac{UW^*}{U^*W}\right) \\ &+ a_2 r\Gamma A^*\left(\frac{B(W)}{B(W^*)} - 1\right)\left(\frac{W}{W^*} - \frac{B(W^*)}{B(W)}\right). \end{aligned} \tag{B4}$$

In Equation (B4), the terms between the brackets are Volterra-type functions. These functions are positive definite. For $B(W)$ with n = 1, we have

$$\frac{B(W)}{B(W^*)} - 1 = \frac{W^* - W}{L + W} \quad \text{and} \quad \frac{W}{W^*} - \frac{B(W^*)}{B(W)} = \frac{(W - W^*)L}{W^*(L + W^*)}.$$

Hence,

$$\left(\frac{B(W)}{B(W^*)} - 1\right)\left(\frac{W}{W^*} - \frac{B(W^*)}{B(W)}\right) = -\frac{(W^* - W)^2 L}{W^*(L + W)(L + W^*)} < 0.$$

Thus, using the arithmetic-geometric means inequality, it follows that $\dot{V}_1 \leq 0$. The proof follows by the conclusion in the proof of Theorem 2 as well. □